



City Research Online

City, University of London Institutional Repository

Citation: Karimalis, Emmanouil (2015). Essays in Multivariate Modelling in Finance. (Unpublished Doctoral thesis, City University London)

This is the accepted version of the paper.

This version of the publication may differ from the final published version.

Permanent repository link: <https://openaccess.city.ac.uk/id/eprint/13549/>

Link to published version:

Copyright: City Research Online aims to make research outputs of City, University of London available to a wider audience. Copyright and Moral Rights remain with the author(s) and/or copyright holders. URLs from City Research Online may be freely distributed and linked to.

Reuse: Copies of full items can be used for personal research or study, educational, or not-for-profit purposes without prior permission or charge. Provided that the authors, title and full bibliographic details are credited, a hyperlink and/or URL is given for the original metadata page and the content is not changed in any way.

Essays in Multivariate Modelling in Finance

by

Emmanouil N. Karimalis

A thesis submitted in fulfilment of the requirements for the Degree of Doctor of
Philosophy in the subject of Finance

City University London
Sir John Cass Business School
Department of Finance
London, UK
May 2015



CITY UNIVERSITY
LONDON

CityLibrary
Your space
Your resources
Your library

**THE FOLLOWING PARTS OF THIS THESIS HAVE BEEN REDACTED
FOR COPYRIGHT REASONS:**

Page ii

Excerpt from: Seferis, George (1937) *Epiphany*

To my parents

[Redacted text block]

[Redacted text block]

(Giorgos Seferis, Epiphany, 1937)

Table of Contents

Table of Contents	v
List of Tables	vi
List of Figures	vii
Acknowledgements	viii
Declaration	x
Abstract	xi
1 Introduction	1
1.1 Motivation and objectives	1
1.2 Copula functions as a modelling tool	2
1.3 Outline of the thesis	4
1.4 Summary of findings and contribution to the literature	8
1.5 Conclusions	12
2 Background material: Copula theory	14
2.1 Introduction	14
2.2 Copulas	14
2.3 Copula and dependence measures	16
2.4 Pair-copula construction	24
2.5 Canonical vines (C-vines)	29
2.6 Inference for a C-vine model	31
2.7 Simulation from a C-vine model	35
2.8 Model selection	37
2.9 Selecting an appropriate C-vine decomposition	38
2.10 Selecting an appropriate copula family	39
2.10.1 Graphical tools	40
2.10.2 Analytical tools	47
2.11 Conclusions	49
3 Extreme value theory and mixed canonical vine copulas	51
3.1 Introduction	51
3.2 Extreme value theory	55
3.2.1 Peak over threshold (POT) method	55
3.3 Copula theory	56
3.3.1 Pair-copula construction	57
3.3.2 Canonical vines (C-vines)	59
3.3.3 Inference for a C-vine model	61
3.3.4 C-vine decomposition and copula selection	64
3.4 Model setup	65
3.5 Data description	67
3.6 Application to Phelix power portfolios	71

3.6.1	Univariate fitting of margins using ARMA-GARCH models	71
3.6.2	Semi-parametric modelling of margins	72
3.6.3	Selection and estimation of C-vine models	74
3.6.4	Baseload selection and estimation results	75
3.7	Empirical results	83
3.7.1	Statistical tests	83
3.7.2	Loss functions	86
3.7.3	Statistical test results	88
3.7.4	Loss function results	89
3.8	Conclusions	90
Appendices		
3.A	Time series models for the conditional mean	95
3.B	Copula family abbreviations	96
3.C	Pair-copulas for the Phelix Baseload portfolio	97
4	Measuring systemic risk in the European banking sector	98
4.1	Introduction	98
4.2	Related literature	100
4.3	<i>CoVaR</i> methodology	102
4.3.1	Definition of <i>CoVaR</i>	102
4.3.2	Copula <i>CoVaR</i> methodology	103
4.3.3	Extension to <i>CoES</i>	107
4.3.4	Systemic risk contributor and dependence consistency	107
4.4	Data	109
4.5	Copula <i>CoVaR</i> estimation	110
4.6	Results	112
4.6.1	Computing <i>CoVaR</i> and <i>CoES</i> measures	112
4.6.2	Systemic risk contribution	116
4.6.3	Backtesting and stress testing <i>CoVaR</i>	123
4.6.4	Systemic risk determinants	125
4.7	Conclusions	134
Appendices		
4.A	<i>CoVaR</i> derivation for Normal and Student- <i>t</i> copulas	136
4.A.1	Normal copula	136
4.A.2	The Student- <i>t</i> copula	136
4.B	<i>CoVaR</i> derivation for Archimedean copulas	137
4.B.1	Clayton copula	137
4.B.2	Frank copula	138
4.B.3	Gumbel copula	138
4.B.4	BB7 copula	139
4.C	Dynamic Copula <i>CoVaR</i>	139
4.D	List of European financial institutions	141
4.E	Systemic risk measure comparisons	142
5	Modelling the dependence of European sovereign yield curves	143
5.1	Introduction	143
5.2	Related literature	146
5.3	Data	150

5.4	The dynamic Nelson-Siegel model	157
5.4.1	Estimation based on the Kalman filter	160
5.4.2	Handling missing data	161
5.5	Estimation of marginal yield curves for each country	162
5.5.1	Significance of coefficients	166
5.5.2	Sensitivity analysis	168
5.6	Covariance regression	171
5.6.1	Covariance regression model	171
5.6.2	Parameter estimation via the EM-algorithm	172
5.7	Covariance regression results	174
5.7.1	Conditional covariance results: low and high-equity market volatility	180
5.7.2	Covariance regression sensitivity analysis	184
5.7.3	Covariance regression sensitivity analysis results	187
5.8	Conclusions	191
6	Conclusions and further research	199
6.1	Conclusions	199
6.2	Further research	202
	Bibliography	220

List of Tables

2.3.1	Theoretical properties of bivariate elliptical copula families	19
2.3.2	Theoretical properties of bivariate Archimedean copula families	19
2.4.1	The h -function of the Gaussian, Student- t , BB1 and BB7 copula	28
3.5.1	Baseload portfolio summary statistics	70
3.5.2	Peakload portfolio summary statistics	71
3.6.1	Maximum likelihood GPD estimates	73
3.6.2	Summary of models investigated for the Phelix Baseload and Peak- load portfolios	75
3.6.3	Kendall's τ correlation matrix and \hat{S} estimates for the Phelix Baseload portfolio	76
3.6.4	Kendall's τ correlation matrix and \hat{S} estimates for the Phelix Baseload portfolio.	77
3.6.5	Vuong and Clarke goodness-of-fit test results	77
3.6.6	Maximum likelihood and sequential estimates of the C-vine-EVT model	80
3.6.7	Maximum likelihood and sequential estimates of the A-C-vine- t model	81
3.8.1	Statistical test results	92
3.8.2	Loss function results: Phelix Baseload	93
3.8.3	Loss function results: Phelix Peakload	94
3.B.1	Copula family abbreviations	96

3.C.1	Determination of unconditional and conditional pair-copulas for C-vine model	97
4.6.1	Contribution to systemic risk for each individual institution	121
4.6.2	Contribution to systemic risk by country	121
4.6.3	Dependence and tail dependence estimates	122
4.6.4	Dependence and tail dependence estimates by country	122
4.6.5	Statistical test results	123
4.6.6	Descriptive statistics of market variables	127
4.6.7	Panel regression results of market variables	128
4.6.8	Descriptive statistics of bank-specific variables	133
4.6.9	Panel regression results of bank-specific variables	133
4.D.1	List of European financial institutions	141
5.3.1	Descriptive Statistics: Sovereign yields	154
5.3.2	Descriptive Statistics: Bid-Ask spreads	154
5.3.3	Descriptive Statistics: Credit Default Swap (CDS) spreads	154
5.3.4	Summary Statistics: Macroeconomic and Financial variables	155
5.3.5	Correlation between credit quality and liquidity	157
5.5.1	Information Criteria results	163
5.5.2	Principal component analysis of the latent level, slope and curvature factors.	165
5.5.3	Estimates of macroeconomic and financial variables	167
5.5.4	Sensitivity analysis	169
5.5.5	Cross-country sensitivity analysis	170
5.7.1	Time-series average correlation estimates	178
5.7.2	Time-series average correlation estimates	179
5.7.3	Likelihood ratio test results	179
5.7.4	Time-series average correlation estimates	184
5.8.1	Sensitivity analysis: Cross-country spreads	192
5.8.2	Sensitivity analysis: Cross-country spreads (calm period)	193
5.8.3	Sensitivity analysis: Cross-country spreads (stress period)	194

List of Figures

2.3.1	CDF and PDF of bivariate Normal, Student- t and Clayton copulas	20
2.3.2	CDF and PDF of bivariate Gumbel, BB1 and BB7 copulas	21
2.3.3	Scatter and contour plots of bivariate Normal, Student- t and Clayton	22
2.3.4	Scatter and contour plots of bivariate Gumbel, BB1 and BB7 copulas	23
2.5.1	Tree representation of a canonical vine structure	30
2.10.1	Empirical and theoretical λ -function comparisons	44
2.10.2	Scatter, Chi and K-plots for various degrees dependence	45
2.10.3	Chi-plots for detecting (tail) dependence	46
3.3.1	Tree representation of a canonical vine with 6 variables, 5 trees and 15 edges.	60

3.5.1	Returns of generic Phelix Baseload futures: roll-over effects	69
3.5.2	Returns of generic Phelix Baseload futures: volatility effects	70
3.6.1	Contour plots of Student- t and BB1 copulas	79
3.6.2	Plots of λ -functions of Student- t and BB1 copulas	79
3.6.3	Dependence structure of residuals in the Baseload portfolio	82
3.6.4	Tail dependence of residuals in the Baseload portfolio	82
3.7.1	VaR forecasts for the A-C-vine-EVT and C-vine-EVT models	84
4.3.1	$CoVaR$ as a function of the copula dependence parameter	109
4.6.1	Time-series average VaR , $CoVaR$ and $CoES$ estimates	114
4.6.2	Time-series average Kendall's τ correlation estimates	114
4.6.3	Scatter plot of VaR and $\Delta CoVaR$ estimates	116
4.6.4	Time-series average $\Delta CoVaR$ and VaR estimates	116
4.6.5	Time-series average tail dependence coefficients	118
4.6.6	$CoVaR$ stress-testing	125
4.6.7	The short-term liquidity spread	129
4.6.8	Time-series average $CoVaR$ estimates and timeline of key events	130
4.6.9	The 3-month Euribor rate	131
4.E.1	Time-series average $CoVaR$ and $CoVaR^=$ estimates	142
4.E.2	Time-series average $CoES$ and $CoES^=$ estimates	142
5.3.1	Bid-ask spreads	153
5.3.2	CDS spreads	153
5.3.3	Cross-country correlation estimates: bid-ask and cds spreads	156
5.4.1	Factor loadings of the Nelson-Siegel model	158
5.5.1	Level, slope and curvature factor estimates	164
5.5.2	Cross-country correlation estimates: level, slope and curvature factors	165
5.7.1	Covariance regression model: significance testing	176
5.7.2	Covariance regression model: signs of coefficients	177
5.7.3	Covariance regression model: significance testing (calm and crisis periods)	182
5.8.1	Sensitivity analysis: shocks at 24 and 60-month maturities	195
5.8.2	Sensitivity analysis: shocks at 120 and 240-month maturities	196
5.8.3	Sensitivity analysis (time-series): shocks at 24 and 60-month maturities	197
5.8.4	Sensitivity analysis (time-series): shocks at 120 and 240-month maturities	198

Acknowledgements

I would like to take this opportunity to thank my first supervisor Prof. Nikos Nomikos for his support, guidance and patience throughout my time as a doctoral PhD candidate. Nikos has provided me with invaluable knowledge and constant encouragement that have been paramount to the completion of this thesis. I am grateful for all his generous support and assistance. My appreciation also goes to my second supervisor Dr. Amir H. Alizadeh. I thank Amir for providing me with valuable and critical comments during my doctoral studies. Furthermore, my gratitude goes to Prof. Costas Grammenos, for his sincere interest in my intellectual development and his useful advice during my years at Cass Business School. Prof. Grammenos has been a constant source of inspiration and optimism and has hugely influenced my personality and my way of thinking.

I am extraordinarily indebted to Dr. Ioannis Kosmidis, a lecturer in Statistical Science at University College London (UCL), for offering me the opportunity to visit the department of Statistical Science at UCL as a visiting PhD student during the third year of my doctoral studies and pursue collaborative research. I am grateful to Dr. Ioannis Kosmidis for his sincere support and guidance ever since my master's studies at Warwick Business School in 2007. He is also the inspiration behind several of the research ideas developed in the present thesis and responsible for convincing me to learn and use R programming for all numerical explorations in my research. I am also grateful to Dr. Gareth Peters, also a lecturer in Statistical Science at UCL, for his help, support and guidance during my visit at UCL. Both Ioannis and Gareth acted as advisors during my research visit at UCL and have provided detailed guidance and supervision on the research presented in Chapter 5 of the present PhD thesis.

This PhD thesis reflects numerous discussions and ideas I have shared with friends and colleagues over the past years. My warmest thanks for their constant help and support go to Dr. Christoforos Bouzanis, Rita Kurpisz, Ioannis Nanos, Orestis Vamvakas, Dr. Nikolaos Karouzakis, Vasilis Zantias, Christos Lelegiannis, Dr. Theodore Koutmeridis, Katerina Papoutsi, Konstantinos Papadatos, Dr. Mariachiara Barzotto, Dr. Mario Campana, Dr. Emmanouil Trachanas, Dr. Olivier Sibai, Dr. Dennis Tuerk, Dr. Chiara Banti, Marianna Russo, Professor Ian Marsh, Professor Giovanni Urga and Professor Lucio Sarno. I am also indebted to Maria Stylogianni for an extremely meticulous proofreading of the manuscript and for the many improvements she has suggested.

Chapter 3 has benefited from the constructive comments and suggestions of the participants in the 2012 Energy Finance conference at Trondheim, Norway, the participants in the 2013 Econometrics, Energy Finance conference at Cass Business School and the participants in the 51st meeting of the Euro Working Group on Commodities and Financial Modelling (EWGCFM) in 2013 at ESCP Europe Business School, London. Chapter 5 has also benefited from the constructive suggestions of the participants in the 4th national conference of the Financial Engineering and Banking Society (FEBS) in 2013 in Athens, Greece, in the 4th Emerging Markets Group (EMG) conference in 2014 at Cass Business School and in the 4th international conference of the Financial Engineering and Banking Society (FEBS) in 2014 at the University of Surrey, UK. Finally, Chapter 5 of the present PhD thesis has benefited from the comments and useful suggestions of the participants in the 2014 Nonlinear time series analysis conference at the London School of Economics.

Finally, the support of my family has been unparalleled. My parents, Nikos and Konstantina, have always believed in me and encouraged me in my decision to quit my job and pursue my childhood dream of studying at a doctoral level. I would like to deeply thank them for their infinite support, continuous encouragement and endless inspiration. Without their love and support, it would not have been possible for me to complete this PhD thesis.

Emmanouil N. Karimalis
Cass Business School
May 2015

Declaration

I grant powers of discretion to the University Librarian to allow this thesis to be copied in whole or in part without further reference to me. This permission covers only single copies made for study purposes, subject to normal conditions of acknowledgement.

Abstract

Modelling the dependence structure of financial variables is of paramount importance for a wide range of financial applications. Financial variables exhibit various forms of dependence and tail dependence whereas the magnitude of dependence is not constant over time but rather time-varying and can also be affected by exogenous factors. The present thesis investigates the effects of multivariate dependence on a broad range of financial applications. In particular, the first empirical part of the thesis investigates the implications of dependence and tail dependence for the accurate risk modelling of financial portfolios. The joint behaviour of the returns of the financial portfolios is modelled employing extreme value theory methods for the univariate distributions and pair-copula constructions for describing the joint dependence. The results indicate that risk estimates, derived within this framework, can be successfully forecasted at extreme quantiles. The second empirical part deals with the estimation of systemic risk in the European banking sector based on the *CoVaR* methodology. In this part, a new methodology, based on copula functions, is proposed and extended to different *CoVaR* definitions and systemic risk measures. The proposed approach also recognises the time-varying dependence of financial variables by allowing the dependence parameters to be functions of lagged information. The results highlight the importance of taking into account accurate specifications for the marginal distributions and the dependence structure when modelling systemic risk. The empirical results also show that systemic risk in the European banking sector can be explained by several macroeconomic and financial variables as well as factors directly related to institution-specific characteristics. Finally, the third empirical part focuses on the modelling of the interdependence structure of European sovereign yield curves as functions of market-wide and country-specific liquidity and credit quality measures. The empirical results highlight the significance of both liquidity and credit measures in explaining the dynamics and covariation of European yields and reveal important contagion and spillover effects among European economies. Overall, the empirical findings of this thesis outline the importance of taking into account the behaviour and the distribution characteristics of the financial variables that are modelled; failure to do so may lead to incorrect inference and erroneous implications.

Chapter 1

Introduction

1.1 Motivation and objectives

The aim of this PhD thesis is to develop multivariate modelling procedures that address the dependence modelling challenges found in financial data and improve methods for risk management, systemic risk measurement and interest rate modelling. In principle, modelling the dependence structure of financial variables is a non-trivial task due to the complex dynamics of individual variables on the one hand, and the varying dependence structure between the variables on the other hand. Evidence that the univariate distributions of many common financial variables are non-normal, exhibiting excess kurtosis (or fat tails) and skewness, has been widely reported in the literature, as far back as [Mills \(1927\)](#). Furthermore, the traditional multivariate time-series approach seems unable to capture the dependence properties and co-movements of financial data. The traditional multivariate time-series approach relies on the assumption of multivariate normality and employs the usual linear correlation as a measure of dependence between financial variables. Nevertheless, the linear correlation measures only linear dependence and does not explore any non-linear dependence. Another drawback of the traditional time-series approach is that correlation is assumed to be constant over time. Several studies in the finance literature have reported deviations from multivariate normality, in the form of asymmetric dependence. One typical example of asymmetric dependence is that returns tend to be more dependent during market downturns than during market upturns.¹ These properties have important implications for a broad range of financial applications.

The contribution of this PhD thesis aims at providing tools for going one step further: What are the stylised facts of dependence and tail dependence in financial data? Can we develop flexible multivariate models that allow us to go beyond normal dependence for applications to financial data? Can we develop high-dimensional models that take into account the stylised facts of dependence and tail dependence between financial variables, while being relatively flexible and computationally tractable at the same time? In addition, we investigate time-varying conditional dependence,

¹For evidence of asymmetry in financial time series, see [Longin and Solnik 1995, 2001](#); [Ang and Bekaert 2002a,b](#); [Das and Uppal 2004](#); [Patton 2004](#); [Garcia and Tsafack 2011](#), among others.

spillover and contagion effects, the interaction of exogenous variables with the dependence structure, as well as the behaviour of correlation under varying market conditions. We explore all the above issues employing different modelling strategies, while focusing on different markets which share distinct dependence modelling challenges.

1.2 Copula functions as a modelling tool

To develop multivariate models that deviate from the normality assumption and, at the same time, address the complex dynamics of financial asset return distributions, we work with copula distributions in Chapters 3 and 4 of this PhD thesis. The copula theory provides an efficient approach for modelling the high-dimensional dependency. The use of copulas, which dates back to [Sklar \(1959\)](#) but was made popular in finance through the pioneering work of [Embrechts et al. \(1999b\)](#), makes it possible to separate the dependence model from marginal distributions. [Patton \(2006\)](#) argues that the copula is a more informative measure of dependence than linear correlation, since the usual correlation coefficient is not sufficient to describe the dependence structure if both the joint distribution and the marginals of financial returns are non-elliptical.² Copulas also allow the modelling of tail dependence, which means that unlike in the case of the Gaussian distribution, the dependence does not vanish as we consider increasingly negative returns.³ Especially in times of financial market turmoil, neglecting the tail dependence between financial time series may have significant effects on multiple financial modelling applications.⁴

A large number of parametric bivariate copulas have been proposed to address various dependency forms. Among the class of non-elliptical copulas, Archimedean copulas have found wide usage in the finance literature recently, because of their simple closed-form cumulative distribution functions and their appropriateness for modelling the dependence between random variables. In this regard, the Archimedean copulas have been found to adequately model the lower tail dependence of financial portfolios (see for example, [Ané and Kharoubi \(2003\)](#) and [Fantazzini \(2009\)](#), among others) because they can capture a broad range of types of tail dependence and asymmetric tail dependence. Nevertheless, the simple parametric copula models

²[Embrechts et al. \(2003c\)](#) and [Rachev \(2003\)](#) illustrate the drawbacks of using linear correlation to analyse dependency.

³Elliptical copula models have been found to perform as poorly as their correlation-based counterparts in many financial applications due to their symmetric tail dependence (see for example, [Cherubini et al. 2004](#); [Fischer et al. 2009](#), among others).

⁴Several studies find that there is more extremal dependence in more volatile periods (see for example, [Longin and Solnik 2001](#); [Ang and Chen 2002](#); [Jondeau and Rockinger 2006](#); [Chollete et al. 2009](#), among others).

are not flexible enough to model the complex dependence structures of multivariate data. For example, only a small set of copulas can be extended to higher dimensions. Moreover, multivariate copulas assume the same form of dependence among marginal series. There have been several attempts to construct multivariate extensions of Archimedean copulas such as the exchangeable multivariate Archimedean copulas (EAC) and the nested Archimedean constructions (NACs) (see for example, [Bandein-Roche and Liang 1996](#); [Joe 1997](#); [Nelsen 2007](#); [Whelan 2004](#); [Embrechts et al. 2003c](#); [McNeil 2008](#); [Savu and Tiede 2009](#), among others). Nevertheless, these models are not flexible enough to model all mutual dependencies among the variables.

The most prominent high-dimensional copula models which are flexible enough to model complex multivariate data are the so-called vine copulas (also called pair-copula constructions, PCC). This structure was originally introduced by [Joe \(1996\)](#) and subsequently extended by [Bedford and Cooke \(2001, 2002\)](#), [Kurowicka and Cooke \(2006\)](#) and [Aas et al. \(2009\)](#). The model is hierarchical in nature and is based on a decomposition of a multivariate density into a cascade of simple bivariate copula densities, applied to original data and to their conditional and unconditional distribution functions. For high-dimensional distributions, there are a significant number of pair-copula constructions. To organise them, [Bedford and Cooke \(2001, 2002\)](#) introduced a graphical model known as *the regular vine* (R-vine). The class of regular vines is still very general; it includes a large number of pair-copula decompositions. Until now, the focus has been on two special cases of regular vines; the *canonical vine* (C-vine) and the *drawable vine* (D-vine). Vine copulas have been used recently in various financial applications such as risk management, asset pricing and portfolio decision problems.⁵

In Chapter 2, we define copulas and provide some of their basic properties. We also present the notion of tail dependence and introduce various dependence coefficients focusing on Kendall's τ correlation coefficient, which is the most popular of the "scale-invariant" measures of dependence. In addition, we introduce various copula families, which are common in the multivariate modelling of financial data, and present their dependence and tail dependence properties. The pair-copula constructions and vines are also presented in this Chapter. In particular, we present in detail the pair-copula construction principle (PCC) and focus on the canonical vine (C-vine) decomposition. Practical issues related to canonical vines such as inference, simulation and model selection are also discussed in this Chapter. In addition,

⁵For the various applications of vine copulas in finance see for example, [Chollete et al. 2009](#); [Heinen and Valdesogo 2008](#); [Min and Czado 2010](#); [Brechmann et al. 2012](#); [Czado et al. 2012](#); [Brechmann and Czado 2013](#), among others.

we present various graphical and analytical goodness-of-fit methodologies for copula selection.

1.3 Outline of the thesis

As explained, the aim of this PhD thesis is to develop modelling techniques that take into account the complex dependence dynamics of financial data and propose procedures that focus on different markets and financial applications. Therefore, each of Chapters 3, 4 and 5 in this PhD thesis can be seen as a standalone research paper that deals with a particular topic in financial modelling and attempts to shed light on distinct research questions employing alternative methodologies and data. More specifically, Chapter 3 deals with portfolio risk modelling and introduces an approach that combines extreme value theory (EVT) methods and the pair-copula construction (PCC) principle for portfolio risk management. In addition, Chapter 4 centres on systemic risk and presents a new methodology, based on copula functions, for systemic risk measurement, while Chapter 5 presents a modelling approach for jointly modelling the evolution of sovereign yield curves and their dependence structure as a function of market-wide and country-specific liquidity and credit quality measures. A more detailed overview of each particular Chapter is provided below.

In Chapter 3, we propose modelling the conditional distribution of financial portfolios using a strategy that combines extreme value theory (EVT) and pair-copula construction methods and forecasting portfolios' *Value-at-Risk* (*VaR*) and *Conditional Value-at-Risk* (*CVaR*, also known as *Expected Shortfall*) by focusing on extreme quantiles. In particular, we propose a combination of semi-parametric modelling for the marginal series, to address the complex dynamics of individual return series, and a vine copula approach, to address all mutual dependences among portfolio constituents. In this respect, the proposed methodology acknowledges the individual characteristics of the marginal series on the one hand and the varying dependence structure of the portfolio components on the other hand, while focusing on the modelling of joint extremes, which is, in practice, the main focus of all risk management applications.

The modelling strategy involves the inference functions for margins (IFM) method (see [Joe and Hu 1996](#); [Joe 1997](#), for more details) which is used for fitting the multivariate models. Within this framework, we model the temporal dependence and dynamic volatility of the marginal series using GARCH-type models and use extreme value theory (EVT) methods to estimate the tails of the innovations' conditional distribution. We employ both sequential estimation (SE) (see [Czado et al. 2012](#), for more details) and full maximum likelihood estimation (MLE) to fit the canonical vine models. The selection of each pair-copula in the canonical vine specification

is based on Akaike's information criterion (AIC). Motivated by the theoretical and empirical findings of [Joe et al. \(2010\)](#) and [Nikoloulopoulos et al. \(2012\)](#) respectively, we also propose an asymmetric canonical vine model specification by replacing the bivariate symmetric Student- t copula models selected by the AIC criterion in the first level of the vine specification with copula families that allow asymmetric tail dependence, in an attempt to address the asymmetries found in multivariate data and further improve the model's fit and forecasting performance.

We apply our methodology focusing on portfolios of energy products because the distribution of returns is characterised by high volatility and extreme price spikes, and thus portfolio risk modelling is a challenging task by its nature. The univariate distribution of the marginal series under study appears highly volatile, being leptokurtotic with fat tails and non-symmetric. Therefore, the assumption of normality cannot be supported for any of the series under study. In addition, the joint distribution of energy return series cannot be sufficiently described by a multivariate normal distribution due to the varying tail dependence between portfolio constituents and the presence of asymmetries in the tails of the joint distribution. We illustrate the superior performance of our proposed methodology in the extreme quantiles over naive benchmark risk models and elliptical vine copula models by performing an out-of-sample *Value-at-Risk* forecasting evaluation. We also compare the *Value-at-Risk* and *Conditional Value-at-Risk* estimates on the basis of several loss functions.

In Chapter 4, we propose a new methodology to estimate the *Conditional Value-at-Risk* (*CoVaR*), the *Value-at-Risk* (*VaR*) of the financial system conditional on an institution being under financial distress. The *Conditional Value-at-Risk* (*CoVaR*) attempts to capture the risk spillovers among financial institutions and has recently attracted great attention from the regulatory and academic community.⁶ The *CoVaR*, originally proposed by [Adrian and Brunnermeier \(2011\)](#), depends on the conditional distribution of the returns representing the entire financial system given that a financial institution is *exactly* at its *Value-at-Risk* (*VaR*) level. Recently, [Girardi and Ergün \(2013\)](#) modified the original *CoVaR* definition to take into account more severe distress events for financial institutions and to overcome some of the shortcomings of the original definition.

In this study, we derive simple, analytical expressions for both *CoVaR* definitions, based on copula distributions, for a broad range of copula families. Given the distinctive characteristics of copula distributions that enable the separation of de-

⁶Prominent research papers in the field also include [Acharya et al. 2012](#); [Brownlees and Engle 2012](#); [Billio et al. 2012](#); [Engle et al. 2014](#), among others. For an overview of the main quantitative systemic risk models which have been proposed over the past years see [Bisias et al. \(2012\)](#).

pendence from marginal distributions, our Copula *CoVaR* methodology provides greater flexibility in the computation of systemic risk, while focusing on the extreme co-movements of financial system returns and financial institution returns. We also propose a dynamic version of the Copula *CoVaR* model to take into account the time-varying dependence between the financial system returns and financial institution returns. Moreover, we extend this methodology and derive expressions that enable the estimation of alternative “co-risk” systemic risk measures such as the *Conditional Expected Shortfall (CoES)*. We also provide numerical examples to illustrate that systemic risk estimates derived from the Copula *CoVaR* framework exhibit the main dependence consistency properties reported in [Mainik and Schaanning \(2014\)](#), and to show that our methodology can easily facilitate stress testing exercises.

We apply the Copula *CoVaR* methodology to measure systemic risk in the European banking system focusing on a portfolio of large European banks. We compute systemic risk estimates employing alternative marginal assumptions to assess the impact of asymmetries in the marginal series on systemic risk measurement. In addition, we compute both *CoVaR* and *CoES* measures to assess the impact of alternative systemic risk models on systemic risk. We also employ a panel regression methodology to investigate the main drivers of systemic risk in the European banking system. In particular, we assess the significance of important financial variables in triggering systemic risk episodes conditional on periods of reduced and heightened market uncertainty and analyse their implications for systemic risk modelling. Finally, we examine the significance of institution-specific characteristics such as institutions’ *VaR*, market-to-book, size, leverage, beta and equity volatility estimates in systemic risk across different forecasting horizons.

In Chapter 5, we jointly model the dynamic evolution and the cross-country dependence structure of European sovereign yield curves as a function of market-wide and country-specific liquidity and credit quality measures. In principle, we deal with three distinct forms of dependence and relate them to market-wide and country-specific liquidity and credit quality measures: the inter-temporal, the term-structure and the cross-country dependence of sovereign yields. There is ample evidence in the finance literature that liquidity and credit concerns are important components of yield spreads (see for example, [Duffie et al., 2003](#); [Longstaff et al., 2005](#); [Ericsson and Renault, 2006](#); [Beber et al., 2009](#), among others). Nevertheless, so far, most studies have explored the effects of liquidity and credit risks on yield levels or yield spreads by concentrating on certain maturities or markets in isolation and neglecting their intrinsic interdependence.

In this study, we seek to understand the dynamic interdependence of European sovereign yield curves and relate them to broader European and country-specific measures of liquidity and credit quality. In other words, we seek to understand how investors in the sovereign fixed income markets react in response to market-wide and country-specific liquidity and credit shocks and to investigate whether their behaviour varies over time, across different investment horizons and across assets of different credit quality. In addition, we investigate the relative importance of liquidity and credit concerns over periods of reduced and heightened economic uncertainty. We also assess the impact of liquidity and credit risks on the European sovereign yields and cross-country spreads and investigate whether market-wide and country-specific shocks can generate significant spillover effects between the European economies.

To model jointly the multiple forms of dependence found in European sovereign yields and relate them to market-wide and country-specific liquidity and credit quality measures, we follow a two-step modelling strategy. In the first step, we model the dynamics of each individual sovereign yield curve under study using the macro-finance Nelson-Siegel model of [Diebold et al. \(2006\)](#), while in the second step, we model the cross-country dependence structure of sovereign yield curves using the covariance regression model of [Hoff and Niu \(2012\)](#). The macro-finance Nelson-Siegel model of [Diebold et al. \(2006\)](#) is a dynamic latent factor model, where the shape and form of the yield curve are governed by three latent factors. We model the dynamics of the latent factors (i.e. level, slope and curvature) as autoregressive processes augmented with observable macroeconomic and financial variables and European proxies for liquidity and credit quality. The heteroskedasticity of the European sovereign yield prediction errors is subsequently modelled as a function of country-specific liquidity and credit quality proxies using the covariance regression model of [Hoff and Niu \(2012\)](#). In this regard, we relate the dynamic evolution of the covariance matrix of the prediction errors to country-specific liquidity and credit quality components.

Finally, we provide a modelling framework that enables quantifying the impact of country-specific liquidity and credit quality shocks directly on the yield curve for each individual country. Given the full state-space model representation, the effects of the shocks to any of the country-specific liquidity and credit quality variables are transmitted via the estimated covariance regression model to the yield curve for each individual country allowing the study of linkages and spillover effects among European economies.

1.4 Summary of findings and contribution to the literature

This PhD thesis contributes to multiple segments of the economics and finance literature and provides a number of significant findings useful for improving portfolio risk management, systemic risk measurement and interest rate modelling. In particular, Chapter 3 contributes to the broad risk management literature (see for example, [Hull and White 1998](#); [Cherubini and Luciano 2001](#); [Embrechts et al. 2002, 2003a](#); [Poon et al. 2004](#), among others) and the segment of the literature that proposes the use of copulas and pair-copula construction methods as a risk management tool for modelling portfolio risk (see for example, [Kole et al. 2007](#); [Brechmann et al. 2012](#); [Czado et al. 2012](#); [Weiß and Scheffer 2012](#); [Nikoloulopoulos et al. 2012](#); [Brechmann and Czado 2013](#); [Weiß and Scheffer 2015](#), among others). We strongly believe that our proposed methodology, which combines extreme value theory (EVT) and pair-copula construction (PCC) methods, contributes to and provides an alternative perspective on the study of multivariate extremes.

The main empirical results in Chapter 3 suggest that elliptical vine copula models are adequate to model portfolio risk at higher quantiles but perform inadequately at extreme quantiles. It is shown that a combination of extreme value theory methods and the pair-copula construction principle can improve the *Value-at-Risk* forecasting performance of the model at extreme quantiles. In addition, it is shown that for inference involving the tails of the joint distribution, pair-copula selection should not be entirely based on likelihood ratio criteria but should also rely on non-parametric dependence measures. These results provide new insight into risk management applications within the vine copula modelling framework and also support the findings of [Joe et al. \(2010\)](#) and [Nikoloulopoulos et al. \(2012\)](#). In particular, [Joe et al. \(2010\)](#) show that vine copulas can have a different upper and lower tail dependence for each bivariate margin when asymmetric bivariate copulas with upper/lower tail dependence are used in the first level of the vine. In addition, [Nikoloulopoulos et al. \(2012\)](#) show that vine copulas with bivariate Student-*t* linking copulas tend to be preferred by likelihood-based selection methods because they provide a better fit in the middle for the first level of the vine.

Motivated by the theoretical and empirical findings of [Joe et al. \(2010\)](#) and [Nikoloulopoulos et al. \(2012\)](#), we also propose an asymmetric vine model where the Student-*t* copula families (selected by the AIC information criterion) in the first level of the vine are replaced by copula families that allow for asymmetric tail dependence. Moreover, the Independence copula is employed for those pair-copulas that could not reject the null hypothesis of independence. The asymmetric canonical vine copula model shows superior performance over alternative modelling specifications accord-

ing to the *Value-at-Risk* forecast evaluations and loss function results, implying that portfolio losses can be satisfactorily forecasted and, at the same time, that the regulatory risk capital can be reduced even further, especially at extreme quantiles.

Furthermore, Chapter 4 contributes directly to the segment of the literature that employs the *Conditional Value-at-Risk* (*CoVaR*) methodology to address the existence of systemic interrelations between financial institutions (see for example, [Adrian and Brunnermeier 2011](#); [Girardi and Ergün 2013](#); [Wong and Fong 2011](#); [Gauthier et al. 2012](#); [López-Espinosa et al. 2012, 2013](#), among others). It also contributes to the broader literature that proposes measures of systemic risk alternative to *CoVaR* and investigates the determinants that trigger systemic episodes (see for example, [Segoviano and Goodhart \(2009\)](#); [Huang et al. \(2009\)](#); [Zhou \(2010\)](#); [Acharya et al. \(2012\)](#); [Nicolò and Lucchetta \(2011\)](#); [Brownlees and Engle \(2012\)](#); [Engle et al. \(2014\)](#); [Billio et al. \(2012\)](#); [Bisias et al. \(2012\)](#), among others). In this respect, the contribution of Chapter 4 to the existing literature is two-fold. On the one hand, we propose a new methodology for estimating *CoVaR*, while extending it to a dynamic setting and to measures of systemic risk alternative to *CoVaR* such as the *Conditional Expected Shortfall* (*CoES*). On the other hand, we investigate the impact of distributional assumptions on the modelling of systemic risk and assess the impact of important financial variables as well as of institution-specific characteristics on the evolution of systemic risk in the European banking sector.

The main empirical results in Chapter 4 suggest that systemic risk estimates can be substantially affected by alternative distribution assumptions in the marginals and the dependence structure but are robust across alternative systemic risk models. Therefore, the ordering of systemically important financial institutions is sensitive to alternative marginal specifications and dependence models. The statistical test results support the use of asymmetric over symmetric marginal distribution assumptions for systemic risk modelling. The use of inappropriate marginal assumptions may also cause biases in the selection of dependence models and thus provide erroneous systemic risk estimates. It is shown that the majority of the selected copula models do not imply any tail dependence when Gaussian marginals are employed. In contrast, the use of the asymmetric Skewed-*t* assumption in the marginal series, favours the preference of dependence models for copulas that allow asymmetric tail dependence. The results of non-parametric tail dependence estimators on return series provide clear evidence of asymmetric tail dependence for the majority of the pairs under study, indicating that systemic risk estimates can be significantly affected by the presence of asymmetries both in the marginals and in the dependence structure, if not addressed properly.

The empirical results show that financial institutions such as BBVA, UBS, Deutsche Bank, Credit Suisse and BNP Paribas are placed among the most systemic European banks under both marginal specifications. The cross-country analysis results also suggest that the French and Spanish banks are the most systemic of all European financial institutions under study. In contrast, financial institutions from Eurozone countries that have been significantly hit by the sovereign debt crisis such as Portugal, Ireland or Greece, appear to be among the least systemic European banks. We attribute these findings to the fact that the financial institutions from these particular countries are typical commercial banks with strong presence in the local market but limited international activity and cross-country exposure. Therefore, the degree of dependence and more importantly the degree of tail dependence implied between the financial system and institution returns is relatively weak generating, on average, lower systemic risk estimates.

Furthermore, the regression results in Chapter 4 highlight the importance of the implied market volatility, liquidity spread, credit risk and short-term funding variables in explaining systemic risk. The large impact of the liquidity spread on systemic risk demonstrates the significant role of liquidity risk in the evolution of the European financial crisis. The conditional regression analysis results also reveal an asymmetric response of financial variables between periods of reduced and heightened economic uncertainty. The asymmetric behaviour of financial variables is partly attributed to the coordinated intervention of central banks to avert the liquidity crunch in the interbank markets and restore financial stability. The majority of these variables are also important in explaining the time-varying correlation and the financial system's volatility estimates, while displaying the same asymmetric response between calm and crisis periods. The regression analysis results also suggest that the effects of the liquidity risk on systemic risk, at the outset of the financial crisis, were transmitted through the financial system's volatility channel and not through the correlation's channel. Finally, leverage and size appear to be the most robust institution-specific determinants of systemic risk implying that larger and highly leveraged banks contribute more to systemic risk.

Finally, Chapter 5 contributes to the segments of the econometrics and finance literature that deal with the modelling of the term structure of interest rates. Specifically, Chapter 5 relates to the research stream that employs the Nelson-Siegel modelling approach of [Diebold and Li \(2006\)](#) and [Diebold et al. \(2006\)](#) to model the dynamic feature of yield curves (see for example, [Yu and Zivot 2011](#); [Yu and Salyards 2009](#); [Bianchi et al. 2009](#); [Koopman et al. 2010](#); [Diebold et al. 2008](#); [Christensen et al. 2011](#), among others) and to the literature that associates macroeconomic variables with the yield curve (see for example, [Kozicki and Tinsley 2001](#); [Ang and Piazzesi 2003](#); [Hördahl et al. 2006](#); [Ang et al. 2006](#); [Dewachter and Lyrio 2006](#); [Balfoussia](#)

and Wickens 2007; Rudebusch and Wu 2008, among others). In addition, Chapter 5 provides new insight into the literature that investigates the determinants of sovereign yields and, more specifically, the extent to which credit and liquidity risks determine the yields in the bond markets (see for example, Longstaff 2004; Duffie et al. 2003; Longstaff et al. 2005; Goldreich et al. 2005; Chordia et al. 2005; Liu et al. 2006; Ericsson and Renault 2006; Chen et al. 2007; Covitz and Downing 2007; Beber et al. 2009; Goyenko et al. 2011; Monfort and Renne 2014, among others). Therefore, Chapter 5 contributes to the existing literature by introducing a methodology that jointly models the dynamic interaction between sovereign yield curves and relates it to broader and country-specific measures of liquidity and credit quality. The proposed methodology is also capable of quantifying the effects of liquidity and credit shocks on the yield curve for each individual country providing a useful tool for studying significant spillover and contagion effects.

The main empirical results, in the first stage of the analysis in Chapter 5, suggest that markets separate Eurozone countries into two distinct groups according to their overall credit risk profiles: peripheral (Spain and Italy) and core (Germany and France) Eurozone countries. The results also suggest that markets distinguish between Eurozone countries and non-Eurozone countries such as the United Kingdom (UK). In addition, the results highlight Germany's significant role in explaining the variation of the estimated latent factors in the Nelson-Siegel specification. The market-wide liquidity and credit quality proxies also appear highly significant in the latent factor specification for Germany, while the significance of these variables is less pronounced for the remaining countries under study. Furthermore, the sensitivity analysis results show that the German yields have a negative relation to both market-wide liquidity and credit quality measures possibly implying that investors view German bonds as a safe haven in periods of increased illiquidity and credit uncertainty in the European fixed income markets.

The covariance regression results, in the second stage of the analysis in Chapter 5, also underscore also the significance of liquidity and credit quality measures in explaining the heteroscedasticity of European sovereign yields both unconditionally and conditional on periods of heightened market volatility. In particular, the unconditional analysis results show that the German bid-ask spreads are the most significant country-specific liquidity explanatory variables, whereas the Italian and Spanish CDS spreads appear to be the most significant country-specific credit quality explanatory variables. The time-series average correlation estimates implied by the estimated covariance regression models are positive for most of the country-pairs under study highlighting the positive dependence among the European sovereign yields.

The conditional analysis results, on the other hand, show that country-specific liquidity and credit quality variables are equally significant in the calm period. Nevertheless, the significance of credit quality measures is considerably more pronounced than that of liquidity proxies in the stress period possibly indicating that investors are more concerned with the credit quality than the liquidity of sovereign debt instruments in times when equity markets are perceived to be more volatile. Additionally, the liquidity and credit quality measures of the peripheral Eurozone countries appear highly significant in the stress period highlighting investors' concerns about their future debt sustainability. The time-series average correlation estimates implied by the estimated covariance models also reveal a change in the dependence structure of European sovereign yields between calm and crisis periods.

In addition, the sensitivity analysis results show that shocks to country-specific liquidity and credit quality variables have a great impact on cross-country spreads. Nevertheless, the impact of the shocks differs across shock types and investment horizons. In general, shocks in the Spanish liquidity and credit variables tend to have, on average, the greatest impact on cross-country spreads. It can also be noted that the effects of the shocks in the short-term liquidity and credit quality measures not only have a significant impact on the corresponding short-term yields, but are also transmitted along the yield curve for each individual country. In contrast, the impact of the shocks in the medium and long-term measures is limited only to the yields of the corresponding maturities. Finally, it is shown that the European sovereign yields appear more sensitive to shocks in liquidity and credit quality variables over periods of increased equity market volatility.

1.5 Conclusions

To sum up, this PhD thesis deals with the modelling of the multiple forms of dependence structure found in financial variables and develops alternative methodologies to tackle important issues in risk management, systemic risk and interest rate modelling. The methodologies followed to address the dependence modelling challenges of financial time-series in Chapter 3 and Chapter 4 are primarily based on copula theory. For this reason, the basic properties of copula theory and some important extensions of it for the purposes of high-dimensional modelling are presented in Chapter 2. In addition, Chapter 3 introduces a methodology that combines extreme value theory and vine copula methods for portfolio risk modelling, whereas Chapter 4 relates to systemic risk modelling and uses copula distribution functions. Finally, Chapter 5 relates to the joint modelling of sovereign yield curves as a function of liquidity and credit quality variables. The results derived from these Chapters reconfirm that the modelling of the multivariate dependence of financial variables is a non-trivial task. It is, therefore, critical to take into account the stylised features of

financial data when modelling their corresponding multivariate distributions because incorrect assumptions or the omission of certain dependence properties may lead to incorrect inference and erroneous results for a broad range of financial applications.

Chapter 2

Background material: Copula theory

2.1 Introduction

In this Chapter we introduce some of the main concepts of copulas and outline some recent developments in the copula theory. Therefore, the present Chapter provides the necessary background material for the study of multivariate dependence in the context of copula modelling and facilitates the understanding of the research ideas presented in Chapters 3 and 4 of the present thesis. In particular, Section 2.2 introduces copulas and presents the theorem of [Sklar \(1959\)](#), which provides the theoretical foundation for the application of copulas. Section 2.3 presents a number of bivariate copula families as well as their association with the common dependence measures Kendall's τ and tail dependence. In addition, Section 2.4 introduces the pair-copula construction (PPC) principle whereas Section 2.5 focuses on the canonical vine (C-vine) model, which suggests a unique way of decomposing the joint distribution into a cascade of bivariate copulas using a star tree methodology. Section 2.6 deals with the estimation of the C-vine model focusing particularly on the maximum likelihood estimation methodology and the sequential estimation methodology. Moreover, Section 2.7 describes an overall selection procedure for the C-vine model whereas Section 2.8 introduces rules that uniquely decompose the C-vine model. Finally, Section 2.9 focuses on the selection of an appropriate C-vine model; Section 2.10 focuses on the selection of appropriate copula models and presents both analytical and graphical tools that facilitate the selection procedure; and Section 2.11 concludes.

2.2 Copulas

A copula is a multivariate distribution function $C(u_1 \dots u_d)$ defined on the unit cube $[0, 1]^d$ with uniformly distributed marginals. It provides a way of isolating the dependence structure between d random variables while allowing for arbitrary marginal distributions. The copula concept was initially developed by [Sklar \(1959\)](#). The famous theorem of [Sklar \(1959\)](#) gives the mapping between the individual distribution functions to the joint distribution. In general, a copula function can be extended for an arbitrary dimension d , but since our mission is to develop multivariate copulas

using only bivariate copulas as building blocks, we will only focus on the bivariate case $d = 2$. The mathematical definitions of this Section are taken from the book of Nelsen (2007) and the papers of Genest (2007), Brechmann (2010), Czado (2010) and Belgorodski (2010).

Definition 2.2.1 (two-dimensional copula) *A two-dimensional copula is a function $C : [0, 1]^2 \rightarrow [0, 1]$ with the following properties:*

- (i) $C(0, u) = C(u, 0) = 0$ for all $u \in [0, 1]$.
- (ii) $C(u, 1) = u$ and $C(1, u) = u$ for all $u \in [0, 1]$.
- (iii) $C(v_1, v_2) - C(v_1, u_1) - C(u_1, v_2) + C(u_1, u_2) \geq 0$ for all $(u_1, u_2), (v_1, v_2) \in [0, 1] \times [0, 1]$ with $u_1 \leq v_1$ and $u_2 \leq v_2$.

Theorem 2.2.1 (Sklar (1959)) *Let $F : \bar{\mathbb{R}}^2 \rightarrow [0, 1]$ with $\bar{\mathbb{R}} = \mathbb{R} \cup \{-\infty, +\infty\}$ be a bivariate distribution with one-dimensional marginals $F_1, F_2 : \bar{\mathbb{R}} \rightarrow [0, 1]$. Then there exists a two-dimensional copula C , such that for all $(x_1, x_2) \in \bar{\mathbb{R}}^2$*

$$F(x_1, x_2) = C(F_1(x_1), F_2(x_2)) \tag{2.1}$$

holds, and vice versa

$$C(u_1, u_2) = F(F_1^{-1}(u_1), F_2^{-1}(u_2)), \tag{2.2}$$

where u_1 and $u_2 \in [0, 1]$ and $F_1^{-1}(u_1)$ and $F_2^{-1}(u_2)$ are the inverse distribution functions of the marginals.

Definition 2.2.2 (Copula density) *Let C be a twice partially differentiable copula. Then the function $c : [0, 1] \times [0, 1] \rightarrow [0, 1]$ with*

$$c(u, v) = \frac{\partial^2 C(u, v)}{\partial u \partial v} \tag{2.3}$$

is called the density of the copula.

Let $f_X(x)$ and $f_Y(y)$ be marginal densities with joint density of $f_{XY}(x, y)$. It can be shown that the joint density can be decomposed as a product of marginal densities

and copula density as follows

$$\begin{aligned}
 f_{XY}(X, Y) &= \frac{\partial^2 F_{XY}(X, Y)}{\partial x \partial y} = \frac{\partial^2 C(F_X(x), F_Y(y))}{\partial x \partial y} \\
 &= \frac{\partial^2 C(F_X(x), F_Y(y))}{\partial F_X(x) \partial F_Y(y)} \cdot \frac{\partial F_X(x)}{\partial x} \cdot \frac{\partial F_Y(y)}{\partial y} \\
 &= \frac{\partial^2 C(u, v)}{\partial u \partial v} f_X(x) f_Y(y) \\
 &= c(u, v) f_X(x) f_Y(y).
 \end{aligned} \tag{2.4}$$

Moreover, it can be shown that the copula density can be expressed in terms of marginals and joint density as

$$c(u, v) = \frac{f_{XY}(F_X^{-1}(u), F_Y^{-1}(v))}{f_X(F_X^{-1}(u)) f_Y(F_Y^{-1}(v))} \tag{2.5}$$

[Embrechts et al. \(2003b\)](#) showed a very important property of copula, namely that it is invariant under any increasing continuous transformation of the margins.

2.3 Copula and dependence measures

Copulas provide a natural way to study and measure the dependence among random variables. There are a variety of ways to measure dependence. Many of these measures are “scale-invariant”, that is, they remain unchanged under strictly increasing transformations. The most popular scale-invariant measures of dependence are the population versions of Spearman’s ρ , Kendall’s τ and Blomqvist’s β . These measures are useful to determine the dependence structure of random variables, on the one hand, and estimate copula parameters from the empirical data, on the other. The most important of these measures for our study is Kendall’s τ . It is not based on any particular distribution assumptions, it is easy to calculate and it helps estimate non-linear dependencies.

Definition 2.3.1 (Kendall’s τ) *Let (X_1, Y_1) and (X_2, Y_2) be independent and identically distributed random vectors with joint distribution F_{XY} and marginal distributions F_X and F_Y . Then the population version of Kendall’s τ is defined as the*

probability of concordance minus the probability of discordance

$$\begin{aligned}
 \tau = \tau_{X,Y} &= P[(X_1 - X_2)(Y_1 - Y_2) > 0] - P[(X_1 - X_2)(Y_1 - Y_2) < 0] \\
 &= E[\text{sgn}(X_1 - X_2)\text{sgn}(Y_1 - Y_2)] \\
 &= P(X_1 < X_2, Y_1 > Y_2) - P(X_1 > X_2, Y_1 < Y_2),
 \end{aligned} \tag{2.6}$$

where sgn is the sign function.

Proposition 2.3.1 *Let F_{XY} be a joint distribution function of a bivariate continuous random variable (X, Y) with marginal distributions F_X and F_Y respectively. Further, let C be a copula distribution function that is $C(F_X(x), F_Y(y)) = F_{XY}(x, y)$. The Kendall's τ dependence measure, can be linked to the copula C as*

$$\tau(X, Y) = 4 \int_0^1 \int_0^1 C(u, v) dC(u, v) - 1. \tag{2.7}$$

Tail dependence is another very useful copula-based measure of extreme co-movements. It is a very important property for applications concerned with the study of the dependence of extreme values. Many empirical studies in finance (e.g. Longin and Solnik (1995, 2001), Ang and Chen (2002), Hong et al. (2007) among others) have indicated the presence of asymmetries in financial data, meaning that lower tail dependence can be stronger than upper tail dependence or vice versa. Therefore, standard symmetric multivariate distributions are inappropriate for addressing this feature.

Moreover, tail dependence is one of the properties that help distinguish between the different copula families. There are copula families that do not allow for tail dependence, such as the Gaussian or the Frank copula, and copula families that only allow for either lower (such as the Archimedean Clayton copula) or upper tail dependence (such as the Archimedean Gumbel copula). There are also “reflection symmetric” copulas, such as the Student- t copula, which imply same upper and lower tail dependence for any bivariate margin, and “reflection asymmetric” copulas, which allow for flexible upper and lower tail dependence, such as the two-parametric bivariate copula families of Joe (1997), known as BB1 and BB7 copulas.

Definition 2.3.2 (Upper tail dependence) *Let X and Y be continuous random variables with marginal distribution functions F_X and F_Y , respectively. The coefficient of **upper tail dependence** λ_U is*

$$\lambda_U = \lim_{u \nearrow 1} P(Y > F_Y^{-1}(u) | X > F_X^{-1}(u)) \tag{2.8}$$

provided that the limit $\lambda_U \in [0, 1]$ exists. If $\lambda_U \in [0, 1]$, we say that X and Y are asymptotically dependent in the upper tail ; if $\lambda_U = 0$, we say that X and Y are asymptotically independent in the upper tail.

Definition 2.3.3 (Lower tail dependence) Let X and Y be continuous random variables with marginal distribution functions F_X and F_Y , respectively. The coefficient of **lower tail dependence** λ_L is

$$\lambda_L = \lim_{u \searrow 0} P(Y \leq F_Y^{-1}(u) | X \leq F_X^{-1}(u)) \quad (2.9)$$

provided that the limit $\lambda_L \in [0, 1]$ exists. If $\lambda_L \in [0, 1]$, we say that X and Y are asymptotically dependent in the lower tail ; if $\lambda_L = 0$, we say that X and Y are asymptotically independent in the lower tail.

Definition 2.3.4 (Upper tail dependence for copulas) If a bivariate copula C is such that

$$\lambda_U = \lim_{u \nearrow 1} \frac{1 - 2u + C(u, u)}{1 - u} \quad (2.10)$$

exists, then C has upper tail dependence if $\lambda_U \in (0, 1]$, and upper tail independence if $\lambda_U = 0$.

Definition 2.3.5 (Lower tail dependence for copulas) If a bivariate copula C is such that

$$\lambda_L = \lim_{u \searrow 0} \frac{C(u, u)}{u} \quad (2.11)$$

exists, then C has lower tail dependence if $\lambda_L \in (0, 1]$, and lower tail independence if $\lambda_L = 0$.

Table 2.3.1 and 2.3.2 summarise the most common copula families, their corresponding Kendall's τ and the degree of tail dependence for each of them. Figures 2.3.1 and 2.3.2 show the probability (pdf) and cumulative (cdf) density functions of a bivariate Normal, Student- t , Clayton, Gumbel, BB1 and BB7 copula with approximately same level of dependence ($\rho = 0.70$) while Figures 2.3.3 and 2.3.4 present the scatter plot and the empirical and theoretical contour plots for the same level of dependence and bivariate copula families.

Table 2.3.1: Theoretical properties of bivariate elliptical copula families

Elliptical distribution	Parameter range	Kendall's τ	Tail dependence
Gaussian	$\rho \in (-1, 1)$	$\frac{2}{\pi} \arcsin(\rho)$	0
Student- t	$\rho \in (-1, 1), \nu > 2$	$\frac{2}{\pi} \arcsin(\rho)$	$2 t_{\nu+1} \left(-\sqrt{\nu+1} \sqrt{\frac{1-\rho}{1+\rho}} \right)$

This table reports parameter range, theoretical Kendall's τ values and tail dependence coefficients of elliptical copula families. **Source:** Brechmann and Schepsmeier (2013).

Table 2.3.2: Theoretical properties of bivariate Archimedean copula families

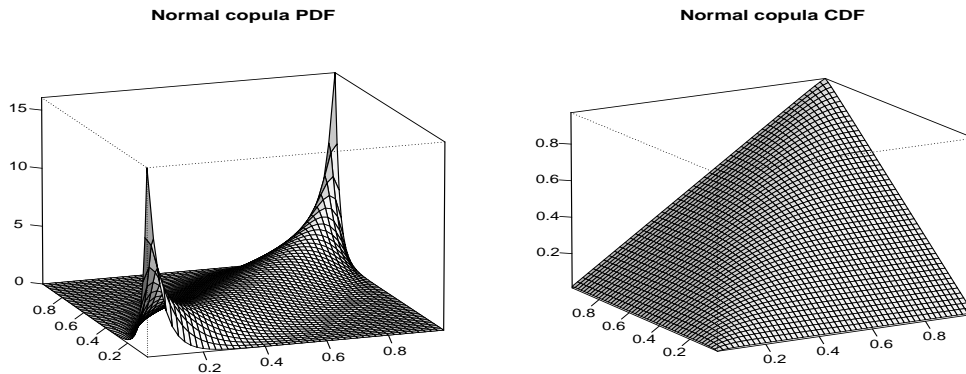
Name	Parameter range	Kendall's τ	Tail dependence (lower, upper)
Clayton	$\theta > 0$	$\frac{\theta}{\theta+2}$	$(2^{-1/\theta}, 0)$
Gumbel	$\theta \geq 1$	$1 - \frac{1}{\theta}$	$(0, 2 - 2^{1/\theta})$
Frank ^a	$\theta \in \mathbb{R} \setminus \{0\}$	$1 - \frac{4}{\theta} + 4 \frac{D_1(\theta)}{\theta}$	$(0, 0)$
Joe	$\theta > 1$	$1 + \frac{4}{\theta^2} \int_0^1 t \log(t) (1-t)^{\frac{2(1-\theta)}{\theta}} dt$	$(0, 2 - 2^{1/\theta})$
BB1	$\theta > 0, \delta \geq 0$	$1 - \frac{2}{\delta(\theta+2)}$	$(2^{-1/(\theta\delta)}, 2 - 2^{1/\delta})$
BB6	$\theta \geq 1, \delta \geq 1$	$1 + 4 \int_0^1 \left(-\log \left(- (1-t)^\theta + 1 \right) \times \frac{(1-t - (1-t)^{-\theta} + t(1-t)^{-\theta})}{\delta\theta} \right) dt$	$(0, 2 - 2^{1/\theta\delta})$
BB7 ^b	$\theta \geq 1, \delta > 0$	$1 - \frac{2}{\delta(2-\theta)} + \frac{4}{\theta^2\delta} B\left(\frac{2-\theta}{\theta}, \delta+2\right)$	$(2^{-1/\delta}, 2 - 2^{1/\theta})$
BB8	$\theta \geq 1, 0 < \delta \leq 1$	$1 + 4 \int_0^1 \left(-\log \left(\frac{(1-t\delta)^\theta - 1}{(1-\delta)^\theta - 1} \right) \times \frac{1-t\delta - (1-t\delta)^{-\theta} + t\delta(1-t\delta)^{-\theta}}{\theta\delta} \right) dt$	$(0, 0^c)$

This table reports parameter range, theoretical Kendall's τ values and tail dependence coefficients of bivariate Archimedean copula families. **Source:** Brechmann and Schepsmeier (2013).

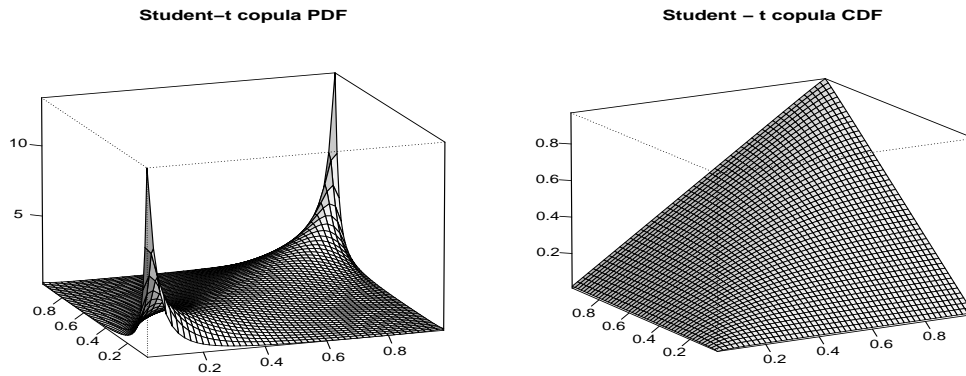
^a $D_1(\theta) = \int_0^\theta \frac{c/\theta}{\exp(x)-1} dx$ (Debye function)

^b $B(x, y) = \int_0^1 t^{x-1} (1-t)^{y-1} dt$ (Beta function)

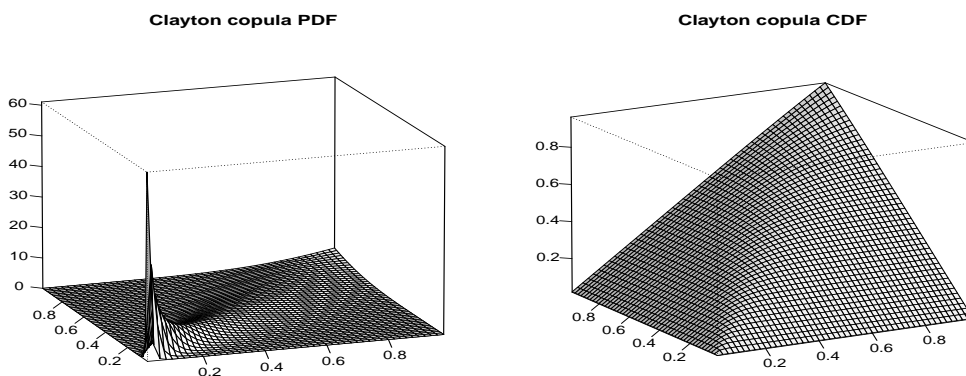
^c Except for $\delta = 1$, then the upper tail dependence coefficient is $2 - 2^{1/\theta}$



(a) CDF and PDF of a bivariate Normal copula with dependence parameter $\tau = 0.7$, $\rho = 0.8910065$ and $\lambda_L = \lambda_U = 0$.

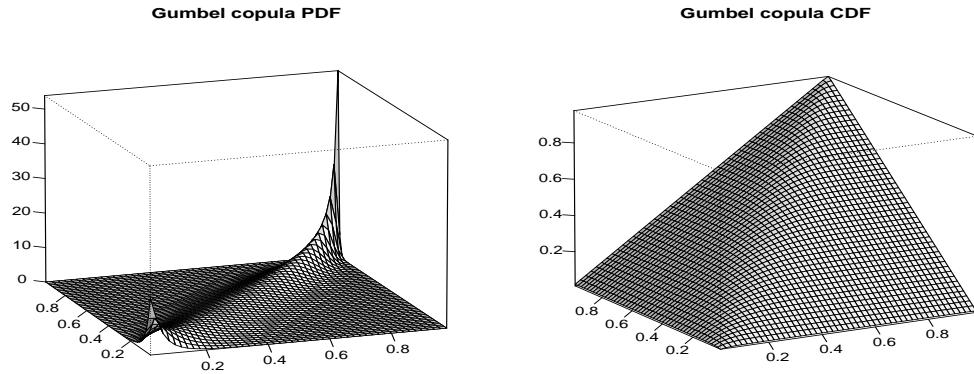


(b) CDF and PDF of a bivariate Student- t copula with dependence parameter $\tau = 0.7$, 3 degrees of freedom and $\lambda_L = \lambda_U = 0.4480999$.

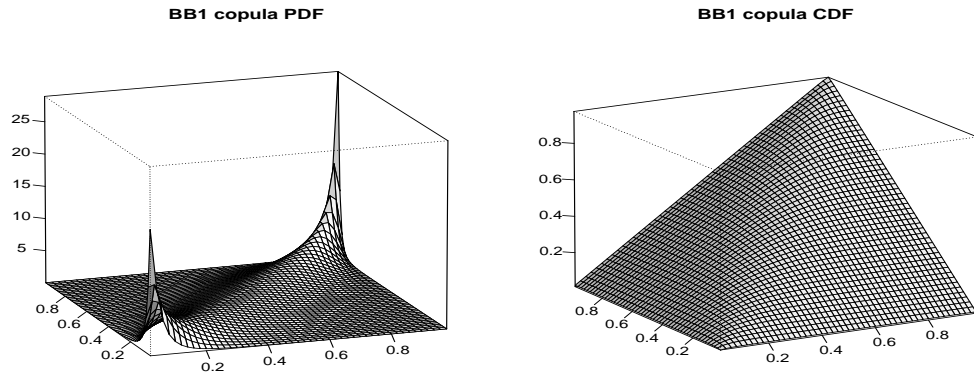


(c) CDF and PDF of a bivariate Clayton copula with dependence parameter $\tau = 0.7$, $\hat{\theta} = 4.666667$, $\lambda_L = 0.8619728$ and $\lambda_U = 0$.

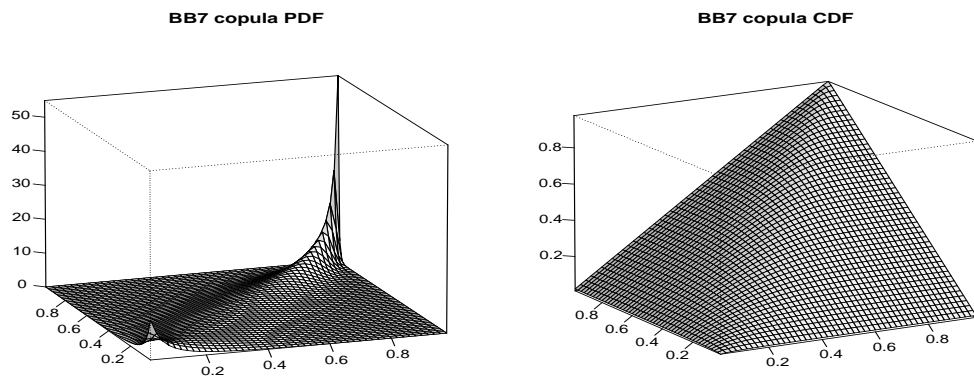
Figure 2.3.1: CDF and PDF of bivariate Normal, Student- t and Clayton copulas with approximately same level of dependence ($\rho = 0.70$).



(a) CDF and PDF of a bivariate Gumbel copula with dependence parameter $\tau = 0.7$, $\hat{\theta} = 3.333333$, $\lambda_L = 0$ and $\lambda_U = 0.7688556$.

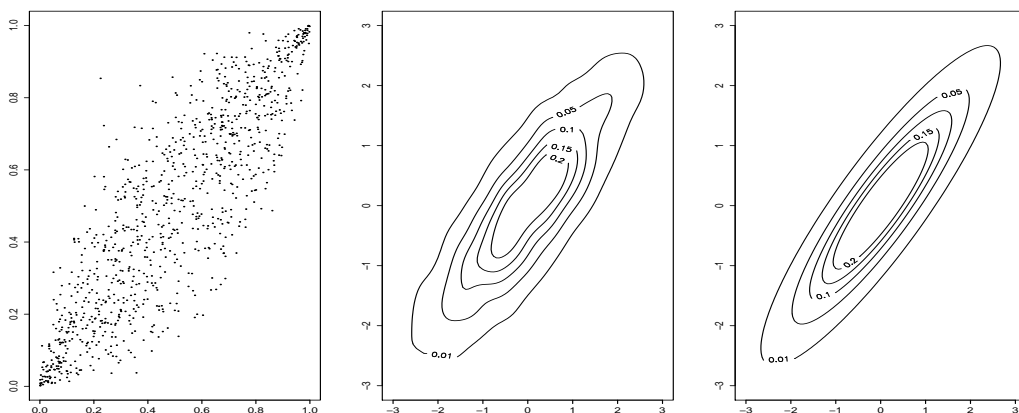


(b) CDF and PDF of a bivariate BB1 copula with dependence parameter $\hat{\tau} = 0.7007108$, $\theta = 0.43$, $\delta = 2.75$, $\lambda_L = 0.5564539$ and $\lambda_U = 0.7133351$.

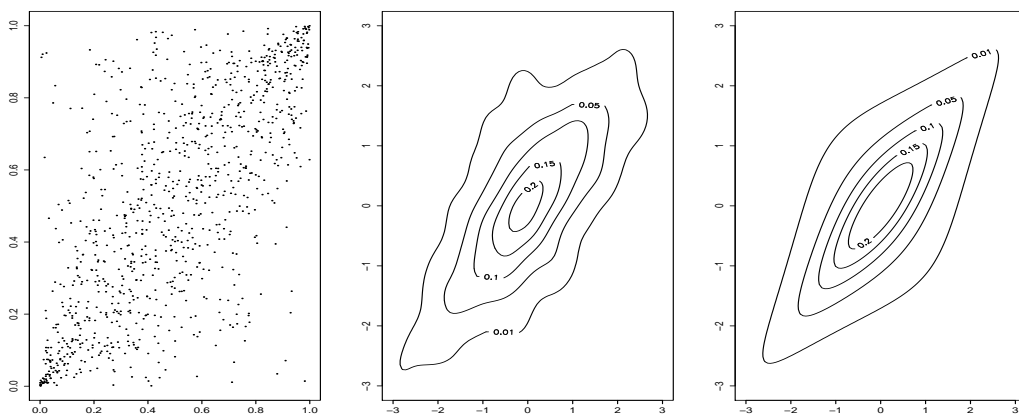


(c) CDF and PDF of a bivariate BB7 copula with dependence parameter $\hat{\tau} = 0.7001527$, $\theta = 4.8$, $\delta = 0.82$, $\lambda_L = 0.4294279$ and $\lambda_U = 0.8446473$.

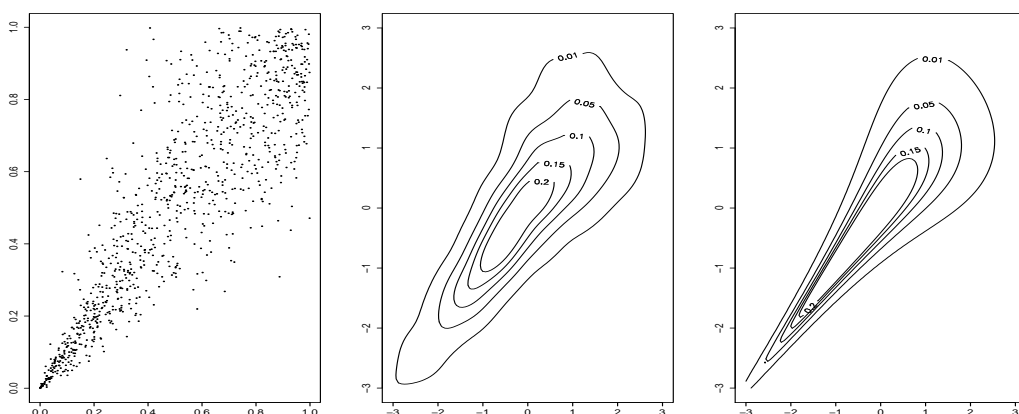
Figure 2.3.2: CDF and PDF of bivariate Gumbel, BB1 and BB7 copulas with approximately same level of dependence ($\rho = 0.70$).



(a) Scatter plot, theoretical and empirical contour plots of a Normal copula with dependence parameter $\tau = 0.7$, $\rho = 0.8910065$ and $\lambda_L = \lambda_U = 0$.

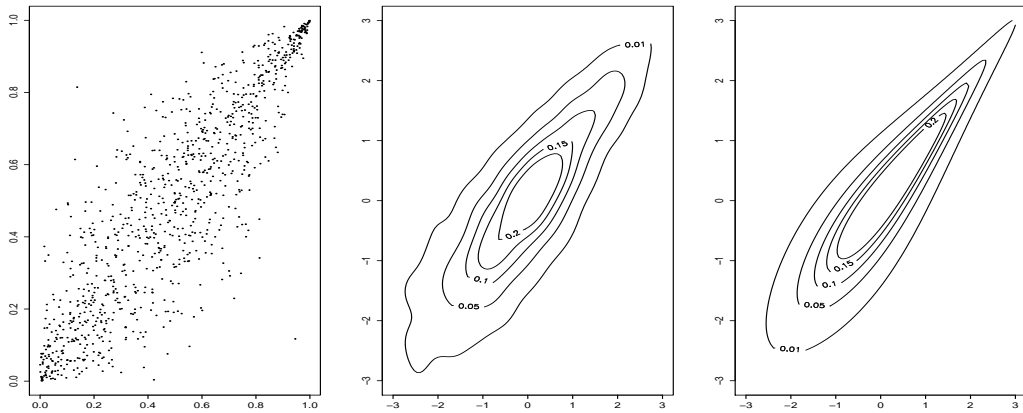


(b) Scatter plot, theoretical and empirical contour plots of a Student- t copula with dependence parameter $\tau = 0.7$, 3 degrees of freedom and $\lambda_L = \lambda_U = 0.4480999$.

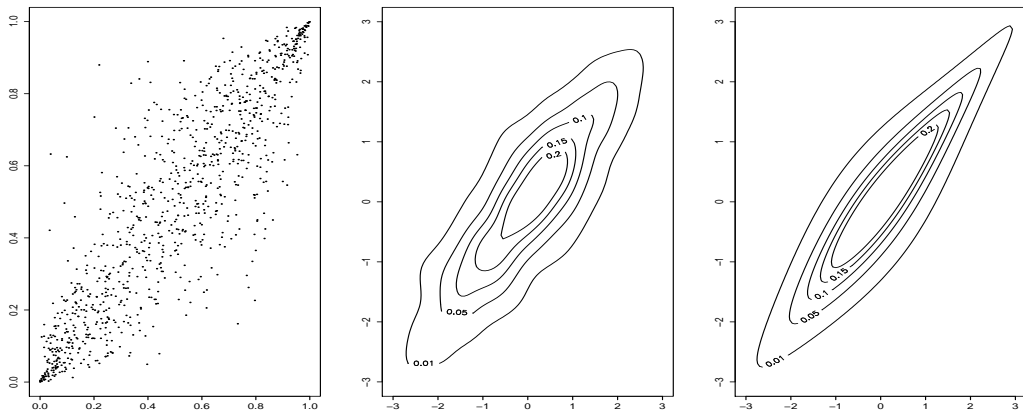


(c) Scatter plot, theoretical and empirical contour plots of a Clayton copula with dependence parameter $\tau = 0.7$, $\hat{\theta} = 4.666667$, $\lambda_L = 0.8619728$ and $\lambda_U = 0$.

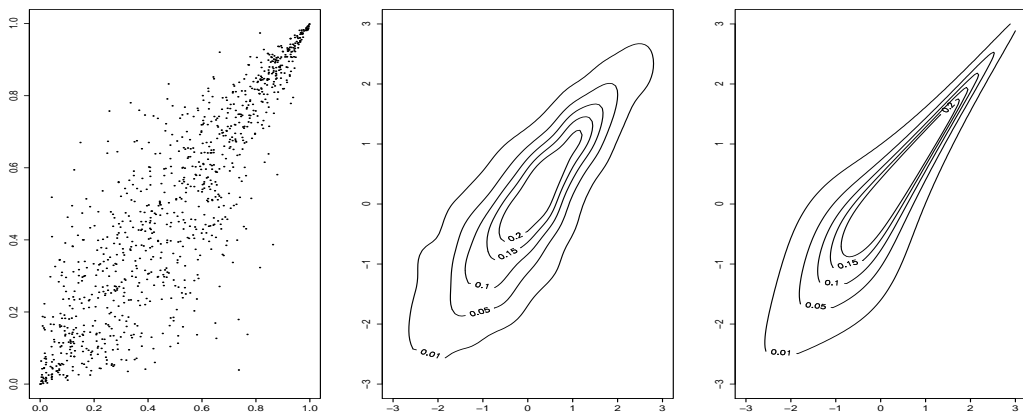
Figure 2.3.3: Scatter plots, theoretical and empirical contour plots of bivariate Normal, Student- t and Clayton copulas with approximately same level of dependence ($\rho = 0.70$).



(a) Scatter plot, theoretical and empirical contour plots of a Gumbel copula with dependence parameter $\tau = 0.7$, $\hat{\theta} = 3.333333$, $\lambda_L = 0$ and $\lambda_U = 0.7688556$.



(b) Scatter plot, theoretical and empirical contour plots of a BB1 copula with dependence parameter $\hat{\tau} = 0.7007108$, $\theta = 0.43$, $\delta = 2.75$, $\lambda_L = 0.5564539$ and $\lambda_U = 0.7133351$.



(c) Scatter plot, theoretical and empirical contour plots of a BB7 copula with dependence parameter $\hat{\tau} = 0.7001527$, $\theta = 4.8$, $\delta = 0.82$, $\lambda_L = 0.4294279$ and $\lambda_U = 0.8446473$.

Figure 2.3.4: Scatter plot, theoretical and empirical contour plots of bivariate Gumbel, BB1 and BB7 copulas with approximately same level of dependence ($\rho = 0.70$).

2.4 Pair-copula construction

Pairwise copula construction constitutes a very useful way of building flexible multivariate distributions. Joe (1996) was the first to introduce the pairwise construction principle based on the theorem of Sklar (1959) and using cumulative distribution functions (cdf). Bedford and Cooke (2001, 2002) realised that there are many different combinations for pair-copula construction and proposed a graphical way based on sequentially designing trees in an attempt to organise them. They called these distributions *regular vines*.

The modelling principle is based on a decomposition of a multivariate density into a cascade of bivariate copulas, which is applied to original variables and to their conditional and unconditional distributions. Aas et al. (2009) were the first to realise that this construction principle can be extended by allowing arbitrary pair-copula families as building blocks, since there are no restrictions on the choice of the bivariate copulas. Therefore, a multivariate distribution that is decomposed by using the pair-copula principle that allows different copula families as building blocks is called *mixed vine*, and it represents a very flexible way to construct higher-dimensional copulas and addresses the complexity of the dependence structure of original variables. Moreover, Aas et al. (2009) proposed algorithms for standard maximum likelihood estimation based on recursive conditioning and simulation from a pair-copula decomposed model.

In general, vine copulas are vine distributions with uniformly distributed marginals. Regular vines include two main types of vines, C-vines and D-vines. Their main difference lies in the way they organise a multivariate density decomposition. C-vines utilise a star tree methodology to decompose a multivariate density whereas D-vines employ a line tree methodology.

Let $\mathbf{X} = (X_1, \dots, X_d)^t$ be a vector of random variables with a joint density $f(x_1, \dots, x_d)$, marginal densities $f(x_1), \dots, f(x_d)$ and marginal distributions $F_1(x_1), \dots, F_d(x_d)$. This density can be decomposed as

$$f(x_1, \dots, x_d) = f_d(x_d) \cdot f(x_{d-1}|x_d) \cdot f(x_{d-2}|x_{d-1}, x_d) \cdots f(x_1|x_2, \dots, x_d), \quad (2.12)$$

and this factorisation is unique up to a re-labelling of the variables. Aas et al. (2009) note that every joint distribution function implicitly contains not only a description of the behaviour of the marginal distribution of each individual variable but also a description of their dependence structure. Therefore, copulas provide a way of isolating the description of their dependence structure.

It can be shown that the joint distribution function $f(x_1, \dots, x_d)$, for an absolutely continuous multivariate distribution F with strictly increasing, continuous marginal densities can be factorised as

$$f(x_1, \dots, x_d) = c_{1\dots d}(F_1(x_1), \dots, F_d(x_d)) \cdot f_1(x_1) \cdots f_d(x_d) \quad (2.13)$$

where $c_{1\dots d}$ is a uniquely identified d -variate copula density. In Section 2.2 we show that a bivariate joint distribution can be factorised as a product of a copula and of marginal densities as follows

$$f(x_1, x_2) = c_{12}(F(x_1), F(x_2))f_1(x_1)f_2(x_2). \quad (2.14)$$

Moreover, the conditional density $f(x_1|x_2)$ can be expressed in terms of a copula as

$$\begin{aligned} f(x_1|x_2) &= \frac{f(x_1, x_2)}{f_2(x_2)} = \frac{c_{12}(F(x_1), F(x_2))f_1(x_1)f_2(x_2)}{f_2(x_2)} \\ &= c_{12}(F(x_1), F(x_2))f_1(x_1). \end{aligned} \quad (2.15)$$

A three-dimensional conditional density can be expressed in terms of copulas in two different ways

$$\begin{aligned} f(x_1|x_2, x_3) &= \frac{f(x_1, x_2, x_3)}{f(x_2, x_3)} = \frac{f(x_1, x_2|x_3)}{f(x_2|x_3)} \\ &= \frac{c_{12|3}(F(x_1|x_3), F(x_2|x_3))f(x_1|x_3)f(x_2|x_3)}{f(x_2|x_3)} \\ &= c_{12|3}(F(x_1|x_3), F(x_2|x_3))f(x_1|x_3) \\ &= c_{12|3}(F(x_1|x_3), F(x_2|x_3))c_{13}(F_1(x_1), F_3(x_3))f_1(x_1), \end{aligned} \quad (2.16)$$

or

$$\begin{aligned} f(x_1|x_2, x_3) &= \frac{f(x_1, x_2, x_3)}{f(x_2, x_3)} = \frac{f(x_1, x_3|x_2)}{f(x_3|x_2)} \\ &= \frac{c_{13|2}(F(x_1|x_2), F(x_3|x_2))f(x_1|x_2)f(x_3|x_2)}{f(x_3|x_2)} \\ &= c_{13|2}(F(x_1|x_2), F(x_3|x_2))f(x_1|x_2) \\ &= c_{13|2}(F(x_1|x_2), F(x_3|x_2))c_{12}(F_1(x_1), F_2(x_2))f_1(x_1). \end{aligned} \quad (2.17)$$

In the d -dimensional case the following general formula can be applied to the conditional density

$$f(x|\boldsymbol{\nu}) = c_{x,\nu_j|\boldsymbol{\nu}_{-j}}(F(x|\boldsymbol{\nu}_{-j}), F(\nu_j|\boldsymbol{\nu}_{-j})) \cdot f(x|\boldsymbol{\nu}_{-j}), \quad (2.18)$$

where $\boldsymbol{\nu}$ is a d -dimensional vector, ν_j is an arbitrary chosen component of $\boldsymbol{\nu}$ and $\boldsymbol{\nu}_{-j}$ represents the $\boldsymbol{\nu}$ vector, excluding this component.

In general, under appropriate regularity conditions, a joint density can be decomposed as a product of bivariate copulas, acting on several different conditional probability distributions. For example, one possible pair-copula decomposition for $d = 3$ is

$$\begin{aligned} f(x_1, x_2, x_3) &= f_3(x_3) \cdot f(x_2|x_3) \cdot f(x_1|x_2, x_3) \\ &= f_3(x_3) \cdot \underbrace{f_2(x_2) \cdot c_{23}(F_2(x_2), F_3(x_3))}_{f(x_2|x_3)} \cdot \\ &\quad \underbrace{c_{12|3}(F(x_1|x_3), F(x_2|x_3)) \cdot c_{12}(F_1(x_1), F_2(x_2)) \cdot f_1(x_1)}_{f(x_1|x_2, x_3)}, \end{aligned} \quad (2.19)$$

and another possible pair-copula decomposition for $d = 3$ can be obtained as follows

$$\begin{aligned} f(x_1, x_2, x_3) &= f_1(x_1) \cdot f(x_2|x_1) \cdot f(x_3|x_2, x_1) \\ &= f_1(x_1) \cdot \underbrace{f_2(x_2) \cdot c_{12}(F_1(x_1), F_2(x_2))}_{f(x_2|x_1)} \cdot \\ &\quad \underbrace{c_{23|1}(F(x_2|x_1), F(x_3|x_1)) \cdot c_{13}(F_1(x_1), F_3(x_3)) \cdot f_3(x_3)}_{f(x_3|x_1, x_2)}. \end{aligned} \quad (2.20)$$

It is also clear that given a specific decomposition, there are still many different reparameterizations. Thus we need to introduce rules that will enable us to decompose a joint density into a cascade of pair-copulas. However, before introducing these rules, we need to introduce another concept related to pair-copula construction. The pair-copula construction involves marginal conditional distributions of the form $F(x|\boldsymbol{\nu})$ and we need a way to evaluate such marginal conditional distribution functions.

Joe (1996) showed that for every u_j in the vector $\boldsymbol{\nu}$, $F(x|\boldsymbol{\nu})$ can be written as

$$F(x|\boldsymbol{\nu}) = \frac{\partial C_{x,\nu_j|\boldsymbol{\nu}_{-j}}(F(x|\boldsymbol{\nu}_{-j}), F(\nu_j|\boldsymbol{\nu}_{-j}))}{\partial F(\nu_j|\boldsymbol{\nu}_{-j})}, \quad (2.21)$$

where $C_{x,\nu_j|\boldsymbol{\nu}_{-j}}$ is an arbitrary copula distribution function. Following the notation

of Aas et al. (2009) we will use the function $h(x, \nu; \boldsymbol{\theta})$ to represent the conditional distribution function when x and ν are uniforms. In this case $f(x) = f(\nu) = 1$, $F(x) = x$ and $F(\nu) = \nu$. Moreover, we assume a parametric specification for $C_{x, \nu_j | \nu_{-j}}$ with a parameter vector $\boldsymbol{\theta}$.

For $x, \nu \sim U[0, 1]$ it holds

$$h_{\boldsymbol{\theta}} = \frac{\partial C_{\boldsymbol{\theta}}(F_x(x), F_{\nu}(\nu))}{\partial F_{\nu}(\nu)} = \frac{\partial C_{\boldsymbol{\theta}(x, \nu)}}{\partial \nu}. \quad (2.22)$$

For the special case where $x = x_1$ and $\nu = x_2$, it follows

$$F(x_1|x_2) = \frac{\partial C_{x_1, x_2}(x_1, x_2; \boldsymbol{\theta}_{1,2})}{\partial F(x_2)}. \quad (2.23)$$

To illustrate the usefulness of h -functions we derive the conditional distribution of $F(x_1|x_2, x_3, x_4)$, where $x_1, x_2, x_3, x_4 \sim U[0, 1]$. One way to obtain the $F(x_1|x_2, x_3, x_4)$ is the following one

$$F(x_1|x_2, x_3, x_4) = \frac{\partial C_{1,2|3,4}(F(x_1|x_3, x_4; \boldsymbol{\theta}_{1,3|4}), F(x_2|x_3, x_4; \boldsymbol{\theta}_{2,3|4}))}{\partial F(x_2|x_3, x_4; \boldsymbol{\theta}_{2,3|4})}, \quad (2.24)$$

or

$$F(x_1|x_2, x_3, x_4) = h_{\boldsymbol{\theta}_{1,2|3,4}}(F(x_1|x_3, x_4), (F(x_2|x_3, x_4))). \quad (2.25)$$

Further, it is clear that we need to evaluate the conditional distributions $F(x_1|x_3, x_4)$ and $F(x_2|x_3, x_4)$ before estimating the final $F(x_1|x_2, x_3, x_4)$. Following the same approach, one possible way to obtain these conditional distributions is

$$F(x_1|x_3, x_4) = \frac{\partial C_{1,3|4}(F(x_1|x_4; \boldsymbol{\theta}_{1,4}), F(x_3|x_4; \boldsymbol{\theta}_{3,4}))}{\partial F(x_3|x_4; \boldsymbol{\theta}_{3,4})}, \quad (2.26)$$

or

$$F(x_1|x_3, x_4) = h_{\boldsymbol{\theta}_{1,3|4}}(F(x_1|x_4), (F(x_3|x_4))), \quad (2.27)$$

$$F(x_2|x_3, x_4) = \frac{\partial C_{2,3|4}(F(x_2|x_4; \boldsymbol{\theta}_{2,4}), F(x_3|x_4; \boldsymbol{\theta}_{3,4}))}{\partial F(x_3|x_4; \boldsymbol{\theta}_{3,4})}, \quad (2.28)$$

or

$$F(x_2|x_3, x_4) = h_{\boldsymbol{\theta}_{2,3|4}}(F(x_2|x_4), (F(x_3|x_4))). \quad (2.29)$$

Finally, the univariate conditional distributions $F(x_1|x_4)$, $(F(x_2|x_4)$ and $F(x_3|x_4)$ can be evaluated in the same way

$$F(x_1|x_4) = \frac{\partial C_{1,4}(F(x_1), F(x_4))}{\partial F(x_4)}, \quad (2.30)$$

or

$$F(x_1|x_4) = h_{\theta_{1,4}}(F(x_1), F(x_4)), \quad (2.31)$$

$$F(x_2|x_4) = \frac{\partial C_{2,4}(F(x_2), F(x_4))}{\partial F(x_4)}, \quad (2.32)$$

or

$$F(x_2|x_4) = h_{\theta_{2,4}}(F(x_2), F(x_4)), \quad (2.33)$$

$$F(x_3|x_4) = \frac{\partial C_{3,4}(F(x_3), F(x_4))}{\partial F(x_4)}, \quad (2.34)$$

or

$$F(x_3|x_4) = h_{\theta_{3,4}}(F(x_3), F(x_4)). \quad (2.35)$$

To summarise, the conditional distribution function $F(x_1|x_2, x_3, x_4)$ can be expressed as a set of nested h -functions as follows

$$F(x_1|x_2, x_3, x_4) = h_{\theta_{1,2|3,4}} \left(h_{\theta_{1,3|4}} \left(h_{\theta_{1,4}}(F(x_1), F(x_4)), h_{\theta_{3,4}}(F(x_3), F(x_4)) \right), h_{\theta_{2,3|4}} \left(h_{\theta_{2,4}}(F(x_2), F(x_4)), h_{\theta_{3,4}}(F(x_3), F(x_4)) \right) \right). \quad (2.36)$$

Table 2.4.1 below gives the h -functions, as obtained from [Czado et al. \(2012\)](#), of the Gaussian, Student- t , BB1 and BB7 copula.

Table 2.4.1: The h -function of the Gaussian, Student- t , BB1 and BB7 copula

Copula	h-function
Gaussian	$h(u v; \rho) = \Phi\left(\frac{\Phi^{-1}(u) - \rho \Phi^{-1}(v)}{\sqrt{1-\rho^2}}\right)$
Student- t	$h(u v; \rho, \nu) = t_{\nu+1}\left\{\frac{t_{\nu}^{-1}(u) - \rho t_{\nu}^{-1}(v)}{\sqrt{\frac{(\nu + (t_{\nu}^{-1}(v))^2)(1-\rho^2)}{\nu+1}}}\right\}$
BB1	$h(u v; \theta, \delta) = \left(1 + ((u^{-\theta} - 1)^{\delta} + (v^{-\theta} - 1)^{\delta})^{\frac{1}{\delta}}\right)^{-\frac{1}{\theta}-1} \cdot ((u^{-\theta} - 1)^{\delta} + (v^{-\theta} - 1)^{\delta})^{\frac{1}{\delta}-1} (v^{-\theta-1})^{\delta-1} v^{-\theta-1}$
BB7	$h(u v; \theta, \delta) = (1 + [(1 - (1-u)^{\theta})^{-\delta} + (1 - (1-v)^{\theta})^{-\delta} - 1]^{-\frac{1}{\delta}})^{-\frac{1}{\delta}-1} \cdot [(1 - (1-u)^{\theta})^{\delta} + (1 - (1-v)^{\theta})^{-\delta} - 1]^{-\frac{1}{\delta}-1} \cdot (1 - (1-v)^{\theta})^{-\delta-1} (1-v)^{\theta-1}$

This table reports the h -function of the Gaussian, Student t , BB1 and BB7 copula. **Source:** [Czado et al. \(2012\)](#).

2.5 Canonical vines (C-vines)

As shown in the previous Section, there are a significant number of possible pair-copula decompositions for high-dimensional distributions. It is therefore crucial to introduce rules that enable us to reduce this complexity. Bedford and Cooke (2001, 2002) have introduced a graphical way of organising pair-copula density decompositions, known as *regular vine*. However, the class of regular vines is still very extended. Canonical vine (C-vine) and drawable vine (D-vine) (Kurowicka and Cooke, 2006) constitute two special cases of regular vines each of which provides a specific way of decomposing the density. In this study, we will concentrate on C-vines because they have not been extensively investigated in financial applications so far.

The joint density decomposition, as organised by a C-vine, is given in the form of a nested set of star trees. For the d -dimensional C-vine, the pairs at level 1 are $(1, i)$, for $i = 2 \dots d$, and for level ℓ , $2 \leq \ell < d$, the (conditional) pairs are $(\ell, i|1, \dots, \ell - 1)$ for $i = \ell + 1, \dots, d$. Figure 2.5.1 shows the specification for a six-dimensional C-vine. It consists of five trees, T_j , $j = 1 \dots, d - 1$. Tree T_j has $d + 1 - j$ nodes and $d - j$ edges. Each edge corresponds to a bivariate copula density, while the edge labels correspond to the subscript of the bivariate copula density. For example, edge $34|12$ corresponds to the conditional copula density $c_{34|12}(\cdot)$, where copula density $c_{34|12}(\cdot)$ can be of any parametric form. In total, $d(d - 1)/2$ pair-copula families should be chosen for the whole decomposition. The nodes in tree T_j are necessary for determining the labels of next tree T_{j+1} .

As can be seen from Figure 2.5.1, there is one node in each tree which is connected with the remaining nodes of this particular tree. C-vines are very useful, when there exists a variable order with sequentially decreasing driving force. The order starts with a variable that has the highest dependency on all remaining variables, the “*pilot*” variable. Conditioning all remaining variables on the first pilot variable, we can obtain the variable with the second highest dependency on all other variables. This approach is completed once we select all pilot variables for every tree (Czado et al., 2012).

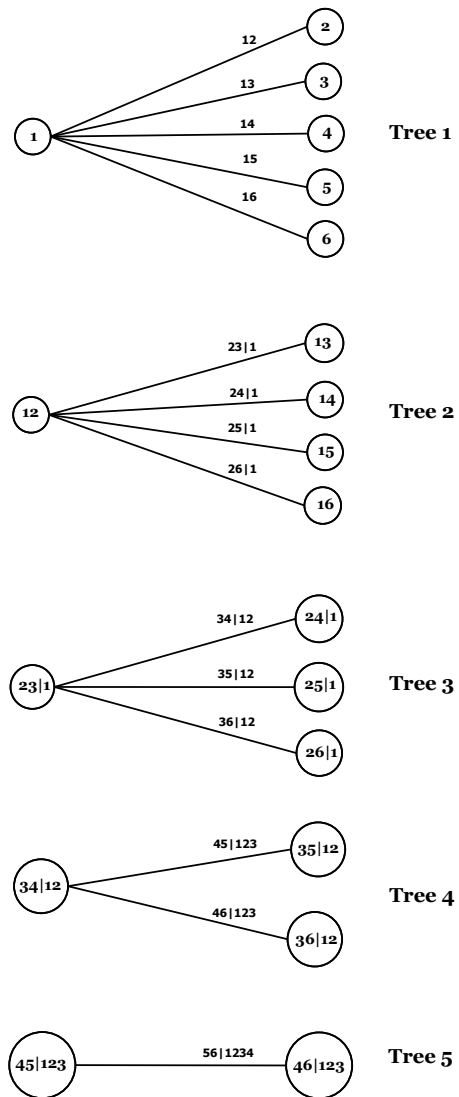


Figure 2.5.1: Tree representation of a canonical vine structure with 6 variables, 5 trees and 15 edges.

The d -dimensional canonical decomposition is given by [Aas et al. \(2009\)](#) as follows

$$f(\mathbf{x}) = \prod_{k=1}^d f_k(x_k) \times \prod_{i=1}^{d-1} \prod_{j=1}^{d-i} c_{i,i+j|1:(i-1)}(F(x_i|x_1, \dots, x_{i-1}), F(x_{i+j}|x_1, \dots, x_{i-1})) \quad (2.37)$$

For example, the six-dimensional canonical vine structure of Figure 2.5.1 can be written as

$$\begin{aligned} f(x_1, x_2, x_3, x_4, x_5, x_6) = & \\ & f_1(x_1)f_2(x_2)f_3(x_3)f_4(x_4)f_5(x_5)f_6(x_6) \cdot c_{1,2}(F(x_1), F(x_2)) \\ & \cdot c_{1,3}(F(x_1), F(x_3)) \cdot c_{1,4}(F(x_1), F(x_4)) \cdot c_{1,5}(F(x_1), F(x_5)) \\ & \cdot c_{1,6}(F(x_1), F(x_6)) \cdot c_{2,3|1}(F(x_{2|1}), F(x_{3|1})) \cdot c_{2,4|1}(F(x_{2|1}), F(x_{4|1})) \\ & \cdot c_{2,5|1}(F(x_{2|1}), F(x_{5|1})) \cdot c_{2,6|1}(F(x_{2|1}), F(x_{6|1})) \cdot c_{3,4|1,2}(F(x_{3|1,2}), F(x_{4|1,2})) \\ & \cdot c_{3,5|1,2}(F(x_{3|1,2}), F(x_{5|1,2})) \cdot c_{3,6|1,2}(F(x_{3|1,2}), F(x_{6|1,2})) \\ & \cdot c_{4,5|1,2,3}(F(x_{4|1,2,3}), F(x_{5|1,2,3})) \cdot c_{4,6|1,2,3}(F(x_{4|1,2,3}), F(x_{6|1,2,3})) \\ & \cdot c_{5,6|1,2,3,4}(F(x_{5|1,2,3,4}), F(x_{6|1,2,3,4})) \end{aligned} \quad (2.38)$$

It is clear that the construction is iterative in nature, and given a specific decomposition in Equation (2.37) there are as many as $\frac{d!}{2}$ possible C-vine structures. As already mentioned, for a mixed C-vine copula model we also need to choose a bivariate copula family for each of the $d(d-1)/2$ pair-copulas. It is worth taking into consideration the special case of a C-vine model with all pair-copulas being Gaussian. In this special case the C-vine model simplifies to a multivariate Gaussian distribution. Similarly, a C-vine structure with all bivariate copulas being Student- t and a common degree of freedom can be viewed as a multivariate Student- t distribution with a common degree of freedom ([Czado et al., 2012](#)). It is therefore quite important to develop selection rules that allow us to select an appropriate copula family for each edge in the C-vine model. However, most of these selection rules are based on estimated C-vines. Thus, we now turn to the parameter estimation in C-vines.

2.6 Inference for a C-vine model

In this Section, we present two main estimation methods for C-vine models, the maximum likelihood estimation (MLE) and the sequential estimation (SE) method. Each estimation approach has its own merits and demerits in terms of mathematical tractability, statistical efficiency and computational feasibility.

Assume a vector $x_i = (x_{i,1}, \dots, x_{i,T})^T$, $i = 1, \dots, d$ of random variables at T points in time. Further, assume that the T observations of each random variable $x_{i,t}$ are independent over time and uniformly distributed on $[0,1]$. The assumption of independence, as [Aas et al. \(2009\)](#) note, is not a limiting assumption. Most of the financial time series are serial correlated and thus univariate time-series models can be fitted to the margins and filter the time dependencies. As a result, the analysis can be continued with the residuals.

The log-likelihood of a C-vine model can be written, according to [Aas et al. \(2009\)](#), as

$$\ell(x; \boldsymbol{\theta}) = \sum_{j=1}^{d-1} \sum_{i=1}^{d-j} \sum_{t=1}^T \log [c_{j,j+i|1,\dots,j-1}(F(x_{j,t}|x_{1,t}, \dots, x_{j-1,t}), F(x_{j+i,t}|x_{1,t}, \dots, x_{j-1,t})))] \quad (2.39)$$

where $F(x_{j,t}|x_{1,t}, \dots, x_{j-1,t})$ and $F(x_{j+i,t}|x_{1,t}, \dots, x_{j-1,t})$ are conditional distributions and determined by Equation (2.21) and the h -function definition of Equation (2.22).

[Schepsmeier \(2010\)](#) shows that the log-likelihood function can also be written as

$$\ell(x; \boldsymbol{\theta}) = \sum_{t=1}^T \left[\sum_{i=1}^{d-1} \log(c(x_{1,t}, x_{i+1,t}; \theta_{1,i})) + \sum_{j=2}^{d-1} \sum_{i=1}^{d-j} \log(c(u_{j-1,i+1,t}, u_{j-1,1,t}; \theta_{j,i})) \right] \quad (2.40)$$

for all $t = 1, \dots, T$ and

$$u_{1,i,t} = h(x_{i+1,t}, x_{1,t}; \theta_{1,i}) \quad i = 1, \dots, d-1,$$

$$u_{j,i,t} = h(u_{j-1,i+1,t}, u_{j-1,1,t}; \theta_{j,i}), \quad j = 2, \dots, d-1 \text{ and } i = 1, \dots, d-j,$$

where $\boldsymbol{\theta}$ is the vector of copula parameters to be estimated while $\theta_{j,i}$ is the set of parameters of the corresponding copula density $c_{j,j+i|1,\dots,j-1}(\cdot, \cdot)$.

For example, the log-likelihood function for a four-variable C-vine model can be given by

$$\begin{aligned}
 \ell(x; \boldsymbol{\theta}) &= l(x_1, x_2, x_3, x_4; \boldsymbol{\theta}) \\
 &= \log(c(x_1, x_2; \theta_{1,1})) + \log(c(x_1, x_3; \theta_{1,2})) + \log(c(x_1, x_4; \theta_{1,3})) \\
 &+ \log(c_{2,3|1}(u_{1,1}, u_{1,2}; \theta_{2,1})) + \log(c_{2,4|1}(u_{1,1}, u_{1,3}; \theta_{2,2})) + \log(c_{3,4|1,2}(u_{2,1}, u_{2,2}; \theta_{3,1})) \\
 &= \log(c(x_1, x_2; \theta_{1,1})) + \log(c(x_1, x_3; \theta_{1,2})) + \log(c(x_1, x_4; \theta_{1,3})) \tag{2.41} \\
 &+ \log(c_{2,3|1}(h(x_2, x_1; \theta_{1,1}), h(x_3, x_1; \theta_{1,2}); \theta_{2,1})) + \log(c_{2,4|1}(h(x_2, x_1; \theta_{1,1}), h(x_4, x_1; \theta_{1,3}); \theta_{2,2})) \\
 &+ \log(c_{3,4|1,2}(h[h(x_2, x_1; \theta_{1,1}), h(x_3, x_1; \theta_{1,2}); \theta_{2,1}], h[h(x_2, x_1; \theta_{1,1}), h(x_4, x_1; \theta_{1,3}); \theta_{2,2}]; \theta_{3,1}))
 \end{aligned}$$

For each bivariate copula in the sum of Equation (2.40) there is at least one parameter to be determined. The number depends on the parametric assumption for each pair-copula in the C-vine model. For example, a Gaussian copula has one parameter whereas a Student- t copula has two parameters. If parametric margins are also estimated, i.e. $f_i(x_{i,t}; \delta_i)$ with $i = 1, \dots, d$, the added contribution to Equation (2.40) is

$$\sum_{t=1}^T \sum_{i=1}^d f_i(x_{i,t}; \delta_i). \tag{2.42}$$

Under this setting, full MLE estimates can be obtained by maximising Equation (2.40) combined with Equation (2.42) with respect to the parameters $(\boldsymbol{\theta}, \delta_1, \dots, \delta_d)$. In general, the full MLE estimation would be our preferred choice due to its well-known optimality properties. However, the Inference Functions for Margins (IFM) method is usually preferred to full MLE due to its computational tractability and comparable efficiency.

The IFM method (see [Joe and Hu \(1996\)](#); [Joe \(1997\)](#), for more details) is a multi-step optimisation technique. It divides the parameter vector into separate parameters for each margin and parameters for the copula model. Therefore, one may break up the optimisation problem into several smaller optimisation steps with fewer parameters. For example, in the first step one may maximise the log-likelihood function of the margins in Equation (2.42) over the parameter vector $(\delta_1, \dots, \delta_d)$ and in the second step the log-likelihood function of the C-vine model in Equation (2.40), given the estimated parameters of the margins from the first step, over the parameter vector $\boldsymbol{\theta}$. The IFM method has been found highly efficient compared to full MLE optimisation for a number of multivariate models in a study by [Joe \(1997\)](#).

Nevertheless, IFM is a fully parametric method and thus a misspecification of the marginal distributions may have an effect on the performance of the estimator. In addition, marginal distributions are almost always unknown in practice. This fact increases the probability of marginal misspecification and as a result non-robust copula estimation. The semi-parametric (SP) method, proposed by [Genest et al. \(1995\)](#), can tackle the marginal misspecification problem since it treats the marginal distributions as unknown functions.

The SP method is also known as *pseudo maximum likelihood* (PML) and as *canonical maximum likelihood* (CML) method. The PML method estimates each marginal distribution non-parametrically by the empirical distribution function (*edf*) without assuming any particular parametric distribution for the marginals. Once this is completed, the dependence structure between the marginals is estimated using a parametric multivariate copula family or in our particular study a C-vine model with appropriate pair-copula families. [Kim et al. \(2007\)](#) have shown that the MLE/IFM methods are non robust against marginals misspecification, and that the SP method performs better than the MLE and IFM methods, overall.

We now turn to the estimation of C-vine models. C-vine parameters can be estimated using the sequential estimator (SE) or the maximum likelihood estimator (MLE). Following [Czado et al. \(2012\)](#) suppose i.i.d. data $\mathbf{u}_t = (u_{1,t}, \dots, u_{d,t})^t$ for $t = 1, \dots, T$ is available. For SE, we first estimate the parameters of the unconditional bivariate copulas of tree 1. Then these estimates are used to estimate pair-copula parameters with a single conditioning variable. The estimation proceeds tree by tree, since the conditional pairs in trees $2, \dots, d - 1$ depend on the specification of the previous trees via the h -function, defined in Equation (2.22). Hence, C-vine models are estimated sequentially until all parameters are estimated. The estimation, in this context, can be carried out using the inversion of Kendall's τ for one parameter bivariate copulas or using MLE.

$$(1, 2), (1, 3), (1, 4), \dots, (1, d), \tag{Tree1}$$

$$(2, 3|1), (2, 4|1), \dots, (2, d|1), \tag{Tree2}$$

$$(3, 4|1, 2), (3, 5|1, 2), \dots, (3, d|1, 2), \tag{Tree3}$$

...

$$(d - 1, d|1, \dots, d - 2). \tag{Tree } d - 1)$$

In particular, the parameter vector $\boldsymbol{\theta}_{1,j+1}$ of bivariate copula families $c_{1,j+1}$ in tree 1 is estimated using data $(u_{1,t}, u_{j+1,t})$, $t = 1, \dots, T$ for $j = 1, \dots, d - 1$. Given the

estimated parameter vector $\hat{\boldsymbol{\theta}}^{SE}$ of tree 1, we next want to estimate the parameter vector $\boldsymbol{\theta}_{2,j+1}$ corresponding to $c_{2,j+2|1}$ for $j = 1, \dots, d-2$ in tree 2. Define

$$\hat{v}_{2|1,t} := F(u_{2,t}|u_{1,t}; \hat{\boldsymbol{\theta}}_{1,1}^{SE}) = h(u_{2,t}|u_{1,t}; \hat{\boldsymbol{\theta}}_{1,1}^{SE}),$$

$$\hat{v}_{j+2|1,t} := F(u_{j+2,t}|u_{1,t}; \hat{\boldsymbol{\theta}}_{1,j+1}^{SE}) = h(u_{j+2,t}|u_{1,t}; \hat{\boldsymbol{\theta}}_{1,j+1}^{SE}),$$

for $j = 1, \dots, d-2$ and denote these estimates by $\hat{\boldsymbol{\theta}}_{2,j}^{SE}$. We can subsequently use data $(\hat{v}_{2|1,t}, \hat{v}_{j+2|1,t})$, $t = 1, \dots, T$ to estimate $\boldsymbol{\theta}_{2,j}$ for $j = 1, \dots, d-2$. In order to estimate the parameter vector $\boldsymbol{\theta}_{3,j}$ corresponding to tree 3 and pair-copula families with double conditioning variables $c_{3,j+3|1,2}$ for $j = 1, \dots, d-3$, we define

$$\hat{v}_{3|1,2,t} := h(\hat{v}_{2|1,t}|\hat{v}_{3|1,t}; \hat{\boldsymbol{\theta}}_{2,1}^{SE}),$$

$$\hat{v}_{j+3|1,t} := h(\hat{v}_{j+3|1,t}|\hat{v}_{3|1,t}; \hat{\boldsymbol{\theta}}_{2,j}^{SE}),$$

and estimate $\boldsymbol{\theta}_{3,j}$ using $(\hat{v}_{3|1,2,t}, \hat{v}_{j+3|1,2,t})$, $t = 1, \dots, T$ for $j = 1, \dots, d-3$.

Following the same reasoning, one can sequentially estimate the pair-copula parameters for each nested set of trees in the C-vine structure until all unconditional and conditional bivariate copula parameters have been estimated. The sequential estimates have been recently found by [Haff \(2013\)](#) to be asymptotically normal under some regularity conditions but their asymptotic covariance properties are intractable ([Czado et al., 2012](#)).

To improve estimation efficiency we can use MLE estimation. The parameters of a C-vine model can be estimated by optimising the log-likelihood function of Equation (2.40). It is clear that MLE requires a high-dimensional optimisation of the log-likelihood and is therefore much more time consuming compared to SE. Moreover, MLE requires good starting values of the parameters in the numerical maximisation of the log-likelihood for quick convergence. Hence, the sequential estimates can be used as starting values for the optimisation.

2.7 Simulation from a C-vine model

Simulation from pair-copula decomposed models is an important element for empirical applications. [Aas et al. \(2009\)](#) have provided simulation algorithms for C-vines and D-vines. Thus, the presentation of the C-vine simulation algorithm in this Section is based on the paper of [Aas et al. \(2009\)](#).

The general algorithm for sampling n dependent uniform $[0, 1]$ variables is common for C-vines and D-vines:

Sample w_1, \dots, w_n , independent uniform on $[0, 1]$

Then set

$$x_1 = w_1,$$

$$x_2 = F^{-1}(w_2|x_1),$$

$$x_3 = F^{-1}(w_3|x_1, x_2),$$

$$\dots = \dots$$

$$x_n = F^{-1}(w_n|x_1, \dots, x_{n-1}).$$

The conditional distribution $F(x_j|x_1, x_2, \dots, x_{j-1})$ for each j , can be evaluated recursively for both vine models through the h -function in Equation (2.22) and the relationship in Equation (2.21). For the C-vine we always choose

$$F(x_j|x_1, \dots, x_{j-1}) = \frac{\partial C_{j,j-1|1,\dots,j-2}(F(x_j|x_1, \dots, x_{j-2}), F(x_{j-1}|x_1, \dots, x_{j-2}))}{\partial F(x_{j-1}|x_1, \dots, x_{j-2})}.$$

The following algorithm (Algorithm 1) gives the procedure for sampling from a C-vine. The variables to be sampled are represented by the outer for-loop. This loop entails two other for-loops. In the first for-loop, the i -th variable is sampled, while in the other, the conditional distribution functions needed for sampling the $(i + 1)$ -th variable are computed. The computation of conditional distribution functions is performed by repeatedly using the h -function defined in Equation (2.22), having previously computed conditional distribution functions, $v_{i,j} = F(x_i|x_1, \dots, x_{j-1})$, as the first two arguments. The last argument of the h -function, $\theta_{j,i}$, is the set of parameters of the corresponding copula density $c_{j,j+i|1,\dots,j-1}(\cdot, \cdot)$.

Algorithm 1: Simulation algorithm for a canonical vine.

Generates one sample x_1, \dots, x_n from the vine.

```

1: Sample  $w_1, \dots, w_n$  independent uniform on  $[0, 1]$ .
2:  $x_{1,1} = v_{1,1} = w_{1,1}$ 
3: for  $i = 2$  to  $n$  do
4:      $v_{i,1} = w_i$ 
5:     for  $k = i - 1$  to  $1$  do
6:          $v_{i,1} = h^{-1}(v_{i,1}, v_{k,k}, \theta_{k,i-k})$ 
7:     end for
8:      $x_i = v_{i,1}$ 
9:     if  $i == n$  then
10:        STOP
11:    end if
12:    for  $j = 1$  to  $i - 1$  do
13:         $v_{i,j+1} = h(v_{i,j}, v_{j,j}, \theta_{j,i-j})$ 
14:    end for
15: end for

```

2.8 Model selection

In Section 2.6, we described how to estimate a specific C-vine structure. However, this is only one piece of the full inference problem. Full inference for a pair-copula decomposition entails (a) the selection of a specific decomposition, (b) the selection of a copula family for each pair-copula and (c) the estimation of the copula parameters.

As shown in the previous Section the complexity (number of possible decompositions, number of possible pair-copula family selections) increases very rapidly with the dimension of the data set. Moreover, in C-vine models we should also determine which bivariate relationships are the most important, since we need to specify the relationships between one specific pilot variable and the others, and consequently determine the appropriate factorisation(s) to estimate.

Therefore, given the empirical observations, it is necessary to choose a specific C-vine factorisation and parametric shape for each pair-copula. For example, in the C-vine decomposition of Figure 2.5.1 we have to select appropriate copula families for the unconditional copulas in the first tree, i.e., $C_{1,2}(\cdot, \cdot), C_{1,3}(\cdot, \cdot), \dots$ etc, and subsequently the copula families for the conditional copulas in the remaining trees, i.e., $C_{2,3|1}(\cdot, \cdot), C_{3,4|1,2}(\cdot, \cdot), \dots$ etc. When the pair-copulas of the C-vine structure do not belong to the same family, the C-vine model is known as *mixed*. The reasoning

behind this mixing procedure is to choose for each pair of variables the parametric copula family that best fits the data and thus improve the overall fit.

We propose the following steps to determine a specific factorisation and copula family for each bivariate copula in the C-vine model:

- (a) Define the pilot variable in tree 1 of the C-vine model based on the empirical rule of [Czado et al. \(2012\)](#).
- (b) Given the empirical data and selected pilot variable, determine which copula families to use in tree 1. The selection of appropriate copula families in tree 1 is based on graphical and analytical tools as well as goodness-of-fit tests.
- (c) Estimate the parameters of the selected copula families using the original data.
- (d) Transform observations as required for tree 2, using the estimated copula parameters from tree 1 and the h -function defined in Equation (2.22).
- (e) Determine the pilot variable in tree 2 in the same way as in tree 1 based on the transformed observations of (d).
- (f) Determine which copula families to use in tree 2 in the same way as in tree 1.
- (g) Iterate.

2.9 Selecting an appropriate C-vine decomposition

As noted in [Aas et al. \(2009\)](#) there are exactly $d!/2$ different C-vine structures available. It is obvious that the variation increases along with the dimension of the dataset. As a result, on the one hand it is necessary to develop selection rules that uniquely decompose a C-vine model and thus reduce the complexity of all available permutations and, on the other hand, to provide an overall good fit to the multivariate distribution of the data.

According to [Aas et al. \(2009\)](#) it is preferable to choose models with high dependence in the bivariate conditional distributions. Moreover, fitting a C-vine model might be more challenging when there is not a particular variable that governs interactions in the data set. So far there exist only empirical selection procedures which propose a specific C-vine decomposition (see [Nikoloulopoulos et al. \(2012\)](#); [Czado et al. \(2012\)](#)). In this study, the empirical selection rule of [Czado et al. \(2012\)](#), which is based on Kendall's τ estimates, is followed.

The rule suggests a data driven sequential approach to determine the pilot variable and the $d - 1$ unconditional pair-copulas needed in tree 1 of the C-vine model. The rule works as follows. Estimate all possible pairwise Kendall's $\tau_{i,j}$ coefficients, noted $\hat{\tau}_{i,j}$, and find the variable i^* that maximises

$$\hat{S}_i := \sum_{j=1}^d |\hat{\tau}_{i,j}|, \quad (2.43)$$

over $i = 1, \dots, d$. Once the variable that is the most dependent on other variables, i^* , is selected for tree 1, we reorder the variables so that i^* becomes the first variable. We can then link the pilot variable i^* with the remaining variables and select the unconditional pair-copulas for $c_{1,j+1}$, $j = 1, \dots, d - 1$. The selection of appropriate copula-families is based on multiple criteria such as graphical and analytical tools as well as goodness-of-fit tests. We will discuss this choice later and assume for the moment that we are able to select a pair-copula family for each unconditional bivariate copula $c_{1,j+1}$, $j = 1, \dots, d - 1$.

As in the sequential estimation procedure $d - 1$ transformed variables

$$\hat{v}_{j+2|1,t} := h(u_{j+2,t}|u_{1,t}; \boldsymbol{\theta}_{1,j+1}^{SE}) \quad j = 0, \dots, d - 2, \quad t = 1, \dots, T \quad (2.44)$$

are formed. Based on $d - 1$ variables of size T all pairwise Kendall's τ coefficients are estimated and the pilot variable i^{**} of tree 2 that maximises Equation (2.43) is selected. Subsequently, we reorder the variables $i = 2, \dots, d$ in such a way that i^{**} is variable 2. Having selected i^{**} as the pilot variable for tree 2, we can consequently select the copula families with single conditioning variable 1, $c_{2,j+2|1}$ for $j = 1, \dots, d - 2$.

This procedure is continued until we determine the pilot variable for each tree and therefore a specific factorisation of the C-vine model as well as all corresponding pair-copulas and their associated sequential parameter estimates $\hat{\boldsymbol{\theta}}^{SE}$.

2.10 Selecting an appropriate copula family

After selecting the pilot variable for the first tree, the next step is to select appropriate parametric copula families for each pair-copula of the first level and, following the sequential selection approach of [Czado et al. \(2012\)](#), to determine a unique C-vine decomposition and choose the copula families for each bivariate copula accordingly.

In general, when modelling the dependence structure of random variables using copulas, the true copula is always unknown. Therefore, we need tools to specify a copula family appropriate for describing the observed dependence structure of the variables. For our sequential selection procedure we only need selection rules for

bivariate copulas and hence our analysis will concentrate only on copula selection in two dimensions.

The problem of selecting an appropriate (bivariate) copula family is a well studied problem in the literature and many procedures have been proposed. In principle there are two different classes of tools that help in the copula selection procedure, *graphical* and *analytical* tools. In our study, we will use both tool sets for our copula selection procedure.

2.10.1 Graphical tools

Two of the most common graphical tools for detecting dependence are the scatter and contour plots, introduced in 2.10.2 1 and particularly in Figures 2.3.3 and 2.3.4. Both plots are rather general tools and provide general information about the description of the dependence structure of the variables. Scatter plots provide a general description of the dependence structure of the variables while contour plots can be used for comparison studies among different copula families. Based on bivariate data, empirical contour plots can be plotted against contour plots with specified margins (standard normal margins are usually used since they allow for direct comparisons and indicate tail dependence) and specified copula families and parameter(s), and useful visual comparisons between empirical contour plots and theoretical copula contour plots can be drawn.

While scatter and contour plots are general tools, there also exist graphical tools that can be used to detect bivariate copula dependence directly. Chi-plots (χ -plots) and Kendall's plots (k -plots) are two of these graphical tools for detecting dependence. Chi-plots can also be helpful for detecting tail dependence. Furthermore, the λ function of [Genest and Rivest \(1993\)](#) is another useful graphical tool that can be employed in the copula selection procedure. The presentation of these tools is based on [Belgorodski \(2010\)](#), [Brechmann and Schepsmeier \(2013\)](#) and [Genest \(2007\)](#) where the properties and practical applications of these tools are well-analysed.

2.10.1.1 Chi-plots

Chi-plots were initially introduced by [Fisher and Switzer \(1985\)](#) and are based on the chi-square statistic for independence in a two way-table. Let $(x_1, y_1), \dots, (x_n, y_n)$ be a random sample from some pair (X, Y) of continuous random variables, where $F_{XY}(x, y)$ is the joint distribution function that characterises their joint behaviour and $F_X(x)$ and $F_Y(y)$ denote their respective marginal distributions. Specifically, introduce

$$\hat{F}_{XY,i} = \hat{F}_{XY,i}(x_i, y_i) = \frac{1}{n-1} \{j \neq i : X_j \leq X_i, Y_j \leq Y_i\} \quad (2.45)$$

$$\hat{F}_{X,i} = \hat{F}_{X,i}(x_i) = \frac{1}{n-1} \{j \neq i : X_j \leq X_i\} \quad (2.46)$$

$$\hat{F}_{Y,i} = \hat{F}_{Y,i}(Y) = \frac{1}{n-1} \{j \neq i : Y_j \leq Y_i\} \quad (2.47)$$

where these quantities depend exclusively on the ranks of the observations, i.e., F_{XY} , F_X and F_Y are estimated by empirical cumulative distribution functions.

Fisher and Switzer propose to plot the pairs (λ_i, x_i) , where

$$x_i = \frac{\hat{F}_{XY,i} - \hat{F}_{X,i}\hat{F}_{Y,i}}{\sqrt{\hat{F}_{X,i}(1 - \hat{F}_{X,i})\hat{F}_{Y,i}(1 - \hat{F}_{Y,i})}} \quad (2.48)$$

$$\lambda_i = 4 \operatorname{sing} \cdot (\tilde{F}_{X,i}, \tilde{F}_{Y,i}) \max (\tilde{F}_{X,i}^2, \tilde{F}_{Y,i}^2) \quad (2.49)$$

and $\tilde{F}_{X,i} = \hat{F}_{X,i} - 1/2$, $\tilde{F}_{Y,i} = \hat{F}_{Y,i} - 1/2$ for $i = 1, \dots, n$. Fisher and Switzer (1985, 2001) argued that $\lambda_i, x_i \in [-1, 1]$. Moreover, λ_i measures the distance between the pairs $(x_1, y_1), \dots, (x_n, y_n)$ and the center of the scatter plot while x_i accords to a correlation coefficient between dichotomised values of X and Y .

Under independence, one would expect $\hat{F}_{XY,i} \approx \hat{F}_{X,i} \cdot \hat{F}_{Y,i}$ for all $i = 1 \dots, n$. Therefore, values of x_i that are far away from zero are indicative of a departure from the hypothesis of independence whereas values of x_i close to zero indicate independence. For positively dependent margins, the pairs (λ_i, x_i) tend to be located on the positive (upper) part of the x_i axis, and vice versa for the negatively dependent margins. Moreover, Fisher and Switzer suggested to draw “control limits” at $\pm c_p/\sqrt{n}$, where c_p is selected in such a way that approximately 100p% of the pairs (λ_i, x_i) lie between these limits, to help identify whether values of x_i lie close enough to zero. They show, through simulations, that the c_p values 1.54, 1.78 and 2.18 correspond to $p = 0.90, 0.95$ and 0.99 , respectively. Figure 2.10.2 and more specifically graphs (iv), (v) and (vi) display Chi-plots for independent, positively dependent and negatively dependent bivariate data, respectively.

As pointed out in Belgorodski (2010), Fisher and Switzer did not discuss the tail dependence problem when they introduced the Chi-plots as a graphical method for detecting dependence. Abberger (2005) was the first to show how the Chi-plots can be employed to detect tail dependence and its form (upper or lower) in a bivariate data set.

To detect tail dependence Abberger proposed to compute Chi-plots for only positive values of λ_i . Since λ_i measures the distance of a data point (x_i, y_i) from the center of a bivariate data set, data points with λ_i values close to -1 are not located far away from the data center whereas data points with λ_i values close to $+1$ are placed far away from the data center. Thus, Abberger argued that λ_i values close to $+1$ can be used to assess tail dependence. In particular, when there is no tail dependence and for λ_i values close to $+1$, the x_i values should return to the zero line at the right edge of the Chi-plot while the presence of tail dependence can be detected by the deviation of x_i values from the zero line. Figure 2.10.3 and particularly panels (c) and (d) display examples of Chi-plots detecting (i) no tail dependence, (ii) symmetric tail dependence, (iii) only upper tail dependence and (iv) only lower tail dependence.

2.10.1.2 K-plots

The Kendall-process-plot (or K-plot), proposed by [Genest and Boies \(2003\)](#), is another rank-based graphical tool for detecting dependence. It is similar in spirit to the familiar QQ-plot. [Genest and Boies \(2003\)](#) proposed to plot the pairs of $(W_{i:n}, \hat{F}_{XY,i:n})$ for $i = 1, \dots, n$, where $\hat{F}_{XY,i:n}$ are the order statistics of $\hat{F}_{XY,i}$ defined in Equation (2.45). As for $W_{i:n}$, it is the expected value of the i -th statistic from a random sample of size n from the random variable $W_i = \hat{F}_{XY}(x_i, y_i)$ under the null hypothesis of independence between X and Y .

The $W_{i:n}$ is given by

$$W_{i:n} = n \binom{n-1}{i-1} \int_0^1 w k_0(w) \{K_0(w)\}^{i-1} \{1 - K_0(w)\}^{n-i} dw \quad (2.50)$$

where

$$K_0(w) = w - w \log(w)$$

and $k_0(\cdot)$ is the corresponding density.

The interpretation of the K-plot is similar to that of the QQ-plot. If the points of the K-plots lie approximately in the line $y = x$, there is no evidence for dependence between X and Y . Any deviation from the main diagonal is a sign of dependence in the K-plot. Further, positive or negative dependence may be detected in the data, depending on whether the points of the K-plots lie above or below the main diagonal. In principle, the further the deviation from the diagonal the greater the dependence. In addition, perfect positive dependence would imply points $(W_{i:n}, \hat{F}_{XY,i:n})$ lying on the bent curve $K_0(w)$ above the main diagonal whereas perfect negative dependence would imply points $(W_{i:n}, \hat{F}_{XY,i:n})$ positioned on the x-axis. Figure 2.10.2 and more specifically graphs (vii), (viii) and (iv) display an example of K-plots for independent, positively dependent and negatively dependent bivariate data, respectively.

2.10.1.3 The λ -function

The λ -function, introduced by [Genest and Rivest \(1993\)](#), is another graphical tool that can be employed for choosing the copula family that best describes the observed dependence. The λ -function is different for each copula family and is defined as follows

$$\lambda(u, \boldsymbol{\theta}) := u - K(u, \boldsymbol{\theta}) \quad (2.51)$$

where $K(u, \boldsymbol{\theta}) := P(C(U_1, U_2 | \boldsymbol{\theta}) \leq u)$ is Kendall's cumulative distribution function for a copula C with parameter (s) $\boldsymbol{\theta}$, $u \in [0, 1]$ and (U_1, U_2) distributed according to C with uniformly distributed margins. For Archimedean copulas the λ -function is given by

$$\lambda(u, \boldsymbol{\theta}) = \frac{\phi(u)}{\phi'(u)} \quad (2.52)$$

where ϕ is the generator function and ϕ' its corresponding derivative. There are no closed form expressions of the theoretical λ -function for the Gaussian and Student- t copula but they can be obtained through simulations. Moreover, control bounds corresponding to independence and comonotonicity ($\lambda = 0$) are usually plotted with the theoretical λ -function.

In general, λ -functions are useful tools for selecting the appropriate copula family. A comparison of the empirical and the theoretical λ -function provides an indication as to whether a selected copula family is adequate to describe the dependence structure of empirical data or not. Figure 2.10.1 displays an illustrative example. In the upper panel of Figure 2.10.1 the empirical λ -function of simulated data ($N = 1000$) from the Joe copula family is plotted whereas in the middle panel the theoretical one is plotted. Finally, the lower panel displays both λ -functions.

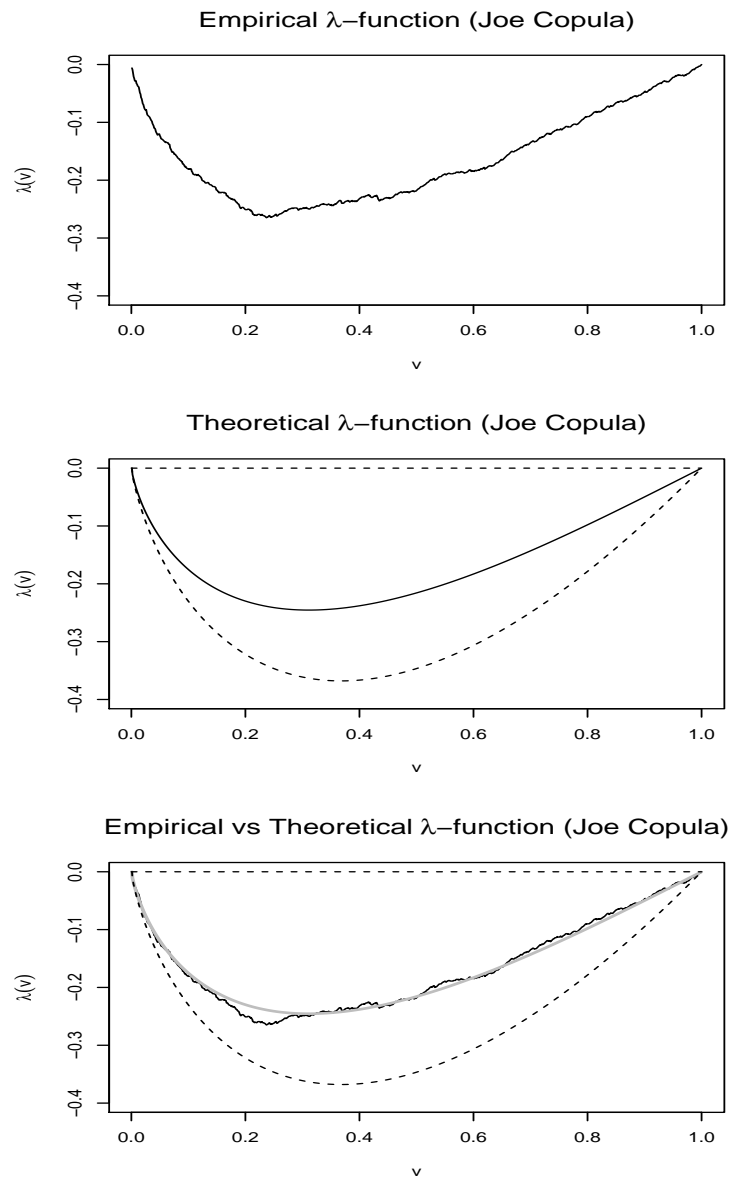


Figure 2.10.1: Upper panel: empirical λ -function of simulated bivariate data from the Joe copula with $\theta = 2$. Middle panel: theoretical λ -function from the Joe Copula with $\theta = 2$. Lower panel: empirical vs theoretical λ -functions. Dashed lines are bounds corresponding to independence and comonotonicity ($\lambda = 0$), respectively.

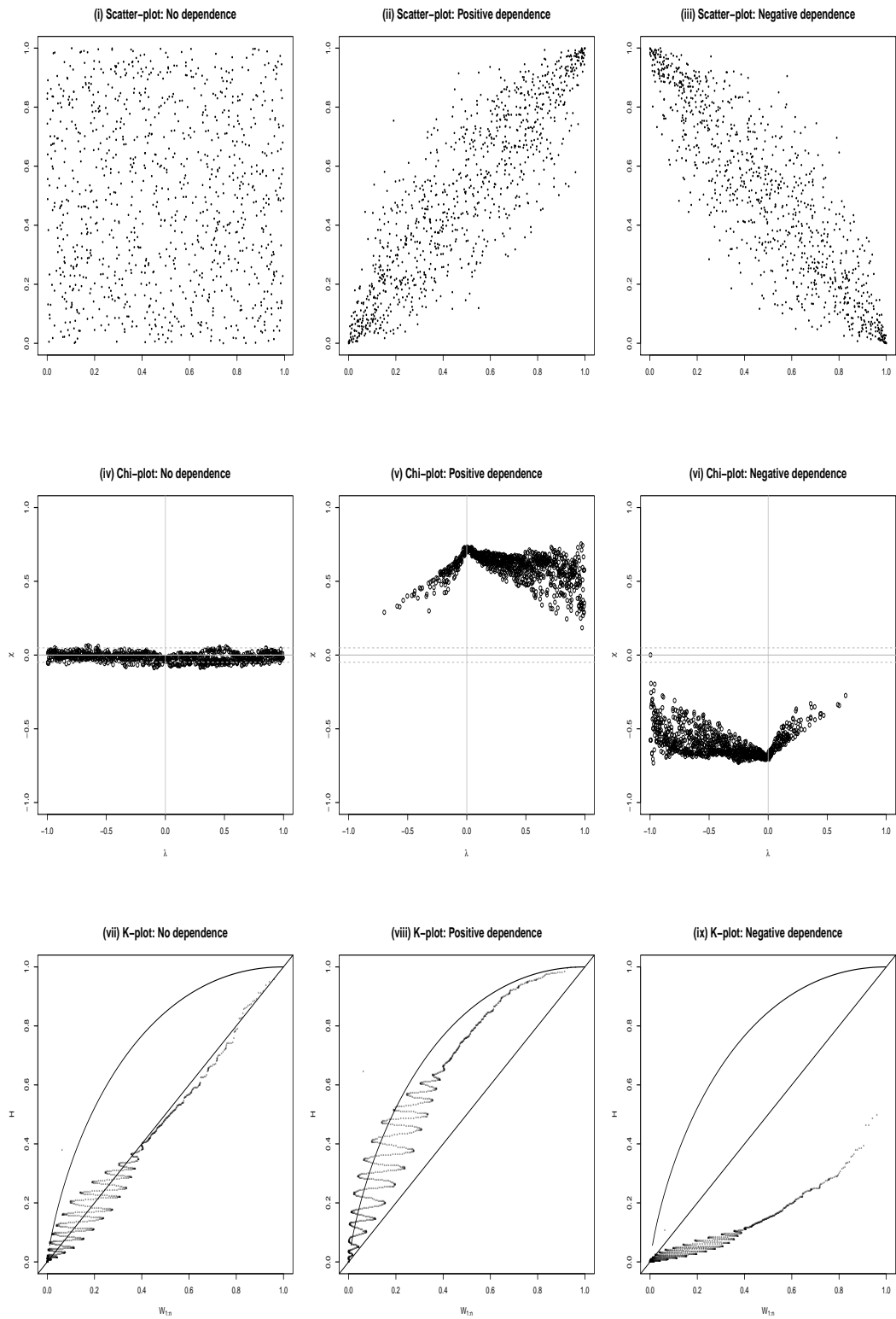


Figure 2.10.2: Panels (i), (iv) and (vii) display scatter, Chi and K-plots for independent data, respectively; panels (ii), (v) and (viii) display scatter, Chi and K-plots for positively dependent data, respectively; panels (iii), (vi) and (ix) display scatter, Chi and K-plots for negatively dependent data, respectively

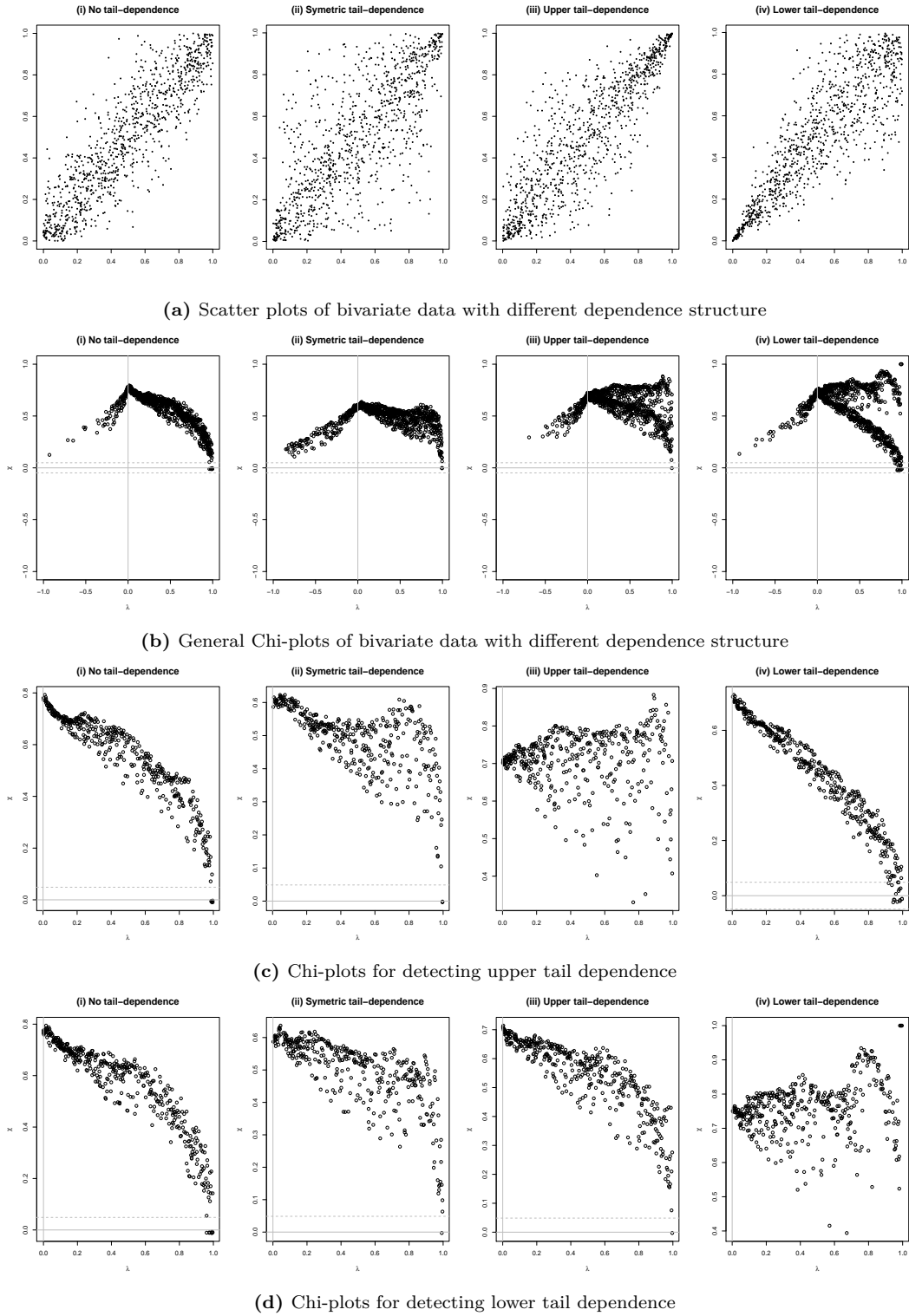


Figure 2.10.3: Chi-plots for detecting (tail) dependence: (a) bivariate scatter plots with different dependence form; (b) General Chi-plots; (c) Chi-plots for upper tail dependence; (d) Chi-plots for lower tail dependence.

2.10.2 Analytical tools

In addition to the graphical tools there are also a broad range of analytical tools that can be employed in the copula selection procedure. In practice, analytical tools consist of various goodness-of-fit tests and information criteria that assist in the selection procedure. A goodness-of-fit test of a statistical model describes how well a given model fits the observed data. Typically, measures of goodness-of-fit summarise the discrepancy between observed and expected values under the model in question. These tests are usually employed in statistical testing. Therefore, in our model selection procedure we test the hypothesis of whether a chosen copula can adequately fit the observed data. On the other hand, information criteria are not tests used in the spirit of hypothesis testing but rather tests used to compare models; in other words, they are tools for model selection. In this study, the Independence test of Genest (2007), the Akaike and Bayesian Information Criteria (AIC and BIC, respectively) and the Vuong (1989) and Clarke (2007) tests are presented and utilized in the copula selection procedure.

2.10.2.1 Independence test

In general, a good initial step for bivariate data analysis, especially when the dependence appears to be weak, is to test for independence between random variables. The independence test of Genest (2007) serves this purpose. The test is based on Kendall's τ estimate. The test relies on the asymptotic normality of the test statistic

$$T := \sqrt{\frac{9N(N-1)}{2(2N+5)}} |\hat{\tau}|, \quad (2.53)$$

where N is the number of observations and $\hat{\tau}$ the empirical Kendall's τ of the data. The p -value of the null hypothesis of bivariate independence is given by

$$p\text{-value} = 2 \times (1 - \Phi(T)).$$

2.10.2.2 Information criteria

In financial econometrics model selection is usually based on so called information criteria. The *Akaike Information Criterion* (AIC) of Akaike (1974) is one of the most popular model selection criteria. Joe (1997) proposed a copula selection procedure based on the Akaike information criterion. Given observations x_i , $i = 1 \dots n$, the Akaike Information Criterion (AIC) is defined as

$$AIC := -2 \sum_{i=1}^N \log f(x_i; \hat{\boldsymbol{\theta}}) + 2k, \quad (2.54)$$

where $\hat{\boldsymbol{\theta}}$ denotes the maximum likelihood estimates of $\boldsymbol{\theta}$ and k is the number of parameters $\boldsymbol{\theta} = (\theta_1, \dots, \theta_k)'$ in the model that penalise the log likelihood function

to avoid over-fitting. The AIC for a copula with density c can be written as

$$AIC := -2 \sum_{i=1}^N \log[c(u_{i,1}, u_{i,2} | \hat{\boldsymbol{\theta}})] + 2k. \quad (2.55)$$

Alternatively, the *Bayesian Information Criterion* (BIC) of Schwarz (1978) can also be used in the copula selection procedure. The BIC for a copula model with density c is given by

$$BIC := -2 \sum_{i=1}^N \log[c(u_{i,1}, u_{i,2} | \hat{\boldsymbol{\theta}})] + \log(N)k. \quad (2.56)$$

Model selection based on AIC or BIC is obtained by choosing the model which minimises the criterion used. In principle, the Bayesian information criterion penalises the log likelihood function more than the Akaike information criterion and hence usually leads to more parsimonious models.

2.10.2.3 Vuong and Clarke Tests

The Vuong test, proposed by Vuong (1989), compares two models that are non-nested and allows for a statistically significant decision between them. The test is based on the Kullback-Leiber information criterion (KLIC), which measures the distance between two statistical models. Let c_1 and c_2 be two competing copula densities with estimated parameters $\hat{\boldsymbol{\theta}}_1$ and $\hat{\boldsymbol{\theta}}_2$, respectively. In general, the model with the smaller KLIC is the preferable one, since it is closer to the true but unknown specification.

Vuong proposes to compute the standardised sum, ν , defined by

$$\nu = \frac{\frac{1}{n} \sum_{i=1}^N m_i}{\sqrt{\sum_{i=1}^N (m_i - \bar{m})^2}} \quad \text{with} \quad \bar{m} = \frac{1}{N} \sum_{i=1}^N m_i, \quad (2.57)$$

of the following statistic

$$m_i := \log \left[\frac{c_1(u_{i,1}, u_{i,2} | \hat{\boldsymbol{\theta}}_1)}{c_2(u_{i,1}, u_{i,2} | \hat{\boldsymbol{\theta}}_2)} \right], \quad (2.58)$$

for observations $u_{i,j}$, $i = 1, \dots, N$, $j = 1, 2$, i.e. Vuong showed that ν is asymptotically standard normal. Therefore, the test favours copula model 1 over copula model 2 if $\nu > z_{1-\frac{\alpha}{2}}$, where $z_{1-\frac{\alpha}{2}}$ is a $(1 - \frac{\alpha}{2})$ -quantile of the standard normal distribution. On the other hand, if $\nu < z_{1-\frac{\alpha}{2}}$, model 2 is preferred. If, however, $|\nu| \leq z_{1-\frac{\alpha}{2}}$, both models are statistically equivalent.

An alternative test for non-nested model comparison is the distribution-free test proposed by Clarke (2007). The Clarke test is similar to the Vuong test since it compares the log-likelihood of two competing models and the one with the higher

value is preferred to the other. Similar to the Vuong test, the Clarke test is based on the Kullback-Leiber Information Criterion (KLIC). The null hypothesis of statistical indistinguishability in the Clarke test, is given by

$$H_0 : P(m_i > 0) = 0.5 \quad \forall i = 1, \dots, N.$$

The intuition behind the null hypothesis is, that under statistical equivalence of the two models, the individual log-likelihood ratios are uniformly distributed around zero i.e. one half of the individual log-likelihood ratios should be greater than zero and the other half should be less than zero. Clarke (2007) proposed the following test statistic

$$B = \sum_{i=1}^N \mathbf{1}_{(0,\infty)}(m_i), \quad (2.59)$$

where $\mathbf{1}$ is an indicator function. B corresponds to the number of positive differences and is distributed as Binomial with parameters N and $p = 0.5$. Model 1 is statistically equivalent to model 2 if B is equal to the expectation $Np = \frac{N}{2}$, under the null hypothesis.

The test statistics of both the Vuong (1989) and the Clarke (2007) test are sensitive to the number of estimated parameters in each model. Both test statistics, Equation (2.57) and Equation (2.59), can be penalised by the number of parameters selected in each model, using the correction specification of the Akaike Information Criterion (AIC) in the case of the Vuong test and the parsimonious Bayesian Information Criterion (BIC) in the case of the Clarke test.

2.11 Conclusions

In this Chapter we formally define copulas and present the dependence and tail dependence properties of some of the most widely used copulas in finance literature such as the classes of elliptical and Archimedean copulas. In addition, we introduce the pair-copula construction (PCC) principle and highlight its flexibility in decomposing a multivariate density into a product of marginal densities and bivariate copula densities. We also address the need of introducing rules that uniquely decompose a joint density and thus simplify the number of possible pair-copula decompositions for high-dimensional distributions. We focus on the C-vine models which provide a distinct approach to decomposing the joint density that uses a star tree methodology. We also describe methods for inference and simulation for the C-vine models and discuss in more detail empirical methods for selecting an appropriate C-vine model. Finally, we present the tools which are commonly employed in the copula selection procedure and discuss their strengths and limitations for identifying an appropriate copula model. The practical implications in the modelling of

multivariate dependence for the majority of the models and methodologies presented in this Chapter are clearly illustrated in the empirical analysis in Chapters 3 and 4 of the present thesis.

Chapter 3

Extreme value theory and mixed canonical vine copulas on modelling energy price risks

3.1 Introduction

The understanding of joint asset return distributions is an integral part of managing portfolio risks successfully. Modelling the joint return distribution of a portfolio, however, is a non-trivial task. What makes this task non-trivial is the complex dynamics and specific characteristics of each particular asset in the portfolio on the one hand, and the varying dependency structure between all portfolio constituents on the other. In this Chapter we are concerned with describing the joint return distribution of power portfolios and computing risk measures such as *Value-at-Risk* (*VaR*) and *Conditional Value-at-Risk* (*CVaR*).

Our modelling strategy comprises two main stages. The first stage combines pseudo-maximum-likelihood fitting of time series models and extreme value theory to estimate both tails of the conditional innovations distribution of time series models. Within this framework we take into account the conditional volatility for each individual return series while assigning an explicit model to each tail of the conditional returns distribution. In the second stage, the dependency structure among portfolio return series is modelled employing a mixed canonical vine copula model. Hence, by combining a semi-parametric approach to the margins and a vine copula methodology for describing the dependency structure we aim to provide a flexible way of modelling the conditional distribution of asset returns while, at the same time, paying particular attention to the tails of the distribution, which is in practice the focus of all risk management applications.

The modelling of extreme events is the central concern of extreme value theory and the main objective of this theory is to provide asymptotic models allowing the modelling of the tails of the distribution. Extreme Value Theory (EVT) has found applications in many fields of modern science such as engineering, insurance, hydrology and many others (see for example, [Embrechts et al. 1999a](#); [Reiss and Thomas 1997](#),

among others). Over the last years, more and more research has been undertaken to analyse extreme events of financial series via EVT (see for example, Embrechts et al. 1999c; Danielsson and de Vries 1997; McNeil and Frey 2000, and references therein). EVT-based methods are suitable for tail estimation of financial time series because they provide better fit in extreme quantiles for heavy-tailed data. Furthermore, EVT-methods treat the tails of the distribution separately, offering a distinct parametric form for each tail of the distribution and allowing for asymmetry and extrapolation beyond the range of the data.

Therefore, EVT has found various risk management applications. For example, McNeil and Frey (2000) propose a method for estimating VaR and related risk measures by filtering return series with GARCH models and then applying threshold-based EVT techniques to residuals series. They found that a conditional approach that models the conditional distribution of returns is better suited for VaR estimation than the unconditional approach. In addition, Gençay and Selçuk (2004) apply EVT to daily stock market returns of emerging markets. They report that the EVT-based model dominates other parametric models in terms of VaR forecasting in extreme quantiles. With respect to the energy markets, Byström (2005) focuses on the Nord Pool intra-daily price changes and calculates extreme quantiles by fitting traditional time-series models and an EVT-based model to empirical data. He found that both in-sample and out-of sample estimates of moderate and extreme tail quantiles are more accurate than the corresponding estimates of time series models with normal or Student- t innovations. Moreover, Fong Chan and Gray (2006) propose an AR-EGARCH-EVT model for forecasting VaR which uses daily electricity prices from various power markets. In markets where the distribution of returns is characterised by high volatility, skewness and kurtosis the AR-EGARCH-EVT model dominates in terms of VaR performance.

Nevertheless, there is only limited multivariate research on the statistical properties of power portfolios. In this regard, Börger et al. (2007) analyse the joint return distribution of various energy futures series. With respect to power data, they focus on monthly and yearly Phelix futures series. According to their findings, the multivariate Normal hypothesis is strongly rejected within a commodity class as well as across commodities. They show that the class of Generalised Hyperbolic (GH) distributions is capable of fitting power futures prices and clearly outperforms the Normal distribution. Moreover, they demonstrate how the multivariate fit of the distributions can be used to estimate risk measures and also state that the exact choice of the distribution has a major influence on risk measures.

To the best of our knowledge, however, there are no studies analysing the dependence of power or other commodities portfolios using the concept of vine copula modelling. The use of copulas enables the separation of the dependence model from the marginal distributions. While over the last years there has been a growing literature on copulas, most of the research is still limited to the bivariate case where a rich variety of different copula families with distinct characteristics is available. Nevertheless, the choice of multivariate copulas is rather limited compared to the bivariate case. Apart from the multivariate Gaussian copula that does not allow for tail dependence and the Student- t copula that can only capture symmetric tail dependence, the exchangeable multivariate Archimedean copulas are extremely restrictive. Therefore, building higher-dimensional copulas is a natural next step.

The so-called *pair-copula constructions* (PCC) provides an alternative and flexible way of building multivariate distributions. The first pairwise structure was proposed by Joe (1996) and further extended by Bedford and Cooke (2001, 2002) and Kurowicka and Cooke (2006). In particular, Bedford and Cooke realised that there are many possible ways to decompose a d -dimensional density using a pairwise construction and hence they organised them graphically in the form of sequentially designed trees where only products of bivariate copulas, the so-called pair-copulas, are involved. They called these distributions *regular vines*. Aas et al. (2009) were the first to recognise that bivariate copulas for any copula family as well as several copula families can be mixed in one pair-copula construction. They also developed algorithms that allow standard maximum likelihood estimation (MLE) and simulation for two special classes of regular vines; the canonical vine (C-vine) and the drawable vine (D-vine), where each model provides a specific way of decomposing the density.

While the use of copulas in finance is popular nowadays, the literature on vine copula modelling is mainly concentrated on illustrative applications. For example, Aas and Berg (2009) fit two different classes of models for constructing higher-dimensional dependence on a four-dimensional equity data set; the nested Archimedean construction (NAC) and the pair-copula construction (PCC). The goodness-of-fit tests employed, strongly reject the NCA while the PCC (D-vine) provides an adequate fit. They also show that the PCC does not overfit the data and works satisfactory for out-of-sample *VaR* calculations. Czado et al. (2012) developed a data driven sequential approach, based on Kendall's τ estimates, for C-vine specifications. They conducted simulation studies that show the satisfactory performance of the maximum likelihood estimation procedure for mixed/non-mixed C-vine models. They also consider an application involving US-exchange rates by fitting univariate time series models to the exchange rate return series and modelling the dependencies among the resulting standardised residuals through a mixed C-vine model.

There are a few recent studies in finance literature that support the use of vine copulas for financial applications. In particular, [Mendes et al. \(2010\)](#) employ a D-vine model on a six-dimensional global portfolio with the Skewed- t distribution as the unconditional model for the marginals. They show how pair-copulas can be used on a daily basis for constructing efficient frontiers and computing VaR . In addition, [Heinen and Valdesogo \(2008\)](#) propose the canonical vine autoregressive (CAVA) model that can be viewed as a time-varying non-linear and non-Gaussian extension of the CAPM model. They focus on high-dimensional vine copula modelling. They show that neither the marginal distribution nor the dependency structure is Gaussian and the persistence in the dependence between all pairs is not the same, as implied by the DCC model. They also show that in terms of in-sample and out-of sample VaR , the CAVA model performs better than the DCC model in all portfolios examined. [Brechmann and Czado \(2013\)](#) also focus on high-dimensional vine copula modelling. They propose a factor model for analysing the dependency structure among European stocks of the Euro Stoxx 50 index, the so-called Regular Vine Market Sector (RVMS) model. The model employs a general R-vine copula construction, thus avoiding imposing the independence assumptions of the CAVA model. The authors show that the RVMS model provides good fits of the data and accurate VaR forecasts. Moreover, they show that their proposed methodology can reduce the required risk capital in contrast to the DCC model with Gaussian innovations when employed for VaR forecasting.

We believe that the contribution of our study to the existing literature is threefold. Firstly, we introduce the concept of vine copula as an alternative and more flexible way to describe the joint return distribution of power portfolios. To our best knowledge, vine copula modelling has never been used before to describe the dependency structure of power related portfolios in the literature. Secondly, we propose an extension of extreme value theory in the context of vine copula modelling that focuses mainly on extreme quantiles. We strongly believe that our proposed methodology adds an alternative perspective to the study of multivariate extremes. Finally, we compute risk measures based on this framework and discuss the implications of our findings for portfolio risk management.

The rest of this Chapter is organised as follows. Section 3.2 summarises the basic concepts of extreme value theory. Section 3.3 introduces the copula theory and presents the pair-copula construction principles and particularly the canonical vine copula modelling. Practical issues related to vines such as inference and model selection are also discussed. The model setup is explained in Section 3.4 whereas Section 3.5 presents the data. Section 3.6 reports the estimated model parameters. Section 3.7 reports VaR and $CVaR$ forecasts and their corresponding backtest results and Section 3.8 concludes.

3.2 Extreme value theory

Let X_1, \dots, X_n be a sequence of n independent and identically distributed (i.i.d.) random variables with distribution function F . Univariate extreme value theory (EVT) centres on the distribution function F with a particular focus on extreme tail quantiles. In general, within the EVT context, there are two approaches of identifying extreme events in real data. The first approach, known as *block maxima*, is the direct modelling of the distribution of minimum or maximum realisations. The other approach, known as *peak over threshold*, concentrates on the realisations that exceed a pre-specified threshold level. The peak over threshold (POT) method is employed in this particular study.

3.2.1 Peak over threshold (POT) method

The peak over threshold method is concerned with the behaviour of large observations that exceed a high threshold. Let's consider an (unknown) distribution function F of a random sample X_1, \dots, X_n . The peak over threshold approach focuses on estimating the distribution function F_u of values of x above a high threshold level u . The distribution function F_u is called *conditional excess distribution function (cedf)* and is defined as

$$F_u(y) = P(X - u \leq y \mid X > u), \quad 0 \leq y \leq x_F - u, \quad (3.1)$$

where X is a random variable, u is a given threshold, $y = x - u$ are the excesses and $x_F \leq \infty$ is the right endpoint of F . This conditional probability may be written as

$$F_u(y) = \frac{\Pr(X - u \leq y, X > u)}{\Pr(X > u)} = \frac{F(u + y) - F(u)}{1 - F(u)} = \frac{F(x) - F(u)}{1 - F(u)}. \quad (3.2)$$

The estimation of F_u is a difficult exercise as we have in general very little observations in this area. A theorem by [Balkema and De Haan \(1974\)](#) and [Pickands \(1975\)](#) is very useful at this point since it provides a powerful result about the *cedf*.

Theorem 3.2.1 ([Pickands \(1975\)](#), [Balkema and De Haan \(1974\)](#)) *For a large number of underlying distribution functions, $F_u(y)$ is well approximated by $G_{\xi, \sigma}$, the Generalised Pareto Distribution (GPD):*

$$F_u(y) \approx G_{\xi, \sigma}(y), \quad u \rightarrow \infty,$$

where

$$G_{\xi, \sigma}(y) = \begin{cases} 1 - (1 + \frac{\xi}{\sigma}y)^{-1/\xi} & \text{if } \xi \neq 0, \\ 1 - e^{-y/\sigma} & \text{if } \xi = 0, \end{cases} \quad (3.3)$$

for $y \in [0, (x_F - u)]$ if $\xi \geq 0$ and $y \in [0, -\frac{\sigma}{\xi}]$ if $\xi < 0$. $G_{\xi, \sigma}$ is the so-called

generalised Pareto distribution (GPD), $\xi = 1/\alpha$ is a shape parameter and α is the tail index.

The GPD includes a number of other distributions. For $\xi > 0$, it takes the form of the ordinary Pareto distribution, which is the most relevant for modelling the fat tails of financial time series. Also, when $\xi > 0$, $E[x^k]$ is infinite for $k > 1/\xi$. Moreover, when $\xi = 0$, the GPD corresponds to the exponential distribution whereas for $\xi < 0$ it corresponds to the Pareto II type distribution. The GPD model can be estimated with the maximum likelihood method. More precisely, [Hosking and Wallis \(1987\)](#) showed that the maximum likelihood estimates are asymptotically normally distributed for $\xi > -0.5$.

3.3 Copula theory

A copula is a multivariate distribution function $C(u_1 \dots u_d)$ defined on the unit cube $[0, 1]^d$ with uniformly distributed marginals. It provides a way of isolating the dependency structure between d random variables while allowing for arbitrary marginal distributions. The copula concept was initially developed by [Sklar \(1959\)](#). The famous theorem of [Sklar \(1959\)](#) gives the connection of marginals and copulas to the joint distribution. In general, a copula function can be extended for an arbitrary dimension d , but since our mission is to develop multivariate copulas using only bivariate copulas as building blocks, we will only focus on the bivariate case $d = 2$.

Theorem 3.3.1 (Sklar (1959)) *Let $F : \overline{\mathbb{R}}^2 \rightarrow [0, 1]$ with $\overline{\mathbb{R}} = \mathbb{R} \cup \{-\infty, +\infty\}$ be a bivariate distribution with one-dimensional marginals $F_1, F_2 : \overline{\mathbb{R}} \rightarrow [0, 1]$. Then there exists a two-dimensional copula C , such that for all $(x_1, x_2) \in \overline{\mathbb{R}}^2$*

$$F(x_1, x_2) = C(F_1(x_1), F_2(x_2)), \quad (3.4)$$

holds, and vice versa

$$C(u_1, u_2) = F(F_1^{-1}(u_1), F_2^{-1}(u_2)), \quad (3.5)$$

where u_1 and $u_2 \in [0, 1]$ and $F_1^{-1}(u_1)$ and $F_2^{-1}(u_2)$ are the inverse distribution functions of the marginals.

Let $f_X(x)$ and $f_Y(y)$ be marginal densities with joint density of $f_{XY}(x, y)$. It can be shown that the joint density can be decomposed as a product of marginal densities and copula density, $c(u, v)$, as follows

$$f_{XY}(X, Y) = \frac{\partial^2 F_{XY}(X, Y)}{\partial x \partial y} = \frac{\partial^2 C(F_X(x), F_Y(y))}{\partial x \partial y} = c(u, v) f_X(x) f_Y(y).$$

Tail dependence is another very useful copula-based measure of extreme co-movements. It is a very important property for applications concerned with the study of the dependence of extreme values, such as risk management. Many empirical studies in finance (see for example, Longin and Solnik 1995, 2001; Ang and Chen 2002; Hong et al. 2007, among others) have indicated the presence of asymmetries in financial data, meaning that lower tail dependence can be stronger than upper tail dependence or vice versa. Therefore, standard symmetric multivariate distributions are inappropriate for addressing this feature. Moreover, tail dependence is one of the properties that help distinguish between the different copula families. There are copula families that do not allow for tail dependence and copula families that only allow for either lower or upper tail dependence. There are also “reflection symmetric” copulas that imply same upper and lower tail dependence for any bivariate margin and “reflection asymmetric” copulas that allow for flexible upper and lower tail dependence.

3.3.1 Pair-copula construction

Pairwise copula construction constitutes a very useful way of building flexible multivariate distributions. The modelling principle is based on a decomposition of a multivariate density into a cascade of bivariate copulas, which is applied to original variables and to their conditional and unconditional distributions. Aas et al. (2009) were the first to realise that this construction principle can be extended by allowing arbitrary pair-copula families as building blocks. Therefore, a multivariate distribution that is decomposed using the pair-copula principle and which allows for different copula families as building blocks is called *mixed vine*. Regular vines include two main types of vines, C-vines and D-vines. Their main difference lies in the way they organise a multivariate density decomposition. C-vines utilise a star tree methodology whereas D-vines employ a line tree methodology.

Let $\mathbf{X} = (X_1, \dots, X_d)^t$ be a vector of random variables with a joint density $f(x_1, \dots, x_d)$, marginal densities $f(x_1), \dots, f(x_d)$ and marginal distributions $F_1(x_1), \dots, F_d(x_d)$. This density can be decomposed as

$$f(x_1, \dots, x_d) = f_d(x_d) \cdot f(x_{d-1}|x_d) \cdot f(x_{d-2}|x_{d-1}, x_d) \cdots f(x_1|x_2, \dots, x_d), \quad (3.6)$$

and this factorisation is unique up to a re-labelling of the variables. It can be shown that the joint distribution function $f(x_1, \dots, x_d)$, for an absolutely continuous multivariate distribution F with strictly increasing, continuous marginal densities can be factorised as

$$f(x_1, \dots, x_d) = c_{1\dots d}(F_1(x_1), \dots, F_d(x_d)) \cdot f_1(x_1) \cdots f_d(x_d), \quad (3.7)$$

where $c_{1\dots d}$ is a uniquely identified d -variate copula density.

At the beginning of this Section, we show that a bivariate joint distribution can be factorised as a product of a copula and marginal densities as follows

$$f(x_1, x_2) = c_{12}(F(x_1), F(x_2))f_1(x_1)f_2(x_2). \quad (3.8)$$

Moreover, the conditional density $f(x_1|x_2)$ can be expressed in terms of a copula as

$$f(x_1|x_2) = \frac{f(x_1, x_2)}{f_2(x_2)} = \frac{c_{12}(F(x_1), F(x_2))f_1(x_1)f_2(x_2)}{f_2(x_2)} = c_{12}(F(x_1), F(x_2))f_1(x_1). \quad (3.9)$$

For the d -dimensional case it holds that

$$f(x|\boldsymbol{\nu}) = c_{x,\nu_j|\boldsymbol{\nu}_{-j}}(F(x|\boldsymbol{\nu}_{-j}), F(\nu_j|\boldsymbol{\nu}_{-j})) \cdot f(x|\boldsymbol{\nu}_{-j}), \quad (3.10)$$

where $\boldsymbol{\nu}$ is a d -dimensional vector, ν_j is an arbitrarily chosen component of $\boldsymbol{\nu}$ and $\boldsymbol{\nu}_{-j}$ represents the $\boldsymbol{\nu}$ vector, excluding this component. In general, under appropriate regularity conditions, a joint density can be decomposed as a product of bivariate copulas, acting on several different conditional probability distributions. For example, one possible pair-copula decomposition for $d = 3$ is

$$\begin{aligned} f(x_1, x_2, x_3) &= f_3(x_3) \cdot f(x_2|x_3) \cdot f(x_1|x_2, x_3) \\ &= f_3(x_3) \cdot \underbrace{f_2(x_2) \cdot c_{23}(F_2(x_2), F_3(x_3))}_{f(x_2|x_3)} \cdot \\ &\quad \underbrace{c_{12|3}(F(x_1|x_3), F(x_2|x_3)) \cdot c_{12}(F_1(x_1), F_2(x_2)) \cdot f_1(x_1)}_{f(x_1|x_2, x_3)}. \end{aligned} \quad (3.11)$$

It is also clear that given a specific decomposition, there are still many different re-parameterizations. Thus we need to introduce rules that will enable us to decompose a joint density into a cascade of pair-copulas. However, before introducing these rules, we need to introduce another concept related to pair-copula construction. The pair-copula construction involves marginal conditional distributions of the form $F(x|\boldsymbol{\nu})$ and we need a way to evaluate such marginal conditional distribution functions. Joe (1996) showed that for every ν_j in the vector $\boldsymbol{\nu}$, $F(x|\boldsymbol{\nu})$ can be written as

$$F(x|\boldsymbol{\nu}) = \frac{\partial C_{x,\nu_j|\boldsymbol{\nu}_{-j}}(F(x|\boldsymbol{\nu}_{-j}), F(\nu_j|\boldsymbol{\nu}_{-j}))}{\partial F(\nu_j|\boldsymbol{\nu}_{-j})}, \quad (3.12)$$

where $C_{x,\nu_j|\boldsymbol{\nu}_{-j}}$ is an arbitrary copula distribution function. Following the notation of Aas et al. (2009) we will use the function $h(x, \nu; \boldsymbol{\theta})$ to represent the conditional

distribution function when x and ν are uniforms. For $x, \nu \sim U[0, 1]$ it holds

$$h_{\theta} = \frac{\partial C_{\theta}(F_x(x), F_{\nu}(\nu))}{\partial F_{\nu}(\nu)} = \frac{\partial C_{\theta(x, \nu)}}{\partial \nu}. \quad (3.13)$$

3.3.2 Canonical vines (C-vines)

There is a significant number of possible pair-copula decompositions for high-dimensional distributions. It is therefore crucial to introduce rules that can help reduce this complexity. Bedford and Cooke (2001, 2002) have introduced a graphical way of organising pair-copula density decompositions, known as *regular vines*. However, the class of regular vines is still very extended. Canonical vine (C-vine) and drawable vine (D-vine) (Kurowicka and Cooke, 2006) constitute two special cases of regular vines. In this study, we concentrate on C-vines because they have not been extensively investigated in financial applications so far.

The joint density decomposition, as organised by a C-vine, is given in the form of a nested set of star trees. For the d -dimensional C-vine, the pairs in level 1 are $(1, i)$, for $i = 2 \dots d$, and for level ℓ , $2 \leq \ell < d$, the (conditional) pairs are $(\ell, i | 1, \dots, \ell - 1)$ for $i = \ell + 1, \dots, d$. Figure 3.3.1 shows the specification for a six-dimensional C-vine. It consists of five trees, T_j , $j = 1 \dots, d - 1$. Tree T_j has $d + 1 - j$ nodes and $d - j$ edges. Each edge corresponds to a bivariate copula density whereas the edge labels correspond to the subscript of the bivariate copula density. For example, edge 34|12 corresponds to the conditional copula density $c_{34|12}(\cdot)$, where copula density $c_{34|12}(\cdot)$ can be of any parametric form. In total, $d(d - 1)/2$ pair-copula families should be chosen for the whole decomposition. The nodes in tree T_j are necessary for determining the labels of next tree T_{j+1} .

As can be seen from Figure 3.3.1, there is one node in each tree which is connected with the remaining nodes of this particular tree. In principle, the order starts with a variable that has the highest dependency on all remaining variables, the “*pilot*” variable. Conditioning all remaining variables on the first pilot variable, we can obtain the variable with the second highest dependency on all other variables. This approach is completed once we select all pilot variables for every tree (Czado et al., 2012).

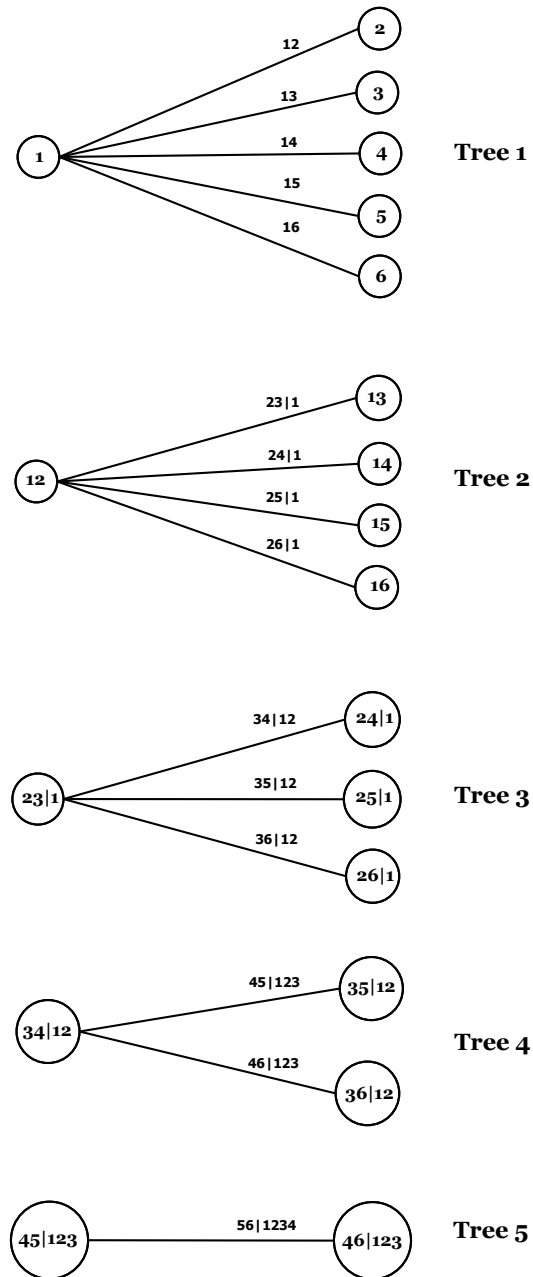


Figure 3.3.1: Tree representation of a canonical vine with 6 variables, 5 trees and 15 edges.

The d -dimensional canonical decomposition is given by [Aas et al. \(2009\)](#) as follows

$$f(\mathbf{x}) = \prod_{k=1}^d f_k(x_k) \times \prod_{i=1}^{d-1} \prod_{j=1}^{d-i} c_{i,i+j|1:(i-1)}(F(x_i|x_1, \dots, x_{i-1}), F(x_{i+j}|x_1, \dots, x_{i-1})). \quad (3.14)$$

For example, the six-dimensional canonical vine structure of Figure 3.3.1 can be written as

$$\begin{aligned} f(x_1, x_2, x_3, x_4, x_5, x_6) = & \\ & f_1(x_1)f_2(x_2)f_3(x_3)f_4(x_4)f_5(x_5)f_6(x_6) \cdot c_{1,2}(F(x_1), F(x_2)) \\ & \cdot c_{1,3}(F(x_1), F(x_3)) \cdot c_{1,4}(F(x_1), F(x_4)) \cdot c_{1,5}(F(x_1), F(x_5)) \\ & \cdot c_{1,6}(F(x_1), F(x_6)) \cdot c_{2,3|1}(F(x_{2|1}), F(x_{3|1})) \cdot c_{2,4|1}(F(x_{2|1}), F(x_{4|1})) \\ & \cdot c_{2,5|1}(F(x_{2|1}), F(x_{5|1})) \cdot c_{2,6|1}(F(x_{2|1}), F(x_{6|1})) \cdot c_{3,4|1,2}(F(x_{3|1,2}), F(x_{4|1,2})) \\ & \cdot c_{3,5|1,2}(F(x_{3|1,2}), F(x_{5|1,2})) \cdot c_{3,6|1,2}(F(x_{3|1,2}), F(x_{6|1,2})) \\ & \cdot c_{4,5|1,2,3}(F(x_{4|1,2,3}), F(x_{5|1,2,3})) \cdot c_{4,6|1,2,3}(F(x_{4|1,2,3}), F(x_{6|1,2,3})) \\ & \cdot c_{5,6|1,2,3,4}(F(x_{5|1,2,3,4}), F(x_{6|1,2,3,4})). \end{aligned} \quad (3.15)$$

It is clear that the construction is iterative by nature, and given a specific decomposition in Equation (3.14) there are as many as $\frac{d!}{2}$ possible C-vine structures. As already mentioned, for a mixed C-vine copula model we also need to choose a bivariate copula family for each of the $d(d-1)/2$ pair-copulas. It is therefore quite important to develop selection rules that allow us to select an appropriate copula family for each edge in the C-vine model. However, most of these selection rules are based on estimated C-vines. Thus, we now turn to the parameter estimation in C-vines.

3.3.3 Inference for a C-vine model

Assume a vector $x_i = (x_{i,1}, \dots, x_{i,T})^T$, $i = 1, \dots, d$ of random variables at T points in time. Further, assume that the T observations of each random variable $x_{i,t}$ are independent over time and uniformly distributed on $[0,1]$. The assumption of independence, as [Aas et al. \(2009\)](#) note, is not a limiting assumption. Most financial time series are serial correlated and thus univariate time-series models can be fitted to the margins and filter the time dependencies. As a result, the analysis can be continued with the residuals. The log-likelihood of a C-vine model can be written,

according to [Aas et al. \(2009\)](#), as

$$\ell(x; \boldsymbol{\theta}) = \sum_{j=1}^{d-1} \sum_{i=1}^{d-j} \sum_{t=1}^T \log [c_{j,j+i|1,\dots,j-1}(F(x_{j,t}|x_{1,t}, \dots, x_{j-1,t}), F(x_{j+i,t}|x_{1,t}, \dots, x_{j-1,t}))], \quad (3.16)$$

where $F(x_{j,t}|x_{1,t}, \dots, x_{j-1,t})$ and $F(x_{j+i,t}|x_{1,t}, \dots, x_{j-1,t})$ are conditional distributions and determined by Equation (3.12) and the h -function definition in Equation (3.13).

For each bivariate copula in the sum of Equation (3.16) there is at least one parameter to be determined. The number depends on the parametric assumption for each pair-copula in the C-vine model. For example, a Gaussian copula has one parameter whereas a Student- t copula has two parameters. If parametric margins are also estimated, i.e. $f_i(x_{i,t}; \delta_i)$ with $i = 1, \dots, d$, the added contribution to Equation (3.16) is

$$\sum_{t=1}^T \sum_{i=1}^d f_i(x_{i,t}; \delta_i). \quad (3.17)$$

Under this setting, full MLE estimates can be obtained by maximising Equation (3.16) combined with Equation (3.17) with respect to the parameters $(\boldsymbol{\theta}, \delta_1, \dots, \delta_d)$. In general, the full MLE estimation would be our preferred choice of estimation due to its well-known optimality properties.

Nevertheless, the Inference Functions for Margins (IFM) method is usually preferred to full MLE due to its computational tractability and comparable efficiency. The IFM method (see [Joe and Hu 1996](#); [Joe 1997](#), for more details) is a multi-step optimisation technique. It divides the parameter vector into separate parameters for each margin and parameters for the copula model. Therefore, one may break up the optimisation problem into several smaller optimisation steps with fewer parameters. For example, in the first step one may maximise the log-likelihood function of the margins in Equation (3.17) over the parameter vector $(\delta_1, \dots, \delta_d)$ and in the second step the log-likelihood function of the C-vine model in Equation (3.16), given the estimated parameters of the margins from the first step, over the parameter vector $\boldsymbol{\theta}$. The IFM method has been found highly efficient compared to full MLE optimisation for a number of multivariate models in a study by [Joe \(1997\)](#).

The IFM is a fully parametric method and thus a misspecification of the marginal distributions may affect the performance of the estimator. In addition, marginal distributions are almost always unknown in practice. This fact increases the probability of marginal misspecification. The semi-parametric (SP) method, proposed by [Genest et al. \(1995\)](#), can tackle the marginal misspecification problem since it treats the marginal distributions as unknown functions. The SP method is also known as *pseudo maximum likelihood* (PML) method. The PML method estimates

each marginal distribution non-parametrically by the empirical distribution function (*edf*) without assuming any particular parametric distribution for the marginals. Once this is completed, the dependency structure between the marginals is estimated using a parametric multivariate copula family or in our particular study a C-vine model. Kim et al. (2007) have shown that the MLE/IFM methods are non robust against marginals misspecification, and that the SP method performs better than the MLE and IFM methods, overall. Note that in our study the estimation of a C-vine model, corresponds to the IFM method when marginals are transformed to uniforms parametrically, or to the PML method when marginal transformations of the data are obtained non-parametrically.

We now turn to the estimation of C-vine models. C-vine parameters can be estimated using the sequential estimator (SE) or the maximum likelihood estimator (MLE). Following Czado et al. (2012) suppose i.i.d. data $\mathbf{u}_t = (u_{1,t}, \dots, u_{d,t})^t$ for $t = 1, \dots, T$ are available. For SE we first estimate the parameters of the unconditional bivariate copulas of tree 1. Then these estimates are used to estimate pair-copula parameters with a single conditioning variable. The estimation proceeds tree by tree, since the conditional pairs in trees $2, \dots, d - 1$ depend on the specification of the previous trees via the h -function, defined in Equation (3.13). Hence, C-vine models are estimated sequentially until all parameters are estimated. The estimation, in this context, can be carried out either using the inversion of Kendall's τ estimates for one parameter bivariate copulas or using MLE.

In particular, the parameter vector $\boldsymbol{\theta}_{1,j+1}$ of bivariate copula families $c_{1,j+1}$ in tree 1 is estimated using data $(u_{1,t}, u_{j+1,t})$, $t = 1, \dots, T$ for $j = 1, \dots, d - 1$. Given the estimated parameter vector $\hat{\boldsymbol{\theta}}^{SE}$ of tree 1, we next want to estimate the parameter vector $\boldsymbol{\theta}_{2,j+1}$ corresponding to $c_{2,j+2|1}$ for $j = 1, \dots, d - 2$ in tree 2. Define

$$\begin{aligned}\hat{v}_{2|1,t} &:= F(u_{2,t}|u_{1,t}; \hat{\boldsymbol{\theta}}_{1,1}^{SE}) = h(u_{2,t}|u_{1,t}; \hat{\boldsymbol{\theta}}_{1,1}^{SE}), \\ \hat{v}_{j+2|1,t} &:= F(u_{j+2,t}|u_{1,t}; \hat{\boldsymbol{\theta}}_{1,j+1}^{SE}) = h(u_{j+2,t}|u_{1,t}; \hat{\boldsymbol{\theta}}_{1,j+1}^{SE}),\end{aligned}$$

for $j = 1, \dots, d - 2$ and denote these estimates by $\hat{\boldsymbol{\theta}}_{2,j}^{SE}$. We can subsequently use data $(\hat{v}_{2|1,t}, \hat{v}_{j+2|1,t})$, $t = 1, \dots, T$ to estimate $\boldsymbol{\theta}_{2,j}$ for $j = 1, \dots, d - 2$. In order to estimate the parameter vector $\boldsymbol{\theta}_{3,j}$ corresponding to tree 3 and pair-copula families with double conditioning variables $c_{3,j+3|1,2}$ for $j = 1, \dots, d - 3$, we define

$$\begin{aligned}\hat{v}_{3|1,2,t} &:= h(\hat{v}_{2|1,t}|\hat{v}_{3|1,t}; \hat{\boldsymbol{\theta}}_{2,1}^{SE}), \\ \hat{v}_{j+3|1,t} &:= h(\hat{v}_{j+3|1,t}|\hat{v}_{3|1,t}; \hat{\boldsymbol{\theta}}_{2,j}^{SE}),\end{aligned}$$

and estimate $\boldsymbol{\theta}_{3,j}$ using $(\hat{v}_{3|1,2,t}, \hat{v}_{j+3|1,2,t})$, $t = 1, \dots, T$ for $j = 1, \dots, d - 3$.

Following the same reasoning, one can sequentially estimate the pair-copula parameters for each nested set of trees in the C-vine structure until all unconditional and conditional bivariate copula parameters have been estimated. The sequential estimates have been recently found by Haff (2013) to be asymptotically normal under some regularity conditions but their asymptotic covariance properties are intractable (Czado et al., 2012). To improve estimation efficiency we can use MLE estimation. It is clear that MLE requires a high-dimensional optimisation of the log-likelihood and therefore it is time consuming compared to SE. Moreover, MLE requires good starting values of the parameters in the numerical maximisation for quick convergence. Sequential estimates can be used as starting values for the optimisation.

3.3.4 C-vine decomposition and copula selection

In general, there are exactly $d!/2$ different C-vine structures available and the variation increases along with the dimension of the dataset. As a result, it is necessary to develop selection rules that uniquely decompose a C-vine model and provide an overall good fit to the data. So far, there exist only empirical selection procedures for a C-vine decomposition (see Nikoloulopoulos et al. (2012); Czado et al. (2012), for more details). The empirical selection rule of Czado et al. (2012) is followed in this study. The rule suggests a data driven sequential approach to determine the pilot variable and the $d-1$ unconditional pair-copulas in level 1 of the C-vine model. The rule works as follows. Estimate all possible pairwise Kendall's $\tau_{i,j}$ coefficients, noted $\hat{\tau}_{i,j}$, and find the variable i^* that maximises

$$\hat{S}_i := \sum_{j=1}^d |\hat{\tau}_{i,j}|, \quad (3.18)$$

over $i = 1, \dots, d$. Once the variable that is the most dependent on other variables, i^* , is selected for tree 1, we reorder the variables so that i^* becomes the first variable. We can then link the pilot variable i^* with the remaining variables and select the unconditional pair-copulas $c_{1,j+1}$, $j = 1, \dots, d-1$. The selection of appropriate copula-families is based on multiple criteria such as graphical and analytical tools as well as goodness-of-fit tests. We will discuss this choice later and assume for the moment that we are able to select a pair-copula family for each unconditional bivariate copula $c_{1,j+1}$, $j = 1, \dots, d-1$. As in the sequential estimation procedure $d-1$ transformed variables are formed.

$$\hat{v}_{j+2|1,t} := h(u_{j+2,t}|u_{1,t}; \boldsymbol{\theta}_{1,j+1}^{SE}) \quad j = 0, \dots, d-2, \quad t = 1, \dots, T. \quad (3.19)$$

Based on $d-1$ variables of size T all pairwise Kendall's τ coefficients are estimated and the pilot variable i^{**} of tree 2 that maximises Equation (3.18) is selected. Subsequently, we reorder the variables $i = 2, \dots, d$ in such a way that i^{**} is variable 2.

Having selected i^{**} as the pilot variable for tree 2, we can consequently select the copula families with single conditioning variable 1 $c_{2,j+2|1}$, $j = 1, \dots, d-2$. This procedure is continued until we determine the pilot variable for each tree as well as all corresponding pair-copulas and their associated sequential parameter estimates $\hat{\theta}^{SE}$.

When modelling the dependency structure of random variables using copulas, the true copula is always unknown. Therefore, we need tools to specify a copula family appropriate for describing the observed dependence structure of the variables. For our sequential selection procedure we only need selection rules for bivariate copulas and hence our analysis will concentrate only on copula selection in two dimensions. The problem of selecting an appropriate (bivariate) copula family is a well studied problem in the literature and many procedures have been proposed. In principle there are two different classes of tools that help in the copula selection procedure, *graphical* and *analytical* tools. In our study, we employ both sets of tools for selecting the appropriate copula family.

3.4 Model setup

To compute risk estimates for given portfolios of power price series $1, \dots, M$ on a daily basis, we choose a moving window size T for each series in the portfolio, a sample size $N = 1,000$ and portfolio weights ω_j , $j = 1, \dots, M$ with $\sum_{j=1}^M \omega_j = 1$ for equally weighted long only and $\sum_{j=1}^M \omega_j = -1$ for equally weighted short only portfolios.

- (a) We fit an ARMA(p,q) - GARCH(m,r) model for each series in the portfolio. Therefore, for $j = 1, \dots, M$ and $t = 1, \dots, T$ we estimate:

$$r_{t,j} = \mu_j + \sum_{k=1}^p \phi_{k,j} r_{t-k,j} + \varepsilon_{t,j} + \sum_{k=1}^q \theta_{k,j} \varepsilon_{t-k,j}, \quad (3.20)$$

$$\sigma_{t,j}^2 = \omega_j + \sum_{k=1}^m \alpha_{k,j} \varepsilon_{t-k,j}^2 + \sum_{k=1}^r \beta_{k,j} \sigma_{t-k,j}^2, \quad (3.21)$$

$$\varepsilon_{t,j} = \sigma_{t,j} z_{t,j}, \quad (3.22)$$

where the error term $z_{t,j}$ in Equation (3.22) is an i.i.d. sequence with zero mean, unit variance and distribution functions, denoted by $F_{\text{norm},j}$ and $F_{t,j}$ (i.e., standard normal and standardised Student- t), respectively. Subsequently, we compute standardised residuals

$$\hat{z}_{t,j} = \frac{1}{\hat{\sigma}_{t,j}} \left(r_{t,j} - \hat{\mu}_j - \sum_{k=1}^p \hat{\phi}_{k,j} r_{t-k,j} - \hat{\sigma}_{t,j} \hat{z}_{t,j} - \sum_{k=1}^q \hat{\theta}_{k,j} \hat{\sigma}_{t-k,j} \hat{z}_{t-k,j} \right). \quad (3.23)$$

- (b) For the C-vine-EVT and A-C-vine-EVT models we fix a high threshold level u for the upper and lower tails of the residuals distribution and assume that excess residuals over this threshold follow the Generalised Pareto Distribution (GPD). The resulting piecewise semi-parametric distribution, denoted by $F_{\text{evt},j}$, encompasses the estimates of the parametric tails and the non-parametric kernel-smoothed interior.
- (c) We transform the standardised residuals to copula data either parametrically (C-vine-Norm, C-vine- t) or non-parametrically (C-Vine-EVT, A-C-vine-EVT).
- (d) We fit a canonical vine model to the set $\mathbf{u} = (\mathbf{u}_{t,1}, \dots, \mathbf{u}_{t,M})$ obtained from the previous step.
- (e) For each $n = 1, \dots, N$, we generate a sample of $\tilde{u}_1, \dots, \tilde{u}_M$ uniforms from the estimated C-vine model, \hat{C}_t , of the previous step.
- (f) We convert $\tilde{u}_1, \dots, \tilde{u}_M$ to standardised residuals $(\hat{z}_{t+1,1}, \dots, \hat{z}_{t+1,M})'$ using the inverse of the corresponding distribution function for each model, $\hat{F}_{\text{evt},j}^{-1}(\tilde{u}_j)$, $\hat{F}_{\text{norm},j}^{-1}(\tilde{u}_j)$ or $\hat{F}_{t,j}^{-1}(\tilde{u}_j)$.
- (g) Based on the estimated conditional mean in Equation (3.20) and variance in Equation (3.21) of step (a), we compute the ex-ante GARCH variance forecasts for $j = 1, \dots, M$,

$$\sigma_{t+1,j}^2 = \hat{\omega}_j + \sum_{k=1}^m \alpha_{k,j} \varepsilon_{t+1-k,j}^2 + \sum_{k=1}^r \beta_{k,j} \sigma_{t+1-k,j}^2. \quad (3.24)$$

- (h) The estimated ARMA parameters and the GARCH variance forecasts in Equation (3.24) are used to compute the ex-ante return forecast for $j = 1, \dots, M$,

$$\hat{r}_{t+1,j} = \hat{\mu}_j + \sum_{k=1}^p \hat{\varphi}_{k,j} r_{t+1-k,j} + \hat{\sigma}_{t+1,j} \hat{z}_{t+1,j} + \sum_{k=1}^q \hat{\theta}_{k,j} \hat{\sigma}_{t+1-k,j} \hat{z}_{t+1-k,j}. \quad (3.25)$$

- (i) The portfolio return forecast, $\hat{r}_{t+1,P}$, is given by

$$\hat{r}_{t+1,P} = \omega_1 \hat{r}_{t+1,1} + \dots + \omega_M \hat{r}_{t+1,M}. \quad (3.26)$$

- (j) We compute VaR and $CVaR$ forecasts by taking α -quantiles of the portfolio return forecasts

$$VaR_{t+1|t}(\alpha) = F^{-1}(q) \hat{r}_{t+1,P}, \quad (3.27)$$

$$CVaR_{t+1|t}(\alpha) = E(\hat{r}_{t+1,P} | \hat{r}_{t+1,P} > VaR_{t+1|t}(\alpha)), \quad (3.28)$$

where $F^{-1}(q)$ is the q th quantile ($q = 1 - \alpha$) of the portfolio return forecasts, $\hat{r}_{t+1,P}$.

3.5 Data description

This study focuses on power portfolios consisting of spot and futures Phelix power contracts traded at the European Energy Exchange (EEX). Phelix Futures are traded for the current week and the next four weeks (Phelix Week Futures), the current month and the next nine months (Phelix Month Futures), the next eleven quarters (Phelix Quarter Futures) and the next six years (Phelix Year Futures). Year and quarter futures are fulfilled by cascading, i.e. futures contracts with longer delivery periods are replaced by equivalent futures contracts with shorter delivery periods on the last day of trading. Therefore, three exchange trading days before the beginning of delivery, year and quarter futures cascade into the respective quarter or month futures whereas the month Phelix futures remain tradeable during the delivery period and reach their expiry date on the exchange trading day before the last delivery day. The power portfolios of the present analysis include time series of spot and futures contracts with delivery during the base (Phelix Baseload) and peak (Phelix Peakload) hours of each day. The choice of the portfolio constituents is based on their high level of trading interest and liquidity. The Baseload and Peakload portfolios include:

- One, two and three months ahead generic time series of daily electricity Phelix Baseload (F1BM, F2BM and F3BM) and Phelix Peakload (F1PM, F2PM and F3PM) futures prices.
- One and two quarters ahead generic time series of daily electricity Phelix Baseload (F1BQ and F2BQ) and Phelix Peakload (F1PQ and F2PQ) futures prices.
- One and two years ahead generic time series of daily electricity Phelix Baseload (F1BY and F2BY) and Phelix Peakload (F1PY and F2PY) futures prices.
- Historical time series of daily day-ahead electricity Phelix Baseload (SpotB) and Phelix Peakload (SpotP) prices.

Both datasets cover a time period of almost 8 years worth of data. The Baseload dataset covers the period from January 2, 2004 to February 7, 2012 whereas the Peakload dataset covers the period from January 2, 2004 to February 22, 2012. In total, there are 2,058 and 2,068 daily price observations for each series in the Baseload and Peakload portfolios, respectively. However, the present study does not analyse the price levels of portfolio constituents directly, but instead focuses on the log-returns of “generic time series”.

Generic time series are artificially constructed time series that represent the prices of futures with (approximately) same time to maturity. For example, a one-month-ahead generic Phelix Baseload futures is the price series that corresponds to the next-to-delivery contract. The employment of generic time series is useful for ruling out the well-known Samuelson effect of futures contracts. In general, the variance of a futures contract increases when the contract approaches maturity. This behaviour is known as the Samuelson effect and is observable both in price levels and in the log-returns of individual contracts. Since generic time series always correspond to futures contracts with same time before delivery, they will not exhibit increasing volatility within any of the time series (Börger et al., 2007).

For generic return series, however, we transform the data further to account for the roll-over of the futures contracts and the large jumps in the returns series that do not stem from price formation at exchanges. For example, the price for a one-month-ahead generic on January 31, 2011 is the price of the Phelix Feb 2011 Month contract and the price of the same contract on the next trading day (February 1, 2011) is the price of the Phelix Mar 2011 Month contract. Calculating the return between these two days may involve a significant jump in the return series due to the possibility of the products having different means. To overcome this problem, we apply an overlap of one day every time that a specific contract approaches its last trading day and a new contract comes into play. Another problem arises with the quarterly and yearly futures contracts because they cease trading three business days before the delivery period. For example, the Phelix Apr 2011 Quarter contract is traded until March 29, 2011. The last return for this contract can be calculated using the prices on March 28 and 29, 2011. The return on March 29 is excluded since it is based on the price of the Phelix Apr 2011 Quarter contract obtained on March 29, 2011 and that of the Phelix Jul 2011 Quarter contract obtained on the next trading day, March 30, 2011. Therefore, as in the monthly contract case, we have an overlap of one day every time that a quarterly or yearly futures contract reaches its last trading day and a new contract comes into play. Nevertheless, monthly and quarterly or yearly contracts, as explained above, expire on different trading days within the same calendar month. Hence, when calculating returns of generic time series, the monthly return overlaps do not tally with the quarterly or yearly return overlaps.

This problem is solved by excluding the monthly returns every time that they correspond to the one day overlap of the quarterly or yearly contracts. Since we deal with multivariate time series and are thus interested in the longest possible joint time series, we also delete trading days which are statutory holidays or weekend days. Phelix futures contracts are not traded during weekends or statutory holidays whereas Phelix day-ahead spot power contracts are traded every day of every single week during the entire year. Figure 3.5.1 displays the actual and transformed generic

return series of the Baseload portfolio. Figure 3.5.1 makes clear the presence of price spikes due to the roll-over of the futures contracts. Therefore, if we do not take this fact into account and exclude them from our estimation sample, their presence will cause severe misspecification problems to our model.

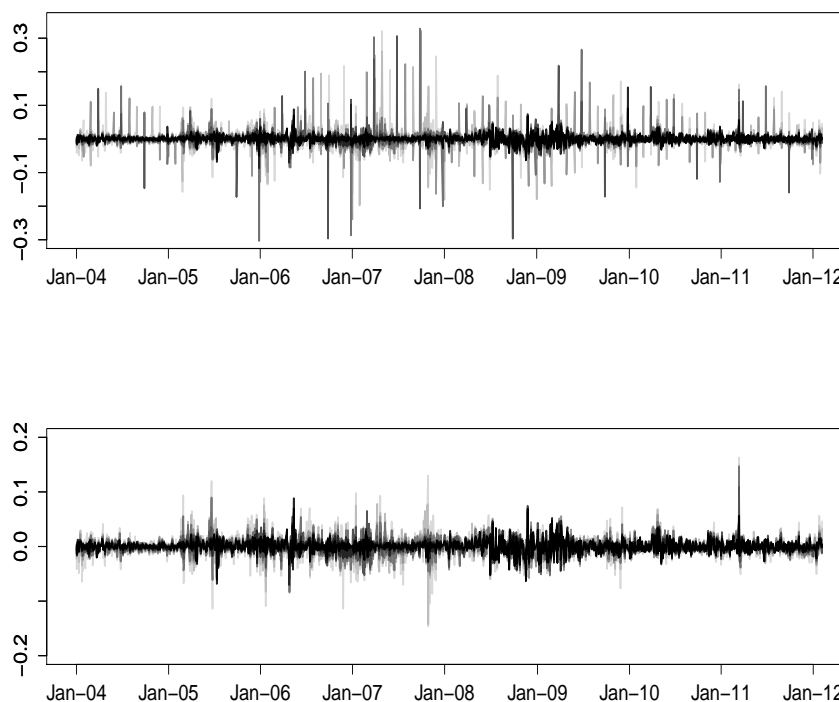


Figure 3.5.1: **Upper:** Log-returns of generic Phelix Baseload futures without adjustment for the roll-over of futures contracts. **Lower:** Log-returns of generic Phelix Baseload futures with adjustment for the roll-over of the futures contracts.

Tables 3.5.1 and 3.5.2 show the descriptive statistics of spot and generic futures returns, after excluding the artificial jumps from each futures contract. At first glance, we can note that the number of observations in both samples has been reduced due to the adjustment in the futures contracts. The mean returns are close to zero and slightly negative for most of the series considered in both datasets. What is also evident is the decrease in volatility as we move from the spot series to futures contracts with longer time to maturity. In other words, the volatility term-structure can be read off across the different generics. Figure 3.5.2 displays the contrast between the one-month-ahead generic Phelix Baseload and Peakload futures returns and the three-months-ahead generic Phelix Baseload and Peakload futures returns. It is clear that the one-month-ahead futures returns are more volatile compared to the three-months-ahead futures returns both in the Baseload and the Peakload portfolios. This behaviour can also be observed in Tables 3.5.1 and 3.5.2 by comparing the sample volatility estimates for each series in the two portfolios.

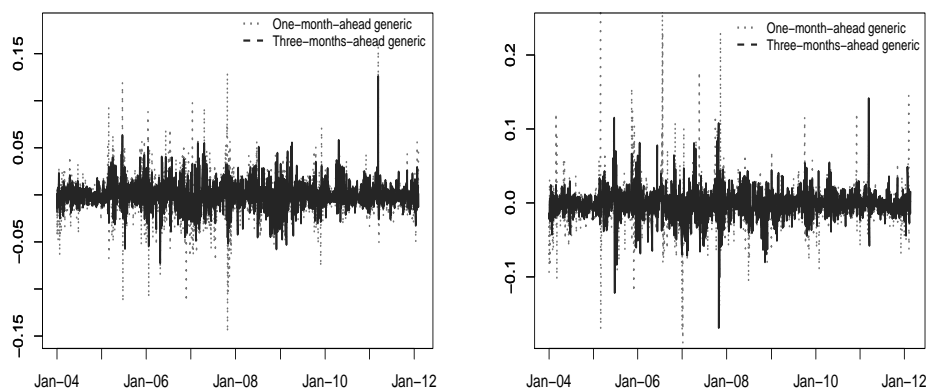


Figure 3.5.2: **Left:** Log-returns of generic Phelix Baseload one-month-ahead and three-months-ahead power futures. **Right:** Log-returns of generic Phelix Peakload one-month-ahead and three-months-ahead power futures.

The volatility of the spot series is the highest among all series in both portfolios whereas it declines gradually as the expiration of the futures contracts increases. The maximum and minimum returns of the spot series reach extreme values in both portfolios, while the maximum and minimum returns of generic futures in the Peakload portfolio are higher compared to the values of the corresponding contracts in the Baseload portfolio. All return series are leptokurtotic with fat tails, as indicated by the positive values of (excess) kurtosis which is present in all series. The spot return series are characterised by negative skewness due to the extreme negative spikes that are present in the spot series whereas almost all generic return series in both portfolios have positive values of skewness. Furthermore, the high values of Jarque-Bera statistics and their respective zero p -values reject the assumption of normality for each series in the two portfolios.

Table 3.5.1: Baseload portfolio summary statistics

	SpotB	F1BM	F2BM	F3BM	F1BQ	F2BQ	F1BY	F2BY
# of Obser.	1934	1934	1934	1934	1934	1934	1934	1934
Mean	0.0025	-0.0012	-0.0005	-0.0002	-0.0003	0.0000	0.0002	0.0002
Variance	0.0260	0.0005	0.0003	0.0002	0.0002	0.0002	0.0001	0.0001
Stand. Dev.	0.1613	0.0218	0.0173	0.0146	0.0144	0.0123	0.0112	0.0097
Min	-1.0764	-0.1461	-0.1423	-0.0727	-0.0836	-0.0615	-0.0705	-0.0634
Max	1.0964	0.1627	0.1489	0.1261	0.1463	0.1091	0.0884	0.0699
Exc. Kurtosis	6.8255	6.0707	7.4221	4.7930	7.9588	6.5901	6.3463	7.0465
Skewness	-0.0677	0.1914	0.2660	0.3097	0.5523	0.3647	0.0118	0.1531
JB	3766.7	29.7	4474.9	18.4	5217.3	3553.1	3255.4	4020.6
p -value	0.0000	0.0000	0.0000	0.0000	0.0000	0.0000	0.0000	0.0000

This table reports summary statistics of spot and generic futures returns for the Baseload portfolio.

Table 3.5.2: Peakload portfolio summary statistics

	SpotP	F1PM	F2PM	F3PM	F1PQ	F2PQ	F1PY	F2PY
# of Obser.	1945	1945	1945	1945	1945	1945	1945	1945
Mean	0.0031	-0.0019	-0.0019	-0.0010	-0.0004	-0.0007	-0.0003	-0.0001
Variance	0.0338	0.0008	0.0007	0.0004	0.0002	0.0002	0.0002	0.0001
Stand. Dev.	0.1838	0.0278	0.0272	0.0195	0.0158	0.0157	0.0123	0.0101
Min	-1.3757	-0.1898	-0.2263	-0.1691	-0.0918	-0.1457	-0.0886	-0.0615
Max	1.3233	0.3295	0.1944	0.1415	0.1549	0.1501	0.1254	0.0670
Exc. Kurtosis	8.8130	27.4211	9.5097	8.2933	9.3500	12.3454	10.4967	4.5930
Skewness	-0.1440	2.1953	-0.1580	0.0194	0.4320	0.2912	0.3861	0.0030
JB	6318.5	62640.4	7356.9	5589.6	7164.6	12410.5	9001.2	1715.4
<i>p</i> -value	0.0000	0.0000	0.0000	0.0000	0.0000	0.0000	0.0000	0.0000

This table reports summary statistics of spot and generic futures returns for the Peakload portfolio

3.6 Application to Phelix power portfolios

In this Section we implement the modelling framework, described in Section 3.4, to forecast daily *VaR* and *CVaR* estimates. First, we model the conditional mean and variance of each return series through time series models. An appropriate ARMA-GARCH model is selected for each individual series. For the C-vine-EVT models, a semi-parametric distribution is fitted to each series of standardised residuals. We transform the standardised residuals to uniforms either parametrically (C-vine-Norm and C-vine-*t*) or non-parametrically (C-vine-EVT and A-C-vine-EVT). The uniforms are used as input data for pair-copula construction. A canonical mixed vine copula structure is fitted to model the joint distribution of the portfolio return series. Both sequential and full maximum likelihood parameters for the C-vine models are estimated. Based on the estimated C-vine structures and ARMA-GARCH models, next-period returns are simulated and *VaR* and *CVaR* estimates are computed.

3.6.1 Univariate fitting of margins using ARMA-GARCH models

The modelling procedure for building an appropriate ARMA-GARCH model, especially when data are “messy”, is not always straightforward. The stylised features of each time series analysed in this study are very complex and hence the selection of an appropriate model is a non-trivial exercise. To select an appropriate model for the conditional mean and variance of each particular series we work as follows. Firstly, the AIC information criterion is applied to every return series of both portfolios and the models, as suggested by the criterion, are estimated. For the conditional variance equation a low-order GARCH(1,1) model is specified for each series and, if we cannot adequately model the volatility dynamics of the series, an extra term is added each time until all “ARCH-effects” have been successfully removed from the squared residual series. If a model cannot remove the serial correlation from the

residual series due to significant higher order autocorrelation and partial autocorrelation lags, then a suitable AR or MA term is added to the mean specification at the specific significant high lag orders, to address the seasonal behaviour, and the model is re-estimated and tested for its adequacy. The conditional mean equations for all series under consideration can be found in Appendix 3.A. With respect to the conditional variance models, it seems that a GARCH(1,1) specification is adequate for all series. The estimated parameters of the ARMA-GARCH models for almost all cases appear statistically significant at 5% level. Moreover, there is clear evidence that the models' assumptions are satisfied¹. Therefore, we assume that the selected time series models are adequate to model the conditional mean and variance of the Phelix Baseload and Peakload portfolio return series.

3.6.2 Semi-parametric modelling of margins

The semi-parametric modelling of margins has the advantage that we have an explicit model for each tail. Therefore, we implement the peak over threshold (POT) method and fit the GPD to observations in the residual series that exceed a high threshold level u . The most important step in estimating the parameters of the GPD is the choice of the threshold u . Theorem 3.2.1 tells us that u should be high enough to approximate the conditional excess distribution by the GPD. On the other hand, the higher the threshold the less observations are left for the estimation of parameters and consequently the variance of the parameter estimates increases. So far, there is no formal method for optimal threshold level selection. In this study we follow [McNeil and Frey \(2000\)](#) and set the threshold level at the 8th and 92th percentiles of the residuals distribution for the lower and upper tail, respectively.

As a result of these threshold levels, 134 observations for the Baseload portfolio residual series and 135 observations for the Peakload portfolio residual series are used in the estimation process. Table 3.6.1 presents the percentage return threshold values u and the maximum likelihood GPD estimates of the tail index ξ and the scale parameter σ with the corresponding standard errors for upper and lower tails. The estimated tail index values for the Phelix Baseload portfolio range between -0.124 (F2BQ, upper tail) and 0.180 (F1BY, lower tail) whereas for the Phelix Peakload portfolio they range between -0.140 (F1PY, upper tail) and 0.138 (F2PM, upper tail). Recall that $\xi > 0$ corresponds to heavy-tailed distributions whose tails decay like power functions, such as the Pareto, Student's- t , Cauchy and Fréchet distributions. The case $\xi = 0$ corresponds to distributions whose tails decay exponentially. In this category belong the normal, exponential, gamma and lognormal distributions. Finally, the case $\xi < 0$ corresponds to short-tailed distributions with a finite

¹The estimation results and residual diagnostic tests are not presented due to space limitation but are available upon request to the authors.

right endpoint, such as the uniform and beta distributions (McNeil and Frey, 2000).

Table 3.6.1: Maximum likelihood GPD estimates

Baseload Portfolio										
Series	Lower tail					Upper tail				
	u (%)	$\hat{\xi}$	$se(\xi)$	$\hat{\sigma}$	$se(\sigma)$	u (%)	$\hat{\xi}$	$se(\xi)$	$\hat{\sigma}$	$se(\sigma)$
SpotB	-1.259	0.126	0.091	0.606	0.076	1.273	0.087	0.099	0.603	0.079
F1BM	-1.342	-0.037	0.078	0.549	0.064	1.340	-0.099	0.092	0.729	0.092
F2BM	-1.340	0.004	0.083	0.503	0.060	1.351	-0.018	0.091	0.650	0.081
F3BM	-1.337	-0.050	0.085	0.592	0.072	1.391	-0.072	0.070	0.610	0.068
F1BQ	-1.337	-0.060	0.095	0.580	0.075	1.391	0.000	0.090	0.577	0.072
F2BQ	-1.363	0.120	0.099	0.477	0.063	1.374	-0.124	0.086	0.612	0.074
F1BY	-1.279	0.180	0.096	0.530	0.068	1.368	-0.096	0.092	0.522	0.066
F2BY	-1.245	0.161	0.093	0.589	0.075	1.378	0.010	0.097	0.517	0.067

Peakload Portfolio										
Series	Lower tail					Upper tail				
	u	$\hat{\xi}$	$se(\xi)$	$\hat{\sigma}$	$se(\sigma)$	u	$\hat{\xi}$	$se(\xi)$	$\hat{\sigma}$	$se(\sigma)$
SpotP	-1.259	0.068	0.101	0.528	0.070	1.323	0.057	0.104	0.704	0.095
F1PM	-1.335	0.065	0.103	0.562	0.075	1.274	-0.013	0.106	0.727	0.099
F2PM	-1.365	-0.056	0.080	0.565	0.066	1.276	0.138	0.098	0.589	0.077
F3PM	-1.326	-0.087	0.091	0.672	0.084	1.285	0.096	0.108	0.612	0.084
F1PQ	-1.387	0.092	0.114	0.476	0.068	1.292	0.069	0.090	0.602	0.075
F2PQ	-1.323	-0.042	0.084	0.697	0.084	1.282	-0.008	0.073	0.613	0.069
F1PY	-1.278	0.110	0.092	0.568	0.071	1.333	-0.140	0.076	0.634	0.072
F2PY	-1.320	0.045	0.076	0.635	0.073	1.336	-0.014	0.106	0.552	0.075

This table reports maximum likelihood estimates (MLE) of the parameters of the Generalised Pareto Distribution (GPD) and threshold percentage returns (u (%)) corresponding to 8% and 92% of empirical quantiles for lower and upper tail, respectively.

High values of the estimated tail index are an indication of extreme values since $\xi > 0$ reflects heavy-tailed distributions. According to the tail index parameter estimates, most of the tail forms do not correspond to fat-tailed distributions. The highest positive tail index value equals to 0.180 and corresponds to the F1BY Phe-lix Baseload series. This value, though, does not imply a very fat-tail form. For example, an empirical study by Byström (2005), using extremely fat-tailed Nord Pool hourly electricity prices, found that a Fréchet distribution applies to the upper tail of standardised residuals. Similar results were also found by Fong Chan and Gray (2006). The above evidence is not strongly supported by our empirical GPD parameter estimates. The upper tail index GPD estimates for Spot Baseload and Peakload data are positive but their numerical values cannot reach the values of

the tail index parameters of the above studies. This is probably an indication that Phelix Spot market does not experience so many extreme price events compared to other electricity markets.

3.6.3 Selection and estimation of C-vine models

Four different C-vine structures are estimated for both portfolios. Table 3.6.2 summarises the specifications of the models investigated. The selection of copula families for each pair-copula in the C-vine specification is mainly based on the Akaike Information Criterion (AIC). There are two main reasons behind this choice. Firstly, it is practically impossible, in large dimensions, for one to investigate every single unconditional and conditional pair-copula in the vine structure and define accordingly an appropriate copula family for each of these pairs. As a result, we use the AIC, which is the most frequently used criterion in copula selection literature. The range of all possible copula families employed by the criterion is defined in Appendix 3.B. The second main reason that drives our copula selection strategy is related to the theoretical and empirical results of the studies by [Joe et al. \(2010\)](#) and [Nikoloulopoulos et al. \(2012\)](#).

[Joe et al. \(2010\)](#) show that vine copulas can have a different upper and lower tail dependence for each bivariate margin when asymmetric bivariate copulas with upper/lower tail dependence are used in level 1 of the vine. In other words, in order for a vine copula to have tail dependence for all bivariate margins, it is necessary for the bivariate copulas in level 1 to have tail dependence but it is not necessary for the conditional bivariate copulas in levels $2, \dots, d - 1$ to have tail dependence, too. At levels 2 or higher, Independence or Gaussian copulas might be adequate to model the dependency structure. Moreover, [Nikoloulopoulos et al. \(2012\)](#) show that vine copulas with bivariate Student- t linking copulas tend to be preferred in likelihood-based selection methods because they provide a better fit in the middle for the first level of the vine. They suggest that for inference involving the tails, the “best-fitting” copula should not be entirely likelihood-based but also depend on matching the non-parametric tail dependence measures and extreme quantiles. Taking these results into account, we also consider a hybrid of the C-vine-EVT model, where all Student- t bivariate linking copulas selected by the AIC in level 1 are replaced by asymmetric copula families. If the empirical data present different degrees of tail dependence, we expect to get more accurate risk measure estimates from vine models that allow asymmetries.

Table 3.6.2: Summary of models investigated for the Phelix Baseload and Peakload portfolios

Model	Model type
C-vine-EVT	Mixed C-vine model with semi-parametric margins
A-C-vine-EVT	Same as C-vine-EVT model but all t-copulas in tree 1 are replaced by asymmetric copula families
C-vine-Norm	C-vine copula with all pair-copulas being Gaussian copulas and normal margins
C-vine- t	C-vine with all pair-copulas being t-copulas and Student-t margins

This table summarises the alternative specifications applied to the Phelix Baseload and Peakload portfolios for modelling their joint distribution and forecasting VaR and $CVaR$.

3.6.4 Baseload selection and estimation results

After filtering the original return series with the appropriate ARMA-GARCH models, the resulting standardised residual series are transformed to uniform pseudo-observations. Figure 3.6.3 displays scatter plots and the estimated Kendall's τ coefficients of standardised residual series. The results highlight the positive dependence among the generic residual series and the almost absolute independence between the spot residual series and the rest of the series in the Phelix Baseload portfolio. Moreover, Figure 3.6.4 provides insight regarding the degree of tail dependence. In particular, Figure 3.6.4 displays Chi-plots of the upper right and lower left quadrants of the series that allow us to detect upper and lower tail dependence. Figure 3.6.4 illustrates a variety of tail dependence behaviours among the residual series. Most of the series either do not show significant tail dependence or show symmetric tail dependence. However, there are a few cases that display some degree of asymmetric tail dependence.

We now apply the sequential procedure of [Czado et al. \(2012\)](#) to select an appropriate C-vine copula model for the Phelix Baseload copula data. Table 3.6.3 reports the empirical Kendall's τ correlation matrix of the transformed residual series and the sum of their absolute values, denoted by \hat{S} and defined in Equation (3.18). According to Table 3.6.3, the i^* variable that maximises the sum of absolute values, \hat{S} , is the F1BQ series and consequently it is placed as the pilot variable in level 1 of the vine structure. Table 3.6.4 presents the empirical Kendall's τ matrix of the series, conditioned on $i^* = \text{F1BQ}$, and the sum over the absolute entries of each row. The i^{**} variable that maximises \hat{S} is the F1BY series and is set as the pilot variable in level 2. Following the same identification procedure, the ordering of the variables for the mixed C-vine structure in the Baseload portfolio is specified as follows

$$F1BQ - F1BY - F1BM - F2BY - F2BQ - SpotB - F3BM - F2BM$$

Table 3.C.1 in Appendix 3.C provides an overview of selected unconditional and conditional pairs for each level of the C-vine model. The above sequential procedure not only identifies an appropriate factorisation for the mixed C-vine model but also identifies the pair-copula families for each tree and provides sequential estimates $\hat{\theta}^{SE}$.

Table 3.6.3: Kendall's τ correlation matrix and \hat{S} estimates for the Phelix Baseload portfolio

	SpotB	F1BM	F2BM	F3BM	F1BQ	F2BQ	F1BY	F2BY	\hat{S}
SpotB	1.00	-0.02	-0.02	-0.03	-0.03	-0.03	-0.04	-0.05	1.20
F1BM	-0.02	1.00	0.66	0.58	0.65	0.48	0.45	0.39	4.22
F2BM	-0.02	0.66	1.00	0.68	0.75	0.57	0.54	0.48	4.70
F3BM	-0.03	0.58	0.68	1.00	0.79	0.61	0.58	0.50	4.76
F1BQ	-0.03	0.65	0.75	0.79	1.00	0.64	0.62	0.54	5.02
F2BQ	-0.03	0.48	0.57	0.61	0.64	1.00	0.72	0.63	4.67
F1BY	-0.04	0.45	0.54	0.58	0.62	0.72	1.00	0.75	4.70
F2BY	-0.05	0.39	0.48	0.50	0.54	0.63	0.75	1.00	4.35

This table reports the unconditional empirical Kendall's τ estimates and the sum over the absolute entries of each row for the Phelix Baseload portfolio copula data. The boldface value in the \hat{S} column indicates the variable that maximises the sum of Kendall's τ absolute values.

Table 3.6.6 presents the resulting mixed C-vine-EVT model and the sequential and maximum likelihood estimates. All pair-copula families are selected by the AIC without testing for independence, and the sequential estimates are used as initial values to obtain maximum likelihood estimates. It can be seen that the sequential $\hat{\theta}^{SE}$ and maximum likelihood $\hat{\theta}^{MLE}$ estimates are pretty close for all estimated models. These findings support the employment of sequential estimation as the preferred optimisation method. With respect to copula selection, 13 different copula types were selected for the 28, in total, different pair-copulas in the C-vine-EVT model. The majority of the selected copula families correspond to the Student- t copula. The empirical results of our likelihood-based copula selection procedure seem to agree with the empirical findings of [Nikoloulopoulos et al. \(2012\)](#). In particular, 5 out of 8 selected copula families in level 1 belong to the Student- t copula. Based on the above results, we specify the A-C-vine-EVT model by replacing the selected Student- t copula families of level 1 with asymmetric copula families. For levels $2 \dots d - 1$, the selection of the appropriate copula family is based on the AIC. We also test for independence in the C-vine model. The Independence copula is selected for pair-copulas that cannot reject the null hypothesis of independence.

Table 3.6.4: Kendall's τ correlation matrix and \hat{S} estimates for the Phelix Baseload portfolio.

	F3BM i^*	F1BY i^*	F2BM i^*	F2BQ i^*	F2BY i^*	F1BM i^*	SpotB i^*	\hat{S}
F3BM i^*	1.00	0.07	-0.01	0.08	0.02	-0.06	0.01	1.25
F1BY i^*	0.07	1.00	-0.00	0.48	0.59	-0.08	-0.02	2.24
F2BM i^*	-0.01	-0.00	1.00	0.01	-0.02	0.20	0.01	1.25
F2BQ i^*	0.08	0.48	0.01	1.00	0.38	-0.07	-0.01	2.03
F2BY i^*	0.02	0.59	-0.02	0.38	1.00	-0.10	-0.03	2.13
F1BM i^*	-0.06	-0.08	0.20	-0.07	-0.10	1.00	0.01	1.52
SpotB i^*	0.01	-0.02	0.01	-0.01	-0.03	0.01	1.00	1.09

This table reports the conditional empirical Kendall's τ estimates and the sum over the absolute entries of each row for the Phelix Baseload portfolio copula data, conditioned on $i^* = \text{F1BQ}$ variable. The boldface value in the \hat{S} column indicates the variable that maximises the sum of Kendall's τ absolute values.

The specification of appropriate asymmetric copula families in place of the selected Student- t copula families in level 1 of the C-vine-EVT model is based on a set of analytical and graphical tools. In particular, we employ the [Vuong \(1989\)](#) and [Clarke \(2007\)](#) goodness-of-fit tests as well as the empirical and theoretical contour plots and λ -function plots to assess the fit of the selected copula families to the empirical data. Table 3.6.5 reports the Vuong and Clarke test results of the selected Student- t pair-copulas in level 1 against copula families with a different tail dependence. We employ copula families with only upper or only lower tail dependence and families whose upper tail dependence is different from their lower tail dependence. The goodness-of-fit results of Table 3.6.5 are in line with the AIC results of the C-vine-EVT model. Both tests provide the highest scores for the Student- t copula for each pair analysed. The BB1 and SBB1 families obtain the second highest scores whereas the rest of the copula families employed obtain negative scores for most of the pairs under consideration.

Table 3.6.5: Vuong and Clarke goodness-of-fit test results

Test	Pairs	Student- t	C	G	J	BB1	BB6	BB7	BB8	SBB1	SBB7
Vuong test	F1BQ-F1BY	8	-8	-1	-8	5	-3	-2	6	5	-2
	F1BQ-F1BM	9	-8	0	-8	6	-2	-1	-1	6	-1
	F1BQ-F2BQ	9	-8	0	-8	5	-2	-1	1	5	-1
	F1BQ-F3BM	9	-8	1	-8	6	-1	0	-5	6	0
	F1BQ-F2BM	9	-8	3	-8	6	1	-3	-3	6	-3
Clarke test	F1BQ-F1BY	9	-8	1	-8	5	-1	-4	5	5	-4
	F1BQ-F1BM	9	-8	3	-8	6	1	-4	-1	6	-4
	F1BQ-F2BQ	9	-7	2	-9	6	0	-4	1	6	-4
	F1BQ-F3BM	9	-8	3	-8	5	1	-2	-5	7	-2
	F1BQ-F2BM	9	-8	3	-8	6	1	-3	-3	6	-3

This table reports results for the Vuong and Clarke goodness-of-fit tests. For each possible pair of copula families the Vuong and the Clarke tests decides which of the two families fits the given data best and assigns a score - pro or contra a copula family - according to this decision.

The above test results imply tail dependence in the pairs analysed, since the copula families with the highest scores suggest symmetric (Student- t copulas) or asymmetric (BB1 and SBB1) upper and lower tail dependence while copula families that have only upper or only lower tail dependence are disregarded. Therefore, it seems that the employment of asymmetric copula families is not necessary for our data set. As indicated by the Chi-plots of Figure 3.6.4 and the likelihood-based goodness-of-fit test results, it seems that there is a symmetric tail dependence and thus Student- t copula is the appropriate copula family for modelling this behaviour.

Nevertheless, we want to investigate whether the specification of asymmetric copula families in place of Student- t selected copula families in level 1 of the vine structure can improve the model performance in VaR and $CVaR$ forecasting. Thus, we replace the Student- t copulas of the F1BQ-F1BY, F1BQ-F1BM, F1BQ-F2BQ and F1BQ-F2BM pairs with the BB1 copula whereas for the F1BQ-F3BM pair we choose the SBB1 copula. Figures 3.6.1 and 3.6.2 compare the fit of Student- t and BB1 copulas on the F1BQ-F1BM pair-copula data through contour and λ -function plots.

In general, the theoretical Student- t contour plots for all pairs analysed match the corresponding empirical contour plots better than the theoretical BB1 contour plots. The same conclusions can be drawn from the λ -function plot comparisons. The simulated Student- t copula λ -function plots seem to fit the interior part of the bivariate distribution better than the corresponding BB1 λ -function plots. However, the BB1 λ -functions appear adequate for fitting the tails of the distribution. Table 3.6.7 presents the resulting mixed A-C-vine-EVT model and the sequential and maximum likelihood estimates.²

²Similar graphs were also plotted for the rest of the pairs under investigation.

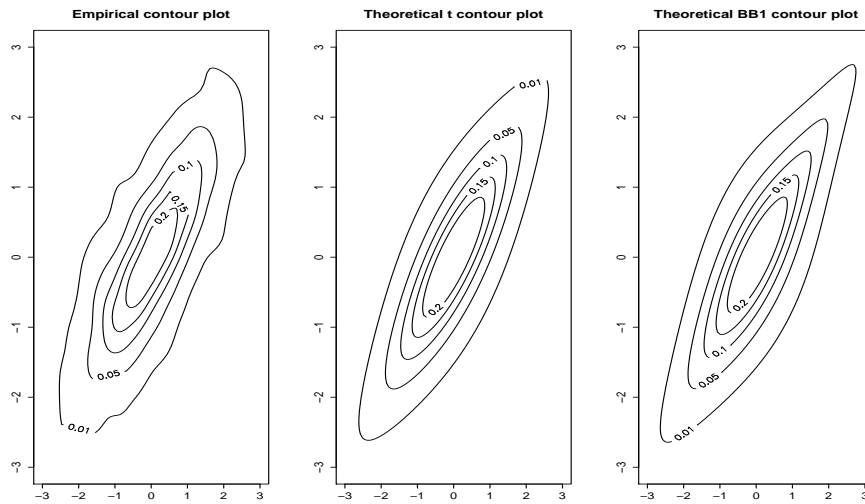


Figure 3.6.1: Empirical and theoretical contour plots for assessing the fit of Student- t and BB1 copulas on the transformed pair-copula F1BQ-F1BY Phelix Baseload data.

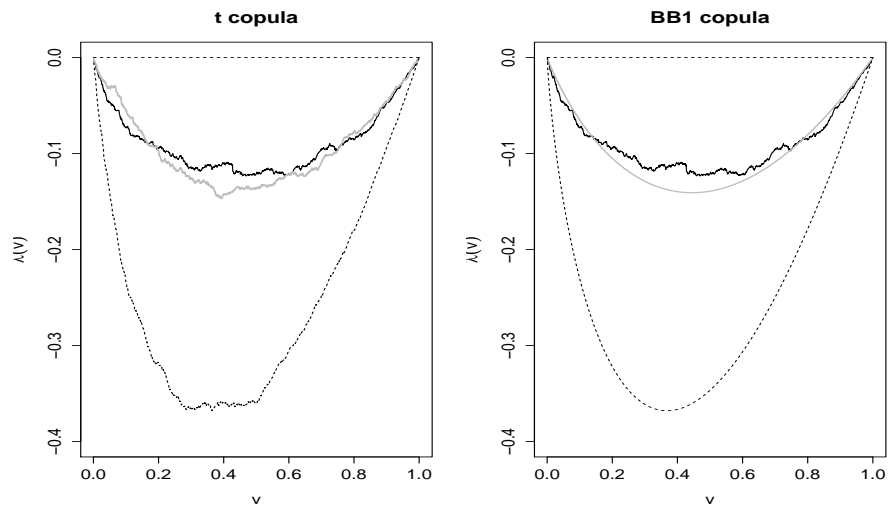


Figure 3.6.2: Plots of λ -functions for assessing the fit of Student- t and BB1 copulas on the transformed pair-copula F1BQ-F1BY Phelix Baseload data.

Table 3.6.6: Maximum likelihood and sequential estimates of the C-vine-EVT model

Level	Block	Family	Param.	$\hat{\theta}^{SE}$	$\hat{\theta}^{MLE}$
1	$C_{1,2}$	t	$\hat{\rho}$	0.81	0.81
			$\hat{\nu}$	7.68	7.79
	$C_{1,3}$	Student- t	$\hat{\rho}$	0.84	0.85
			$\hat{\nu}$	7.48	7.47
	$C_{1,4}$	F	$\hat{\theta}$	6.55	6.37
	$C_{1,5}$	Student- t	$\hat{\rho}$	0.83	0.83
			$\hat{\nu}$	9.59	9.6
	$C_{1,6}$	BB8_90	$\hat{\theta}$	-1.08	-1.09
$\hat{\delta}$			-0.97	-0.95	
$C_{1,7}$	Student- t	$\hat{\rho}$	0.94	0.94	
		$\hat{\nu}$	6.98	6.93	
$C_{1,8}$	Student- t	$\hat{\rho}$	0.92	0.92	
		$\hat{\nu}$	6.69	6.69	
2	$C_{2,3 1}$	N	$\hat{\rho}$	-0.12	-0.12
	$C_{2,4 1}$	Student- t	$\hat{\rho}$	0.79	0.8
			$\hat{\nu}$	6.31	6.33
	$C_{2,5 1}$	Student- t	$\hat{\rho}$	0.68	0.68
			$\hat{\nu}$	6.93	6.95
	$C_{2,6 1}$	F	$\hat{\theta}$	-0.21	-0.18
			$\hat{\rho}$	0.11	0.12
$C_{2,7 1}$	Student- t	$\hat{\rho}$	8.28	8.31	
		$\hat{\nu}$	-0.01	-0.01	
3	$C_{3,4 1,2}$	BB8_270	$\hat{\theta}$	-1.12	-1.13
			$\hat{\delta}$	-0.96	-0.94
	$C_{3,5 1,2}$	F	$\hat{\theta}$	-0.17	-0.15
			$\hat{\rho}$	0.04	0.04
	$C_{3,6 1,2}$	SC	$\hat{\theta}$	-0.07	-0.09
			$\hat{\nu}$	9.34	9.38
$C_{3,7 1,2}$	Student- t	$\hat{\theta}$	1.29	1.29	
		$\hat{\delta}$	0.26	0.24	
4	$C_{4,5 1,2,3}$	G	$\hat{\theta}$	1.04	1.04
			$\hat{\rho}$	-0.04	-0.04
	$C_{4,6 1,2,3}$	Student- t	$\hat{\rho}$	10.84	10.84
			$\hat{\nu}$	-0.08	-0.08
$C_{4,7 1,2,3}$	N	$\hat{\rho}$	-0.03	-0.03	
		$\hat{\nu}$	18.69	18.69	
5	$C_{5,6 1,2,3,4}$	C90	$\hat{\theta}$	-0.03	-0.03
			$\hat{\rho}$	0.06	0.05
	$C_{5,7 1,2,3,4}$	Student- t	$\hat{\nu}$	16.72	16.72
6	$C_{5,8 1,2,3,4}$	SJ	$\hat{\theta}$	1.05	1.05
			$\hat{\rho}$	1.02	1.01
7	$C_{6,7 1,2,3,4,5}$	J	$\hat{\theta}$	0.01	0
			$\hat{\rho}$	0.01	0.01
7	$C_{6,8 1,2,3,4,5}$	SC	$\hat{\theta}$	0.01	0
			$\hat{\rho}$	0.01	0.01
7	$C_{7,8 1,2,3,4,5,6}$	Student- t	$\hat{\rho}$	0.01	0.01
			$\hat{\nu}$	6.1	6.09

This table reports the estimated parameters of the C-vine-EVT model for the Phelix Baseload portfolio. $\hat{\theta}^{SE}$ and $\hat{\theta}^{MLE}$ correspond to sequential and maximum likelihood estimated parameters, respectively. Selected copula families are explained in Table 3.B.1.

Table 3.6.7: Maximum likelihood and sequential estimates of the A-C-vine- t model

Level	Block	Family	Param.	$\hat{\theta}^{SE}$	$\hat{\theta}^{MLE}$
1	$C_{1,2}$	BB1	$\hat{\theta}$	0.49	0.49
			$\hat{\delta}$	1.91	1.91
	$C_{1,3}$	BB1	$\hat{\theta}$	0.54	0.54
			$\hat{\delta}$	2.05	2.05
	$C_{1,4}$	F	$\hat{\theta}$	6.55	6.55
	$C_{1,5}$	BB1	$\hat{\theta}$	0.58	0.58
			$\hat{\delta}$	1.95	1.95
	$C_{1,6}$	Ind.			
$C_{1,7}$	SBB1	$\hat{\theta}$	0.29	0.29	
		$\hat{\delta}$	3.76	3.76	
$C_{1,8}$	BB1	$\hat{\theta}$	0.56	0.56	
		$\hat{\delta}$	2.87	2.87	
2	$C_{2,3 1}$	N	$\hat{\rho}$	-0.1	-0.1
	$C_{2,4 1}$	Student- t	$\hat{\rho}$	0.78	0.78
			$\hat{\nu}$	6.6	6.6
	$C_{2,5 1}$	Student- t	$\hat{\rho}$	0.68	0.68
			$\hat{\nu}$	6.97	6.97
	$C_{2,6 1}$	Ind.			
$C_{2,7 1}$	Student- t	$\hat{\rho}$	0.11	0.11	
		$\hat{\nu}$	8.29	8.29	
$C_{2,8 1}$	Ind.				
3	$C_{3,4 1,2}$	BB8_270	$\hat{\theta}$	-1.15	-1.15
			$\hat{\delta}$	-0.97	-0.97
	$C_{3,5 1,2}$	Ind.			
	$C_{3,6 1,2}$	Ind.			
	$C_{3,7 1,2}$	Student- t	$\hat{\rho}$	-0.07	-0.07
$\hat{\nu}$			10.08	10.08	
$C_{3,8 1}$	SBB7	$\hat{\theta}$	1.29	1.29	
		$\hat{\delta}$	0.26	0.26	
4	$C_{4,5 1,2,3}$	G	$\hat{\theta}$	1.04	1.04
	$C_{4,6 1,2,3}$	Ind.			
	$C_{4,7 1,2,3}$	N	$\hat{\rho}$	-0.09	-0.09
	$C_{4,8 1,2,3}$	Ind.			
5	$C_{5,6 1,2,3,4}$	Ind.			
	$C_{5,7 1,2,3,4}$	Student- t	$\hat{\rho}$	0.06	0.06
			$\hat{\nu}$	18.45	18.45
$C_{5,8 1,2,3,4}$	Ind.				
6	$C_{6,7 1,2,3,4,5}$	Ind.			
	$C_{6,8 1,2,3,4,5}$	Ind.			
7	$C_{7,8 1,2,3,4,5,6}$	Ind.			

This table reports the estimated parameters of the A-C-vine- t model for the Phelix Baseload portfolio. $\hat{\theta}^{SE}$ and $\hat{\theta}^{MLE}$ correspond to sequential and maximum likelihood estimated parameters, respectively. Selected copula families are explained in Table 3.B.1.

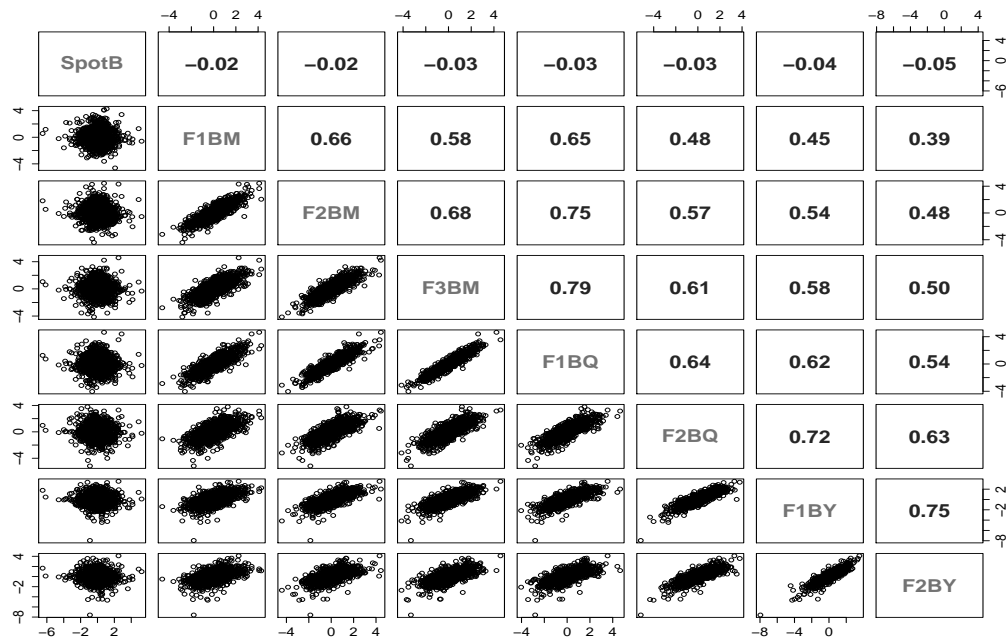


Figure 3.6.3: Dependence structure of standardised residuals in the Baseload portfolio. **Upper diagonal matrix:** Sample Kendall's τ correlation coefficients for each pair of standardised residual series. **Lower diagonal matrix:** Bivariate scatter plots for each pair of standardised residual series.

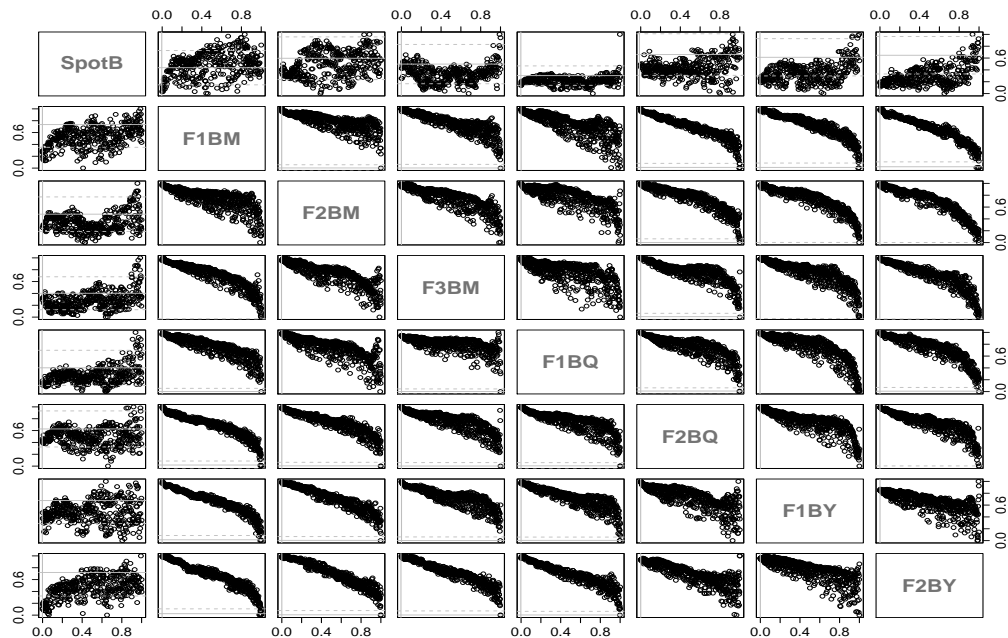


Figure 3.6.4: Tail dependence of transformed standardised residuals in the Baseload portfolio. **Upper diagonal matrix:** Chi-plots for each pair of transformed standardised residuals for the upper right quadrat. **Lower diagonal matrix:** Chi-plots for each pair of transformed standardised residuals for the lower left quadrat.

3.7 Empirical results

We forecast the one-day-ahead VaR and $CVaR$ of equally weighted long only and short only Phelix Baseload and Peakload portfolios. The competing models are specified in Table 3.6.2. We also employ the RiskMetrics (RM) model with smoothing constant $\lambda = 0.94$ as a naive benchmark. To backtest the models we use a period of 250 trading days that corresponds approximately to one year of trading. The forecasting period for the Baseload portfolio corresponds to the period from January 25, 2011 to February 07, 2012 and that of the Peakload portfolio spans the period from February 10, 2011 to February 22, 2012. We evaluate all risk estimates at 1% and 5% confidence levels, since they constitute the levels most commonly used for model evaluation both in literature and in financial markets. Figure 3.7.1 displays the Baseload portfolio return series and the 95%- VaR forecasts for the mixed C-vine-EVT and A-C-vine-EVT models. For a backtesting period of 250 observations and confidence levels 1% and 5% we expect 2.5 and 12.5 exceedances, respectively. According to Figure 3.7.1, both models seem to respond well to volatility changes and produce an acceptable number of failures. However, the VaR performance for each single model is hard to assess visually and hence a two-stage selection procedure, similar to [Sarma et al. \(2003\)](#), is followed. In the first stage, all models are tested for statistical accuracy and, if they survive rejection, a second stage filtering of the surviving models is employed using subjective loss functions.

3.7.1 Statistical tests

The first-stage of the model selection procedure is useful for examining whether the VaR estimates coming from alternative models satisfy the appropriate theoretical statistical properties. A well-specified VaR model should produce statistically meaningful VaR forecasts. Therefore, the proportion of exceedances should approximately equal the VaR confidence level (unconditional coverage) while the exceedances should not occur in clusters but instead independently. For example, a well-specified model should produce low VaR forecasts in times of low volatility and high VaR forecasts in times of high volatility, so that exceedances are spread over the entire sample period, and do not come in clusters. Therefore, a model which fails to capture the volatility dynamics of the underlying return distribution will suffer from a clustering of failures, even if it can produce the correct unconditional coverage. The term “conditional coverage” includes both properties. In the literature, there have been proposed a wide range of tests designed to test for these two properties. In principle, there are no universal guidelines on which tests to employ, since each test has its own merits and demerits. Thus, we employ the [Kupiec \(1995\)](#) unconditional coverage test, the conditional coverage test by [Christoffersen \(1998\)](#) and the duration-based Weibull test of independence by [Christoffersen and Pelletier \(2004\)](#), which are very popular, in the literature, for testing the above two properties.

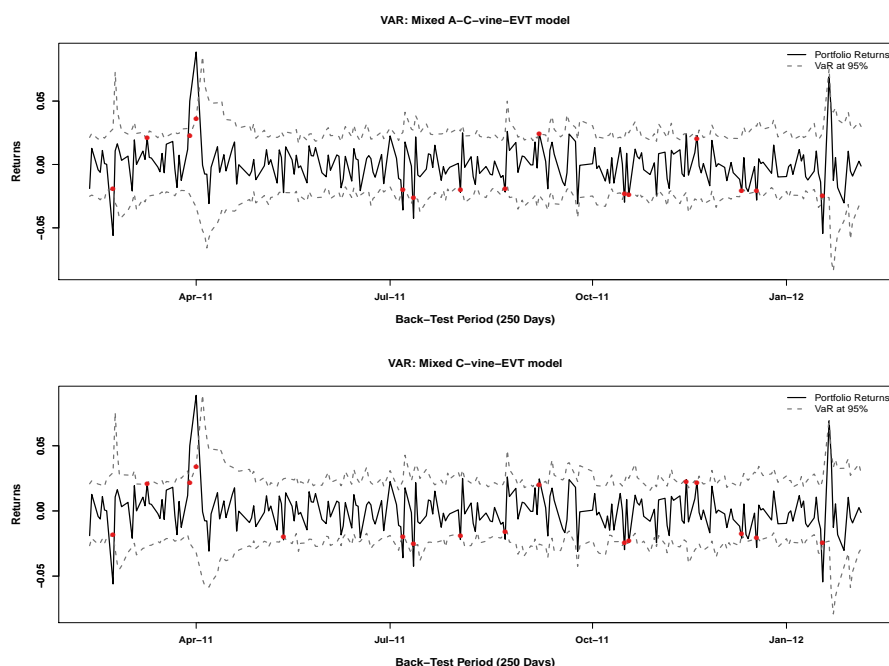


Figure 3.7.1: Baseload portfolio returns and 95%-*VaR* forecasts for the A-C-vine-EVT and C-vine-EVT models. *VaR* exceedances are marked by red points

3.7.1.1 Kupiec (1995) test for unconditional coverage (LR_{uc})

The most well-known test based on failure rates has been proposed by Kupiec (1995). The test is a likelihood-ratio test and measures whether the number of exceedances is consistent with the confidence level. Under the null hypothesis that the model is “well-specified”, the number of exceedances should follow the binomial distribution. Therefore, the idea is to examine whether the observed failure rate $\hat{\pi}$ is significantly different from α , the failure rate implied by the confidence level. The likelihood-ratio test statistic is given by

$$LR_{uc} = -2\log \left[\frac{\alpha^{n_1} (1 - \alpha)^{n_0}}{\hat{\pi}^{n_1} (1 - \hat{\pi})^{n_0}} \right] \sim \chi^2_{(1)}, \quad (3.29)$$

where n_1 is the number of exceedances, n_0 is the number of non-exceedances, α is the confidence level at which *VaR* measures are estimated and $\hat{\pi} = n_1 / (n_0 + n_1)$ is the MLE estimate of α . Under the null hypothesis, LR_{uc} is asymptotically χ^2 distributed with one degree of freedom. Nevertheless, Kupiec’s test exhibits two major shortcomings. First, the test is statistically weak with sample sizes consistent with the current regulatory framework (one year). Second, the test only considers the frequency of exceedances and does not take into account the time when they occur. This means that it may fail to reject a model which suffers from clustered exceedances. Therefore, backtesting should not rely entirely on unconditional coverage but clustered exceedances should also be taken into account.

3.7.1.2 Christoffersen (1998) test for conditional coverage (LR_{cc})

Christoffersen (1998) proposed a “conditional coverage” test that jointly examines whether the total number of exceedances is equal to the expected one, and whether the VaR failures are independently distributed. The test is carried out, given the realisation of return series r_t and the *ex-ante* VaR for a $\alpha\%$ coverage rate by first defining an indicator function I_{t+1} that gets the value of 1 if a VaR violation occurs and 0 otherwise. If the model is “well-specified”, then an exception today should not depend on whether or not an exception occurred on the previous day and the total number of exceedances should be consistent with the confidence level. Therefore, by combining the test statistic of independence (LR_{ind}) with Kupiec’s test statistic (LR_{uc}), we obtain a conditional coverage test $LR_{cc} = LR_{uc} + LR_{ind}$ that jointly tests for these two properties - i.e. the correct VaR failures and the independence of the exceedances. The LR_{cc} test statistic for the correct conditional coverage is given by

$$LR_{cc} = -2\log \frac{(1 - \alpha)^{n_0} \alpha^{n_1}}{(1 - \hat{\pi}_{01})^{n_{00}} \hat{\pi}_{01}^{n_{01}} (1 - \hat{\pi}_{11})^{n_{10}} \hat{\pi}_{11}^{n_{11}}} \sim \chi^2_{(2)}, \quad (3.30)$$

where n_{ij} is the number of i values followed by a j value in the I_{t+1} series ($i, j = 0, 1$), $\pi_{ij} = \Pr\{I_{t+1} = i | I_t = j\}$ ($i, j = 0, 1$), $\hat{\pi}_{01} = n_{01}/(n_{00} + n_{01})$, $\hat{\pi}_{11} = n_{11}/(n_{00} + n_{01})$. LR_{cc} is χ^2 distributed too, but with two degrees of freedom. The above tests are reliable for detecting misspecified risk models when the temporal dependence in the sequence of VaR violations is a simple first-order Markov structure. However, we are interested in tests that have power against more general forms of dependence. The duration-based Weibull test of Christoffersen and Pelletier (2004) deals with this issue.

3.7.1.3 Christoffersen and Pelletier (2004) duration based test

The intuition behind the duration-based tests is that the clustering of exceedances will result in an excessive number of relatively short or relatively long no-hit durations (i.e., the duration of time (in days) between two VaR violations), corresponding to market turmoil and market calm, respectively. Following Christoffersen and Pelletier (2004), we denote by d_i the duration between two consecutive VaR violations (i.e., the no-hit duration)

$$d_i = t_i - t_{i-1},$$

where t_i denotes the day of the i^{th} exceedance. Under the conditional coverage hypothesis, the duration process d_i follows a geometric distribution with probability equal to α and a probability density function, given by

$$f(d; \alpha) = \alpha(1 - \alpha)^{d-1} \quad d \in \mathbb{N}^*. \quad (3.31)$$

The general idea of the test is to specify a distribution that nests Equation (3.31), so that the memoryless property can be tested via parameter restriction (Hurlin and Pérignon, 2011). The only memory free (continuous) random distribution is the exponential one, and thus under the null hypothesis the distribution of the no-hit durations should be

$$f_{\text{exp}}(d; p) = p \exp(-pd). \quad (3.32)$$

In Equation (3.32) we have $\mathbb{E}(d) = 1/\alpha$ and, since the conditional coverage hypothesis implies a mean of duration equal to $1/\alpha$, it also implies the condition $p = a$. With regard to statistical testing for independence, Christoffersen and Pelletier (2004), specify an alternative distribution that allows dependence. They consider the Weibull distribution where

$$f_w(d; p, b) = p^b b d^{b-1} \exp((-pd)^b). \quad (3.33)$$

This particular type of distribution is able to capture violation clustering. When $b < 1$, the Weibull will have a decreasing hazard function that corresponds to a high number of very short durations (very volatile period) and a high number of very long durations (low volatile period). This can be evidence of misspecified volatility dynamics in the risk model (Christoffersen and Pelletier, 2004).

Since the exponential distribution corresponds to a Weibull with a flat hazard function, i.e., $b = 1$, the test for independence (Christoffersen and Pelletier, 2004) is

$$H_{0,\text{ind}} : b = 1. \quad (3.34)$$

Berkowitz et al. (2009) extended this approach to address the conditional coverage hypothesis, which is

$$H_{0,\text{cc}} : b = 1 \ \& \ p = \alpha. \quad (3.35)$$

3.7.2 Loss functions

The idea of employing loss functions to assess *VaR* performance was firstly introduced by Lopez (1998, 1999). The loss function evaluation method is not based on a hypothesis-testing framework, but rather on assigning to *VaR* estimates a numerical score that reflects the evaluator's specific concerns. As such, it provides a measure of relative performance that can be utilised to assess the performance of *VaR* estimates. Under this approach, a model which minimises the loss is preferred to other models (Lopez, 1998). The general form of a loss function for the i^{th} model is

$$L_{i,t+1} = \begin{cases} f(r_{t+1}, VaR_{i,t+1|t}) & \text{if } r_{t+1} < VaR_{i,t+1|t}, \\ g(r_{t+1}, VaR_{i,t+1|t}) & \text{if } r_{t+1} \geq VaR_{i,t+1|t}, \end{cases} \quad (3.36)$$

where $f(x, y)$ and $g(x, y)$ are functions such that $f(x, y) \geq g(x, y)$ for a given y . Lower values of $L_{i,t+1}$ are preferred because exceedances are given higher scores than non exceedances. The total numerical score for each risk model i , is obtained by summing out the individual loss function estimates for the complete regulatory sample.

Under general conditions, accurate VaR estimates generate the lowest possible numerical scores. This approach for evaluating VaR performance is very flexible since the loss function can take different forms that represent the evaluator's specific concerns. However, this approach is vulnerable to misspecification of the loss function. Various loss functions have been proposed in the literature in order to address specific regulatory concerns. In this study, we employ the magnitude loss function (MLF) of Lopez (1998), the regulatory loss function (RLF) of Sarma et al. (2003) and the predictive quantile loss function (PQLF) of Koenker and Bassett (1978) in order to evaluate the VaR performance of our risk models. We also evaluate the $CVaR$ performance by employing the mean absolute error (MAE) and mean squared error (MSE) loss functions of Angelidis and Degiannakis (2007).

The magnitude loss function of Lopez (1998) incorporates two main regulatory concerns: the magnitude as well as the number of exceedances. The magnitude loss function has the following general representation

$$QL_{i,t+1} = \begin{cases} 1 + (r_{i,t+1} - VaR_{i,t+1|t})^2 & \text{if } r_{i,t+1} < VaR_{i,t+1|t}, \\ 0 & \text{if } r_{i,t+1} \geq VaR_{i,t+1|t}. \end{cases} \quad (3.37)$$

A score of 1 is given when a violation occurs, and an additional quadratic term, based on its magnitude, is also included. The numerical score increases with the magnitude of the exception and hence can provide additional information about the VaR relative performance. The second type of loss function we apply is the regulatory loss function of Sarma et al. (2003), which is similar to the magnitude loss function of Lopez (1998). This function does not penalise for the number of exceedances but only for the magnitude of the failure. It takes the following form

$$RLF_{i,t+1} = \begin{cases} (r_{i,t+1} - VaR_{i,t+1|t})^2 & \text{if } r_{i,t+1} < VaR_{i,t+1|t}, \\ 0 & \text{if } r_{i,t+1} \geq VaR_{i,t+1|t}. \end{cases} \quad (3.38)$$

As in the loss function in Equation (3.37), the quadratic term in Equation (3.38) ensures that large VaR exceedances are penalised more than small VaR exceedances. The predictive quantile loss function of Koenker and Bassett (1978) penalises more heavily observations for which an exception occurs, and represents a measure of the predicted tail at a given confidence level. The loss function may take the following

form

$$PQLF_{i,t+1} = \begin{cases} |r_{i,t+1} - VaR_{i,t+1|t}| \cdot (1 - \alpha) & \text{if } r_{i,t+1} < VaR_{i,t+1|t}, \\ |r_{i,t+1} - VaR_{i,t+1|t}| \cdot \alpha & \text{if } r_{i,t+1} \geq VaR_{i,t+1|t}. \end{cases} \quad (3.39)$$

A backtest based on this loss functional form is carried out by calculating the sample average loss

$$PQLF_i = \frac{1}{T} \sum_{j=1}^T PQLF_{i,t+j}, \quad (3.40)$$

where T denotes the total number of observations. The economic intuition behind the PQLF is that capital charges should also be considered in the evaluation of VaR performance. Therefore, the capital foregone for over-predicting the true VaR should not be disregarded.

The above loss functions only take into account the magnitude and do not consider the size of the expected loss, given a VaR violation. Since the size of the expected loss is also an integral part in a regulator's utility function, we backtest the risk models' performance by using loss functions that take into account the *Expected Shortfall* (ES) or the *Conditional-VaR* ($CVaR$), if a VaR violation occurs. Therefore, we employ the mean absolute error (MAE) and mean squared error (MSE) loss functions of [Angelidis and Degiannakis \(2007\)](#). The MAE loss function can be described by the following equation

$$\Psi_{i,t+1}^1 = \begin{cases} |r_{i,t+1} - CVaR_{i,t+1|t}| & \text{if } r_{i,t+1} < VaR_{i,t+1|t}, \\ 0 & \text{if } r_{i,t+1} \geq VaR_{i,t+1|t}, \end{cases} \quad (3.41)$$

whereas the MSE loss function can obtain the following form

$$\Psi_{i,t+1}^2 = \begin{cases} (r_{i,t+1} - CVaR_{i,t+1|t})^2 & \text{if } r_{i,t+1} < VaR_{i,t+1|t}, \\ 0 & \text{if } r_{i,t+1} \geq VaR_{i,t+1|t}. \end{cases} \quad (3.42)$$

A backtest based on the loss functional forms of Equation (3.41) and Equation (3.42) is carried out by calculating the sample average expected loss (T observations) for MAE and MSE:

$$MAE_i = \frac{1}{T} \sum_{j=1}^T \Psi_{i,t+j}^1, \quad MSE_i = \frac{1}{T} \sum_{j=1}^T \Psi_{i,t+j}^2.$$

3.7.3 Statistical test results

Table 3.8.1 presents the number of exceedances and p -values of the statistical tests for the Phelix Baseload and Peakload long only and short only portfolios. It is evident from the p -values of the tests that almost all VaR forecasts at 1% and 5%

confidence levels are sufficiently accurate. For most of the risk models, the null hypotheses of independence (Weibull), unconditional coverage (uc) and conditional coverage (cc) cannot be rejected at 5% significance level. The only exceptions are the rejection of the null hypothesis for the conditional coverage test at 5% significance level (but not at 1%) for the Phelix Baseload short portfolio 99%-*VaR* forecasts for all C-vine models and the rejection of the null hypothesis of independence in the [Christoffersen and Pelletier \(2004\)](#) test for C-vine-*t* model 99%-*VaR* forecasts for the Phelix Peakload long portfolio.

The rejection of the conditional coverage null hypothesis, at 5% significance level, for all C-vine models 99%-*VaR* forecasts of the Phelix Baseload short portfolio is due to the first-order Markov structure of the independence test, which is embedded in the conditional coverage test. As explained, the unconditional and conditional coverage tests have low statistical power with the current regulatory backtest sample. This weakness is the reason for the rejection of the conditional coverage test in our particular case. Nevertheless, the hypothesis of independence is pretty strong, since the Weibull independence test cannot be rejected at 5% level for any risk model except for the C-vine-*t* model 99%-*VaR* forecasts for the Phelix Peakload long portfolio. This exception, however, is not of great concern since there is only 1 exceedance in this level and this affects the respective test statistic. The corresponding unconditional and conditional coverage tests cannot be rejected.

Moreover, the number of exceedances for all risk models are very close to the expected number of exceedances and therefore the hypothesis of unconditional coverage cannot be rejected. The *p*-values of the corresponding Kupiec tests are very high for all *VaR* forecast levels and all risk models. As expected, the benchmark RM model most of the time produces the highest number of exceedances without being rejected, though, by any statistical test at 5% level. It also seems that the C-vine-EVT and A-C-vine-EVT models obtain the highest *p*-values in the unconditional coverage tests at 1% level whereas for the 5% *VaR* forecast level, no clear conclusion can be drawn on the basis of the Kupiec test. In this stage, all *VaR* model forecasts can be considered statistically adequate and hence can be subsequently used in the second stage of the backtesting procedure, which entails evaluation through the employment of the subjective loss functions introduced in Section 3.7.2.

3.7.4 Loss function results

The second-stage of the selection procedure entails the employment of loss functions in order to assess the *VaR* and *CVaR* forecast performance of the various risk models under consideration. Tables 3.8.2 and 3.8.3 report the average out-of-sample *VaR* and *CVaR* estimates, the numerical scores for the *VaR*-based regulatory

(RLF), magnitude (MLF) and predictive quantile (PQLF) loss functions as well as the numerical scores of the *CVaR*-based MAE and MSE loss functions for the Phelix Baseload and Peakload long only and short only portfolios, respectively.

The numerical scores of the *VaR*-based loss functions are highly supportive of the A-C-vine-EVT model at 1% confidence level. In particular, almost all numerical scores for every possible Phelix Baseload and Peakload long only and short only portfolio combination tend to favour the A-C-vine-EVT model over the rest of the models at 1% significance level. The A-C-vine-EVT model's numerical scores are minimised in this level in 9 out of 12 cases for all *VaR*-based loss functions employed. The C-vine-EVT model also produces satisfactory results in this level. Moreover, the *CVaR*-based loss function results favour the A-C-Vine-EVT model. In total, 3 out of 8 times the corresponding MAE and MSE loss functions are minimised by the A-C-vine-EVT model.

Therefore, the statistical test results in the previous Section and the loss function findings in this Section, support our modelling approach for the extreme quantiles. It seems that a mixed A-C-vine structure can successfully describe the dependency structure of portfolio return series while the employment of extreme value theory can provide better fit in the tails. Moreover, these findings support the theoretical and empirical findings of [Joe et al. \(2010\)](#) and [Nikoloulopoulos et al. \(2012\)](#). Based on the loss function results at 1% level, it seems that the *VaR* and *CVaR* forecasts produced by the A-C-vine-EVT model outperform those of the C-Vine-EVT model. Therefore, for inference involving the tails, the pair-copula selection procedure should not be entirely likelihood-based.

At 5% level the numerical score results seem to be mixed, since there is no strong preference towards a specific risk model. In general, the C-vine-Norm model estimates most of the time tend to minimise the *VaR*-based loss functions. Nevertheless, there is not the case where the C-vine-Norm model is preferred by all three loss functions simultaneously. The A-C-vine-EVT and C-vine-EVT models tend to minimise the *VaR*-based loss functions in some cases too, with the C-vine-*t* model and the RM model being the least preferred models according to the *VaR*-based loss function numerical scores at this level. The *CVaR*-based loss function results at 5% level also fail to provide more insight.

3.8 Conclusions

In this study we introduced the vine copula modelling as an alternative and more flexible way to describe the joint distribution of power portfolios. Our approach combines pseudo-maximum-likelihood fitting of time series models and extreme value

theory to model the tails of the resulting innovations conditional distribution. We modelled the dependency structure of portfolios using a canonical vine copula modelling approach. We also employed an alternative vine specification based on the theoretical and empirical results of [Joe et al. \(2010\)](#) and [Nikoloulopoulos et al. \(2012\)](#). In particular, we replaced the AIC selected Student- t copula families in level 1 of the vine with copula families having asymmetric tail dependence whereas the Independence copula was employed for pair-copulas that could not reject the null hypothesis of independence. Baseload and Peakload portfolio VaR and $CVaR$ forecasts were computed by five alternative models. The evaluation of their forecasting performance was conducted using standard statistical and subjective loss function techniques. In general, the statistical tests for all models show good unconditional and conditional coverage. However, the A-C-vine-EVT model shows superior performance according to the VaR and $CVaR$ -based loss function results at extreme quantiles ($\alpha = 0.01$) compared to the rest of the models employed.

These results provide new insight regarding risk management applications within the vine copula modelling framework and also support the findings of [Joe et al. \(2010\)](#) and [Nikoloulopoulos et al. \(2012\)](#). It seems that the A-C-vine-EVT model provides better fit in the tails of the joint distribution and hence better risk estimates compared to the entirely AIC selected C-vine-EVT model. Even though neither data set shows significant tail asymmetries, it seems that the asymmetric copulas, instead of the likelihood-selected Student- t copulas, in level 1 of the vine structure as well as the employment of Independence copulas for the pairs that display independence improve the fit in the tails and as a consequence the risk measure estimates. We strongly believe that the employment of the A-C-vine-EVT model for risk management applications in portfolios that exhibit more significant asymmetric tail dependences will further enhance the importance and predictive ability of the model in extreme quantiles.

The fit and performance of the model can also be improved in various ways. For example, the selection of asymmetric copula families in level 1 of the vine should not be entirely based on empirical and theoretical scatter and λ -function plots comparisons but also on matching the empirical tail dependence of the data with the theoretical tail dependence of the corresponding asymmetric copula families. Moreover, the fit of the semi-parametric marginals and of the canonical vine copula model can be improved by re-estimating the model at fixed periods of time, i.e., every month, when considering forecasting applications. All risk measure forecasts presented in this study were obtained by a static version of the model. To sum up, we believe that the proposed methodology has a lot of potential in modelling large-scale portfolios and can substantially improve the existing portfolio risk management methods.

Table 3.8.1: Statistical test results

		Phelix Baseload Long Portfolio				Phelix Baseload Short Portfolio			
Model	Level	No. of exceed.	Kupiec (uc)	Christoff. (cc)	Weibull (ind.)	No. of exceed.	Kupiec (uc)	Christoff. (cc)	Weibull (ind.)
RM	99%	4	0.38048	0.63771	0.93515	3	0.75799	0.06329	1.00000
	95%	14	0.66907	0.39618	0.74427	13	0.88535	0.36735	0.57266
C-vine-EVT	99%	3	0.75799	0.91938	0.25047	2	0.74193	0.02235	1.00000
	95%	11	0.65706	0.54490	0.26182	8	0.16322	0.18966	0.19264
A-C-vine-EVT	99%	3	0.75799	0.91938	0.25047	2	0.74193	0.02235	1.00000
	95%	10	0.45291	0.49648	0.83140	7	0.08281	0.08830	0.30945
C-vine-Norm	99%	4	0.38048	0.63771	0.93515	2	0.74193	0.02235	1.00000
	95%	9	0.28602	0.40385	0.70539	7	0.08281	0.08830	1.00000
C-vine- <i>t</i>	99%	4	0.38048	0.63771	0.93515	2	0.74193	0.02235	1.00000
	95%	11	0.65706	0.54490	0.26182	9	0.28602	0.05618	1.00000

		Phelix Peakload Long Portfolio				Phelix Peakload Short Portfolio			
Model	Level	No. of exceed.	Kupiec (uc)	Christoff. (cc)	Weibull (ind.)	No. of exceed.	Kupiec (uc)	Christoff. (cc)	Weibull (ind.)
RM	99%	6	0.05935	0.14575	0.86344	6	0.05935	0.05032	0.56562
	95%	16	0.32937	0.62119	0.71425	15	0.48124	0.43564	0.18624
C-vine-EVT	99%	3	0.75799	0.91938	0.52624	4	0.38048	0.08733	1.00000
	95%	10	0.45291	0.49648	0.39991	10	0.45291	0.53023	0.82869
A-C-vine-EVT	99%	4	0.38048	0.63771	0.78387	3	0.75799	0.06329	1.00000
	95%	9	0.28602	0.40385	0.60371	11	0.65706	0.71727	0.65718
C-vine-Norm	99%	4	0.38048	0.63771	0.78387	5	0.16185	0.07766	1.00000
	95%	7	0.08281	0.18141	0.90648	10	0.45291	0.53023	0.48095
C-vine- <i>t</i>	99%	1	0.27807	0.55307	0.00686	4	0.38048	0.08733	1.00000
	95%	9	0.28602	0.40385	0.64173	11	0.65706	0.71727	0.31980

This table reports Phelix Baseload and Peakload Long and Short portfolio p -values of statistical tests, described in Section 3.7.1, and number of VaR exceedances for each risk model at $\alpha = 0.01$ and $\alpha = 0.05$ level.

Table 3.8.2: Loss function results: Phelix Baseload

Phelix Baseload Long Portfolio								
Model	Level	Av.VaR	RLF	MLF	PQLF	Av.CVaR	MAE	MSE
RM	99%	-0.03515	0.0015646	4.0015646	0.00063489	-0.04027	0.0002127	0.00000418
	95%	-0.02485	0.0032817	14.0032817	0.00181747	-0.03117	0.0004567	0.00000871
C-vine-EVT	99%	-0.04351	0.0009507	3.0009507	0.00060692	-0.05586	0.0001885	0.00000273
	95%	-0.02706	0.0030201	11.0030201	0.00188056	-0.03779	0.0006105	0.00001073
A-C-vine-EVT	99%	-0.04447	0.0004391	3.0004391	0.00057180	-0.05717	0.0001387	0.00000171
	95%	-0.02780	0.0028869	10.0028869	0.00187775	-0.03869	0.0005913	0.00000869
C-vine-Norm	99%	-0.03965	0.0011447	4.0011447	0.00062836	-0.04553	0.0001531	0.00000272
	95%	-0.02828	0.0027324	9.0027324	0.00189274	-0.03541	0.0005316	0.00000921
C-vine- <i>t</i>	99%	-0.04275	0.0010770	4.0010770	0.00061632	-0.05578	0.0002377	0.00000403
	95%	-0.02650	0.0030967	11.0030967	0.00186608	-0.03723	0.0005666	0.00001030
Phelix Baseload Short Portfolio								
Model	Level	Av.VaR	RLF	MLF	PQLF	Av.CVaR	MAE	MSE
RM	99%	-0.03515	0.0033335	3.0033335	0.00072408	-0.04027	0.0003077	0.00000939
	95%	-0.02485	0.0060319	13.0060319	0.00188622	-0.03117	0.0005375	0.00001741
C-vine-EVT	99%	-0.04209	0.0015976	2.0015976	0.00062577	-0.05348	0.0001290	0.00000268
	95%	-0.02638	0.0039360	8.0039360	0.00174001	-0.03658	0.0003646	0.00001235
A-C-vine-EVT	99%	-0.04274	0.0015196	2.0015196	0.00062027	-0.05440	0.0001639	0.00000261
	95%	-0.02705	0.0037340	7.0037340	0.00175258	-0.03733	0.0003497	0.00001051
C-vine-Norm	99%	-0.03850	0.0019666	2.0019666	0.00061009	-0.04421	0.0001832	0.00000524
	95%	-0.02728	0.0037337	7.0037337	0.00176239	-0.03436	0.0003213	0.00001163
C-vine- <i>t</i>	99%	-0.04189	0.0017390	2.0017390	0.00062869	-0.05528	0.0001372	0.00000529
	95%	-0.02557	0.0042147	9.0042147	0.00171525	-0.03635	0.0005921	0.00003091

This table reports Phelix Baseload Long and Short portfolio *VaR* and *CVaR* loss function results, described in Section 3.7.2; Av.VaR is the average forecasted *Value-at-Risk* for the out-of-sample period; Av.CVaR is the average forecasted *Conditional Value-at-Risk* (*Expected Shortfall*) for the out-of-sample period; Bold values indicate the minimum loss function scores across different risk models and at same confidence level.

Table 3.8.3: Loss function results: Phelix Peakload

Phelix Peakload Long Portfolio								
Model	Level	Av.VaR	RLF	MLF	PQLF	Av.CVaR	MAE	MSE
RM	99%	-0.03476	0.0002246	6.0002246	0.00046690	-0.03982	0.0000514	0.00000015
	95%	-0.02457	0.0018197	16.0018197	0.00170577	-0.03082	0.0003675	0.00000328
C-vine-EVT	99%	-0.04013	0.0000530	3.0000530	0.00044744	-0.04959	0.0005616	0.00002937
	95%	-0.02607	0.0017057	10.0017057	0.00167023	-0.03511	0.0008263	0.00001875
A-C-vine-EVT	99%	-0.04040	0.0000103	4.0000103	0.00041746	-0.04941	0.0004356	0.00001614
	95%	-0.02653	0.0015422	9.0015422	0.00164987	-0.03537	0.0008030	0.00001670
C-vine-Norm	99%	-0.03912	0.0000829	4.0000829	0.00043210	-0.04475	0.0003761	0.00001305
	95%	-0.02790	0.0013726	7.0013726	0.00168505	-0.03496	0.0007567	0.00001505
C-vine- <i>t</i>	99%	-0.04444	0.0000004	1.0000004	0.00044276	-0.05827	0.0008244	0.00004366
	95%	-0.02748	0.0013035	9.0013035	0.00168213	-0.03881	0.0008689	0.00002239

Phelix Peakload Short Portfolio								
Model	Level	Av.VaR	RLF	MLF	PQLF	Av.CVaR	MAE	MSE
RM	99%	-0.03476	0.0034548	6.0034548	0.00078469	-0.03982	0.0003358	0.00000990
	95%	-0.02457	0.0064371	15.0064371	0.00205432	-0.03082	0.0006236	0.00001797
C-vine-EVT	99%	-0.04402	0.0022995	4.0022995	0.00076175	-0.05596	0.0002175	0.00000536
	95%	-0.02721	0.0051004	10.0051004	0.00199222	-0.03807	0.0005311	0.00001767
A-C-vine-EVT	99%	-0.04482	0.0010725	3.0010725	0.00064555	-0.05705	0.0001116	0.00000300
	95%	-0.02794	0.0048558	11.0048558	0.00201820	-0.03898	0.0005384	0.00001737
C-vine-Norm	99%	-0.03852	0.0028474	5.0028474	0.00074071	-0.04417	0.0002642	0.00000686
	95%	-0.02714	0.0052233	10.0052233	0.00201169	-0.03427	0.0004958	0.00001775
C-vine- <i>t</i>	99%	-0.04364	0.0017716	4.0017716	0.00070101	-0.05916	0.0000865	0.00000123
	95%	-0.02678	0.0055913	11.0055913	0.00200585	-0.03841	0.0005459	0.00001618

This table reports Phelix Peakload Long and Short portfolio *VaR* and *CVaR* loss function results, described in Section 3.7.2; Av.VaR is the average forecasted *Value-at-Risk* for the out-of-sample period; Av.CVaR is the average forecasted *Conditional Value-at-Risk (Expected Shortfall)* for the out-of-sample period; Bold values indicate the minimum loss function scores across different risk models and at same confidence level.

Appendices

3.A Time series models for the conditional mean

The conditional mean time series models for the Phelix Baseload portfolio return series are:

SpotB-ARMA(1,1):	$r_t = \varphi_1 r_{t-1} + \varepsilon_t + \theta_1 \varepsilon_{t-1}$
F1BM - ARMA(15,1):	$r_t = \varphi_8 r_{t-8} + \varphi_{15} r_{t-15} + \varepsilon_t + \theta_1 \varepsilon_{t-1}$
F2BM - ARMA(8,1):	$r_t = \varphi_8 r_{t-8} + \varepsilon_t + \theta_1 \varepsilon_{t-1}$
F3BM - ARMA(8,1):	$r_t = \varphi_8 r_{t-8} + \varepsilon_t + \theta_1 \varepsilon_{t-1}$
F1BQ - ARMA(8,1):	$r_t = \varphi_8 r_{t-8} + \varepsilon_t + \theta_1 \varepsilon_{t-1}$
F2BQ - ARMA(4,1):	$r_t = \varphi_4 r_{t-4} + \varepsilon_t + \theta_1 \varepsilon_{t-1}$
F1BY - MA(1):	$r_t = \varepsilon_t + \theta_1 \varepsilon_{t-1}$
F2BY - ARMA(4,1):	$r_t = \varphi_4 r_{t-4} + \varepsilon_t + \theta_1 \varepsilon_{t-1}$

The conditional mean time series models for the Phelix Peakload portfolio return series are:

SpotP-ARMA(1,1):	$r_t = \varphi_1 r_{t-1} + \varepsilon_t + \theta_1 \varepsilon_{t-1}$
F1PM - ARMA(15,1):	$r_t = \varphi_8 r_{t-8} + \varphi_9 r_{t-9} + \varphi_{15} r_{t-15} + \varepsilon_t + \theta_1 \varepsilon_{t-1}$
F2PM - ARMA(18,1):	$r_t = \varphi_8 r_{t-8} + \varphi_{18} r_{t-18} + \varepsilon_t + \theta_1 \varepsilon_{t-1}$
F3PM - ARMA(15,1):	$r_t = \varphi_8 r_{t-8} + \varphi_{15} r_{t-15} + \varepsilon_t + \theta_1 \varepsilon_{t-1}$
F1PQ - ARMA(18,1):	$r_t = \varphi_8 r_{t-8} + \varphi_{15} r_{t-15} + \varphi_{18} r_{t-18} + \varepsilon_t + \theta_1 \varepsilon_{t-1}$
F2PQ - ARMA(8,1):	$r_t = \varphi_3 r_{t-3} + \varphi_4 r_{t-4} + \varphi_8 r_{t-8} + \varepsilon_t + \theta_1 \varepsilon_{t-1}$
F1PY - ARMA(9,1):	$r_t = \varphi_4 r_{t-4} + \varphi_8 r_{t-8} + \varphi_9 r_{t-9} + \varepsilon_t + \theta_1 \varepsilon_{t-1}$
F2PY - ARMA(4,1):	$r_t = \varphi_4 r_{t-4} + \varepsilon_t + \theta_1 \varepsilon_{t-1}$

3.B Copula family abbreviations

Table 3.B.1: Copula family abbreviations

No.	Short name	Long name
0	I	Independence
1	N	Gaussian
2	t	t
3	C	Clayton
4	G	Gumbel
5	F	Frank
6	J	Joe
7	BB1	Clayton-Gumbel
8	BB6	Joe-Gumbel
9	BB7	Joe-Clayton
10	BB8	Frank-Joe
13	SC	Survival Clayton
14	SG	Survival Gumbel
16	SJ	Survival Joe
17	SBB1	Survival Clayton-Gumbel
18	SBB6	Survival Joe-Gumbel
19	SBB7	Survival Joe-Clayton
20	SBB8	Survival Joe-Frank
23	C90	Rotated Clayton 90 degrees
24	G90	Rotated Gumbel 90 degrees
26	J90	Rotated Joe 90 degrees
27	BB1_90	Rotated Clayton-Gumbel 90 degrees
28	BB6_90	Rotated Joe-Gumbel 90 degrees
29	BB7_90	Rotated Joe-Clayton 90 degrees
30	BB8_90	Rotated Frank-Joe 90 degrees
33	C270	Rotated Clayton 270 degrees
34	G270	Rotated Gumbel 270 degrees
36	J270	Rotated Joe 270 degrees
37	BB1_270	Rotated Clayton-Gumbel 270 degrees
38	BB6_270	Rotated Joe-Gumbel 270 degrees
39	BB7_270	Rotated Joe-Clayton 270 degrees
40	BB8_270	Rotated Frank-Joe 270 degrees

This table reports the number, short and long names of copula families in **CDVine** package, R statistical software.

3.C Pair-copulas for the Phelix Baseload portfolio

Table 3.C.1: Determination of unconditional and conditional pair-copulas for C-vine model

Level	Numerical representation	Unconditional & Conditional pair-copulas
1	1,2	F1BQ,F1BY
	1,3	F1BQ,F1BM
	1,4	F1BQ,F2BY
	1,5	F1BQ,F2BQ
	1,6	F1BQ,SpotB
	1,7	F1BQ,F3BM
	1,8	F1BQ,F2BM
2	2,3 1	F1BY,F1BM F1BQ
	2,4 1	F1BY,F2BY F1BQ
	2,5 1	F1BY,F2BQ F1BQ
	2,6 1	F1BY,SpotB F1BQ
	2,7 1	F1BY,F3BM F1BQ
	2,8 1	F1BY,F2BM F1BQ
3	3,4 12	F1BM,F2BY F1BQ F1BY
	3,5 1,2	F1BM,F2BQ F1BQ,F1BY
	3,6 1,2	F1BM,SpotB F1BQ,F1BY
	3,7 1,2	F1BM,F3BM F1BQ,F1BY
	3,8 1,2	F1BM,F2BM F1BQ,F1BY
4	4,5 123	F2BY,F2BQ F1BQ,F1BY,F1BM
	4,6 1,2,3	F2BY,SpotB F1BQ,F1BY,F1BM
	4,7 1,2,3	F2BY,F3BM F1BQ,F1BY,F1BM
	4,8 1,2,3	F2BY,F2BM F1BQ,F1BY,F1BM
5	5,6 1234	F2BQ,SpotB F1BQ,F1BY,F1BM,F2BY
	5,7 1,2,3,4	F2BQ,F3BM F1BQ,F1BY,F1BM,F2BY
	5,8 1,2,3,4	F2BQ,F2BM F1BQ,F1BY,F1BM,F2BY
6	6,7 12345	SpotB,F3BM F1BQ,F1BY,F1BM,F2BY,F2BQ
	6,8 1,2,3,4,5	SpotB,F2BM F1BQ,F1BY,F1BM,F2BY,F2BQ
7	7,8 1,2,3,4,5,6	F3BM,F2BM F1BQ,F1BY,F1BM,F2BY,F2BQ,SpotB

This table reports the specification of unconditional and conditional pair-copulas for all levels of canonical vine structure selected by the empirical rule of [Czado et al. \(2012\)](#).

Chapter 4

Measuring systemic risk in the European banking sector: A Copula *CoVaR* approach

4.1 Introduction

The recent financial crisis has highlighted in the most prominent way the need for prudent monitoring and assessment of systemic risk. Systemic risk can be seen as the adverse consequence, for the financial system and the broader economy, of a financial institution being in distress. The failure of large credit institutions can not only threaten the stability of the financial system but also have dramatic effects on the real economy. It is well-documented that conditional correlations between asset returns are much stronger in periods of financial distress (see e.g. [Longin and Solnik 2001](#); [Ang and Chen 2002](#)) and typically arise from exposure to common shocks, although amplifications of financial shocks are also associated with balance sheet channels and liquidity spirals (see e.g. [Brunnermeier 2009](#); [Adrian and Shin 2010](#)). As a result, losses tend to spread across financial institutions during stress times, amplifying the risk of systemic contagion.

Assessing the level of contribution of the so-called systemically important financial institutions (SIFIs) to systemic risk and designing a regulatory framework capable of ensuring financial stability is the foremost objective of international financial regulatory institutions. The *Value-at-Risk* (*VaR*), the risk measure most widely used by financial institutions, is not capable of capturing the systemic nature of risk since it focuses on the risk of an individual institution when viewed in isolation. As a result, there has been recently a growing interest in developing alternative risk measures that reflect systemic risk and avoid the shortcomings of *VaR*.

One such measure of systemic risk is the *Conditional Value-at-Risk* (*CoVaR*) of [Adrian and Brunnermeier \(2011\)](#), which attempts to capture risk spillovers among financial institutions and has attracted a lot of attention by the regulatory and academic community, especially after the financial crisis in the summer of 2007. The general framework of *CoVaR* depends on the conditional distribution of a random variable

$R_{s,t}$ representing the returns of the entire financial system at time t given that another financial institution i , represented by a random variable $R_{i,t}$, is in distress. Currently, there are two different definitions of *CoVaR* in the literature. In the original definition by [Adrian and Brunnermeier \(2011\)](#), *CoVaR* is defined as the conditional distribution of $R_{s,t}$ given that $R_{i,t} = VaR_t^i$, while in the modified definition of *CoVaR*, proposed by [Girardi and Ergün \(2013\)](#), the conditioning event is $R_{i,t} \leq VaR_t^i$. In other words, the former definition represents the *VaR* of the system assuming that institution i is *exactly* at its *VaR* level whereas the latter definition of *CoVaR* represents the same risk metric assuming that institution i is *at most* at its *VaR* level. This change in the *CoVaR* definition is arguably very useful. First of all, it considers more severe distress events for institution i that are further in the tail of the loss distribution (below VaR_t^i level) in contrast to the highly selective and over-optimistic scenario $R_{i,t} = VaR_t^i$. Moreover, the *CoVaR* estimates based on $R_{i,t} \leq VaR_t^i$ can be tested for statistical accuracy and independence using modified versions of the standard [Kupiec \(1995\)](#) and [Christoffersen \(1998\)](#) tests, respectively. Finally, and perhaps most importantly, [Mainik and Schaanning \(2014\)](#) show that conditioning on $R_{i,t} \leq VaR_t^i$ has great advantages for dependence modelling.

In this study, we propose a new methodology based on copula functions to estimate *CoVaR* under both definitions. We derive simple closed-form expressions for a broad range of copula families that allow us to model various forms of dependence, while focusing on extreme co-movements of financial system-institution returns, which is, in practice, the main concern of all systemic risk measures. Given the distinctive characteristics of copula families, our modelling approach enables the separation of dependence from marginal distributions providing greater flexibility and eliminating misspecification biases. A dynamic version of the model is also proposed - one that is capable of incorporating time-varying correlation into *CoVaR* calculations. Through counterexamples, we show that *CoVaR* measures generated by our modelling approach share the dependence consistency properties found in [Mainik and Schaanning \(2014\)](#). In addition, we extend the Copula *CoVaR* methodology to other “co-risk” measures. In this respect, we derive expressions for *Conditional Expected Shortfall (CoES)* under both definitions. Furthermore, we show that our approach can be easily employed by financial regulators as a useful stress testing tool for assessing the impact of extreme market conditions on the stability of the financial system.

Focusing on a portfolio of large European banks, we measure the contribution of each individual bank to systemic risk using both *CoVaR* and *CoES* systemic risk metrics. We show that distribution assumptions are extremely important for the accurate modelling of systemic risk. In this respect, we show that the ordering of

systemically important institutions and the magnitude of the corresponding systemic risk measures are substantially affected by the alternative distribution assumptions both in marginals and dependence but are robust across different systemic risk measures with the same assumptions. In a cross-country comparison, we find that banks from Spain and France have, on average, the highest contribution to systemic risk. Moreover, we investigate whether common market factors or institution specific characteristics are important determinants of systemic risk. We show that liquidity risk is an important determinant of systemic risk contribution. The large impact of funding liquidity in the pre-crisis period partly explains the “liquidity spirals” that occurred after the break out of the financial crisis in summer 2007. Its relative impact has been reduced in the post-crisis period due to the coordinated intervention of the European Central Bank (ECB) and the Federal Reserve in the interbank market. We also find that size and leverage are the most robust determinants of systemic risk contribution concluding that larger and more leveraged financial institutions can be harmful for the overall stability of the financial system.

The rest of the Chapter is organised as follows: Section 4.2 discusses the relevant literature, while Section 4.3 formally defines the *CoVaR* and *CoES* measures and presents the Copula *CoVaR* methodology. The derivation of closed-form expressions both for *CoVaR* and *CoES* systemic risk measures is also presented in this Section. Section 4.4 describes the data we use in the empirical part of this study and Section 4.5 presents the computation of systemic risk measures. Section 4.6 reports the results of financial institutions’ contribution to systemic risk. This Section also analyses the determinants of systemic risk and discusses their implications for the stability of the financial system. Section 4.7 concludes.

4.2 Related literature

Our study builds on the *CoVaR* methodology initially proposed by [Adrian and Brunnermeier \(2011\)](#) and subsequently modified by [Girardi and Ergün \(2013\)](#) to address the shortcomings of the original *CoVaR* definition. Recently, a number of papers have extended the *CoVaR* methodology and applied it to different financial sectors. For example, [Wong and Fong \(2011\)](#) analyse interconnectivity among economies using sovereign credit default swap (CDS) spreads of 11 Asia-Pacific economies. [Gauthier et al. \(2012\)](#) estimate systemic risk exposures for the Canadian banking system and set macro-prudential capital requirements equal to an institution’s contribution to systemic risk using $\Delta CoVaR$ as a risk allocation mechanism. Recently, [López-Espinosa et al. \(2012, 2013\)](#) have used the *CoVaR* methodology to analyse the impact of bank-specific factors on an institution’s solvency risk and its contribution to systemic risk in a portfolio of large international banks.

There also exists a growing literature that proposes a number of quantitative measures of systemic risk alternative to *CoVaR* using different approaches and data. For instance, [Segoviano and Goodhart \(2009\)](#) work with credit default swap (CDS) data and develop bank stability measures that assess banks' contribution to systemic risk within a multivariate framework. [Huang et al. \(2009\)](#) propose a systemic risk indicator measured by the price of insurance against systemic financial distress based on *ex-ante* measures of default probabilities of individual banks and equity return correlation forecasts. [Zhou \(2010\)](#) assesses the systemic importance of financial institutions within a multivariate Extreme Value Theory (EVT) framework and suggests two measures of systemic risk: the systemic impact index (SII), which measures the size of the systemic impact if one bank fails, and the vulnerability index (VI), which measures the impact on a particular bank when the other part of the system is in financial distress.

In addition, [Acharya et al. \(2012\)](#) use equity returns of financial institutions to calculate the systemic expected shortfall (SES), which represents the propensity of a financial institution to be undercapitalised when the financial system as a whole is undercapitalised, and the marginal expected shortfall (MES), which denotes an institution's average loss when the financial system is in its left tail. Systemic expected shortfall measures are calculated as the weighted average of an institution's MSE and its leverage. Alternatively, [Nicolò and Lucchetta \(2011\)](#) use a dynamic factor model on quarterly time-series sets of indicators of financial and real activity for the G-7 economies and obtain joint forecasts and stress-tests of indicators of systemic real risk and systemic financial risk. More recently, [Brownlees and Engle \(2012\)](#) have introduced the SRISK index, the expected capital shortage of a firm conditional on a substantial market decline, as an alternative measure of systemic risk. The SRISK index is a function of the leverage, size and marginal expected shortfall (MES) of an institution. Moreover, [Engle et al. \(2014\)](#) develop an econometric approach to measure the systemic risk of European financial institutions, with several factors explaining the dynamics of European financial institutions' returns. Finally, [Billio et al. \(2012\)](#) propose several econometric measures to capture the connectedness among financial institutions based on principal components analysis and Granger-causality networks. An extensive survey of the main quantitative measures of systemic risk proposed over the past several years in the literature can be found in [Bisias et al. \(2012\)](#).

4.3 CoVaR methodology

4.3.1 Definition of CoVaR

Consider a random variable $R_{i,t}$ that represents the returns of financial institution i at time t ($i = 1, \dots, N; t = 1, \dots, T$). The *Value-at-Risk* (VaR)¹ of the random variable $R_{i,t}$ at the confidence level $\alpha \in (0, 1)$, $VaR_{\alpha,t}^i$, is defined as the α -quantile of the return distribution

$$VaR_{\alpha,t}^i = F_{i,t}^{-1}(\alpha), \quad (4.1)$$

where $F_{i,t}^{-1}$ is the generalised inverse distribution function of the return distribution $F_{i,t}$, i.e., $F_{i,t}^{-1}(\alpha) := \inf \{r_{i,t} \in \mathbb{R} : F_{i,t}(r_{i,t}) \geq \alpha\}$. Equivalently, Equation (4.1) can also be written as

$$Pr(R_{i,t} \leq VaR_{\alpha,t}^i) = \alpha. \quad (4.2)$$

Two alternative definitions of *Conditional Value-at-Risk* (*CoVaR*) appear in the literature using different conditioning events. The notion of $CoVaR_{\alpha,\beta,t}^-$ denotes the original definition, introduced by [Adrian and Brunnermeier \(2011\)](#), representing the β -quantile of the returns of financial system $R_{s,t}$ conditional on $R_{i,t} = VaR_{\alpha,t}^i$, while the notion of $CoVaR_{\alpha,\beta,t}$ denotes the alternative definition of *CoVaR*, proposed by [Girardi and Ergün \(2013\)](#), where the conditioning event is $R_{i,t} \leq VaR_{\alpha,t}^i$. Formally, $CoVaR_{\alpha,\beta,t}^-$ and $CoVaR_{\alpha,\beta,t}$ are defined as the β -quantiles of the following conditional distributions

$$Pr(R_{s,t} \leq CoVaR_{\alpha,\beta,t}^- | R_{i,t} = VaR_{\alpha,t}^i) = \beta, \quad (4.3)$$

$$Pr(R_{s,t} \leq CoVaR_{\alpha,\beta,t} | R_{i,t} \leq VaR_{\alpha,t}^i) = \beta, \quad (4.4)$$

where $s \neq i$. The confidence levels α and β are decided *ex-ante* by the financial regulator. Typical values are 1% or 5%. In most studies a common confidence level for α and β is used, i.e., $\alpha = \beta$; however, working with different confidence levels, i.e., $\alpha \neq \beta$, is also feasible.

To obtain $CoVaR_{\alpha,\beta,t}^-$ estimates, [Adrian and Brunnermeier \(2011\)](#) employ linear quantile regressions.² Within this framework, time-varying $VaR_{\alpha,t}^i$ and $CoVaR_{\alpha,\beta,t}^-$ measures are generated from the predicted values of quantile regression specifica-

¹It is common to present downside risk statistics, such as VaR , in positive values. In this study, we do not follow this sign convention and instead maintain the original (negative) sign of the conditional quantile for all downside risk measures reported in the subsequent Sections, such as VaR , $CoVaR$, $\Delta CoVaR$, $CoES$, $\Delta CoES$.

²They also show in the appendix of their study that $CoVaR_{\alpha,\beta,t}^-$ can be estimated using *GARCH*-type models, providing closed-form expressions for $CoVaR$ estimation in the bivariate Gaussian framework.

tions, that is

$$VaR_{\alpha,t}^i = \hat{\phi}^i + \hat{\gamma}^i M_{t-1},$$

$$CoVaR_{\alpha,\beta,t}^- = \hat{\mu}^i + \hat{\theta}^i VaR_{\alpha,t}^i + \hat{\psi}^i M_{t-1},$$

where M_{t-1} is a vector of exogenous variables and $\hat{\phi}^i, \hat{\gamma}^i, \hat{\mu}^i, \hat{\theta}^i$ and $\hat{\psi}^i$ denote the estimated parameters of quantile regressions for each institution i . The $CoVaR_{\alpha,\beta,t}^-$ estimates derived from this procedure, however, do not have a time-varying exposure to its $VaR_{\alpha,t}^i$. The effect of $VaR_{\alpha,t}^i$ on $CoVaR_{\alpha,\beta,t}^-$, which is given by the coefficient estimate $\hat{\theta}^i$, remains the same regardless of any changes in the correlation between the returns of the financial system and the financial institution over time.

On the contrary, [Girardi and Ergün \(2013\)](#) follow a three-step procedure to obtain time-varying $CoVaR_{\alpha,\beta,t}$ estimates. In step one, they fit univariate time-series models on $R_{s,t}$ and $R_{i,t}$ returns, while in step two they apply the DCC model of [Engle \(2002\)](#) to the residuals of these regressions to obtain time-varying correlations. In the final step, given the $VaR_{\alpha,t}^i$ estimates obtained in step one and the time-varying correlations obtained in step two, they solve numerically the following two-dimensional integral for $CoVaR_{\alpha,\beta,t}$

$$\int_{-\infty}^{CoVaR_{\alpha,\beta,t}} \int_{-\infty}^{VaR_{\alpha,t}^i} pdf_t(x, y) dy dx = \alpha \cdot \beta, \quad (4.5)$$

where $pdf_t(x, y)$ denotes the bivariate density of $R_{s,t}$ and $R_{i,t}$. The time-varying correlations for each $R_{s,t}$ and $R_{i,t}$ pair imply that $CoVaR_{\alpha,\beta,t}$ measures reflect time-varying exposure to an institution's $VaR_{\alpha,t}^i$. Nevertheless, solving numerically for $CoVaR_{\alpha,\beta,t}$ in Equation (4.5) for each time-point correlation estimate is a non-trivial task. It is computationally intensive and time expensive, especially when the bivariate density $pdf_t(x, y)$ is mathematically more involved. In addition, the marginal specification in this framework is restricted and needs to result from the choice of the bivariate distribution of $R_{s,t}$ and $R_{i,t}$. In practice, the distributional characteristics of $R_{s,t}$ and $R_{i,t}$ can differ substantially and hence restricting the marginal specification may introduce misspecification bias in the computation of $CoVaR_{\alpha,\beta,t}$.

4.3.2 Copula *CoVaR* methodology

In this Section we show how the *Conditional Value-at-Risk* (*CoVaR*) can be estimated using copula functions. We provide simple analytical expressions for a broad range of copula families for both *CoVaR* definitions. In this respect, our Copula *CoVaR* approach overcomes the burden of numerical integration and also incorporates the time-varying dependence between $R_{s,t}$ and $R_{i,t}$ into the computation of the systemic risk measure through the copula parameter(s), which is allowed to vary over

time as a function of lagged information. Furthermore, the Copula *CoVaR* approach provides greater flexibility in the specification of the marginals and the dependence structure, i.e., the marginal specification is not restricted by the choice of the bivariate copula distribution, eliminating in this way potential misspecification bias in the computation of risk measures. This modelling setting also enables the decomposition of systemic risk into three main components: 1) the dependence structure, 2) the magnitude of dependence and 3) the marginal series. As a result, we can assess the relevant contribution of any of these three components to systemic risk.

The joint distribution function of bivariate random variables (Y, X) can be represented as

$$F_{YX}(y, x) = Pr(Y \leq y, X \leq x).$$

The famous theorem of Sklar (1959) gives the connection of marginals and copulas with the joint distribution. Let F_{YX} represent a bivariate cumulative distribution function with marginal distributions F_Y and F_X , then there exists a two dimensional copula cumulative distribution function C on $[0, 1]^2$, such that for all $(y, x) \in \overline{\mathbb{R}}^2$ it holds that

$$F_{YX}(y, x) = C(F_Y(y), F_X(x)).$$

For continuous F_Y and F_X , C is uniquely determined by

$$C(u, v) = F_{YX}(F_Y^{-1}(u), F_X^{-1}(v)),$$

where random variables $u = F_Y(y)$ and $v = F_X(x)$ (i.e., obtained by the probability integral transform) are uniformly distributed on $[0, 1]$, while $F_Y^{-1}(u)$ and $F_X^{-1}(v)$ are the generalised inverse distribution functions of the marginals.

It can be shown³, that the conditional probability distribution $Pr(Y \leq y|X = x)$ can be expressed in terms of a copula function as

$$Pr(Y \leq y|X = x) = \frac{\partial C(u, v)}{\partial v}. \quad (4.6)$$

In contrast, the conditional probability distribution $Pr(Y \leq y|X \leq x)$ can be expressed in terms of a copula function as

$$Pr(Y \leq y|X \leq x) = \frac{Pr(Y \leq y, X \leq x)}{Pr(X \leq x)} = \frac{C(F_Y(y), F_X(x))}{F_X(x)} = \frac{C(u, v)}{v}. \quad (4.7)$$

The class of Archimedean copulas has recently found wide usage in the economics and finance literature, because of their simple closed-form cumulative distribution

³See proof in Bouyè and Salmon (2009, p. 726).

functions and due to their properties allowing the modelling of the dependence between random variables. The Archimedean copulas can capture a broad range of forms of asymmetric tail dependence, which we know to be extremely important for modelling multiple relationships between financial asset returns. Bivariate Archimedean copulas are defined as

$$C(u, v) = \varphi^{-1} [\varphi(u) + \varphi(v)] ,$$

where $\varphi : [0, 1] \rightarrow [0, \infty)$ is a continuous strictly decreasing convex function such that $\varphi(1) = 0$ and φ^{-1} is the inverse of φ . The function φ is called *generator function* of the copula C (see [Nelsen \(2007\)](#), for further details).

We begin with the presentation of $CoVaR_{\alpha, \beta, t}^-$ in terms of Archimedean copulas and provide general solutions through their corresponding generator functions.⁴ From the general result in Equation (4.6) we have

$$Pr(Y \leq y | X = x) = \frac{\partial C(u, v)}{\partial v} = \frac{\varphi'(v)}{\varphi'(C(u, v))} = \frac{\varphi'(v)}{\varphi'(\varphi^{-1} [\varphi(u) + \varphi(v)])} . \quad (4.8)$$

Assuming that the above random variables Y and X represent the returns of the financial system, $R_{s,t}$, and the returns of the institution i , $R_{i,t}$, with distribution functions $F_{s,t}$ and $F_{i,t}$, respectively; the conditional distribution $Pr(R_{s,t} \leq CoVaR_{\alpha, \beta, t}^- | R_{i,t} = VaR_{\alpha, t}^i)$ can be equivalently expressed in terms of a copula generator function as follows

$$Pr(R_{s,t} \leq CoVaR_{\alpha, \beta, t}^- | R_{i,t} = VaR_{\alpha, t}^i) = \frac{\varphi'(v)}{\varphi'(\varphi^{-1} [\varphi(u) + \varphi(v)])} = \beta .$$

Solving for u , under the general condition that $\partial/\partial v C(u, v)$ is partially invertible in its first argument u , we obtain the copula conditional quantile

$$u^- \equiv u = \varphi^{-1} \left[\varphi \left(\varphi'^{-1} \left(\frac{1}{\beta} \varphi'(v) \right) \right) - \varphi(v) \right] . \quad (4.9)$$

Applying the probability integral transform in Equation (4.9), we derive an explicit expression for $CoVaR_{\alpha, \beta, t}^-$ for a broad range of Archimedean copula functions, that

⁴In Appendix 4.A we also provide general solutions for elliptical copula families, i.e., Gaussian and Student- t copulas. Even though these particular families do not have copula distributions in closed form, an explicit solution for $CoVaR_{\alpha, \beta, t}^-$ can be derived. Unfortunately, there is no explicit solution for $CoVaR_{\alpha, \beta, t}$ and hence numerical integration is needed.

is

$$CoVaR_{\alpha,\beta,t}^- = F_{s,t}^{-1} \left(\varphi^{-1} \left[\varphi \left(\varphi'^{-1} \left(\frac{1}{\beta} \varphi' \left(F_{i,t} (VaR_{\alpha,t}^i) \right) \right) \right) \right] - \varphi \left(F_{i,t} (VaR_{\alpha,t}^i) \right) \right), \quad (4.10)$$

where $F_{s,t}^{-1}$ is the generalised inverse distribution function of $F_{s,t}$. From the definition of VaR it holds that $v = F_{i,t}(VaR_{\alpha,t}^i) = F_{i,t}(F_{i,t}^{-1}(\alpha)) = \alpha$. Therefore, the expression for $CoVaR_{\alpha,\beta,t}^-$ in Equation (4.10) can be simplified further as follows

$$CoVaR_{\alpha,\beta,t}^- = F_{s,t}^{-1} \left(\varphi^{-1} \left[\varphi \left(\varphi'^{-1} \left(\frac{1}{\beta} \varphi'(\alpha) \right) \right) - \varphi(\alpha) \right] \right). \quad (4.11)$$

Alternatively, an analytical expression can also be given for $CoVaR_{\alpha,\beta,t}$ for a wide range of Archimedean copula families. Given the general result in Equation (4.7), the conditional distribution $Pr(R_{s,t} \leq CoVaR_{\alpha,\beta,t} | R_{i,t} \leq VaR_{\alpha,t}^i)$ can be equivalently written as

$$Pr(R_{s,t} \leq CoVaR_{\alpha,\beta,t} | R_{i,t} \leq VaR_{\alpha,t}^i) = \frac{\varphi^{-1} [\varphi(u) + \varphi(v)]}{v} = \beta. \quad (4.12)$$

Similarly, from the definition of VaR it holds that $v = F_{i,t}(VaR_{\alpha,t}^i) = F_{i,t}(F_{i,t}^{-1}(\alpha)) = \alpha$. Therefore, the expression in Equation (4.12) can be expressed as

$$\varphi^{-1} [\varphi(u) + \varphi(\alpha)] = \alpha \cdot \beta. \quad (4.13)$$

Finally, after solving for u and applying the probability integral transform, under the general condition that $C(u, v)$ is partially invertible in its first argument u , $CoVaR_{\alpha,\beta,t}$ has a general representation for Archimedean copulas, that is

$$u^{\leq} \equiv u = \varphi^{-1} [\varphi(\alpha \cdot \beta) - \varphi(\alpha)], \quad (4.14)$$

$$CoVaR_{\alpha,\beta,t} = F_{s,t}^{-1} \left(\varphi^{-1} [\varphi(\alpha \cdot \beta) - \varphi(\alpha)] \right). \quad (4.15)$$

The general representation of $CoVaR$ in Equation (4.11) or Equation (4.15) implies a constant correlation between $R_{s,t}$ and $R_{i,t}$. Nevertheless, it is known that the dependence structure between financial asset returns is not constant over a long horizon but rather time-varying. Numerous studies have also indicated that the correlation between financial series tends to be more pronounced during downturns than during upturns, a stylised feature that should be considered in the estimation of systemic risk. In this respect, the use of constant correlations may severely affect the risk estimates and lead to incorrect inferences. We follow the specification proposed by Patton (2006) in order to introduce a dynamic version of the Copula $CoVaR$ model and hence incorporate time-varying correlation into $CoVaR$ estimation. Patton (2006) proposed observation driven copula models for which the time-varying

dependence parameter(s) of a copula is a parametric function of transformed lagged data. It is essentially an ARMA(1,10)-type process. In Appendix 4.B we derive analytical expressions for $CoVaR_{\alpha,\beta,t}^-$ and $CoVaR_{\alpha,\beta,t}$, while in Appendix 4.C we present the time-varying parameter specification for the Clayton, Frank, Gumbel⁵ and BB7 copulas. These copula families are very popular in the literature for modelling the dependence between financial asset returns since they allow for very flexible dependency structures and can capture various forms of tail dependence.

4.3.3 Extension to *CoES*

The *CoVaR* concept can be easily adopted for other “co-risk” measures. One of them is the *Conditional Expected Shortfall (CoES)*. We denote by $CoES_{\alpha,\beta,t}^-$ the expected shortfall of the financial system conditional on $R_{i,t} = VaR_{\alpha,t}^i$ and similarly by $CoES_{\alpha,\beta,t}$ the expected shortfall of the financial system conditional on $R_{i,t} \leq VaR_{\alpha,t}^i$. In this respect, *CoES* estimates can be easily obtained for both definitions within our framework as follows

$$CoES_{\alpha,\beta,t}^- = \frac{1}{\beta} \int_0^\beta CoVaR_{\alpha,q,t}^- dq, \quad (4.16)$$

$$CoES_{\alpha,\beta,t} = \frac{1}{\beta} \int_0^\beta CoVaR_{\alpha,q,t} dq, \quad (4.17)$$

where $CoVaR_{\alpha,q,t}^- = Pr(R_{s,t} \leq F_{s,t}^{-1}(q) | R_{i,t} = VaR_{\alpha,t}^i)$ and $CoVaR_{\alpha,q,t} = Pr(R_{s,t} \leq F_{s,t}^{-1}(q) | R_{i,t} \leq VaR_{\alpha,t}^i)$.

4.3.4 Systemic risk contributor and dependence consistency

[Adrian and Brunnermeier \(2011\)](#) define institution i 's contribution to systemic risk by

$$\Delta CoVaR_{\alpha,\beta,t}^- = CoVaR_{\alpha,\beta,t}^- - CoVaR_{0.5,\beta,t}^-,$$

where $\Delta CoVaR_{\alpha,\beta,t}^-$ denotes the difference between the *VaR* of the financial system conditional on $R_{i,t} = VaR_{\alpha,t}^i$ and the *VaR* of the financial system conditional on $R_{i,t} = VaR_{0.5,t}^i$ (institution i being *exactly* at its median state). Following [Adrian and Brunnermeier \(2011\)](#), we adopt $\Delta CoVaR$ as a measure of institution i 's contribution to systemic risk and also define by $\Delta CoVaR_{\alpha,\beta,t}$ the difference between the *CoVaR* of the financial system conditional on $R_{i,t} \leq VaR_{\alpha,t}^i$ and the *CoVaR* of the financial system conditional on $R_{i,t} \leq VaR_{0.5,t}^i$ (institution i being *at most* at

⁵The $\partial/\partial v C(u, v)$ of the Gumbel copula is not partially invertible in its u and hence we cannot derive analytical expressions for $CoVaR_{\alpha,\beta,t}^-$.

its median state)⁶, that is

$$\Delta CoVaR_{\alpha,\beta,t} = CoVaR_{\alpha,\beta,t} - CoVaR_{0.5,\beta,t}.$$

The computation of $CoVaR_{0.5,\beta,t}^-$ or $CoVaR_{0.5,\beta,t}$ is straightforward and can be carried out as in the $CoVaR_{\alpha,\beta,t}^-$ or $CoVaR_{\alpha,\beta,t}$ procedure by simply modifying the stress scenario. We also employ $\Delta CoES$ as a measure of institution i 's contribution to systemic risk where the contribution is measured in terms of $CoES$. Therefore, we define

$$\Delta CoES_{\alpha,\beta,t}^- = CoES_{\alpha,\beta,t}^- - CoES_{0.5,\beta,t}^-,$$

$$\Delta CoES_{\alpha,\beta,t} = CoES_{\alpha,\beta,t} - CoES_{0.5,\beta,t},$$

where $\Delta CoES_{\alpha,\beta,t}^-$ denotes the difference between the $CoES$ of the financial system conditional on $R_{i,t} = VaR_{\alpha,t}^i$ and on the $CoES$ of the financial system conditional on $R_{i,t} = VaR_{0.5,t}^i$, while $\Delta CoES_{\alpha,\beta,t}$ denotes the same risk metric with stress scenarios being $R_{i,t} \leq VaR_{\alpha,t}^i$ and $R_{i,t} \leq VaR_{0.5,t}^i$, respectively.

To investigate whether the different representations for measuring contribution to systemic risk, derived within the Copula $CoVaR$ framework, encompass the dependence consistency properties reported in [Mainik and Schaanning \(2014\)](#), we compare $\Delta CoVaR$ estimates for the bivariate distribution with a Clayton copula.⁷ Figure 4.3.1 presents $\Delta CoVaR_{\alpha,\beta,t}^-$ and $\Delta CoVaR_{\alpha,\beta,t}$ measures as a function of the dependence parameter θ for a Clayton copula with Student- t marginals with three degrees of freedom at three different confidence levels, i.e., 1%, 5% and 10%. The behaviour of risk measures in these two models confirms the results in [Mainik and](#)

⁶[Girardi and Ergün \(2013\)](#) define the systemic risk contribution of a particular institution i by

$$\Delta CoVaR_{\alpha,\beta,t} = 100 \times (CoVaR_{\alpha,\beta,t} - CoVaR_{b_i,\beta,t}) / CoVaR_{b_i,\beta,t},$$

that is the percentage difference of the VaR of the financial system conditional on the distressed state of institution i from the VaR of the financial system conditional on the benchmark state of institution i . They define the benchmark state b_i as a one-standard deviation about the mean event: $\mu_{i,t} - \sigma_{i,t} \leq R_{i,t} \leq \mu_{i,t} + \sigma_{i,t}$, where $\mu_{i,t}$ and $\sigma_{i,t}$ are the conditional mean and the standard deviation of institution i 's returns, respectively. Nevertheless, the VaR of the financial system conditional on the benchmark state of institution i can not be derived in explicit form within our framework and thus numerical integration is needed. So far, there is no consensus in the literature regarding the definition of systemic risk contribution. For example, [Adrian and Brunnermeier \(2011\)](#) changed the definition of $\Delta CoVaR$ twice in two earlier versions of their paper. Nevertheless, [Mainik and Schaanning \(2014\)](#) show that the primary deficiency of $\Delta CoVaR$ is due to the underlying stress scenario $R_{i,t} = VaR_{\alpha,t}^i$. As a result, we decided to adopt $\Delta CoVaR$, as defined in [Adrian and Brunnermeier \(2011\)](#), as a measure of an institution's contribution to systemic risk but modified the distress events to ensure that $CoVaR$ is a continuous function of the dependence parameter.

⁷We have also compared $\Delta CoVaR$ for the bivariate distribution with a Frank copula. The dependence consistency properties are in line with the results reported for the bivariate distribution with a Clayton copula.

Schaanning (2014). Initially, $\Delta CoVaR_{\alpha,\beta,t}^=$ increases with respect to the dependence parameter; however, after a certain threshold it counter-intuitively starts to decrease. In other words, $\Delta CoVaR_{\alpha,\beta,t}^=$ fails to detect dependence when it becomes more pronounced. On the other hand, $\Delta CoVaR_{\alpha,\beta,t}$ increases with respect to the dependence parameter. Therefore, conditioning on $R_{i,t} \leq VaR_{\alpha,t}^i$ gives a much more consistent response to dependence than conditioning on $R_{i,t} = VaR_{\alpha,t}^i$.⁸

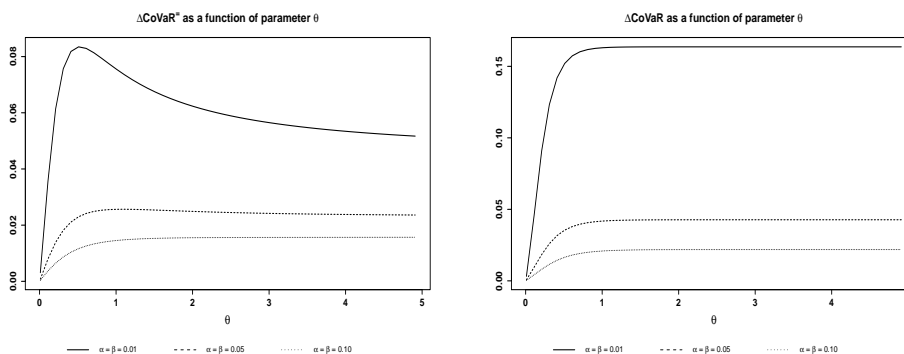


Figure 4.3.1: Clayton with Student- t margins with 3 degrees of freedom: $\Delta CoVaR_{\alpha,\beta,t}^=$ and $\Delta CoVaR_{\alpha,\beta,t}$ as a function of θ .

4.4 Data

We focus on the STOXX Europe 600 Banks Index that consists of 46 large European banks from 15 European countries, characterised by a large market capitalisation, international activity, cross-country exposure and a representative size in the local market. The STOXX Europe 600 Banks Index is a component of the STOXX Europe 600 Index that represents large, mid and small capitalisation companies across 18 countries of the European region. It is the largest, in market capitalisation, sector index of STOXX Europe 600 Index (€748.5 billion as of June, 2013), which indicates the relative importance and size of the banking sector in Europe. We exclude 4 institutions from the initial sample because the history of their corresponding datasets is narrow and does not cover the time period we want to analyse. Therefore, the resulting sample is formed by a total of 42 European banks, starting on 01/04/2002 and ending on 31/12/2012. This time period provides a good platform to assess the level of contribution of the systemically important financial institutions in Europe to systemic risk since it includes a number of significant events (e.g. the U.S subprime mortgage crisis, the Lehman Brothers collapse, the European sovereign-debt crisis etc.). We assign the Q3 2007 - Q4 2012 as the crisis period because the majority of these events occurred within this time window.

⁸Similar dependence consistency results are obtained when $\Delta CoES$ is employed for the same stochastic models.

We obtain weekly equity adjusted prices, to account for capital operations (i.e., splits, dividends etc.), from the Datastream database and convert them to weekly log returns. There are 562 weekly returns for each institution in our sample. Appendix 4.D lists these institutions. For each bank, an equally-weighted average of the returns of the remaining banks in the sample is used as a proxy for the financial system. In this way, the resulting system return portfolios can be considered representative of the European financial system, allowing the study of possible spillover effects between a stressed institution and the financial system. Moreover, this approach rules out any spurious correlation that may be induced due to the sizeable disparity in the composition of the financial system proxy. For example, HSBC has a total contribution of 20.5% to the composition of the STOXX Europe 600 Banks Index. As a result, if the corresponding index is used as a proxy for the financial system, systemic risk estimates generated conditional on HSBC will be severely affected by the presence and the large scale factor of HSBC in the financial system's portfolio proxy.

4.5 Copula *CoVaR* estimation

The computation of *CoVaR* or *CoES* requires the estimation of the parameter(s) of the marginal densities and the copula function that captures the dependence between $R_{s,t}$ and $R_{i,t}$. Assume a vector of system and institution returns $\mathbf{R}_t = (R_{s,t}, R_{i,t})'$, ($t = 1, \dots, T$; $i = 1, \dots, N$) where $s \neq i$. Given that a copula function and the marginals are continuous, their joint probability density function can be expressed in terms of the copula density function, $c(\cdot, \cdot; \theta_t)$, and the univariate marginal densities, $f_{s,t}(R_{s,t}; \phi_s)$ and $f_{i,t}(R_{i,t}; \phi_i)$, as follows

$$f(R_{s,t}, R_{i,t}) = c(u_t, v_t; \theta_t) \cdot f_{s,t}(R_{s,t}; \phi_s) \cdot f_{i,t}(R_{i,t}; \phi_i), \quad (4.18)$$

where θ_t denotes the copula parameter while ϕ_s and ϕ_i denote the parameters for the system's and institution i 's marginal distributions, respectively. In the above expression $u_t = F_{R_{s,t}}(R_{s,t}; \phi_s)$ and $v_t = F_{R_{i,t}}(R_{i,t}; \phi_i)$ are the uniformly transformed marginal series. The log-likelihood function of Equation (4.18) is given by

$$L(\theta_t, \phi_s, \phi_i) = \sum_{t=1}^T [\log c(u_t, v_t; \theta_t) + \log f_{s,t}(R_{s,t}; \phi_s) + \log f_{i,t}(R_{i,t}; \phi_i)] . \quad (4.19)$$

The marginal densities $f_{s,t}(R_{s,t}; \phi_s)$ and $f_{i,t}(R_{i,t}; \phi_i)$ can be conditional densities and the series $R_{s,t}$ and $R_{i,t}$ are usually modelled by a GARCH-type model, whose residuals are treated as *i.i.d* random variables. Under this setting, full maximum likelihood estimates (MLE) can be obtained by maximising Equation (4.19) with respect to the parameters $(\theta_t, \phi_s, \phi_i)$. In general, the full MLE estimation would be our first choice due to the well-known optimality properties of the maximum likelihood.

However, the Inference Functions for Margins (IFM) method is usually preferred to full MLE due to its computational tractability and comparable efficiency. The IFM method (see [Joe and Hu \(1996\)](#); [Joe \(1997\)](#), for further details) is a multi-step optimisation technique. It divides the parameter vector into separate parameters for each marginal distribution and parameters for the copula model. Therefore, one may break up the optimisation problem into two parts. In this study we adopt the IFM method to estimate the parameters of the marginal distributions and copula function and subsequently obtain *CoVaR* and *CoES* estimates.

When modelling the distribution of financial asset returns, the critical issues are dynamic volatility and the modelling of asymmetries. It is well-documented that asset return distributions are skewed and fat-tailed. Moreover, the volatility of asset returns is not constant; it is mean-reverting and it tends to cluster. Another important stylised characteristic of asset returns volatility is that a large negative price shock increases volatility much more than a positive price shock of the same magnitude, which is also known as “leverage-effect”. To address these features we assume that the returns of the financial system and institution i at time t , $\mathbf{R}_t = (R_{s,t}, R_{i,t})'$, follow an AR(1)-GJR-GARCH(1,1) model.⁹ Therefore for $j \equiv s, i$ and time $t = 1, \dots, T$ we estimate

$$R_{j,t} = \mu_{j,t} + \varepsilon_{j,t} = \phi_{j,0} + \phi_{j,1}R_{j,t-1} + \sigma_{j,t}z_{j,t}, \quad (4.20)$$

$$\sigma_{j,t}^2 = \omega_j + \alpha_j\sigma_{j,t-1}^2 + \beta_j\varepsilon_{j,t-1}^2 + \xi_j I_{t-1}\varepsilon_{j,t-1}^2, \quad (4.21)$$

where I_{t-1} is an indicator function equal to 1 if $\varepsilon_{j,t-1} < 0$, and 0 otherwise. We assume that the distribution of the innovations $z_{j,t}$ is a white noise process with zero mean, unit variance and a distribution function given by $F_{z_j,t}$. To allow for asymmetry in the marginal distributions, we assume that the distribution of the innovations follows the Skewed- t distribution, as introduced in [Fernández and Steel \(1998\)](#). It is very common, however, when modelling asset returns, to assume normality. In this respect, we also estimate the time-series models in Equation (4.20) and Equation (4.21) based on the assumption of normal distributed innovations.¹⁰ We denote the cumulative distribution functions of the financial system and institution i 's innovations by $u_t \equiv F_{z_s,t}(z_{s,t})$ and $v_t \equiv F_{z_i,t}(z_{i,t})$, respectively.¹¹ The

⁹The asymmetric GJR-GARCH model is developed in [Glosten et al. \(1993\)](#).

¹⁰Note that given the innovations distributional assumptions we can easily obtain time-varying *VaR* estimates for each institution i (see [Duffie and Pan \(1997\)](#); [Jorion \(2001\)](#) among others, for further details)

¹¹The innovations can also be transformed to uniformly distributed data non-parametrically by their corresponding empirical distribution functions without assuming any particular parametric distribution for the marginals. This semi-parametric (SP) method is also known as pseudo maximum

dependence parameter is then estimated by maximising the log-likelihood function in Equation (4.19), given the estimated parameters of the marginal series.

In this respect, *CoVaR* estimates can be obtained by evaluating the analytical expressions derived in Section 4.3.2. Note that the conditional quantiles implied by Equation (4.9) and Equation (4.14) correspond to the conditional quantiles of innovations. To obtain time-varying *CoVaR* measures, we rescale $CoVaR_{\alpha,\beta,t}^-$ or $CoVaR_{\alpha,\beta,t}$ estimates with the fitted conditional mean $\mu_{s,t}$ and standard deviation $\sigma_{s,t}$ of $R_{s,t}$, obtained from estimated Equation (4.20) and Equation (4.21), as follows

$$CoVaR_{\alpha,\beta,t}^- = \mu_{s,t} + \sigma_{s,t} F_{z_{s,t}}^{-1}(u_t^-),$$

$$CoVaR_{\alpha,\beta,t} = \mu_{s,t} + \sigma_{s,t} F_{z_{s,t}}^{-1}(u_t^{\leq}),$$

where $F_{z_{s,t}}^{-1}$ is the generalised inverse of the financial system's innovation distribution function and u_t^- and u_t^{\leq} are the conditional quantiles of the general solutions in Equation (4.9) and Equation (4.14), respectively.¹² Also note that the conditional quantiles in Equation (4.9) and Equation (4.14) correspond to a static model (i.e., θ is constant). However, the dynamic version of the model (i.e., θ_t is time-varying) implies that conditional quantiles are also time-varying. Therefore, we use the subscript t in u_t^- and u_t^{\leq} to distinguish between the dynamic and static model.

4.6 Results

4.6.1 Computing *CoVaR* and *CoES* measures

In this Section we present results based on the representation of *CoVaR* by Girardi and Ergün (2013).¹³ In our search for the copula model that can sufficiently describe the dependence between financial system and institution returns, we consider four alternative copula functional forms: Clayton, Frank, Gumbel and BB7. Each of these copula families allows for positive dependence but implies a different type of

likelihood (PML) method (see Genest et al. (1995), for further details). The semi-parametric (SP) method can tackle the marginal misspecification problem since it treats the marginal distributions as unknown functions.

¹²To obtain time-varying *CoES* measures, the same process as in the computation of *CoVaR* is followed; however, the copula conditional quantiles u_t^- and u_t^{\leq} are obtained from the corresponding expressions in Equation (4.16) and Equation (4.17), respectively.

¹³As discussed earlier, *CoVaR* under this definition is a dependent consistent measure of systemic risk, which is an essential property for a well-specified model. Another attractive characteristic of it is that *CoVaR* estimates generated under this framework can be statistically evaluated, providing a distinctive opportunity to assess the statistical adequacy of systemic risk models. In Appendix 4.E, we present a graphical comparison between *CoVaR* and *CoES* measures under both definitions conditional on HSBC returns. Similar results are also obtained for the rest of the pairs analysed.

tail dependence between the variables. For example, the Clayton copula only allows for negative tail dependence and would hence fit best if negative changes in financial system and institution returns are more highly correlated than positive changes. In contrast, the Gumbel copula only allows for positive tail dependence, while the Frank copula does not allow for tail dependence. Finally, the BB7 copula allows for asymmetric upper and lower tail dependence. In practice, *CoVaR* focuses on the joint tail distribution of the financial system-institution pair returns and thus tail dependence is a rather important concept for *CoVaR* computation.

We estimate dynamic $CoVaR_{\alpha,\beta,t}$ and $CoES_{\alpha,\beta,t}$ measures for each institution i . We employ two alternative distributional assumptions for the marginal series: Gaussian and Skewed- t . The selection of the best-fitting copula model for each system-institution pair is based on the Akaike Information Criterion (AIC) (Akaike, 1974).¹⁴ All risk measures ($Var_{\alpha,t}^i$, $CoVaR_{\alpha,\beta,t}$, $CoES_{\alpha,\beta,t}$) are computed at the same confidence level, i.e., $\alpha = \beta = 5\%$. We also evaluate $CoVaR_{\alpha,\beta,t}$ estimates for statistical accuracy and independence using modified versions of the standard Kupiec (1995) and Christoffersen (1998) tests (see Girardi and Ergün (2013), for further details on the implementation of the modified tests). Figure 4.6.1 shows time-series average $Var_{\alpha,t}^i$, $CoVaR_{\alpha,\beta,t}$ and $CoES_{\alpha,\beta,t}$ measures, while Figure 4.6.2 shows time-varying average Kendall's τ correlations implied by the estimated bivariate copula families, across all financial system-institution pairs with Skewed- t marginals. The light blue shaded area in the graphs corresponds to Q3 2007 - Q4 2012 crisis period. It is clear that $CoVaR_{\alpha,\beta,t}$ and $CoES_{\alpha,\beta,t}$ estimates are higher in absolute value during this period. This is partly due to the increasing correlation between financial system and institution returns as shown in Figure 4.6.2.

¹⁴The Bayesian Information Criterion (BIC) of Schwarz (1978) was also employed in the selection procedure for the best-fitting copula model; however, the results remained unaffected.

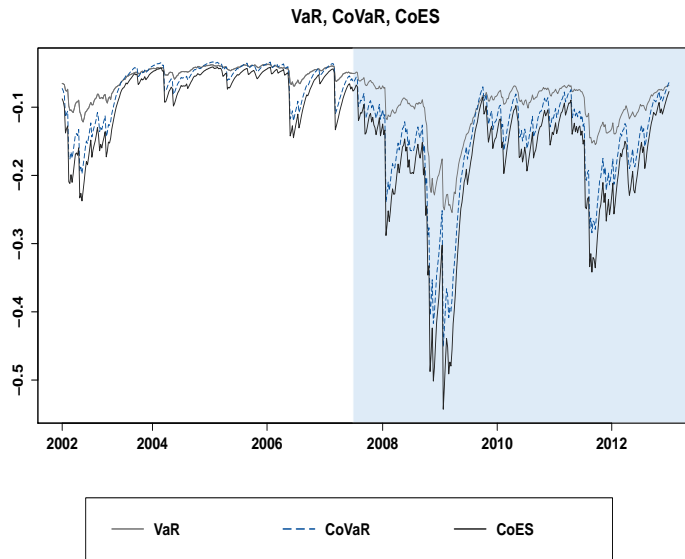


Figure 4.6.1: This figure shows time-series average values of weekly $VaR_{\alpha,t}^i$, $CoVaR_{\alpha,\beta,t}$ and $CoES_{\alpha,\beta,t}$ measures across all financial system-institution pairs. All risk measures are generated under the assumption of Skewed- t margins and computed at $\alpha = \beta = 5\%$ level. The light blue shaded area corresponds to Q3 2007 - Q4 2012 crisis period.

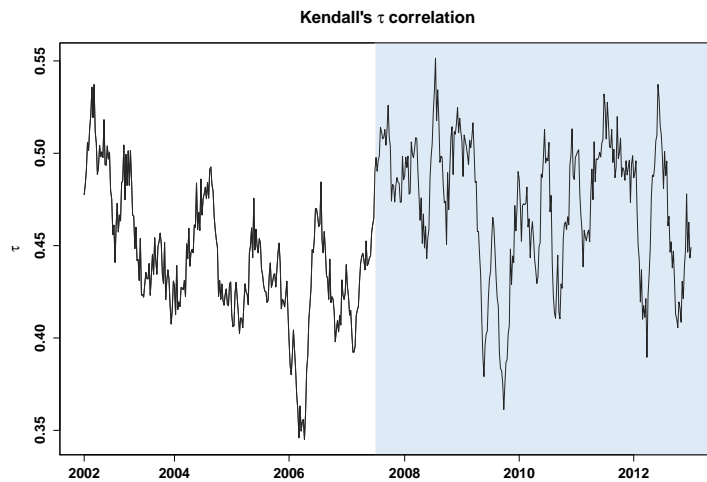


Figure 4.6.2: This figure shows time-series average Kendall's τ correlation estimates implied by estimated copula families across all financial system-institution pairs. All risk measures are generated under the assumption of Skewed- t margins and computed at $\alpha = \beta = 5\%$ level. The light blue shaded area corresponds to Q3 2007 - Q4 2012 crisis period.

Nevertheless, the time-varying correlation results cannot fully support the empirical findings in Longin and Solnik (2001) and Ang and Chen (2002), indicating that conditional correlations between financial asset returns are much stronger in downturns than in upturns. The time-varying Kendall's τ correlations are slightly more pronounced during the crisis period than in the pre-crisis period for most of the pairs; the average value is 0.44 in the pre-crisis period and 0.47 in the crisis period for all

pairs under consideration. Figures 4.6.1 and 4.6.2 also indicate the importance of consistency of systemic risk measures with respect to dependence. It is clear from the two graphs that high values of Kendall's τ correlations are associated with high in absolute value systemic risk estimates. Therefore, a systemic risk measure that provides an inconsistent response to dependence may fail to detect systemic risk when it is more pronounced, i.e., during periods of financial distress, and thus lead financial system regulators to make inappropriate policy decisions. Therefore, the notion of consistency of systemic risk measures with respect to dependence becomes rather significant during crisis periods.

Figure 4.6.3 displays a cross-section plot of an institution's average $VaR_{\alpha,t}^i$ and its contribution to systemic risk, measured by average $\Delta CoVaR_{\alpha,\beta,t}$. It is clear that there is a weak relationship between an institution's $VaR_{\alpha,t}^i$ and its $\Delta CoVaR_{\alpha,\beta,t}$ in the cross-section. Similar findings are also reported in [Adrian and Brunnermeier \(2011\)](#) and [Girardi and Ergün \(2013\)](#) leading to the conclusion that regulating the risk of financial institutions in isolation, through institutions' VaR , might not be the optimal policy for protecting the financial sector against systemic risk. In contrast, Figure 4.6.4 plots the time-series average of $VaR_{\alpha,t}^i$ and $\Delta CoVaR_{\alpha,\beta,t}$ over time. It is evident that $VaR_{\alpha,t}^i$ and $\Delta CoVaR_{\alpha,\beta,t}$ measures have a strong relationship in the time series. [Adrian and Brunnermeier \(2011\)](#) report the same strong relationship, while [Girardi and Ergün \(2013\)](#) confirm a weak relationship between these two risk measures in the time series. Given our findings, we can conclude that the association between these two measures over time is primarily determined by the alternative definitions of $\Delta CoVaR$ and not by the alternative $CoVaR$ definitions.¹⁵

¹⁵This conclusion results from estimating $CoVaR$ under both stress scenarios $R_{i,t} = VaR_{\alpha,t}^i$ and $R_{i,t} \leq VaR_{\alpha,t}^i$ and employing alternative $\Delta CoVaR$ definitions for three copula models: Clayton, Gumbel and Frank. Numerical integration is used to estimate $CoVaR$ when explicit expressions are not available in our Copula $CoVaR$ framework (see also footnote 6). The weak relationship between $\Delta CoVaR$ and VaR in the time series is supported only when the definition of $\Delta CoVaR$ employed is that of [Girardi and Ergün \(2013\)](#) is used, regardless of alternative $CoVaR$ definitions.

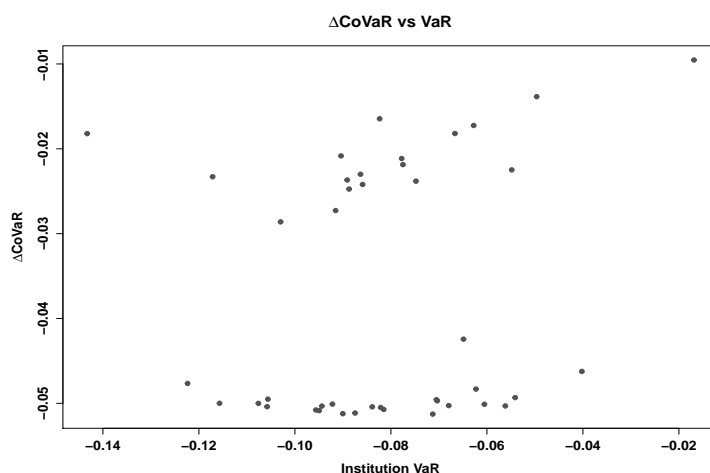


Figure 4.6.3: This scatter plot shows the cross-sectional link between the time-series average of each financial institution's risk in isolation, measured by $VaR_{\alpha,t}^i$, and the time-series average contribution to systemic risk, measured by $\Delta CoVaR_{\alpha,\beta,t}$. All risk measures are generated under the assumption of Skewed- t margins and computed at $\alpha = \beta = 5\%$ level.

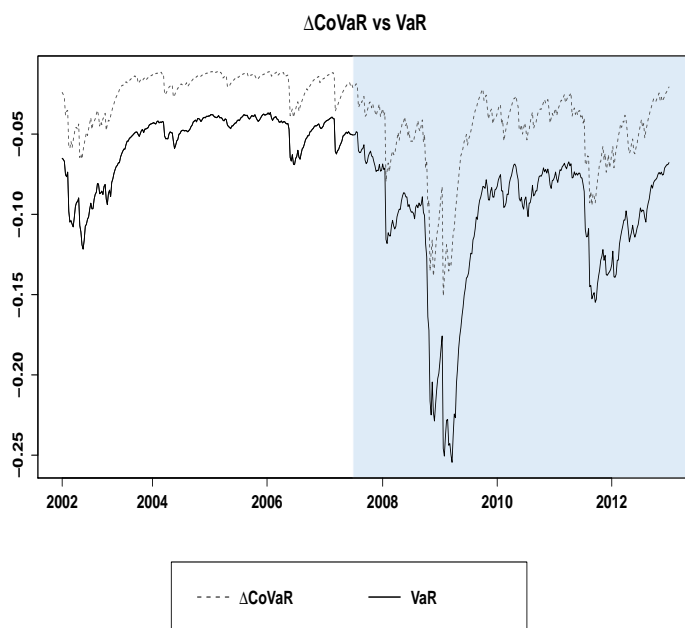


Figure 4.6.4: This figure shows the time-series average of weekly $\Delta CoVaR_{\alpha,\beta,t}$ and $VaR_{\alpha,t}^i$ measures. All risk measures are generated under the assumption of Skewed- t margins and computed at $\alpha = \beta = 5\%$ level. The light blue shaded area corresponds to Q3 2007 - Q4 2012 crisis period.

4.6.2 Systemic risk contribution

Table 4.6.1 ranks the contribution of each individual bank to overall systemic risk, as measured by the time-series average of $\Delta CoVaR_{\alpha,\beta,t}$ and $\Delta CoES_{\alpha,t}$ estimates, under the assumption of Gaussian and Skewed- t margins, respectively. Table 4.6.1 also displays the selected copula functions and the average value of Kendall's τ cor-

relation coefficients implied by the estimated copula parameters of each financial system-institution pair. The Frank copula is the most preferred functional form for describing the dependence between financial system and institution returns and the Gumbel copula is the second most popular choice under the assumption of Gaussian marginals. In contrast, the BB7 copula is the most popular functional form for modelling the dependence under the Skewed- t marginals assumption, while the Frank copula is the second most favoured choice. The Clayton copula has not been selected for any of the pairs analysed under both marginal assumptions. It is clear from Table 4.6.1 that the distribution assumptions in the marginals affect the selection of the best-fitting copula and hence the overall $CoVaR_{\alpha,\beta,t}$ and $CoES_{\alpha,\beta,t}$ results. Therefore, particular attention should be paid when specifying marginals since the use of inappropriate marginals not only introduces biases directly but also affects systemic risk measures indirectly, through copula parameter estimation or copula misspecification.¹⁶

The average $\Delta CoVaR_{\alpha,\beta,t}$ and $\Delta CoES_{\alpha,\beta,t}$ estimates with Skewed- t margins are much higher in absolute value than those generated under the assumption of Gaussian marginals. The size differences in systemic risk measures, however, result not only from the alternative marginal assumptions but also from the characteristics of the copula functions that model the dependence for each pair. The dominant copula function when assuming Gaussian marginals is Frank, while BB7 is the most popular copula family under Skewed- t marginals. As explained, the Frank copula does not imply tail dependence, while the BB7 copula allows for asymmetric tail dependence. In this regard, the general dependence structure, and especially the dependence structure in extremes, affects substantially the computation of $CoVaR_{\alpha,\beta,t}$ and $CoES_{\alpha,\beta,t}$. This is also confirmed by the implied Kendall's τ estimates reported in Table 4.6.1. It is clear from Table 4.6.1 that for those copula families that do not imply lower tail dependence, such as the Frank or the Gumbel copula family, the average $\Delta CoVaR_{\alpha,\beta,t}$ and $\Delta CoES_{\alpha,\beta,t}$ estimates are primarily driven by the degree of dependence.

The stronger the dependence between financial system and institution returns the higher the average values of $\Delta CoVaR_{\alpha,\beta,t}$ and $\Delta CoES_{\alpha,\beta,t}$. In contrast, when the dependence between the financial system and an institution's returns is modelled by an asymmetric BB7 copula, the average $\Delta CoVaR_{\alpha,\beta,t}$ and $\Delta CoES_{\alpha,\beta,t}$ estimates are not monotonic functions of Kendall's τ correlation estimates but their values are also affected by the degree of tail dependence. Figure 4.6.5 shows the average time-varying upper (λ^U) and lower (λ^L) tail dependence indices estimated from

¹⁶The effects on the computation of the VaR when there is a misspecification in the marginals and in the copulas has been investigated by Fantazzini (2009).

those pairs modelled by a BB7 copula under the assumption of Skewed- t marginals. There is clear evidence of asymmetric tail dependence.

The average value of upper and lower tail dependence indices is 0.45 and 0.50, respectively, leading to the conclusion that joint negative extremes occur more often than joint positive extremes. To investigate further the impact of asymmetries in the tails on the computation of systemic risk metrics, we compute non-parametric (N-P) estimates (an average of non-parametric estimates in Dobrić and Schmid (2005)) for upper (λ^U) and lower (λ^L) tail dependence coefficients and sample Kendall's τ correlation coefficients for each financial system-institution pair of standardised residuals, obtained from the fit of the univariate time-series models in Section 4.5. Table 4.6.3 reports average $\Delta CoVaR_{\alpha,\beta,t}$, sample Kendall's τ and non-parametric tail dependence indices for each pair. It is not surprising that banks having high coefficients of lower tail dependence appear among the most systemic financial institutions, indicating in this way the importance of asymmetries in systemic risk modelling.

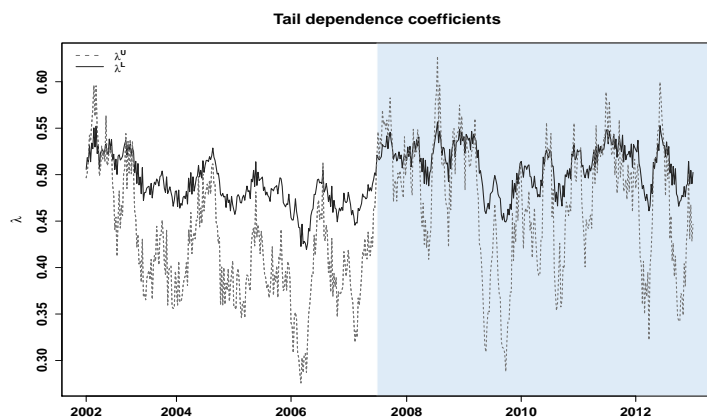


Figure 4.6.5: This figure shows time-varying average values of upper (λ^U) and lower (λ^L) tail dependence coefficients implied by BB7 copulas under the assumption of Skewed- t margins. All risk measures are computed at $\alpha = \beta = 5\%$ level. The light blue shaded area corresponds to Q3 2007 - Q4 2012 crisis period.

The ranking of the systemically important financial institutions in Table 4.6.1 varies significantly across different marginal distributional assumptions but is more consistent across alternative systemic risk measures within the same marginal distributional assumptions. For example, Santander bank is ranked as the 2nd most systemic financial institution according to its average contribution to systemic risk, measured by $\Delta CoVaR_{\alpha,\beta,t}$, under the assumption of Gaussian margins, while it is ranked in the 7th place when Skewed- t margins are assumed instead. Moreover, BNP Paribas is ranked as the 3rd most systemic bank based on its average $\Delta CoES_{\alpha,\beta,t}$ measure under normality, but under the assumption of Skewed- t margins it is ranked in the 26th place. Nevertheless, the hierarchy of systemic banks across $\Delta CoVaR_{\alpha,\beta,t}$

and $\Delta CoES_{\alpha,\beta,t}$ does not differ significantly under the same marginal distribution assumptions, implying that qualitative results depend more on the underlying distribution assumptions in the margins and dependence structure and less on the systemic risk measures *per se*.

From the ranking results in Table 4.6.1 and the market capitalisation values of financial institutions reported in Table 4.D.1 in the Appendix 4.D, it can also be shown that banks which are large in size with strong cross-country exposure and international activity appear among the most systemic financial institutions under both distribution assumptions. For instance, banks such as BBVA, UBS, Deutsche Bank, Credit Suisse or BNP Paribas, are placed among these institutions. Table 4.6.2 displays a cross-country comparison of systemic risk contribution measured by the average $\Delta CoVaR_{\alpha,\beta,t}$ and $\Delta CoES_{\alpha,\beta,t}$ of financial firms belonging to the same country. Financial institutions from France and Spain appear to be the most systemic ones according to their average $\Delta CoVaR_{\alpha,\beta,t}$ and $\Delta CoES_{\alpha,\beta,t}$ estimates under Gaussian and Skewed- t marginal distribution assumptions, respectively. In contrast, banks from Portugal, Ireland or Greece are classified among the least systemic financial institutions in our sample.

One may regard this classification as an economic paradox since banks that belong to those national economies that have suffered the most from the European sovereign debt crisis - and the market value of whose corresponding share prices has declined significantly during the crisis - appear among the least systemic financial institutions in the cross-country comparison. However, banks from these particular countries are typical commercial banks with substantial presence in the local market but limited international activity and cross-country exposure. Therefore, the implied correlation and more importantly the dependence in extreme events between these banks and the financial system is typically reduced generating in this way lower in absolute value systemic risk estimates. This is also confirmed by the fact that the Frank copula which does not allow for tail dependence is the preferred copula functional form for most of these particular pairs.

These findings should not be regarded as a weakness of the *CoVaR* model but rather as a merit. According to Brunnermeier et al. (2009), a systemic risk measure should be able to identify the risk to the system by individually “systemically important” institutions, which are highly interconnected and large enough to cause negative spill over effects on others, as well as by small institutions that are “systemic” when acting as parts of a herd. In this respect, the relative size and the interconnectedness of each particular financial institution are factors that should be considered in systemic risk measurement. The *CoVaR* methodology implicitly incorporates institution size and interconnectedness into systemic risk estimation through correlation

and dependence on extreme events. In our study, the financial system is represented by components of the STOXX Europe 600 Banks Index, which includes the largest banks in terms of market capitalisation in Europe. It is a portfolio of 42 financial institutions from 15 different European countries.

The majority of and the largest in size among these financial institutions come from countries such as Germany, France, Spain, Italy and Great Britain. Therefore, the implied dependence between each of these particular institutions and the financial system is, by construction, stronger due to within-country dependence (e.g increased commonalities for institution returns from same country) and the dependence that arises from their large size and dominant position in the European market. This may partly explain why banks from these particular countries are listed among the most systemic financial institutions in our study. The results in Table 4.6.4 support this argument. Table 4.6.4 reports average sample Kendall's τ and non-parametric upper (λ^U) and lower (λ^L) tail dependence estimates for each country. It is evident that Kendall's τ correlations and non-parametric tail dependence coefficients are much stronger for these particular countries, implying a stronger dependence and dependence in the tails of the joint distribution and consequently higher, on average, systemic risk estimates.

Table 4.6.1: This table ranks the average contribution to systemic risk for each individual institution.

ΔCoVaR results								ΔCoES results							
Normal Margins				Skewed- t Margins				Normal Margins				Skewed- t Margins			
Bank	Copula	ΔCoVaR	τ	Bank	Copula	ΔCoVaR	τ	Bank	Copula	ΔCoES	τ	Bank	Copula	ΔCoES	τ
BBVA	Gumbel	-2.741	0.62	POP	BB7	-5.127	0.46	BBVA	Gumbel	-2.549	0.62	POP	BB7	-5.236	0.46
SCH	Gumbel	-2.709	0.61	DBK	BB7	-5.122	0.55	SCH	Gumbel	-2.522	0.61	DBK	BB7	-5.227	0.55
BNP	Gumbel	-2.691	0.60	UBSN	BB7	-5.114	0.53	BNP	Gumbel	-2.507	0.60	UBSN	BB7	-5.226	0.53
CRDA	Gumbel	-2.585	0.57	CSGN	BB7	-5.086	0.51	CRDA	Gumbel	-2.417	0.57	CSGN	BB7	-5.186	0.51
UCG	Gumbel	-2.524	0.55	CRDA	BB7	-5.078	0.53	UCG	Gumbel	-2.365	0.55	CRDA	BB7	-5.181	0.53
SEA	Gumbel	-2.488	0.54	SEA	BB7	-5.073	0.50	SEA	Gumbel	-2.336	0.54	LLOY	BB7	-5.178	0.46
NDA	Gumbel	-2.476	0.54	SCH	BB7	-5.049	0.56	NDA	Gumbel	-2.326	0.54	BSAB	BB7	-5.168	0.38
BARC	Gumbel	-2.450	0.54	BBVA	BB7	-5.041	0.57	BARC	Gumbel	-2.302	0.54	SEA	BB7	-5.160	0.50
LLOY	Gumbel	-2.334	0.50	LLOY	BB7	-5.039	0.46	LLOY	Gumbel	-2.203	0.50	SVK	BB7	-5.155	0.41
SGE	Frank	-1.934	0.64	UCG	BB7	-5.033	0.50	SGE	Frank	-1.746	0.64	SCH	BB7	-5.125	0.56
DBK	Frank	-1.883	0.63	BSAB	BB7	-5.031	0.38	DBK	Frank	-1.700	0.63	UCG	BB7	-5.124	0.50
KB	Frank	-1.802	0.60	NDA	BB7	-5.027	0.50	KB	Frank	-1.626	0.60	BP	BB7	-5.123	0.47
UBSN	Frank	-1.798	0.60	SVK	BB7	-5.011	0.41	UBSN	Frank	-1.623	0.60	DNB	BB7	-5.121	0.38
CSGN	Frank	-1.798	0.59	BP	BB7	-5.009	0.47	CSGN	Frank	-1.622	0.59	NDA	BB7	-5.118	0.50
CBK	Frank	-1.713	0.57	KB	BB7	-5.000	0.52	CBK	Frank	-1.545	0.57	DAB	BB7	-5.111	0.38
ISP	Frank	-1.704	0.56	CBK	BB7	-4.999	0.49	ISP	Frank	-1.537	0.56	BBVA	BB7	-5.110	0.57
BMPS	Frank	-1.664	0.55	DNB	BB7	-4.971	0.38	BMPS	Frank	-1.500	0.55	BARC	BB7	-5.085	0.48
KNF	Frank	-1.660	0.53	DAB	BB7	-4.956	0.38	KNF	Frank	-1.497	0.53	CBK	BB7	-5.078	0.49
MB	Frank	-1.652	0.56	BARC	BB7	-4.951	0.48	MB	Frank	-1.490	0.56	KB	BB7	-5.075	0.52
RBS	Frank	-1.645	0.54	SYD	BB7	-4.932	0.33	RBS	Frank	-1.483	0.54	SYD	BB7	-5.073	0.33
POP	Frank	-1.594	0.53	JYS	BB7	-4.832	0.34	POP	Frank	-1.437	0.53	JYS	BB7	-5.033	0.34
PMI	Frank	-1.587	0.53	ETE	BB7	-4.766	0.35	PMI	Frank	-1.430	0.53	BPSO	BB7	-4.888	0.29
HSBA	Frank	-1.580	0.52	BPSO	BB7	-4.624	0.29	HSBA	Frank	-1.424	0.52	ETE	BB7	-4.887	0.35
BP	Frank	-1.575	0.53	BCV	BB7	-4.244	0.27	BP	Frank	-1.419	0.53	BCV	BB7	-4.582	0.27
SWED	Frank	-1.526	0.50	SGE	Frank	-2.862	0.62	SWED	Frank	-1.374	0.50	SGE	Frank	-2.910	0.62
STAN	Frank	-1.492	0.50	BNP	Frank	-2.728	0.61	STAN	Frank	-1.343	0.50	BNP	Frank	-2.769	0.61
ERS	Frank	-1.464	0.50	ISP	Frank	-2.474	0.53	ERS	Frank	-1.318	0.50	ISP	Frank	-2.507	0.53
SVK	Frank	-1.455	0.48	BMPS	Frank	-2.420	0.53	SVK	Frank	-1.310	0.48	BMPS	Frank	-2.460	0.53
DAB	Frank	-1.383	0.46	MB	Frank	-2.382	0.54	DAB	Frank	-1.244	0.46	MB	Frank	-2.422	0.54
BSAB	Frank	-1.357	0.45	KNF	Frank	-2.368	0.50	BSAB	Frank	-1.220	0.45	KNF	Frank	-2.405	0.50
POH	Frank	-1.321	0.45	RBS	Frank	-2.330	0.51	POH	Frank	-1.188	0.45	RBS	Frank	-2.354	0.51
BKIR	Frank	-1.315	0.44	PMI	Frank	-2.300	0.51	BKIR	Frank	-1.183	0.44	PMI	Frank	-2.335	0.51
DNB	Frank	-1.305	0.44	HSBA	Frank	-2.249	0.51	DNB	Frank	-1.173	0.44	HSBA	Frank	-2.285	0.51
BES	Frank	-1.274	0.42	SWED	Frank	-2.187	0.48	BES	Frank	-1.145	0.42	SWED	Frank	-2.216	0.48
JYS	Frank	-1.260	0.39	STAN	Frank	-2.115	0.48	JYS	Frank	-1.132	0.39	STAN	Frank	-2.144	0.48
SYD	Frank	-1.227	0.41	ERS	Frank	-2.084	0.47	SYD	Frank	-1.102	0.41	ERS	Frank	-2.118	0.47
ETE	Frank	-1.217	0.40	BKIR	Frank	-1.821	0.41	ETE	Frank	-1.093	0.40	BKIR	Frank	-1.845	0.41
BCP	Frank	-1.212	0.40	POH	Frank	-1.820	0.42	BCP	Frank	-1.088	0.40	POH	Frank	-1.840	0.42
BPE	Frank	-1.081	0.37	BES	Frank	-1.725	0.39	BPE	Frank	-0.969	0.37	BES	Frank	-1.744	0.39
BPSO	Frank	-1.016	0.34	BCP	Frank	-1.646	0.37	BPSO	Frank	-0.910	0.34	BCP	Frank	-1.659	0.37
BCV	Frank	-1.011	0.33	BPE	Frank	-1.386	0.33	BCV	Frank	-0.905	0.33	BPE	Frank	-1.399	0.33
VATN	Frank	-0.813	0.28	VATN	Frank	-0.953	0.23	VATN	Frank	-0.726	0.28	VATN	Frank	-0.953	0.23

This table reports average $\Delta\text{CoVaR}_{\alpha,\beta,t}$, $\Delta\text{CoES}_{\alpha,\beta,t}$ and implied Kendall's τ estimates along with the selected copula families of each financial system-institution pair in our sample under two marginals specifications: Normal and Skewed- t . All risk measures are computed at $\alpha = \beta = 5\%$ level.

Table 4.6.2: This table ranks the average contribution to systemic risk by country.

ΔCoVaR results				ΔCoES results			
Normal Margins		Skewed- t Margins		Normal Margins		Skewed- t Margins	
Country	ΔCoVaR	Country	ΔCoVaR	Country	ΔCoES	Country	ΔCoES
France	-0.0222	Spain	-0.0506	France	-0.0204	Spain	-0.0516
Spain	-0.0210	Germany	-0.0505	Spain	-0.0193	Germany	-0.0515
Sweden	-0.0199	Belgium	-0.0499	Sweden	-0.0184	Norway	-0.0512
Great Britain	-0.0190	Norway	-0.0497	Great Britain	-0.0175	Belgium	-0.0507
Belgium	-0.0180	Denmark	-0.0490	Belgium	-0.0163	Denmark	-0.0507
Germany	-0.0180	Greece	-0.0476	Germany	-0.0162	Greece	-0.0489
Italy	-0.0160	Sweden	-0.0432	Italy	-0.0145	Sweden	-0.0441
Austria	-0.0146	Swiss	-0.0384	Austria	-0.0132	Swiss	-0.0399
Swiss	-0.0136	Great Britain	-0.0333	Swiss	-0.0122	Great Britain	-0.0341
Finland	-0.0132	France	-0.0326	Finland	-0.0119	France	-0.0332
Ireland	-0.0132	Italy	-0.0320	Ireland	-0.0118	Italy	-0.0328
Norway	-0.0131	Austria	-0.0208	Norway	-0.0117	Austria	-0.0212
Denmark	-0.0129	Ireland	-0.0182	Denmark	-0.0116	Ireland	-0.0185
Portugal	-0.0124	Finland	-0.0182	Portugal	-0.0112	Finland	-0.0184
Greece	-0.0122	Portugal	-0.0168	Greece	-0.0109	Portugal	-0.0170

This table reports average $\Delta\text{CoVaR}_{\alpha,\beta,t}$ and $\Delta\text{CoES}_{\alpha,\beta,t}$ estimates for each country in our sample under two marginal specifications: Normal and Skewed- t . All risk measures are computed at $\alpha = \beta = 5\%$ level.

Table 4.6.3: Dependence and tail dependence estimates.

Bank	Copula	ΔCoVaR	τ	λ^L	λ^U
POP	BB7	-5.127	0.51	0.46	0.24
DBK	BB7	-5.122	0.62	0.65	0.42
UBSN	BB7	-5.114	0.57	0.59	0.44
CSGN	BB7	-5.086	0.56	0.49	0.41
CRDA	BB7	-5.078	0.57	0.46	0.54
SEA	BB7	-5.073	0.54	0.62	0.40
SCH	BB7	-5.049	0.61	0.59	0.44
BBVA	BB7	-5.041	0.63	0.62	0.53
LLOY	BB7	-5.039	0.50	0.41	0.42
UCG	BB7	-5.033	0.56	0.48	0.28
BSAB	BB7	-5.031	0.43	0.42	0.24
NDA	BB7	-5.027	0.54	0.48	0.51
SVK	BB7	-5.011	0.47	0.30	0.34
BP	BB7	-5.009	0.51	0.55	0.29
KB	BB7	-5.000	0.57	0.56	0.33
CBK	BB7	-4.999	0.55	0.57	0.24
DNB	BB7	-4.971	0.42	0.45	0.21
DAB	BB7	-4.956	0.43	0.38	0.26
BARC	BB7	-4.951	0.54	0.54	0.43
SYD	BB7	-4.932	0.37	0.34	0.16
JYS	BB7	-4.832	0.37	0.31	0.27
EYS	BB7	-4.766	0.38	0.34	0.23
BPSO	BB7	-4.624	0.31	0.30	0.11
BCV	BB7	-4.244	0.28	0.19	0.21
SGE	Frank	-2.862	0.63	0.60	0.50
BNP	Frank	-2.728	0.61	0.44	0.52
ISP	Frank	-2.474	0.53	0.42	0.33
BMPS	Frank	-2.420	0.54	0.50	0.24
MB	Frank	-2.382	0.53	0.36	0.19
KNF	Frank	-2.368	0.50	0.37	0.26
RBS	Frank	-2.330	0.51	0.47	0.41
PMI	Frank	-2.300	0.51	0.50	0.24
HSBA	Frank	-2.249	0.51	0.33	0.32
SWED	Frank	-2.187	0.48	0.46	0.31
STAN	Frank	-2.115	0.48	0.36	0.23
ERS	Frank	-2.084	0.47	0.38	0.26
BKIR	Frank	-1.821	0.41	0.29	0.15
POH	Frank	-1.820	0.42	0.20	0.22
BES	Frank	-1.725	0.38	0.25	0.18
BCP	Frank	-1.646	0.37	0.41	0.00
BPE	Frank	-1.386	0.33	0.13	0.17
VATN	Frank	-0.953	0.24	0.17	0.12

This table reports average $\Delta\text{CoVaR}_{\alpha,\beta,t}$, sample Kendall's τ correlations and non-parametric upper (λ^U) and lower (λ^L) tail dependence estimates (an average of non-parametric estimates in Dobrić and Schmid (2005)) of each financial system-institution pair in our sample. $\Delta\text{CoVaR}_{\alpha,\beta,t}$ estimates are obtained under the assumption of Skewed- t margins. All risk measures are computed at $\alpha = \beta = 5\%$ level.

Table 4.6.4: Dependence and tail dependence estimates by country.

Country	τ	λ^L	λ^U
Germany	0.58	0.61	0.33
Belgium	0.57	0.56	0.33
Spain	0.54	0.52	0.37
France	0.58	0.47	0.46
Sweden	0.51	0.46	0.39
Norway	0.42	0.45	0.21
Great Britain	0.51	0.42	0.36
Italy	0.48	0.41	0.23
Austria	0.47	0.38	0.26
Swiss	0.41	0.36	0.30
Greece	0.38	0.34	0.23
Denmark	0.39	0.34	0.23
Portugal	0.38	0.33	0.09
Ireland	0.41	0.29	0.15
Finland	0.42	0.20	0.22

This table reports average sample Kendall's τ correlations and non-parametric upper (λ^U) and lower (λ^L) tail dependence estimates (an average of non-parametric estimates in Dobrić and Schmid (2005)) for each country in our sample.

4.6.3 Backtesting and stress testing *CoVaR*

A well-specified risk model should satisfy the appropriate theoretical statistical properties. Therefore, the proportion of violations should approximately equal the confidence level, while the violations should not occur in clusters but independently. Table 4.6.5 reports the average p -values from the modified Kupiec (1995) and Christoffersen (1998) statistical tests for the unconditional coverage, independence and conditional coverage of $CoVaR_{\alpha,\beta,t}$ estimates under both Gaussian and Skewed- t distribution assumptions computed at $\alpha = \beta = 5\%$ level.

The null hypotheses of unconditional and conditional coverage are rejected at the 5% level of significance under the Gaussian assumption. On the other hand, the average p -values from statistical tests under the assumption of Skewed- t margins are pretty high and hence the null hypotheses cannot be rejected at any conventional level of significance. Thus, it seems that a combination of copula functions - with asymmetric marginals - that allow for asymmetries in the tails is a better candidate for systemic risk modelling. Our test results are in line with the *CoVaR* backtest results in Girardi and Ergün (2013) and the *VaR* test results in the vast literature that reject the underlying normality assumption of risk models suggesting alternative distribution assumptions that allow for asymmetries.

Table 4.6.5: Statistical test results

Test	Normal Margins	Skewed- t Margins
Unconditional coverage	0.0206	0.3633
Independence	0.5649	0.8802
Conditional coverage	0.0286	0.5410

This table reports average p -values of statistical tests for unconditional coverage, independence and conditional coverage properties for $CoVaR_{\alpha,\beta,t}$ estimates. All risk estimates are computed at $\alpha = \beta = 5\%$ level.

On the other hand, stress testing exercises are useful in order financial regulators to gauge the potential implications of extreme market conditions for the stability of the financial system as a whole. Before the outset of the financial crisis, financial stability stress tests were largely focused on the implications of system-wide macroeconomic shocks and rarely considered idiosyncratic shocks such as the failure of a single large firm. Recently, there has been a growing interest in such systemic stress testing exercises by central banks and financial regulators. Our modelling framework can be easily employed as part of the tool-kit for financial stability assessment. Stress testing exercises under this framework can simulate scenarios that are absent from historical data or are more likely to occur than historical observation suggests, as well as simulate shocks that reflect permanent structural breaks or temporal dependence breakdowns.

Figure 4.6.6 displays a scenario analysis example for HSBC and demonstrates its influence on systemic risk as measured by $CoVaR_{\alpha,\beta,t}$ under certain scenarios. In particular, Figure 4.6.6 plots the implied $CoVaR_{\alpha,\beta,t}$ measures generated by the Clayton, Gumbel, Frank and BB7 copulas for $\beta = 0.01$ to 0.80 , $\alpha = 0.05$ and the dependence parameter(s) estimated for each particular copula family assuming Skewed- t margins.¹⁷ Thus, the discrepancies in $CoVaR_{\alpha,\beta,t}$ measures are due to the employment of different copula models and do not arise from margin specifications. The implied $CoVaR_{\alpha,\beta,t}$ results in Figure 4.6.6 have an appealing interpretation. For instance, we are 99% confident, given that HSBC is at most at its 95% VaR level, that the financial system will not experience a distress event worse than -16.84% according to the Clayton copula. For the same confidence level, $CoVaR_{\alpha,\beta,t}$ estimates implied by the Gumbel, Frank and BB7 copulas are -15.08% , -13.56% and -16.74% , respectively.¹⁸

Given the unique ability of copula functions to enable the separation of dependence from marginal distributions, we are able to quantify the potential effects on the stability of the financial system of risks associated with marginal distribution assumptions or risks related to the dependence structure. For example, a scenario that implies a structural break in the correlation between the financial system and an institution's returns can be analysed by modifying the level of Kendall's τ parameter, while a change in the dependence structure can be studied through alternative copula functional forms. Similarly, a scenario that implies high volatility or severe equity price declines can be examined through alternative marginal specifications. Complex stress test exercises that combine all the above scenarios can also be analysed simultaneously, thus providing a powerful tool for systemic risk assessment.

¹⁷We could also set the parameters for the Clayton, Gumbel and Frank copulas to a pre-specified value such as the Kendall's τ sample correlation coefficient because there is a one-to-one relationship between these particular one-parameter copula families and Kendall's τ . Such a relationship, however, does not exist for the two-parameter BB7 copula. To maintain the consistency of the implied systemic risk estimates, we use the estimated parameter(s) for each particular copula family instead.

¹⁸Similar stress testing exercises can also be obtained using $CoES_{\alpha,\beta,t}$ as a measure of systemic risk.

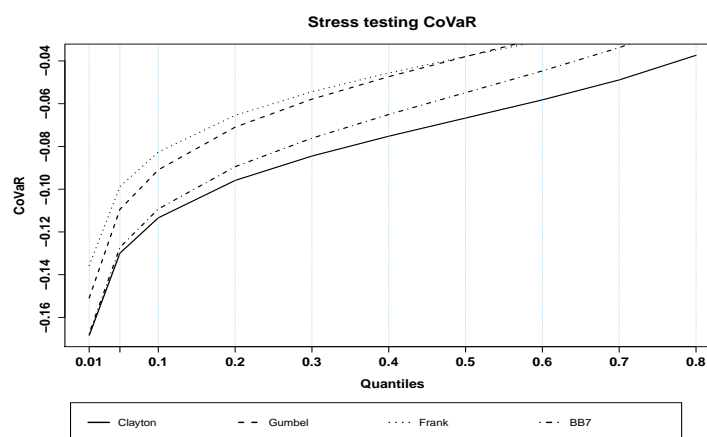


Figure 4.6.6: This figure shows the implied $CoVaR_{\alpha,\beta,t}$ estimates of the financial system conditional on HSBC returns generated by the Clayton, Gumbel, Frank and BB7 copulas with Skewed- t marginals across different quantile levels ($\beta = 0.01$ to 0.8 and $\alpha = 0.05$). The Kendall's τ sample correlation parameter is equal to 0.51, i.e., $\tau = 0.51$.

Figure 4.6.6 also provides a distinct graphical way to illustrate the importance of tail dependence in systemic risk computation and facilitate the interpretation of the results in Tables 4.6.1 and 4.6.2. It is clear from Figure 4.6.6 that the Clayton and BB7 copulas which allow for lower tail dependence produce much larger in absolute value $CoVaR_{\alpha,\beta,t}$ measures compared to the corresponding measures generated by the Frank or Gumbel copulas, which do not allow for lower tail dependence. As already explained, the average $\Delta CoVaR_{\alpha,\beta,t}$ or $\Delta CoES_{\alpha,\beta,t}$ measures reported in Tables 4.6.1 and 4.6.2 do not differ in size only due to alternative distribution assumptions in margins but also due to the different characteristics of the alternative copula functional forms employed. Therefore, copula misspecification may critically affect the systemic risk estimates and therefore dependence modelling should proceed with caution.

4.6.4 Systemic risk determinants

In this Section, we investigate the main drivers of systemic risk in the European banking system. The analysis is split into two main parts. In the first part, we investigate whether there are common market factors explaining an institution's contribution to systemic risk and seek to understand how this relationship is altered in the face of changes in the market environment. We also investigate how and in which direction these factors affect systemic risk. As explained, systemic risk measures can be decomposed within the Copula $CoVaR$ framework due to the unique ability of copula functions to enable the separation of dependence from marginal distributions. Thus, $CoVaR$ is an increasing non-linear function of the correlation between the financial system and institution i and of the financial system's volatility. This separation allows us to assess the impact of market factors on these variables and analyse their importance for the stability of the financial system.

Therefore, the dependent variables in our formal empirical work are $\Delta CoVaR_{\alpha,\beta,t}$, Kendall's τ correlations and the financial system's volatility σ_s estimates, obtained in Section 4.6.2.¹⁹ In particular, we run the following panel regression model:

$$\begin{aligned}
 y_{i,t} = & \beta_0 + \beta_1 Vix_{t-1} + \beta_2 Liquidity_{t-1} + \beta_3 \Delta Euribor_{t-1} + \beta_4 \Delta Slope_{t-1} + \beta_5 \Delta Credit_{t-1} \\
 & + \beta_6 S\&P_{t-1} + \beta_7 I_{crisis} Vix_{t-1} + \beta_8 I_{crisis} Liquidity_{t-1} + \beta_9 I_{crisis} \Delta Euribor_{t-1} \\
 & + \beta_{10} I_{crisis} \Delta Slope_{t-1} + \beta_{11} I_{crisis} \Delta Credit_{t-1} + \beta_{12} I_{crisis} S\&P_{t-1} + \varepsilon_{i,t}, \quad (4.22)
 \end{aligned}$$

where $y_{i,t}$ are the $\Delta CoVaR_{\alpha,\beta,t}^i$, Kendall's τ_t^i and financial system's volatility $\sigma_{s,t}^i$ estimates, for each financial institution i and week t . The I_{crisis} represents a dummy variable that takes the value of zero in the pre-crisis period and the value of one in the period we designate as the crisis period. In addition, the right-hand side of Equation (4.22) includes the following market variables:

- (i) *Vix*, which is a proxy for the implied volatility in the stock market reported by the Chicago Board Options Exchange (CBOE).
- (ii) *Liquidity*, which is a short term “liquidity spread” defined as the difference between the three-month interbank offered rate and the three-month repo rate. This spread is a common proxy for short-term funding liquidity risk. We use the three-month Euribor rate and the three-month Eurepo rate, both reported by the European Banking Federation (EBF).
- (iii) $\Delta Euribor$, which is the change in the three-month Euribor rate.
- (iv) $\Delta Slope$, which is the change in the slope of the yield curve, measured by the spread between the German ten-year government bond yield and the German three-month Bubill rate.
- (v) $\Delta Credit$, which is the change in the credit spread between the ten-year Moody's seasoned BAA-rated corporate bond and the German ten-year government bond.
- (vi) *S&P*, which is the S&P 500 Composite Index returns and used as a proxy for equity market returns.

The data have been obtained from Bloomberg and are sampled weekly. Table 4.6.6 reports the summary statistics of market variables. Almost all extreme values of these variables occur during stress periods. It is also evident that the distributions of the variables are highly skewed.

¹⁹All results are based on Skewed- t marginal distribution assumptions. We also analysed the same relationships based on the results from Gaussian margins. Moreover, we employed $\Delta CoES_{\alpha,\beta,t}$ as an alternative measure of an institution's contribution to systemic risk. The qualitative results, however, remained unchanged.

Table 4.6.6: Market variables summary statistics

	<i>Vix</i>	<i>Liquidity</i>	$\Delta Euribor$	$\Delta Slope$	$\Delta Credit$	<i>S&P</i>
Mean	21.834	35.642	-0.706	-0.085	0.086	0.070
Median	19.090	20.000	0.000	-0.700	0.000	0.138
Std. dev	10.219	34.721	6.198	14.261	11.892	3.125
Min	9.970	7.300	-51.100	-50.200	-41.100	-15.723
Max	80.060	188.800	21.100	119.500	126.200	13.604
Skewness	1.973	1.700	-2.555	1.560	2.498	-0.318
Kurtosis	5.246	2.995	15.362	11.278	27.012	4.834

This table reports summary statistics for the weekly market variables. *Vix* denotes the CBOE implied volatility. *Liquidity* represents the difference between the 3-month Euribor rate and the 3-month Eurepo rate. $\Delta Euribor$ denotes the change in the 3-month Euribor rate. $\Delta Slope$ denotes the change in the yield slope between the 10-year and the 3-month German government bond rates. $\Delta Credit$ represents the change in the yield spread between the ten-year Moody's seasoned BAA-rated corporate bond and the German ten-year government bond. *S&P* is the market equity returns. The spreads and spread changes are expressed in basis points, while returns and the *Vix* in percentage points.

Table 4.6.7 reports bank fixed-effect panel regression estimates for $\Delta CoVaR_{\alpha,\beta,t}$, Kendall's τ and the financial system's volatility σ_s estimates on the above lagged market variables. Across both sub-periods, the lagged values of the *Vix*, *Liquidity* and $\Delta Euribor$ variables appear highly significant in explaining the variation in $\Delta CoVaR_{\alpha,\beta,t}$ at conventional significance levels. In particular, higher lagged values of implied market volatility are associated with more negative $\Delta CoVaR_{\alpha,\beta,t}$ measures in the pre-crisis period. In contrast, the impact of lagged *S&P Return*, $\Delta Spread$ and $\Delta Slope$ variables on $\Delta CoVaR_{\alpha,\beta,t}$ does not appear statistically significant in this period ($\Delta Slope$ is significant only at 10% level).

The results in Table 4.6.7 also highlight the importance of funding liquidity in systemic risk contribution. Banks typically raise short-term funding in the unsecured interbank market or through over-the-counter collateralised repurchase agreements (repos). In times of uncertainty, banks charge higher rates for unsecured loans and thus interbank offered rates increase. The spread between the Euribor and the Eurepo rates measures the difference in interest rates between short-term fundings of different risks. As Figure 4.6.7 shows, this spread had shrunk to historical low levels during the pre-crisis period but it began to surge upward during the crisis period. The positive impact of funding liquidity on $\Delta CoVaR_{\alpha,\beta,t}$ in the pre-crisis period is confirmed by the results in Table 4.6.7. The coefficient of *Liquidity* in this period is negative and rather significant in magnitude. On average, a 1% increase in *Liquidity*, which indicates a worsening of funding liquidity, contributes almost 13.7% to systemic risk as measured by $\Delta CoVaR_{\alpha,\beta,t}$.

Table 4.6.7: Panel regression results.

Variables	ΔCoVaR	Kendall's τ	Volatility σ_s
Vix_{t-1}	-0.149***	0.004***	0.140***
$Liquidity_{t-1}$	-13.739***	-0.313***	13.997***
$\Delta Euribor_{t-1}$	-3.691***	0.057	3.453***
$\Delta Slope_{t-1}$	0.658*	-0.024	-0.607*
$\Delta Credit_{t-1}$	-0.089	-0.027***	0.101
$S\&P_{t-1}$	-0.021	0.001	0.019
$Vix_{t-1} \cdot I_{crisis}$	0.044***	-0.003***	-0.044***
$Liquidity_{t-1} \cdot I_{crisis}$	11.866***	0.337***	-12.234***
$\Delta Euribor_{t-1} \cdot I_{crisis}$	5.951***	-0.035	-5.494**
$\Delta Slope_{t-1} \cdot I_{crisis}$	-0.301	0.017	0.276
$\Delta Credit_{t-1} \cdot I_{crisis}$	-0.932***	-0.014***	0.947***
$S\&P_{t-1} \cdot I_{crisis}$	0.032	-0.002	-0.029
Adj. R^2	0.770	0.219	0.876

This table displays results from bank fixed-effects panel data methodology (within estimator). The columns ΔCoVaR , Kendall's τ and Volatility report estimated coefficients from regressions of weekly $\Delta\text{CoVaR}_{\alpha,\beta,t}$ measures, Kendall's τ estimates and the financial system's volatility σ_s estimates on the same lagged values of market variables: Vix , $Liquidity$, $\Delta Euribor$, $\Delta Slope$, $\Delta Credit$ and $S\&P$. The I_{crisis} is a crisis dummy that takes the value of 0 for the Q2 2002 - Q2 2007 pre-crisis period and 1 for the Q3 2007 - Q4 2012 crisis period. Estimated coefficients for spreads, yield changes, Vix and market returns correspond to percent changes. The results are based on weekly data from Q2 2002 - Q4 2012. All $\Delta\text{CoVaR}_{\alpha,\beta,t}$ measures are estimated at 5% level. Kendall's τ correlations are obtained after transforming the time-varying copula parameters for each financial system-institution i pair to theoretical Kendall's τ values. The financial system's volatility σ_s estimates are obtained by a univariate asymmetric AR(1)-GJR-GARCH(1,1) model for each financial system portfolio. Following [Thompson \(2011\)](#), we compute standard errors that cluster by both firm and time. *** denotes significant at 1%, ** denotes significant at 5% and * denotes significant at 10%.

The results are in line with a large number of theoretical and empirical research papers that associate market declines with liquidity dry-ups to explain the triggering of systemic episodes (see e.g., [Brunnermeier 2009](#); [Adrian and Shin 2010](#); [Brunnermeier and Pedersen 2009](#); [Hameed et al. 2010](#), and references therein). The burst of the crisis in summer 2007, caused two “liquidity spirals”. Financial institutions' capital eroded due to the initial decline in asset prices and the increase in wholesale funding cost. Consequently, both events triggered fire-sales, pushing asset prices further down, and increased the uncertainty in the interbank lending market. As a result, European banks that relied excessively on short-term funding were particularly exposed to a dry-up in liquidity. In this respect, the large size of the pre-crisis liquidity spread coefficient estimate partly explains why the sudden dry-up in liquidity had such a severe impact on the stability of the financial system.

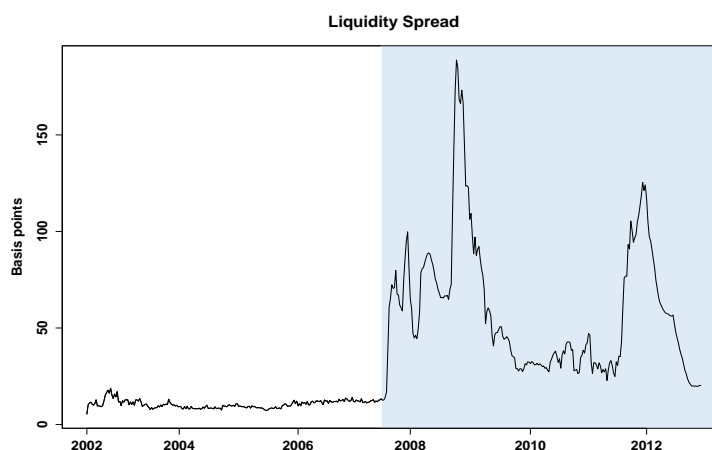


Figure 4.6.7: This figure shows the short-term Liquidity Spread between the 3-month Euribor rate and the 3-month Eurepo rate measured in basis points. The light blue shaded area corresponds to Q3 2007 - Q4 2012 crisis period.

The regression results in Table 4.6.7 for the $\Delta Euribor$ variable are also of great interest. As explained, the Euribor rate represents the unsecured rate at which a large panel of European banks borrow funds from one another. An increase in short-term rates implies a higher borrowing cost for banks. In this respect, banks relying on short-term funding are more vulnerable to liquidity risk. The pre-crisis coefficient estimate of the change in the three-month Euribor rate variable indicates the positive relation between changes in the short-term rates and systemic risk contribution. On average, an increase by 1% in the change of the three-month Euribor rate adds an additional 3.7% to $\Delta CoVaR_{\alpha,\beta,t}$.

In contrast, the signs of almost all estimated coefficients have switched in the crisis period indicating an asymmetric response of market factors to systemic risk in these sub-periods. In particular, the coefficient estimates of the *Liquidity* and $\Delta Euribor$ variables have switched from negative in the pre-crisis period to positive in the crisis period. One of the main reasons behind this behaviour is the coordinated intervention of central banks in both the United States and Europe in response to the freezing up of the interbank market. To alleviate the liquidity crunch, the European Central Bank (ECB) and the Federal Reserve (Fed) reduced the interest rates at which financial institutions borrow from them; they also expanded their balance sheets by broadening the type of collateral that banks could use, and increased the maturity of their loans to the banks (see [Giannone et al. \(2012\)](#), for further details). Figure 4.6.8 shows average $CoVaR_{\alpha,\beta,t}$ estimates and a timeline of key events and measures taken by the European Central Bank (ECB) to provide liquidity and restore financial stability over the recent financial crisis. We note in Figure 4.6.8 that the highest $CoVaR_{\alpha,\beta,t}$ measures (in absolute value) are reported after the Lehman Brothers collapse in September 2008. Figure 4.6.8 also depicts the measures taken by the European Central Bank (ECB) in response to the liquidity crunch and

the overall financial market turmoil. It can be shown that the systemic risk measures returned to lower levels (in absolute value) while the initial liquidity dry-up in the interbank market calmed down and the short-term interbank rates returned to lower levels, as Figure 4.6.7 and Figure 4.6.9 display, respectively.



Figure 4.6.8: This figure shows time-series average $CoVaR_{\alpha,\beta,t}$ estimates, key events (in red) and measures taken by the European Central Bank (ECB) to provide liquidity to the interbank market and restore financial stability. The light blue shaded area corresponds to Q3 2007 - Q4 2012 crisis period. Source of timeline events: European Central Bank (ECB), www.ecb.europa.eu.

The overall increase in systemic risk during the crisis period, however, is not only driven by the solvency problems of several Euro-area financial institutions, but also by the sovereign debt crisis of a large number of Eurozone member countries. As Figure 4.6.8 suggests, systemic risk estimates reached their highest levels after the collapse of Lehman Brothers in September 2008; however, high values are also associated with the inability of several countries in the Eurozone to repay or refinance their government debt without the assistance of third parties. As Shambaugh (2012) points out, the euro area faced three interdependent crises, that is, a sovereign debt crisis, a banking crisis and a growth and competitiveness crisis. In this respect, the problems of undercapitalised banks and high sovereign debt are mutually reinforcing, and both are amplified by slow and unequally distributed - among Eurozone member countries - growth. Therefore, our regression results and the asymmetric response of market factors to systemic risk should be viewed in conjunction with the overall characteristics of the crisis in the Eurozone.

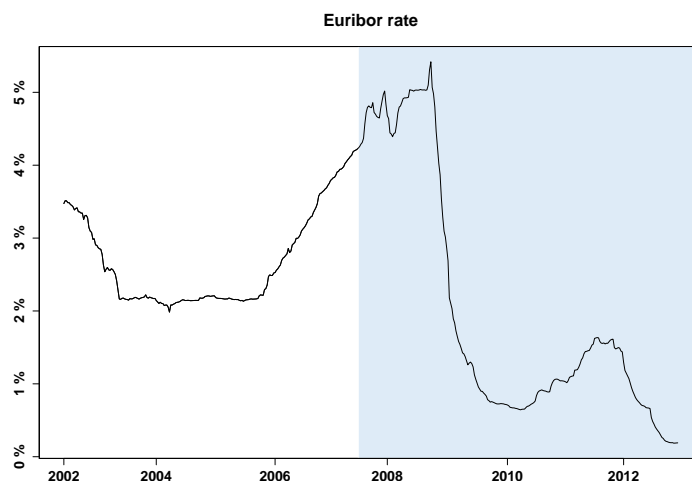


Figure 4.6.9: This figure shows the 3-month euro interbank offered rate (Euribor), the interest rate at which euro interbank 3-month deposits are offered by one prime bank to another prime bank within the euro area. The light blue shaded area corresponds to Q3 2007 - Q4 2012 crisis period.

It is also of great interest to investigate the effect of market factors on Kendall's τ correlation estimates and the financial system's volatility σ_s estimates. Kendall's τ correlation estimates are asymmetrically related to lagged values of the *Vix* and *Liquidity* variables, although the magnitude of the asymmetries is not large. Interestingly, liquidity shocks (the widening of liquidity spread) reduce Kendall's τ correlation in the pre-crisis period, while having a positive impact on it in the crisis period. A widening in $\Delta Credit$ also suggests a decrease in Kendall's τ correlation in both periods. The above market factors also appear significant in explaining the financial system's volatility and demonstrate the same asymmetric behaviour. In the pre-crisis period, an increase in the *Vix*, *Liquidity* or $\Delta Credit$ variables increases the financial system's volatility and as a consequence the level of systemic risk, while the impact of these factors on the financial system's volatility is the opposite in the post-crisis period. The $\Delta Euribor$ variable is also asymmetrically related to the financial system's volatility; however, the degree of asymmetry is pretty high between these sub-periods, with the regression coefficients changing from 3.453 to -5.494. This substantial asymmetric response also highlights the impact of the European Central Bank's (ECB) intervention in the interbank market.

In the post-crisis period, an increase in the change of the three-month Euribor rate, counterintuitively suggests a reduction in the financial system's volatility. Nevertheless, as shown in Figures 4.6.8 and 4.6.9, the action taken by the European Central Bank (ECB) during the crisis period eventually reduced the level of short-term interest rates and, thus, distorted the positive pre-crisis relationship between the change in short-term rates and the financial system's volatility. From the results in Table 4.6.7, it can also be seen that the impact of funding liquidity is primar-

ily transmitted on $\Delta CoVaR_{\alpha,\beta,t}$ through the financial system's volatility and not through Kendall's τ correlation. In other words, the sudden dry-up of liquidity in the pre-crisis period reduced the level of correlation among financial institutions but considerably increased the volatility of the financial system. This can also be confirmed by comparing the estimated coefficients of the *Liquidity* variable with the estimated coefficients of the $\Delta CoVaR_{\alpha,\beta,t}$ and volatility variables, which are almost identical in absolute value.

In the second part of our analysis, we investigate how individual characteristics of financial institutions contribute to systemic risk. In this regard, we employ panel regressions and regress quarterly-aggregated $\Delta CoVaR_{\alpha,\beta,t}$ measures on a set of institution-specific variables. In particular, we consider the following panel regression model with fixed effects:

$$\begin{aligned} \Delta CoVaR_{\alpha,\beta,t}^i = & \beta_0 + \beta_1 VaR_{\alpha,t-k}^i + \beta_2 MtB_{i,t-k} + \beta_3 Size_{i,t-k} + \beta_4 Leverage_{i,t-k} \\ & + \beta_5 Beta_{i,t-1} + \beta_6 Vol_{i,t-k} + \varepsilon_{i,t}. \end{aligned} \quad (4.23)$$

where $\Delta CoVaR_{\alpha,\beta,t}^i$ represents the quarterly-aggregated $\Delta CoVaR$ measures for institution i computed from the first stage as described in Section 4.6.2. In addition, we use the following set of quarterly bank-specific characteristics:

- (i) $VaR_{\alpha,t-k}^i$ defined as the quarterly-aggregated VaR measures for bank i at quarter $t-k$, calculated by averaging the corresponding weekly measures within each quarter.
- (ii) $MtB_{i,t-k}$ defined as the ratio of the market to book value of total equity for bank i at quarter $t-k$ and used as a proxy for growth opportunities.
- (iii) $Size_{i,t-k}$ defined as the log of total book value of equity for bank i at quarter $t-k$.
- (iv) $Leverage_{i,t-k}$ defined as the ratio of the total assets to total book value of equity for bank i at quarter $t-k$ and used as a proxy for the solvency of the bank.
- (v) $Beta_{i,t-k}$ is the equity market beta for bank i at quarter $t-k$, calculated from weekly equity return data within each quarter.
- (vi) $Vol_{i,t-k}$ is the equity return volatility for bank i at quarter $t-k$, calculated from weekly equity return data within each quarter.

The balance-sheet data for each individual bank are obtained from Worldscope database. Table 4.6.8 below provides the summary statistics for $\Delta CoVaR_{\alpha,\beta,t}^i$ and $VaR_{\alpha,t}^i$ measures and the bank-specific characteristics at quarterly frequency.

Table 4.6.8: Bank-specific variables summary statistics

Variable	Mean	Median	Std. dev.
$\Delta CoVaR$	-0.0469	-0.0353	0.0334
VaR	-0.0798	-0.0649	0.0552
MtB	1.2684	1.2406	0.8558
$Size$	8.4790	8.5084	0.6605
$Leverage$	21.6602	19.7551	14.7454
$Beta$	0.7232	0.6433	0.5415
Vol	0.0214	0.0172	0.0151

This table reports summary statistics of quarterly-aggregated bank-specific variables. VaR estimates are obtained by averaging the corresponding weekly measures within each quarter. All risk measures are estimated at 5% level of significance under the assumption of Skewed- t marginals.

Table 4.6.9 reports results from panel regressions, after controlling for bank fixed-effects and, additionally, allowing for bank and time clustered errors. We report results from three different specifications based on the forecast horizon of explanatory variables: one quarter, one year and two years. Across forecast periods, $Size$ and $Leverage$ appear to be the most robust determinants of systemic risk. The estimated coefficient of the $Size$ variable is negative and highly significant, suggesting that bigger institutions contribute more to systemic risk than smaller institutions.

Table 4.6.9: Determinants of systemic risk - Individual institution characteristics.

Variable	1-Quarter	1-Year	2-Year
VaR_{t-k}	-0.213 49**	0.128 39*	0.004 43
MtB_{t-k}	0.000 03	-0.010 95*	-0.015 09**
$Size_{t-k}$	-0.015 66***	-0.040 46***	-0.038 94***
$Leverage_{t-k}$	-0.000 74***	-0.001 28***	-0.000 76***
$Beta_{t-k}$	0.008 47	-0.004 08	-0.015 95***
$Volatility_{t-k}$	-1.834 96***	0.436 13*	0.341 99
$Adj. R^2$	0.440	0.288	0.325

This table displays results from the bank fixed-effects panel regression methodology (within estimator). The columns report estimated coefficients from regressions of lagged quarterly bank-specific data on quarterly aggregated $\Delta CoVaR_{\alpha,\beta,t}$ measures. The column 1-Quarter corresponds to results based on lagged variables equal to one-quarter, while columns 1-Year and 2-Year correspond to results based on lagged variables equal to one year and two years, respectively. The results are based on quarterly data from Q2 2002 - Q4 2012. All $\Delta CoVaR_{\alpha,\beta,t}$ measures are estimated at 5% level. Following [Thompson \(2011\)](#), we compute standard errors that cluster by both firm and time. *** denotes significant at 1%, ** denotes significant at 5% and * denotes significant at 10%.

These findings support the empirical results in Section 4.6.2. Several of the largest banks in our sample are placed among the most systemic financial institutions based on their average $\Delta CoVaR$ or $\Delta CoES$ measures as reported in Table 4.6.1. Furthermore, $Leverage$ is negative and significant across all forecasting horizons. As explained, $Leverage$ is used as a proxy for the solvency of the financial institution. The negative coefficient estimates of $Leverage$ across all forecasting horizons imply that highly leveraged banks contribute more to systemic risk than low leveraged

banks. In addition, the *VaR* of each financial institution and equity return volatility are statistically significant at the one quarter horizon, whereas equity beta is statistically significant at the two year horizon. Overall, our results in Table 4.6.9 are in line with other studies. Similar to [Acharya et al. \(2012\)](#), [Adrian and Brunnermeier \(2011\)](#) and [Girardi and Ergün \(2013\)](#), we find that size, leverage and equity beta are important determinants of systemic risk. However, we found no statistical support for the hypothesis that the market to book value of total equity ratio is important in explaining institutions' contribution to systemic risk.

4.7 Conclusions

In this study we propose a new method for estimating the *Conditional Value-at-Risk* (*CoVaR*), a method based on copula functions. The proposed Copula *CoVaR* methodology provides simple, explicit expressions for a broad range of copula families, while allowing the *CoVaR* of an institution to have time-varying exposure to its *VaR*. In this respect, we avoid the burden of numerical integration in *CoVaR* computation and offer a dynamic and more flexible approach to systemic risk modelling, while eliminating potential biases that may arise from misspecification in the marginals or the joint distribution. This approach is also extended to other systemic risk measures, such as the *Conditional Expected Shortfall* (*CoES*). The systemic risk measures generated from our framework share the main properties reported in [Mainik and Schaanning \(2014\)](#) for each particular *CoVaR* specification. Furthermore, we illustrate how the Copula *CoVaR* methodology can facilitate stress testing exercises employed by financial regulators to measure the impact of extreme market scenarios on the stability of the financial system.

We focus on a portfolio of large European banks and estimate *CoVaR* and *CoES* measures using alternative distribution assumptions in the margins and the dependence structure. We illustrate the importance of taking asymmetries into account and highlight the threats to accurate systemic risk measurement posed by misspecification biases in the margins or the dependence model. We measure an institution's contribution to systemic risk using both $\Delta CoVaR$ and $\Delta CoES$ measures. Banks such as BBVA, UBS, Deutsche Bank, Credit Suisse and BNP Paribas appear among the most systemic European banks, whereas French and Spanish banks generate the highest average $\Delta CoVaR$ and $\Delta CoES$ estimates. We also investigate whether there are common market factors explaining an institution's contribution to systemic risk. In principle, lagged values of the implied market volatility, of funding liquidity, of the credit spread and of the change in the three month Euribor rate are significant in explaining $\Delta CoVaR$. They also appear important in explaining the correlation between the financial system and each institution, as well as the financial system's volatility. The asymmetric behaviour of market factors in the pre-crisis and the crisis period is

partly attributed to the coordinated intervention of central banks in response to the financial crisis. Finally, we investigate the impact of bank-specific characteristics on systemic risk and regress $\Delta CoVaR$ measures on a set of balance-sheet variables. Across all alternative model specifications considered, size and leverage appear to be the most robust determinants of systemic risk, implying that bigger and highly leveraged financial institutions can generate large systemic risk externalities.

Appendices

4.A *CoVaR* derivation for Normal and Student-*t* copulas

4.A.1 Normal copula

The Normal copula does not have a closed form distribution. Its distribution is given by

$$C(u, v) = \Phi_2(\Phi^{-1}(u), \Phi^{-1}(v); \rho),$$

where Φ_2 is the bivariate distribution of two standard normal distributed random variables with correlation ρ , Φ is the $N(0, 1)$ cdf and Φ^{-1} is the inverse of Φ . Nevertheless, the *CoVaR* in [Adrian and Brunnermeier \(2011\)](#) can be given in explicit form, that is

$$CoVaR_{\alpha, \beta, t}^- = F_{s, t}^{-1} \left(\Phi \left(\rho \Phi^{-1}(v) + \sqrt{1 - \rho^2} \Phi^{-1}(\beta) \right) \right).$$

Unfortunately, the *CoVaR* can not be given in explicit form under the definition in [Girardi and Ergün \(2013\)](#). In this respect, *CoVaR* is obtained numerically by first solving the Normal copula density for the conditional quantile u , that is

$$\int_0^u \int_0^v \frac{1}{\sqrt{1 - \rho^2}} \exp \left(- \frac{\rho^2(s^2 + t^2) - 2\rho s t}{2(1 - \rho^2)} \right) ds dt = \alpha^2.$$

Note that from the *VaR* definition it holds that $v = F_{R_{i, t}}(VaR_{\alpha, t}^i) = F_{R_{i, t}}(F_{R_{i, t}}^{-1}(\alpha)) = \alpha$. Since we work on a common significance level for *VaR* and *CoVaR* measures it also holds that $\alpha = \beta$. In this regard, *CoVaR* is given by applying the probability integral transform to the conditional quantile u , i.e., $CoVaR_{\alpha, \beta, t} = F_{s, t}^{-1}(u)$. In practice, this method for *CoVaR* computation is similar to that proposed by [Girardi and Ergün \(2013\)](#), the only difference being that we work with a copula density function instead of a probability density function (*pdf*).

4.A.2 The Student-*t* copula

Similar to the Norman copula, the Student-*t* copula does not have a closed-form density. However, the *CoVaR* definition based on [Adrian and Brunnermeier \(2011\)](#) can be given in explicit form as

$$CoVaR_{\alpha, \beta, t} = F_{s, t}^{-1} \left(t_\nu \left(\rho t_\nu^{-1}(v) + \sqrt{(1 - \rho^2)(\nu + 1)^{-1}(\nu + t_\nu^{-1}(v)^2)} t_{\nu+1}^{-1}(\beta) \right) \right).$$

In contrast, the *CoVaR* definition given by Girardi and Ergün (2013) can be obtained numerically by solving the following numerical integral

$$\int_0^u \int_0^v \frac{1}{\sqrt{1-\rho^2}} \frac{\Gamma(\frac{\nu+2}{2})\Gamma(\frac{\nu}{2})}{\Gamma(\frac{\nu+2}{2})^2} \frac{(1 + \frac{s^2-2st\rho+t^2}{\nu(1-\rho^2)})^{-\frac{\nu+1}{2}}}{(1 + \frac{s^2}{\nu})^{-\frac{\nu+1}{2}}(1 + \frac{t^2}{\nu})^{-\frac{\nu+1}{2}}} ds dt = \alpha \cdot \beta.$$

After solving for u and applying the probability integral transform, the *CoVaR* is given by $CoVaR_{\alpha,\beta,t} = F_{s,t}^{-1}(u)$. As in the case with the Normal copula, we work on a common significance level for both risk metrics, i.e., $\alpha = \beta$, while $v = F_{R_{i,t}}(VaR_{\alpha,t}^i) = F_{R_{i,t}}(F_{R_{i,t}}^{-1}(\alpha)) = \alpha$, which it holds from the definition of *VaR*.

4.B *CoVaR* derivation for Archimedean copulas

4.B.1 Clayton copula

The Clayton copula is a member of the Archimedean copula family with dependence parameter $\theta \in (0, \infty)$ and generator function $\varphi = \frac{(u^{-\theta}-1)}{\theta}$. The perfect dependence is observed as $\theta \rightarrow \infty$ whereas $\theta \rightarrow 0$ implies independence. The Clayton copula allows for the modelling of positive dependence and asymmetric (lower) tail dependence. The distribution function is given by

$$C(u, v; \theta) = (u^{-\theta} + v^{-\theta} - 1)^{-\frac{1}{\theta}}.$$

Following the notation introduced in Section 4.3.2, an explicit expression for $CoVaR_{\alpha,\beta,t}^-$ for the Clayton copula can be derived, that is

$$\frac{\partial C(u, v)}{\partial v} = \left(1 + u^\theta (v^{-\theta} - 1)\right)^{\frac{-(1+\theta)}{\theta}} = \beta. \quad (4.24)$$

Solving for u and applying the probability integral transform, $CoVaR_{\alpha,\beta,t}^-$ is obtained as follows

$$u^- \equiv u = \left(1 + v^{-\theta} \cdot (\beta^{-\frac{\theta}{1+\theta}} - 1)\right)^{-\frac{1}{\theta}},$$

$$CoVaR_{\alpha,\beta,t}^- = F_{s,t}^{-1}\left(\left(1 + \alpha^{-\theta} \cdot (\beta^{-\frac{\theta}{1+\theta}} - 1)\right)^{-\frac{1}{\theta}}\right). \quad (4.25)$$

Alternatively, using the general expression in Equation (4.12) an explicit expression for $CoVaR_{\alpha,\beta,t}$ for the Clayton copula can be given as follows

$$\frac{C(u, v)}{v} = \beta,$$

$$\left(u^{-\theta} + v^{-\theta} - 1\right)^{-\frac{1}{\theta}} = v \cdot \beta.$$

Thus, solving for u and applying the probability integral transform, $CoVaR_{\alpha,\beta,t}$ can be obtained in a closed-form expression, that is

$$u^{\leq} \equiv u = \left(1 + (v \cdot \beta)^{-\theta} - v^{-\theta}\right)^{-\frac{1}{\theta}},$$

$$CoVaR_{\alpha,\beta,t} = F_{s,t}^{-1}\left(\left(1 + (\alpha \cdot \beta)^{-\theta} - \alpha^{-\theta}\right)^{-\frac{1}{\theta}}\right). \quad (4.26)$$

4.B.2 Frank copula

This copula is also a member of the Archimedean copula family with dependence parameter $\theta \in (-\infty, \infty) \setminus \{0\}$ and generator function $\varphi = -\ln\left(\frac{e^{-\delta u}-1}{e^{-\delta}-1}\right)$. The Frank copula allows for both positive and negative dependence structures; however, it does not imply tail dependence. The distribution function is given by

$$C(u, v; \delta) = -\frac{1}{\delta} \ln\left(\frac{1}{1-e^{-\delta}} [(1-e^{-\delta}) - (1-e^{-\delta u})(1-e^{-\delta v})]\right).$$

An analytical expression for $CoVaR_{\alpha,\beta,t}^=$ for this copula family can be derived as

$$CoVaR_{\alpha,\beta,t}^= = F_{s,t}^{-1}\left(-\frac{1}{\delta} \ln\left(1 - (1-e^{-\delta}) \cdot [1 + e^{-\delta\alpha} \cdot (\beta^{-1} - 1)]^{-1}\right)\right). \quad (4.27)$$

In contrast, an explicit expression for $CoVaR_{\alpha,\beta,t}$ for the Frank copula is given as follows

$$CoVaR_{\alpha,\beta,t} = F_{s,t}^{-1}\left(-\frac{1}{\delta} \ln\left[1 - \frac{(1-e^{-\delta}) - (1-e^{-\delta})(e^{-\delta\beta\alpha})}{(1-e^{-\delta\alpha})}\right]\right). \quad (4.28)$$

4.B.3 Gumbel copula

The Gumbel copula with dependence parameter $\theta \in [1, \infty]$ and generator function $\varphi(t) = (-\log t)^\theta$ belongs to the Archimedean copula family, too. The Gumbel copula only captures positive dependence and it allows for asymmetric (upper) tail dependence. For $\theta = 1$, the Gumbel copula implies independence while the perfect positive dependence is observed as $\theta \rightarrow \infty$. The distribution function is given by

$$C(u, v; \theta) = \exp\left(-\left((-\log u)^\theta + (-\log v)^\theta\right)^{\frac{1}{\theta}}\right).$$

Unfortunately, the $\partial/\partial v C(u, v)$ of the Gumbel copula is not partially invertible in its first argument u and hence we cannot derive an analytical expression for $CoVaR_{\alpha,\beta,t}^=$. However, an analytical expression for $CoVaR_{\alpha,\beta,t}$ can be given as follows

$$CoVaR_{\alpha,\beta,t} = F_{s,t}^{-1}\left(\exp\left(-\left[(-\log(\alpha \cdot \beta))^\theta - (-\log \alpha)^\theta\right]^{\frac{1}{\theta}}\right)\right). \quad (4.29)$$

4.B.4 BB7 copula

The BB7 copula, known as the Joe-Clayton copula, is a two-parametric Archimedean copula family with $\theta \geq 1$ and $\delta > 0$. This copula family captures positive dependence while also allowing for asymmetric upper and lower tail dependence. In particular, the δ parameter measures lower tail dependence and the θ parameter measures upper tail dependence. Moreover, the Joe copula is the limiting case of BB7 for $\delta \rightarrow 0$ whereas for $\theta = 0$ one obtains the Clayton copula. The distribution function for this copula family is given by

$$C(u, v; \theta, \delta) = 1 - \left(1 - [(1 - (1 - u)^\theta)^{-\delta} + (1 - (1 - v)^\theta)^{-\delta} - 1]^{-\frac{1}{\delta}}\right)^{\frac{1}{\theta}}.$$

Analytical expressions for $CoVaR_{\alpha, \beta, t}^-$ and $CoVaR_{\alpha, \beta, t}$ can be obtained from the general solutions in Equation (4.11) and Equation (4.15), respectively, with

$$\begin{aligned}\varphi(v; \theta, \delta) &= [1 - (1 - v)^{-\theta}]^{-\delta} - 1, \\ \varphi^{-1}(v; \theta, \delta) &= 1 - [1 - (1 + v)^{-1/\delta}]^{1/\theta}, \\ \varphi'(v; \theta, \delta) &= -[1 - (1 - v)^\theta]^{-\delta-1} \delta [-(1 - v)^\theta \theta / (-1 + v)].\end{aligned}$$

4.C Dynamic Copula *CoVaR*

For the Clayton and Gumbel copulas the following parametric representation is proposed

$$\theta_t = \Lambda_1\left(\omega + \beta \cdot \theta_{t-1} + \alpha \cdot \frac{1}{10} \sum_{j=1}^{10} |u_{t-j} \cdot v_{t-j}|\right),$$

where $\Lambda_1(x)$ is an appropriate transformation to ensure the parameter always remains in its domain: $\exp(x)$ for the Clayton copula and $(\exp(x) + 1)$ for the Gumbel one. On the other hand, the parameter δ of the Frank copula is defined in $[-\infty, \infty] \setminus \{0\}$ at all times. Thus, we employ the following evolution equation for this particular copula family

$$\delta_t = \omega + \beta \cdot \delta_{t-1} + \alpha \cdot \frac{1}{10} \sum_{j=1}^{10} |u_{t-j} \cdot v_{t-j}|,$$

where the evolution of δ_t is constrained to ensure that the parameter remains in its domain. For the two-parametric Archimedean BB7 copula a similar parametric representation for each tail dependence coefficient is considered. The BB7 copula is constructed by taking a particular Laplace transformation of the Clayton copula. The BB7 copula distribution is given by

$$C(u, v; \theta, \delta) = 1 - \left(1 - [(1 - (1 - u)^\theta)^{-\delta} + (1 - (1 - v)^\theta)^{-\delta} - 1]^{-\frac{1}{\delta}}\right)^{\frac{1}{\theta}},$$

where $\theta = 1/\log_2(2 - \tau^U)$, $\delta = -1/\log_2(\tau^L)$ and $\tau^U, \tau^L \in (0, 1)$. Therefore, the following evolution equations can be considered for the BB7 copula

$$\tau_t^U = \Lambda_2\left(\omega_U + \beta_U \cdot \tau_{t-1}^U + \alpha_U \cdot \frac{1}{10} \sum_{j=1}^{10} |u_{t-j} \cdot v_{t-j}|\right),$$

$$\tau_t^L = \Lambda_2\left(\omega_L + \beta_L \cdot \tau_{t-1}^L + \alpha_L \cdot \frac{1}{10} \sum_{j=1}^{10} |u_{t-j} \cdot v_{t-j}|\right),$$

where $\Lambda_2(x) \equiv (1 + \exp(-x))^{-1}$ is the logistic transformation, used to keep τ^U and τ^L in $(0, 1)$ at all times.

4.D List of European financial institutions

Table 4.D.1: List of European financial institutions

Bank	Datastream tickers	Country	Weight (%)	MCap (€ Bil.)
HSBC	HSBA	Great Britain	20.44	142.65
BCO SANTANDER	SCH	Spain	7.33	51.17
UBS	UBSN	Swiss	6.60	46.08
BNP PARIBAS	BNP	France	6.17	43.09
BARCLAYS	BARC	Great Britain	5.37	37.50
BCO BILBAO VIZCAYA ARGENTARIA	BBVA	Spain	4.95	34.56
STANDARD CHARTERED	STAN	Great Britain	4.64	32.38
DEUTSCHE BANK	DBK	Germany	4.43	30.92
LLOYDS BANKING GRP	LLOY	Great Britain	4.34	30.28
CREDIT SUISSE GRP	CSGN	Swiss	4.32	30.12
NORDEA BANK	NDA	Sweden	3.14	21.89
GRP SOCIETE GENERALE	SGE	France	3.00	20.92
UNICREDIT	UCG	Italy	2.82	19.69
INTESA SANPAOLO	ISP	Italy	2.44	17.00
SWEDBANK	SWED	Sweden	2.28	15.88
SVENSKA HANDELSBANKEN A	SVK	Sweden	2.11	14.69
SKANDINAVISKA ENSKILDA BK A	SEA	Sweden	1.59	11.07
DNB	DNB	Norway	1.49	10.38
DANSKE BANK	DAB	Denmark	1.21	8.41
CREDIT AGRICOLE	CRDA	France	1.02	7.15
ROYAL BANK OF SCOTLAND GRP	RBS	Great Britain	1.00	6.95
COMMERZBANK	CBK	Germany	0.89	6.21
KBC GRP	KB	Belgium	0.88	6.13
ERSTE GROUP BANK	ERS	Austria	0.86	6.00
BCO POPULAR ESPANOL	POP	Spain	0.56	3.93
BCO SABADELL	BSAB	Spain	0.55	3.85
NATIXIS	KNF	France	0.40	2.77
BANK OF IRELAND	BKIR	Ireland	0.37	2.55
POHJOLA BANK	POH	Finland	0.33	2.27
MEDIOBANCA	MB	Italy	0.32	2.23
JYSKE BANK	JYS	Denmark	0.29	2.03
BCO POPOLARE	BP	Italy	0.24	1.65
BCA POPOLARE EMILIA ROMAGNA	BPE	Italy	0.23	1.63
BCA MONTE DEI PASCHI DI SIENA	BMPS	Italy	0.20	1.43
BCO ESPIRITO SANTO	BES	Portugal	0.20	1.38
BCO COMERCIAL PORTUGUES	BCP	Portugal	0.19	1.31
NATIONAL BANK OF GREECE	ETE	Greece	0.18	1.29
BCA POPOLARE DI SONDRIO	BPSO	Italy	0.17	1.21
SYDBANK	SYD	Denmark	0.17	1.17
BCA POPOLARE DI MILANO	PMI	Italy	0.15	1.07
BANQUE CANTONALE VAUDOISE	BCV	Swiss	0.15	1.05
VALIANT	VATN	Swiss	0.15	1.03

This table lists 42 out of the 46 banks (from 15 European countries) that belong to the to STOXX 600 Banks Index and their corresponding Datastream tickers, Market Capitalisation values and relative STOXX 600 Banks Index weights as of June, 2013. Source: STOXX Limited (www.stoxx.com).

4.E Systemic risk measure comparisons

This Appendix presents a graphical comparison of $CoVaR$ and $CoES$ measures, based on the $CoVaR$ definitions in [Adrian and Brunnermeier \(2011\)](#) and [Girardi and Ergün \(2013\)](#). Figure 4.E.1 shows dynamic $CoVaR_{\alpha,\beta,t}^=$ and $CoVaR_{\alpha,\beta,t}$ estimates, while Figure 4.E.2 displays dynamic $CoES_{\alpha,\beta,t}^=$ and $CoES_{\alpha,\beta,t}$ estimates. All measures are generated by a Frank copula function with Skewed- t marginals conditional on HSBC returns. It is clear that the systemic risk estimates do not differ significantly from each other. Similar patterns are also observed for the rest of the pairs in our study.

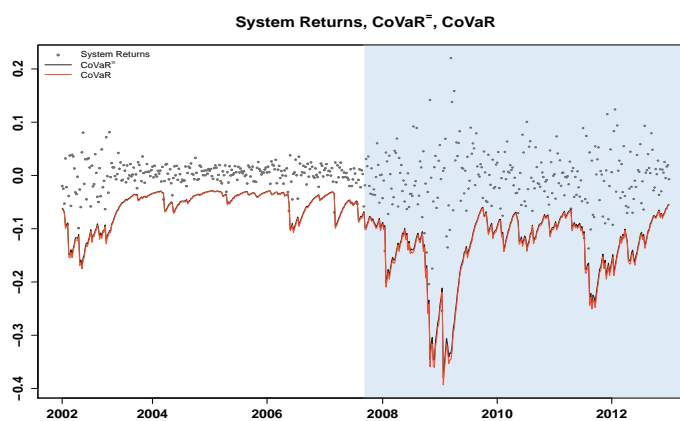


Figure 4.E.1: This figure shows financial system returns (grey points), dynamic $CoVaR_{\alpha,\beta,t}^=$ (black line) and $CoVaR_{\alpha,\beta,t}$ (red line) estimates conditional on HSBC returns. Both systemic risk measure estimates are generated by a Frank copula function with Skewed- t marginals. The light blue shaded area corresponds to Q3 2007 - Q4 2012 crisis period.

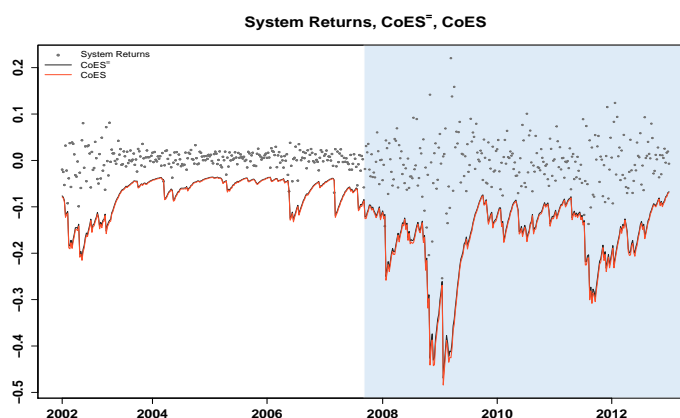


Figure 4.E.2: This figure shows financial system returns (grey points), dynamic $CoES_{\alpha,\beta,t}^=$ (black line) and $CoES_{\alpha,\beta,t}$ (red line) estimates conditional on HSBC returns. Both systemic risk measure estimates are generated by a Frank copula function with Skewed- t marginals. The light blue shaded area corresponds to Q3 2007 - Q4 2012 crisis period.

Chapter 5

Modelling the dependence of European sovereign yield curves

5.1 Introduction

How do investors react in the light of market-wide and country-specific liquidity and credit quality shocks in the sovereign fixed-income markets? Does their behaviour change when equity markets become more volatile? Can we quantify the effects of these shocks on the sovereign yield curves and cross-country spreads? Understanding the implications of market-wide and country-specific liquidity and credit risks for sovereign yield curves and their dependence structure is of key importance for understanding the sources of risk premia and cross-market dynamics and consequently for monetary policy, investment decisions and prudent risk management.

It is well-documented in the finance literature that liquidity and credit concerns are important components of the yield spreads (see for example, [Duffie et al., 2003](#); [Longstaff et al., 2005](#); [Beber et al., 2009](#), among others). Nevertheless, so far, most studies have related liquidity and credit concerns to the yields or yield spreads focusing on certain maturities or markets in isolation without taking into account the dynamic interaction of these risks with the term structure of interest rates and the cross-markets dependence. In this study, we focus on the yield curve of several Euro-area countries and model *jointly* their temporal and dependence structure as a function of market-wide and country-specific liquidity and credit quality measures. Said differently, we study the dynamic interaction between sovereign yield curves and European measures of liquidity and credit quality, while relating the dynamic dependence between sovereign yield curves to country-specific liquidity and credit quality measures. We also investigate the interaction of these measures with the sovereign yield curves unconditionally, as well as conditional on periods of heightened equity market volatility.

The present analysis is split into two main parts. In the first part, we model the evolution of the yield curve for each particular country using the macro-finance Nelson-Siegel model of [Diebold et al. \(2006\)](#) augmented with key macroeconomic and financial variables, as well as European measures of liquidity and credit quality.

The inclusion of market-wide liquidity and credit quality measures in the latent factor specification of the model enables the study of the dynamic interaction between these risks and the yield curve for each particular country. The correlation and principal component analysis (PCA) results of the estimated latent factors support the view that markets separate Eurozone countries according to their corresponding credit quality into two distinct groups: the peripheral and the core Eurozone countries. The analysis also supports the view that investors tend to differentiate between Eurozone countries and non-Euro countries, such as the UK. The large contribution of Germany to the construction of the first principal component (PC1) for the level, slope and curvature factors reveals the country's leading role in explaining the variation of the European sovereign yields.

The statistical significance of the estimated European liquidity and credit quality measures in the latent factor specification is also rather pronounced for Germany, while the statistical significance of the corresponding measures is less pronounced and varies across Italy, Spain, France and the UK. In addition, the sensitivity analysis results suggest significant effects on the European sovereign yield curves and cross-country spreads after shocks to market-wide measures of liquidity and credit quality, while the impact of liquidity and credit quality shocks differs across countries and term structure maturities. Specifically, the German yields tend to be negatively related to market-wide liquidity and credit quality shocks, while being, on average, the most sensitive ones, implying a significant reduction in the German yields after a shock in the European liquidity and credit quality measures. In addition, the spreads between the German yields and the yields of the peripheral Eurozone countries increase in response to market-wide liquidity and credit shocks, while the impact of these shocks on the remaining cross-country spreads varies across shock types (i.e. shock to market-wide liquidity or credit quality measures) and term structure maturities.

In the second part, we model the covariance structure of European sovereign yields employing the covariance regression model of [Hoff and Niu \(2012\)](#). In this respect, we parametrise the covariance matrix of sovereign yields as a function of country-specific liquidity and credit quality measures and explore the effects of liquidity and credit concerns on the heteroscedasticity of European sovereign yields unconditionally, as well as conditional on times of heightened equity market volatility. The unconditional statistical significance results and likelihood-ratio tests indicate that country-specific liquidity and credit quality measures are jointly important in explaining the covariation of European sovereign yields, while their importance is robust across different investment horizons. The German bid-ask spreads appear to be the most significant country-specific liquidity measures, whereas the Italian and Spanish credit default swap (CDS) spreads are the most significant country-specific

credit quality measures across maturities. The time-series average correlation estimates, derived from the fitted models, tend to be positively signed for the majority of the country pairs and are more pronounced for the medium and longer-term maturity bonds.

In addition, the conditional analysis covariance regression results reveal significant changes in the behaviour of country-specific liquidity and credit quality variables during periods of low and high-equity market volatility. The significance of credit quality variables is slightly more pronounced than the significance of liquidity measures in the low-equity market volatility period. In contrast, the significance of credit quality measures is considerably more pronounced than the significance of liquidity measures in the high-equity market volatility period. Specifically, the significance of liquidity measures is reduced in the high-equity market volatility period, while the significance of credit quality measures is more pronounced in this period. The majority of time-series average correlation estimates differ significantly from each other, reflecting the change in the behaviour of country-specific liquidity and credit quality measures and consequently the change in the dependence structure of sovereign yields across these sub-periods.

The impact of country-specific liquidity and credit quality shocks on European sovereign curves and the corresponding cross-country spreads is rather significant and varies across countries, shock types and maturities. In particular, credit shocks have, on average, a greater impact on cross-country spreads than liquidity shocks of the same magnitude. In addition, shocks tend to have a greater impact on medium and longer-term bonds, such as 60, 120 and 240-month maturities. The unconditional sensitivity analysis results also suggest that shocks to Spanish liquidity and credit quality measures have, on average, the greatest impact on cross-country spreads. Moreover, the short-term liquidity and credit quality shocks appear to have more persistent effects on the sovereign yield curves than shocks in medium and longer-term maturities. The conditional sensitivity analysis results suggest that European sovereign yield changes are more pronounced in high-equity than low-equity market volatility periods; however, the cross-country spread changes do not show significant evidence of asymmetries over either sub-period for the majority of the cross-country spreads under study.

To sum up, our empirical findings suggest that both market-wide and country-specific liquidity and credit measures are important in explaining the dynamic behaviour of European sovereign yield curves and their dependence structure unconditionally, as well as conditional on periods of heightened equity market volatility. Nevertheless, the importance of these measures varies across time, shock types and investment horizons. Investors appear to be more concerned with credit quality over

periods of high-equity market volatility, while investors' liquidity concerns cannot be disregarded. The German yields tend to be the most sensitive to market-wide liquidity and credit shocks, while shocks to Spanish liquidity and credit quality measures have the greatest impact on the cross-country spreads suggesting significant spillover effects among European economies.

The rest of the Chapter is organised as follows: Section 5.2 discusses the relevant literature, while Section 5.3 describes in detail the data we use in the empirical part of this study. Section 5.4 presents the macro-finance Nelson-Siegel model of [Diebold et al. \(2006\)](#) and discusses the associated state-space representation, whereas Section 5.5 reports the empirical results from the fit of the European sovereign yield curve models. Significance testing, a principal component analysis of the extracted latent factors and a sensitivity analysis are also presented in this Section. Section 5.6 presents the covariance regression model of [Hoff and Niu \(2012\)](#) and describes in detail the model's estimation procedure. Section 5.7 presents the empirical results obtained from the covariance regression model. The significance testing of country-specific liquidity and credit quality variables and the correlation estimates are also presented in this Section. Moreover, Section 5.7 describes in detail a sensitivity analysis procedure aimed at quantifying the impact of country-specific liquidity and credit quality shocks on the European sovereign yield curves and cross-country spreads, respectively. Section 5.8 concludes with discussion and suggestions for further work.

5.2 Related literature

Our study is related to multiple segments of the econometrics and finance literature. Firstly, our analysis is related to studies focused on modelling the dynamic futures of the term structure of interest rates. There are two main strands of term structure models in finance literature, each with its particular focus; the no-arbitrage models and the equilibrium models. The non-arbitrage models ([Ho and Lee, 1986](#); [Hull, 1990](#); [Heath, Jarrow, and Morton, 1992](#)) focus on fitting the term structure at a given point in time to ensure that no arbitrage possibilities exist. In contrast, the affine equilibrium models ([Vasicek, 1977](#); [Cox, Ingersoll, and Ross, 1985](#); [Duffie and Kan, 1996](#); [Dai and Singleton, 2000](#)) focus on modelling the instantaneous short rates, and thus the yields of longer maturities are derived under certain assumptions for the risk premium. [Duffie \(2002\)](#) shows that the affine equilibrium models result in poor out-of-sample yield curve forecasts.

In this study we use neither the no-arbitrage approach nor the equilibrium approach. Our modelling strategy builds primarily on the yield curve models proposed by [Diebold and Li \(2006\)](#) and [Diebold et al. \(2006\)](#), respectively. [Diebold and](#)

Li (2006) extended the parsimonious three-factor (exponential components) yield curve model of Nelson and Siegel (1987) to a dynamic model. They employ a two-step approach, in which they first estimate autoregressive models for the latent level, slope and curvature factors, and then use models to produce term structure forecasts. Diebold et al. (2006) proposed a latent factor model for the yield curve that explicitly incorporates observable macroeconomic factors to study the dynamic interactions between the macroeconomy and the yield curve. In this respect, their model's state-space representation enables estimations, the extraction of latent factors, and hypothesis testing concerning the dynamic interactions between the macroeconomy and the yield curve. After fitting the model on a set of US Treasury securities, Diebold et al. (2006) extract three latent factors (specifically, level, slope and curvature) and relate these factors to three observable macroeconomic variables (essentially measures for real economic activity, monetary policy and inflation). Diebold et al. (2006) conclude that the level and slope factors are highly correlated with inflation and real economic activity respectively, while the curvature factor appears uncorrelated with key macroeconomic variables. Consequently, their work is more closely connected to research that relates macroeconomic variables to the yield curve, including, for example, Kozicki and Tinsley (2001), Ang and Piazzi (2003), Hördahl et al. (2006), Ang et al. (2006), Dewachter and Lyrio (2006), Balfoussia and Wickens (2007) and Rudebusch and Wu (2008), among others.

There are a number of papers that have further extended the work of Diebold and Li (2006) and Diebold et al. (2006) on the Nelson-Siegel model. For example, Yu and Zivot (2011) extended the Nelson-Siegel model by providing a forecasting evaluation of the two-step and one-step procedures of Diebold and Li (2006) and Diebold et al. (2006), respectively, using corporate bonds of different credit ratings. Yu and Salayards (2009) investigate the sensitivity of the out-of-sample forecasting performance of the dynamic Nelson-Siegel model concluding that the ad hoc selection of the λ parameter, which determines the rate of exponential decay, is not optimal. Bianchi et al. (2009) extended the framework of Diebold et al. (2006) proposing a VAR model with time-varying coefficients and stochastic volatility for the latent level, slope and curvature factors. In addition, Koopman et al. (2010) extended the dynamic Nelson-Siegel model by allowing time-varying factor loadings and time-varying volatility in the observation disturbances. Moreover, Diebold et al. (2008) extended the Diebold et al. (2006) model to a global context, modelling a large set of country yields in a framework that allows both global and country-specific factors. More recently, Christensen et al. (2011) modified the Nelson-Siegel framework to impose the arbitrage-free condition.

Secondly, our analysis is naturally related to the literature studying the determinants of sovereign yield changes or sovereign yield spreads and the extent to which

credit and liquidity determine yields in the bond markets. Early work by [Duffie et al. \(2003\)](#) and [Longstaff et al. \(2005\)](#) suggests that both liquidity and credit risks are important components of yield spreads. In particular, [Longstaff et al. \(2005\)](#) work with corporate yield spreads of various credit ratings and investigate the extent to which corporate yields are directly attributed to corporate default risk and factors such as liquidity and taxes. They find that the majority of the corporate spreads are due to the default risk across all bond ratings. They also find a significant non-default component that is strongly related to bond-specific and market-wide measures of liquidity indicating that there are significant individual and market-wide liquidity dimensions in spreads. Furthermore, [Covitz and Downing \(2007\)](#) study the determinants of very short-term corporate yield spreads. They find that liquidity is significant in the determination of yield spreads, but credit quality is the dominant determinant of spreads, even at horizons of less than 1 month.

More recently, [Beber et al. \(2009\)](#) have used intraday Euro-area government bond spreads and order flow data to explore the association of sovereign yield spreads with measures of liquidity and credit quality unconditionally, as well as conditional on periods of heightened market uncertainty. [Beber et al. \(2009\)](#) show that the majority of European sovereign yield spreads can be explained by differences in credit quality, though liquidity is also significant, especially for low credit risk countries and during times of increased market uncertainty. [Beber et al. \(2009\)](#) also show that flights (large flows into and out of the bond market) are significantly determined by liquidity and that liquidity also explains the majority of sovereign yield spreads conditional on periods of large flows into or out of the bond markets. In addition, [Monfort and Renne \(2014\)](#) develop a multi-issuer no-arbitrage affine term structure framework to model the dynamics of Euro-area sovereign yield spreads and identify the part of liquidity and credit spreads corresponding to the risk premium. [Monfort and Renne \(2014\)](#) provide evidence of causal relationships between credit- and liquidity-stress periods. Liquidity effects are also found to account for a sizeable share of spreads' fluctuations.

There is strong empirical and theoretical evidence that yields and yield spreads are affected by liquidity concerns (for a survey, see [Amihud et al., 2005](#)).¹ For example, [Longstaff \(2004\)](#) investigates whether there are flight-to-liquidity premia in the U.S Treasury bond prices, comparing Treasury bond prices with prices of bonds issued by Refcorp, a U.S government agency whose bonds are fully collateralised by Treasury bonds and essentially have the same credit risk as Trea-

¹Studies on bond liquidity also include [Balduzzi et al. \(2001\)](#), [Krishnamurthy \(2002\)](#), [Goldreich et al. \(2005\)](#), [Chordia et al. \(2005\)](#), [Liu et al. \(2006\)](#), [Dick-Nielsen et al. \(2012\)](#), [de Jong and Driessen \(2012\)](#), [Kempf et al. \(2012\)](#) among others.

sury bonds. Longstaff (2004) finds significant liquidity premia in Treasury bond prices. Longstaff (2004) also finds that the liquidity premia are related to a variety of market sentiment measures such as changes in consumer confidence, in the amount of Treasury debt available to investors, and in the amount of funds flowing into equity and money market mutual funds. Furthermore, Chen et al. (2007) assess bond-specific liquidity for a broad range of investment and speculative grade corporate bonds and examine the association between bond-specific liquidity estimates and corporate bond yield spreads. They find, employing three different liquidity measures, that liquidity is priced in both levels and changes of the yield spread. For all three liquidity measures, they show that an increase in illiquidity is significantly and positively associated with an increase in yield spreads after controlling for changes in credit rating, macroeconomic effects, or firm-specific factors. They also find that the explanatory power of liquidity persists across both types of bonds, but is more pronounced for speculative grade bonds.

Recently, Goyenko et al. (2011) have studied the time series of illiquidity for different bond maturities, over an extended period of time that spans over 35 years, in order to explore whether illiquidities are differentially affected by macroeconomic conditions, and to analyse variations in the illiquidity premium across bonds. They find that illiquidity increases in recessions across all maturities, but the increase is more pronounced for short-term bonds. In addition, they find that off-the-run illiquidity is affected by a larger set of economic variables - such as inflation, monetary policy surprises, bond returns, and volatility - than its on-the-run counterpart. They also show that bond returns across maturities are forecastable by off-the-run but not on-the-run bond illiquidity, concluding that off-the-run illiquidity is the primary source of the liquidity premium in the Treasury market.

In addition to the empirical papers, there are a number of theoretical papers that highlight the role of liquidity in asset pricing. For example, Vayanos (2004) proposes a dynamic equilibrium model with multiple assets, stochastic volatility and transaction costs. The empirical implication of the model is that the preference for liquidity is time-varying and increases with volatility. Moreover, assets' pairwise correlation and illiquid assets' market beta increase during more volatile times. Similarly, Acharya and Pedersen (2005) propose an equilibrium model with liquidity risk. The model can explain the empirical findings that return sensitivity to market liquidity is priced, that average liquidity is priced, and that liquidity co-moves with returns and predicts expected returns. Moreover, Ericsson and Renault (2006) develop a structural bond pricing model with liquidity and credit risk to study the interaction between these two sources of risk and their relative contributions to the yield spreads on corporate bonds. Their main findings suggest that the levels of liquidity spreads are positively correlated with credit risk and decrease with time to

maturity. More recently, [Brunnermeier and Pedersen \(2009\)](#) have developed a model that links an asset's market liquidity with traders' funding liquidity. The model is capable of explaining the main empirical features of market liquidity and also implies that speculators' capital is a driver of market liquidity and risk premiums.

5.3 Data

The data, which will be described in detail below, consists of end-of-day sovereign bond yields, sovereign bid-ask spreads, credit default swap (CDS) spreads, and macroeconomic and financial variables. The data spans security trading in 5 major economies in the European Union: two "peripheral" Eurozone countries (Italy and Spain), two "core" Eurozone countries (Germany and France) and one non-euro European country (United Kingdom).² We consider daily end-of-day sovereign yields (midpoints of the quoted daily closing bid and ask yields) with maturities of 12, 24, 36, 48, 60, 72, 84, 96, 108, 120, 180, 240 and 360 months for each country over the period from November 11, 2008 to February 28, 2014. In this respect, the full sample consists of 1372 daily yield observations for each maturity and each country, respectively. This period is of great interest as it includes a significant number of events, for example the sovereign debt crisis faced by several Eurozone countries such as Greece, Ireland, Portugal, Spain and Cyprus as well as a range of policy interventions including the Securities Market Programme (SMP) and the Outright Monetary Transactions (OMT) programme launched by the European Central Bank (ECB) in response to the financial crisis and the liquidity dry-ups in the interbank lending markets. We argue that it therefore constitutes a rich period in which to study a variety of effects on the behaviour of the European fixed-income markets and the relative importance of credit quality and liquidity during both calm and distress periods.

In our analysis we quantify liquidity in the European sovereign bonds via the quoted bid-ask spreads. This is a standard measure of liquidity in the bond markets. [Goyenko et al. \(2011\)](#) argue that the quoted bid-ask spread is a reasonable liquidity proxy and is highly correlated with other liquidity measures in the bond market.³ The daily end-of-day bid and ask quotes are obtained from Bloomberg for

²The exclusion of several "peripheral" Eurozone countries, such as Greece, Portugal, and Ireland, and "core" Eurozone countries, such as Austria, Belgium, Finland, and the Netherlands, from the analysis is mainly driven by the lack of sovereign yields, liquidity and credit quality data for the time period and time-to-maturity contracts we want to analyse. However, [González-Hermosillo and Johnson \(2014\)](#) show that Spain and Italy played a more pivotal role in the transmission of financial shocks after 2009. In addition, [Alter and Beyer \(2014\)](#) show that the systemic contributions of Greece, Portugal, and Ireland decreased markedly after the implementation of IMF/EU bailout programs.

³For example, [Chordia et al. \(2001\)](#), show that the daily correlations between quoted and effective

each maturity studied, using the Bloomberg Generic Quote (BGN) pricing source, which reflects consensus quotes among market participants regarding the value of the bond. The measures based on quoted bid-ask spreads from Bloomberg are among the most widely used daily liquidity measures in fixed-income markets (see, e.g., Bao et al. (2011); Longstaff et al. (2005); Chen et al. (2007) amongst others). Schestag et al. (2013) also show that the daily bid-ask quotes from Bloomberg can capture effective transaction costs.

In addition to the sovereign yield data, we use sovereign credit default swap (CDS) spreads to obtain a market estimate of the credit quality for each of the countries in our sample. A credit default swap is an over-the-counter (OTC) derivative contract that provides protection against the risk of a credit event by a particular company or country. The sovereign CDS data used for the analysis are midpoints of the daily closing spreads with maturities of 6, 12, 24, 36, 48, 60, 84, 120, 240 and 360 months from the Thomson Reuters Eikon database, which also consists of market consensus CDS quotes that are published by Thomson Reuters using a highly standardised quality assurance data process.

The macroeconomic and financial variables consist of inflation data, major exchange rates and proxies for short-term liquidity and credit quality. In particular, the Harmonised Index of Consumer Prices (HICP) is used as a measure of inflation and price stability. The HICP monthly time series for each individual country are obtained from the statistics database of the European Central Bank (ECB) and are subsequently interpolated to daily series using cubic spline techniques. The daily US Dollar (USD), Great Britain Pound (GBP) and Japanese Yen (JPN) exchange rates against the Euro are also obtained from the ECB's database. The spread between the 3-month Euribor rate and the 3-month Eurepo rate, both reported by the European Banking Federation (EBF), is used as a proxy for short-term liquidity risk. In addition, the 5-year Markit iTraxx Europe index is employed as a credit proxy for the overall credit quality in the European bond market. The Markit iTraxx Europe is a benchmark index comprising 125 equally weighted CDS on investment grade European corporate entities. The contract with 5 years to maturity is the most actively traded contract. The daily 3-month Euribor and Eurepo rates are obtained from Bloomberg, while the daily 5-year Markit iTraxx Europe index is obtained from the Thomson Reuters Eikon database.

spread changes are 0.68 in the bond market over their 9-year sample period, while Chordia et al. (2005) show that the correlation between daily quoted spreads and depth is -0.49.

Table 5.3.1 presents descriptive statistics for the sovereign bond yields, while Table 5.3.2 and Table 5.3.3 present descriptive statistics for the quoted sovereign bid-ask and CDS spreads for each country and maturity, respectively. We note that the typical yield curve for each country is upward sloping, and that the short-term rates are generally more volatile than the long-term rates, especially for Italy and Spain. The German yields are the lowest, on average, across all maturities, followed by the UK and French bond yields.⁴ The Spanish and Italian bond yields are the highest across all countries and maturities in our sample highlighting investors' increased credit and liquidity concerns. Table 5.3.2 and 5.3.3 also show that average bid-ask and CDS spreads are much greater in size when compared with the corresponding German, French and UK spreads. The evolution of the 5-year bid-ask and CDS spreads, plotted in Figures 5.3.1 and 5.3.2, also confirms investors' risk aversion and negative sentiment toward the sovereign debts of the "peripheral" Eurozone countries. As can be seen in Figures 5.3.1 and 5.3.2, both bid-ask and CDS spreads for Italy and Spain peaked between end-2011 and mid-2012. This period corresponds to the peak of the Spanish crisis and the official request of the Spanish government for financial support from Eurozone members.⁵

The turning point of the Eurozone sovereign debt crisis was the July 26, 2012 policy statement by Mario Draghi, president of the European Central Bank (ECB), that "the ECB is ready to do whatever it takes to preserve the euro."⁶ This policy statement was followed on September 6, 2012, by the announcement of the Outright Monetary Transactions (OMT) programme.⁷ This change in the policy stance triggered a lasting scaling-down in the bond yields of Eurozone countries. The benchmark Spanish 10-year bond yield stayed below 6%, having reached 5% by year's end. [Saka et al. \(2014\)](#) provided empirical evidence regarding the contagion-mitigating effects of the new ECB policy embodied in the OMT programme.

⁴Germany's 12, 24 and 36 month bond yields turned negative between end-2011 and mid-2012 since investors sought refuge in Europe's safest assets over concerns about the solvency of several European economies.

⁵On June 9, 2012, the Eurogroup granted to Spain a financial support package of up to €100 billion in order for the country's financial institutions to be recapitalised. In addition, on June 25, 2012, the Cypriot Government requested financial aid from the euro area members and the International Monetary Fund (IMF) in order to tackle the distress in the country's banking sector and the macroeconomic imbalances.

⁶Mario Draghi, 26 July 2012. See www.ecb.europa.eu/press/key/date/2012/html/sp120726.en.html

⁷The Outright Monetary Transactions (OMT) programme is a programme of the European Central Bank (ECB) under which the bank makes purchases of sovereign bonds of Eurozone countries having difficulty issuing debt.

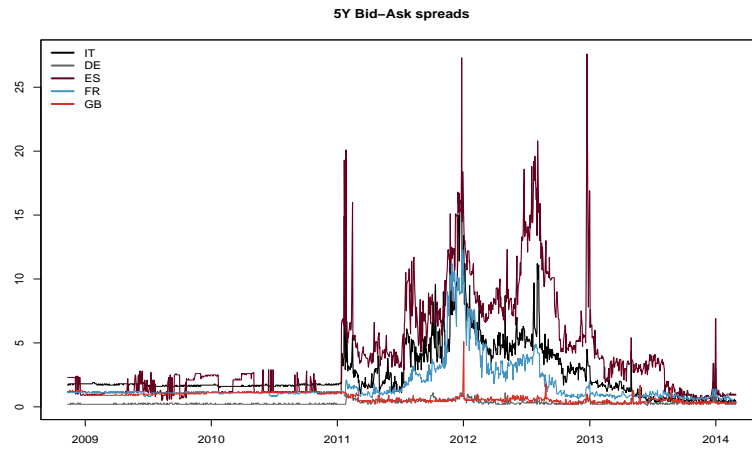


Figure 5.3.1: Sovereign 5-year bid-ask spreads for Italy, Germany, Spain, France and the United Kingdom.

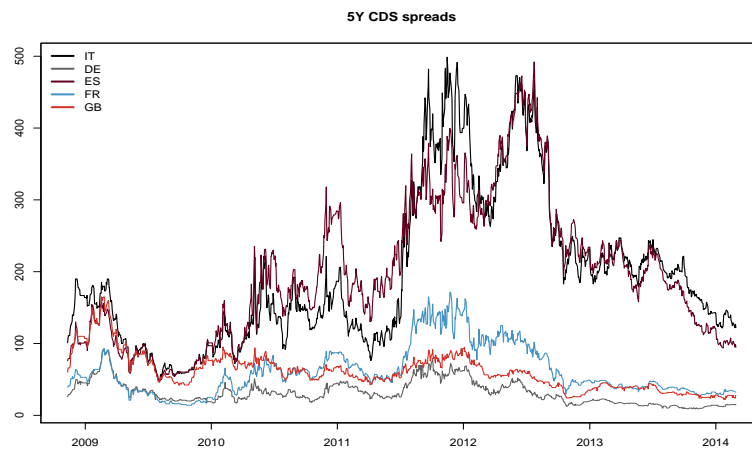


Figure 5.3.2: Sovereign 5-year credit default swap (CDS) spreads for Italy, Germany, Spain, France and the United Kingdom.

Table 5.3.1: Descriptive Statistics: Sovereign yields

Maturity	Italy					Germany					Spain					France					UK				
	N	Mean	Sd	Min	Max	N	Mean	Sd	Min	Max	N	Mean	Sd	Min	Max	N	Mean	Sd	Min	Max	N	Mean	Sd	Min	Max
12	1368	1.66	1.00	0.57	7.67	1349	0.50	0.49	-0.11	2.19	665	2.06	1.14	0.55	5.47	1356	0.58	0.47	-0.01	2.32	1372	0.52	0.25	0.07	2.29
24	1372	2.34	1.10	0.75	7.58	1366	0.72	0.61	-0.09	2.35	1372	2.51	0.99	0.76	6.57	1372	0.92	0.59	0.02	2.60	1372	0.75	0.44	0.05	2.55
36	1372	2.87	1.10	1.25	7.63	1372	0.91	0.71	-0.05	2.55	1372	3.04	0.98	1.36	7.37	1372	1.19	0.67	0.10	2.82	1372	1.12	0.67	0.08	3.02
48	1372	3.27	1.00	1.71	7.68	1372	1.18	0.80	0.05	2.82	1372	3.35	0.95	1.58	7.40	1372	1.54	0.71	0.29	3.07	1372	1.48	0.77	0.23	3.32
60	1372	3.62	0.99	2.04	7.70	1372	1.45	0.81	0.24	2.90	1372	3.73	0.94	1.99	7.50	1372	1.88	0.71	0.60	3.28	1372	1.78	0.77	0.45	3.49
72	1372	3.81	0.95	2.28	7.66	1372	1.68	0.84	0.41	3.19	1372	3.96	0.95	2.19	7.56	1372	2.10	0.73	0.70	3.45	1241	1.94	0.82	0.62	3.68
84	1372	4.04	0.91	2.59	7.67	1372	1.90	0.84	0.56	3.40	1372	4.21	0.91	2.50	7.53	1372	2.34	0.70	0.91	3.65	1372	2.28	0.82	0.80	3.98
96	1372	4.23	0.83	2.89	7.55	1372	2.09	0.82	0.77	3.60	1372	4.40	0.87	2.84	7.42	1372	2.58	0.68	1.16	3.88	1372	2.52	0.79	1.05	4.06
108	1372	4.43	0.74	3.21	7.28	1371	2.25	0.78	0.98	3.65	1372	4.56	0.87	3.07	7.54	1372	2.77	0.64	1.40	3.94	1249	2.62	0.74	1.35	3.85
120	1372	4.65	0.75	3.46	7.24	1371	2.38	0.75	1.16	3.72	1372	4.77	0.83	3.49	7.57	1372	2.95	0.60	1.66	4.05	1372	2.88	0.77	1.44	4.23
180	1372	5.04	0.70	3.95	7.72	1372	2.82	0.74	1.61	4.27	1329	5.23	0.83	3.94	7.70	1370	3.39	0.54	2.29	4.42	1372	3.40	0.75	2.10	4.85
240	1372	5.32	0.71	4.18	8.04	1372	3.08	0.74	1.75	4.48	1372	5.34	0.79	3.97	7.71	1371	3.56	0.53	2.48	4.64	1372	3.65	0.67	2.46	4.86
360	1372	5.40	0.61	4.45	7.63	1371	3.10	0.70	1.67	4.47	1372	5.43	0.75	3.85	7.54	1371	3.69	0.43	2.77	4.62	1372	3.81	0.53	2.84	4.69

This table reports summary statistics for our sample daily sovereign yields (end-of-day midpoints of the quoted bid and ask yields), expressed in percentages, for various maturities, measured in months, for Italy, Germany, Spain, France and the UK. N is the number of daily observations for each maturity/country.

Table 5.3.2: Descriptive Statistics: Bid-Ask spreads

Maturity	Italy					Germany					Spain					France					UK				
	N	Mean	Sd	Min	Max	N	Mean	Sd	Min	Max	N	Mean	Sd	Min	Max	N	Mean	Sd	Min	Max	N	Mean	Sd	Min	Max
12	1368	10.72	14.84	1.10	176.70	1349	2.14	2.13	0.80	25.30	665	29.36	28.56	2.40	148.30	1356	4.08	2.13	0.80	17.00	1372	3.33	1.88	0.70	19.80
24	1372	4.78	3.58	0.50	35.90	1366	0.57	0.21	0.20	2.20	1372	7.29	6.10	1.00	40.70	1372	3.04	2.37	0.50	15.90	1372	1.79	0.95	0.50	4.90
36	1372	3.92	3.60	0.30	26.60	1372	0.47	0.24	0.10	1.90	1372	5.65	5.40	0.60	41.00	1372	2.38	1.87	0.50	12.50	1372	1.17	0.60	0.30	2.60
48	1372	3.10	2.59	0.40	20.30	1372	0.36	0.18	0.10	1.70	1372	4.87	4.63	0.70	33.60	1372	2.05	1.83	0.40	11.70	1372	0.90	0.44	0.20	2.00
60	1372	2.58	2.21	0.20	18.10	1372	0.31	0.16	0.10	1.10	1372	4.15	3.97	0.40	27.60	1372	1.72	1.73	0.20	12.30	1372	0.73	0.35	0.20	5.10
72	1372	2.41	1.87	0.30	19.40	1372	0.31	0.15	0.10	1.10	1372	3.81	3.38	0.50	24.50	1372	1.23	1.01	0.20	8.80	1241	0.60	0.25	0.10	1.70
84	1372	2.12	1.56	0.20	16.50	1372	0.37	0.14	0.10	1.60	1372	3.35	2.96	0.30	17.10	1372	1.00	0.70	0.20	6.60	1372	0.55	0.20	0.10	1.60
96	1372	1.89	1.32	0.20	12.40	1372	0.33	0.13	0.10	1.70	1372	3.06	2.84	0.20	16.30	1372	0.96	0.71	0.20	5.40	1372	0.51	0.18	0.10	1.70
108	1372	1.75	1.30	0.30	18.40	1371	0.27	0.12	0.00	0.60	1372	2.73	2.34	0.30	11.60	1372	0.86	0.63	0.20	4.50	1249	0.45	0.19	0.10	1.60
120	1372	1.72	1.28	0.20	15.80	1371	0.34	0.18	0.10	0.80	1372	2.48	2.22	0.20	12.60	1372	0.83	0.59	0.20	5.90	1372	0.46	0.18	0.10	1.80
180	1372	2.06	1.78	0.20	19.10	1372	0.82	0.39	0.40	3.00	1329	2.86	2.41	0.40	16.80	1370	0.94	0.77	0.20	7.00	1372	0.52	0.14	0.20	1.50
240	1372	2.24	2.22	0.50	21.80	1372	0.76	0.40	0.30	2.60	1372	2.93	2.82	0.10	13.30	1371	0.96	0.81	0.20	6.50	1372	0.47	0.11	0.20	1.50
360	1372	1.70	1.56	0.30	14.00	1371	0.59	0.34	0.20	6.00	1372	2.57	2.65	0.00	12.90	1371	0.77	0.62	0.10	5.00	1372	0.43	0.10	0.20	1.40

This table reports summary statistics for our sample sovereign bid-ask spreads (end-of-day quoted bid-ask spreads), expressed in basis points, for various maturities, measured in months, for Italy, Germany, Spain, France and the UK. N is the number of daily observations for each maturity/country.

Table 5.3.3: Descriptive Statistics: Credit Default Swap (CDS) spreads

Maturity	Italy					Germany					Spain					France					UK				
	N	Mean	Sd	Min	Max	N	Mean	Sd	Min	Max	N	Mean	Sd	Min	Max	N	Mean	Sd	Min	Max	N	Mean	Sd	Min	Max
12	1367	128.93	113.04	6.00	550.85	1357	12.48	11.43	0.28	50.48	1366	139.18	94.61	14.00	426.63	1343	27.31	24.99	2.02	128.78	1372	27.65	25.53	1.92	140.00
24	1367	155.67	116.55	20.00	542.02	1357	16.26	12.79	1.09	59.23	1366	162.89	101.88	24.00	476.87	1343	35.25	28.16	3.86	142.49	1372	35.40	26.03	4.02	147.50
36	1367	176.13	116.53	34.00	530.17	1357	20.15	14.07	2.53	69.70	1366	180.27	102.82	34.00	494.40	1343	43.80	31.72	6.39	156.98	1372	42.29	26.61	6.11	155.00
48	1367	187.40	111.85	41.00	513.91	1357	25.58	15.14	5.19	81.10	1366	190.23	100.76	40.50	493.25	1343	52.33	32.77	12.01	161.37	1372	51.22	25.94	15.59	160.00
60	1367	196.88	107.76	48.00	498.66	1357	31.47	16.25	9.16	92.50	1370	197.94	98.44	47.00	492.07	1343	61.14	34.23	14.01	171.56	1372	60.25	25.65	22.09	165.00
84	1367	201.46	103.86	49.20	480.66	1356	36.92	15.33	16.95	92.24	1366	202.18	94.28	47.80	468.87	1343	68.84	34.02	15.60	176.03	1372	67.78	21.82	34.58	165.00
120	1367	201.63	98.53	51.00	468.19	1357	41.92	15.01	21.48	91.98	1366	201.27	89.31	49.00	444.51	1343	75.15	34.79	17.00	181.36	1372	74.94	19.80	45.50	165.00
240	1365	195.82	94.21	46.00	463.11	1357	41.85	15.15	20.71	96.02	1364	196.83	83.46	49.00	419.07	1343	75.17	33.69	19.00	182.37	1372	82.54	18.63	45.50	165.00
360	1367	192.90	92.86	41.00	460.04	1357	41.90	15.44	18.18	96.34	1366	194.93	81.12	49.00	408.36	1343	75.83	32.88	25.00	183.86	1372	84.44	18.53	45.50	165.00

This table reports summary statistics for our sample credit default swap (CDS) spreads, expressed in basis points, for various maturities, measured in months, for Italy, Germany, Spain, France and the UK. N is the number of daily observations for each maturity/country.

In addition, Table 5.3.4 presents descriptive statistics for the macroeconomic and financial variables employed in the analysis. The inflation rates for all four Eurozone countries in our sample collectively turned negative over the third quarter of 2009. This period is characterised by severe liquidity dry-ups in the interbank lending markets. The 3-month Euribor-Eurepo spread that measures the difference in interest rates between short-term unsecured and collateralised funding skyrocketed to almost 172 basis points, while the iTraxx Europe index that provides an exogenous credit quality estimate on investment grade European entities, soared to approximately 216 basis points at the end of 2008 illustrating the widespread market concerns about the solvency of several European financial institutions over this period. The volatility for all major exchange rates is also fairly large in our sample period.

Table 5.3.4: Summary Statistics: Macroeconomic and Financial variables

Variable	Mean	Sd	Min	Max
HICP.IT	1.97	1.08	-0.14	3.84
HICP.DE	1.39	0.69	-0.50	2.41
HICP.ES	1.69	1.35	-1.40	3.80
HICP.FR	1.30	0.80	-0.72	2.54
HICP.UK	3.07	0.90	1.10	5.23
GBP	0.86	0.03	0.78	0.98
JPY	118.78	12.57	94.63	145.02
USD	1.34	0.06	1.19	1.51
Liquidity	44.22	31.55	12.70	171.70
iTraxx	119.93	33.73	65.30	215.92

This table reports summary statistics for our sample macroeconomic and financial variables. The Harmonised Index of Consumer Prices (HICP), measured in percentages, is used as an inflation proxy for Italy (HICP.IT), Germany (HICP.DE), Spain (HICP.ES), France (HICP.FR) and the UK (HICP.UK). GBP, JPY and USD represent the Great Britain Pound, Japanese Yen and US Dollar exchange rates against the Euro. Liquidity and iTraxx represent liquidity and credit quality variables expressed in basis points.

Figure 5.3.3 presents average cross-country correlation coefficient estimates for liquidity and credit quality variables. We note that the variability of liquidity correlation estimates is more pronounced when compared with that of credit quality correlation estimates. It can also be noted that there is a strong positive correlation between bond liquidity measures across all Eurozone countries and a negative correlation between all Eurozone countries and the UK. The correlations between credit quality measures are also of great interest. As expected, the correlation between Spanish and Italian credit default swap (CDS) spreads is very strong and positive indicating the widespread market concerns about the sovereign credit default risk of the two “peripheral” Eurozone countries. Interestingly, Spanish and Italian CDS spreads are also strongly and positively correlated with French CDS spreads. Although we lack the statistical power to make more qualitative statements, the increased correlation of the French credit quality measures with those

of the “peripheral” Eurozone countries can be partly attributed to the increased concerns over the country’s economy and public finances.⁸ We also note the weak correlation between the UK credit default swap (CDS) spreads and those of the Eurozone countries, with the exception of the correlation coefficient for Germany, which is strong and positive, and reflects the country’s superior credit quality.

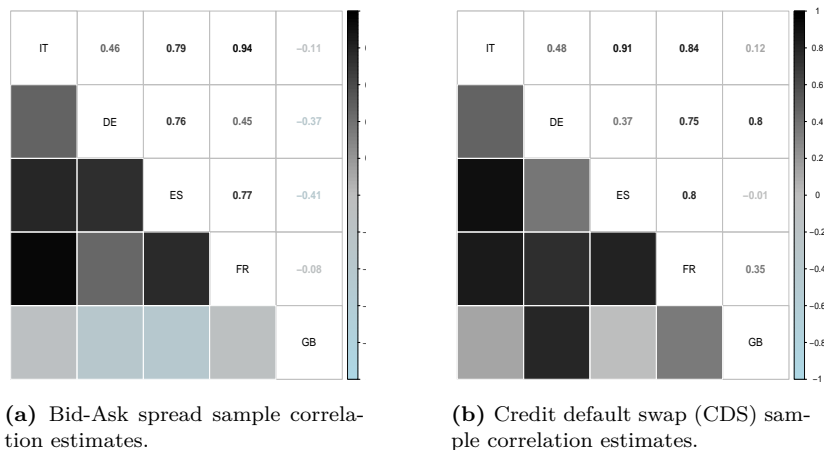


Figure 5.3.3: This figure presents average cross-country bond liquidity correlation estimates, calculated using the average quoted bid-ask spreads across maturities for each country, and average cross-country credit quality correlation estimates, calculated using the average credit default swap (CDS) spreads across maturities for each country.

Table 5.3.5 presents cross-sectional correlation coefficients between our average liquidity and credit quality measures for several maturities. It reports the correlation coefficients of the above measures for all countries in our sample (All countries column) as well as for Eurozone only countries (Eurozone column) to assess the impact of the exclusion of the UK, a non-Eurozone EU country, on the correlation estimates. The correlation estimates between average liquidity and credit quality measures across all maturities in both columns (All countries and Eurozone) are strong and positive suggesting that as liquidity in the sovereign bonds decreases, via the widening of the bid-ask spreads, credit quality also decreases. The qualitative results in Table 5.3.5 differ from the qualitative findings of [Beber et al. \(2009\)](#) and, more specifically, from the corresponding correlation estimates reported in Table 2 of their paper. [Beber et al. \(2009\)](#), using intraday European government bond quotes and credit default swap (CDS) data, report a negative relation between credit quality and liquidity measures. The discrepancy in the correlation estimates can be attributed to differences in the sample size and in the proxies for measuring liquidity

⁸France lost its Standard & Poor’s top-grade AAA rating in January 2012. In November 2013, Standard & Poor’s cut France’s credit rating from AA+ to AA, the third tier of credit quality, for the second time in less than two years due to the country’s weak economic growth, high unemployment and government spending constraints.

in the European bond markets.⁹

Table 5.3.5: Correlation between credit quality and liquidity

Maturity	All countries	Eurozone
12	0.65	0.67
24	0.77	0.78
36	0.74	0.75
48	0.79	0.81
60	0.79	0.80
84	0.79	0.80
120	0.76	0.77
240	0.78	0.79
360	0.80	0.81

This table reports the correlation between the average country credit risk, measured by credit default swap (CDS) spreads quoted for each country/maturity, and the average country bond liquidity, measured by the quoted bid-ask spread for each country/maturity. Column All countries reports the correlation for all countries in the sample, namely Italy, Germany, Spain, France and the UK, while column Eurozone, reports the correlation for all countries in the sample excluding the United Kingdom, which is the only non-euro EU country in our sample.

5.4 The dynamic Nelson-Siegel model

In this Section we introduce the latent factor model for the yield curve, initially proposed by [Nelson and Siegel \(1987\)](#), and subsequently extended, by [Diebold and Li \(2006\)](#), to a dynamic latent factor model to allow for time-varying parameters. We also discuss the state-space representation of the model as introduced in [Diebold et al. \(2006\)](#). Denote the set of yields as $y_t(\tau_i)$, where τ_i denotes the maturity of a zero-coupon bond for a set of N different maturities $\tau_1 \leq \dots \leq \tau_N$ available at time t . The term structure of yields for $i = 1, \dots, N$ at any point in time t is modelled by the three factor model of [Nelson and Siegel \(1987\)](#) as follows¹⁰

$$y_t(\tau_i) = \beta_1 + \beta_2 \left(\frac{1 - e^{-\lambda\tau_i}}{\lambda\tau_i} \right) + \beta_3 \left(\frac{1 - e^{-\lambda\tau_i}}{\lambda\tau_i} - e^{-\lambda\tau_i} \right) + \varepsilon(\tau_i), \quad (5.1)$$

⁹[Beber et al. \(2009\)](#) use intraday inter-dealer European government bond quotes for the period from April 2003 to December 2004. They also consider four alternative measures to capture the liquidity of sovereign bonds: the effective bid-ask spread, the average quoted depth, the cumulative limit-order book depth and the average quoted depth divided by the percentage bid-ask spreads. In contrast, our sample period is more extensive since it includes securities trading from November 11, 2008 to February 28, 2014; however, we are limited to the use of the quoted bid-ask spread for measuring the liquidity of the European sovereign bonds due to lack of limit-order book data.

¹⁰The original Nelson-Siegel model representation is slightly different from Equation (5.1), which has been modified by [Diebold and Li \(2006\)](#) to improve estimation tractability and to facilitate an intuitive interpretation of the factors.

where β_1 , β_2 , β_3 and λ are parameters. The disturbances $\varepsilon(\tau_i), \dots, \varepsilon_t(\tau_N)$ are assumed to be independent with zero mean and constant variance. The Nelson-Siegel model in Equation (5.1) was extended by Diebold and Li (2006) to a dynamic latent factor model where β_1 , β_2 and β_3 are interpreted as dynamic latent level, slope and curvature factors; the terms multiplied by these factors are factor loadings. In this respect, the dynamic Nelson-Siegel (DNS) model of Diebold and Li (2006) can be rewritten as follows

$$y_t(\tau_i) = L_t + S_t \left(\frac{1 - e^{-\lambda\tau_i}}{\lambda\tau_i} \right) + C_t \left(\frac{1 - e^{-\lambda\tau_i}}{\lambda\tau_i} - e^{-\lambda\tau_i} \right) + \varepsilon_t(\tau_i), \quad (5.2)$$

where $t = 1, \dots, T$, $i = 1, \dots, N$ while L_t , S_t and C_t are the time-varying β_1 , β_2 and β_3 parameters. The λ parameter determines the exponential decay rate of the slope and curvature factors. The shape and the form of the yield curve are governed by the three latent factors and their corresponding factor loadings. The loading on the first factor takes the value 1 and is interpreted as *level factor* because it affects all yields equally and, hence, changes the level of the yield curve. The loading on the second factor is $(1 - e^{-\lambda\tau_i})/(\lambda\tau_i)$, a function that starts at 1 and converges quickly and monotonically to 0 as τ increases. This factor is interpreted as *slope factor* because it affects short rates more heavily than long rates; consequently, it changes the slope of the yield curve. The loading on the third factor is $((1 - e^{-\lambda\tau_i})/\lambda\tau_i) - e^{-\lambda\tau_i}$, which is a function that starts at 0, increases, and then decays to 0. This factor is interpreted as *curvature factor* because it loads medium rates more heavily and, therefore, changes the yield curve curvature.¹¹ Figure 5.4.1 plots the Nelson-Siegel factor loadings with fixed $\lambda = 0.0609$ as in Diebold and Li (2006).

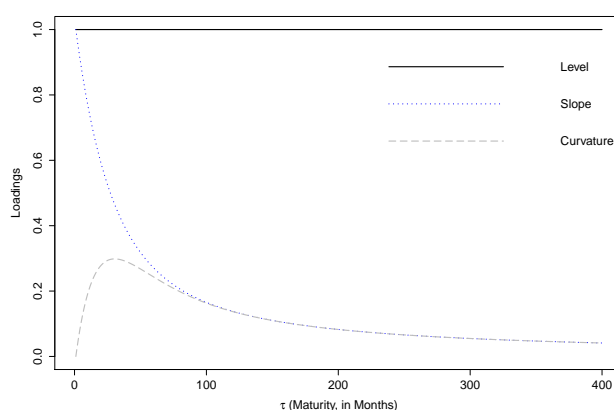


Figure 5.4.1: Factor loadings of the Nelson-Siegel model with fixed $\lambda = 0.0609$.

¹¹The *level*, *slope* and *curvature* factors are also known as *long-term*, *short-term* and *medium-term* factors respectively because, given their corresponding factor loadings, they affect more heavily long-term, short-term and medium-term interest rates, respectively (see for example, Yu and Zivot (2011), among others).

Diebold and Li (2006) estimate the parameters, $\boldsymbol{\theta}_t = \{L_t, S_t, C_t, \lambda\}$, of the dynamic Nelson-Siegel (DNS) model in Equation (5.2) by nonlinear least squares for each time period t after fixing λ at a pre-specified value (i.e. $\lambda = 0.0609$). Diebold et al. (2006) go a step further by recognising that the dynamic Nelson-Siegel (DNS) model naturally forms a state-space system when treating $\boldsymbol{\beta}_t = [L_t, S_t, C_t]'$ as a latent vector. The *measurement* equation that relates a set of N yields to the three unobserved factors can be written as

$$\begin{pmatrix} y_t(\tau_1) \\ y_t(\tau_2) \\ \vdots \\ y_t(\tau_N) \end{pmatrix} = \begin{pmatrix} 1 & \frac{1-e^{-\lambda\tau_1}}{\lambda\tau_1} & \frac{1-e^{-\lambda\tau_1}}{\lambda\tau_1} - e^{-\lambda\tau_1} \\ 1 & \frac{1-e^{-\lambda\tau_2}}{\lambda\tau_2} & \frac{1-e^{-\lambda\tau_2}}{\lambda\tau_2} - e^{-\lambda\tau_2} \\ \vdots & \vdots & \vdots \\ 1 & \frac{1-e^{-\lambda\tau_N}}{\lambda\tau_N} & \frac{1-e^{-\lambda\tau_N}}{\lambda\tau_N} - e^{-\lambda\tau_N} \end{pmatrix} \begin{pmatrix} L_t \\ S_t \\ C_t \end{pmatrix} + \begin{pmatrix} \varepsilon_t(\tau_1) \\ \varepsilon_t(\tau_2) \\ \vdots \\ \varepsilon_t(\tau_N) \end{pmatrix}, \quad (5.3)$$

In a matrix notation, Equation (5.3) can be written as

$$\mathbf{y}_t = \boldsymbol{\Lambda}(\lambda)\boldsymbol{\beta}_t + \boldsymbol{\varepsilon}_t, \quad (5.4)$$

with observation vector $\mathbf{y}_t = [y_t(\tau_1), \dots, y_t(\tau_N)]'$, latent vector $\boldsymbol{\beta}_t = [L_t, S_t, C_t]'$, disturbance vector $\boldsymbol{\varepsilon}_t = [\varepsilon_t(\tau_1), \dots, \varepsilon_t(\tau_N)]'$ and the $N \times 3$ factor loadings matrix $\boldsymbol{\Lambda}(\lambda)$, whose (i, l) element is given by

$$\boldsymbol{\Lambda}_{il}(\lambda) = \begin{cases} 1, & \text{for } l = 1, \\ (1 - e^{-\lambda\tau_i})/\lambda \cdot \tau_i, & \text{for } l = 2, \\ (1 - e^{-\lambda\tau_i} - \lambda \cdot \tau_i e^{-\lambda\tau_i})/\lambda \cdot \tau_i, & \text{for } l = 3. \end{cases} \quad (5.5)$$

The dynamics of L_t , S_t and C_t in Diebold et al. (2006) follow a vector autoregressive process of first order, VAR(1).¹² In general, the time-series dynamics for the 3×1 latent vector $\boldsymbol{\beta}_t$ are modelled as a VAR(p)-process, that is

$$\boldsymbol{\beta}_t = \boldsymbol{\mu} + \sum_{j=1}^p \boldsymbol{\Phi}_j \boldsymbol{\beta}_{t-j} + \boldsymbol{\eta}_t, \quad (5.6)$$

for $t = 1, \dots, T$, where $\boldsymbol{\mu} = [\mu_s, \mu_l, \mu_c]'$ is a vector of constants, $\boldsymbol{\Phi}_j$ is a 3×3 coefficient matrix for $j = 1 \dots p$ and $\boldsymbol{\eta}_t = [\eta_{lt}, \eta_{st}, \eta_{ct}]'$ is the disturbance vector. The system is complete once the covariance structure of the *transition errors* \mathbf{Q} and the covariance of *measurement errors* \mathbf{H} are specified. Diebold et al. (2006) make the standard assumption that the white noise errors in the *measurement* and *transition*

¹²Diebold and Li (2006) employ the VAR(1) assumption only for the sake of transparency and parsimony; however, ARMA state vector dynamics of any order can be easily accommodated in state-space form.

equations are orthogonal to each other and to the initial state, such that

$$\begin{pmatrix} \boldsymbol{\eta}_t \\ \boldsymbol{\varepsilon}_t \end{pmatrix} = WN \left(\begin{pmatrix} 0 \\ 0 \end{pmatrix}, \begin{pmatrix} \mathbf{Q} & 0 \\ 0 & \mathbf{H} \end{pmatrix} \right), \quad \mathbb{E}(\boldsymbol{\beta}_0 \boldsymbol{\eta}'_t) = 0 \quad \text{and} \quad \mathbb{E}(\boldsymbol{\beta}_0 \boldsymbol{\varepsilon}'_t) = 0.$$

In Diebold et al. (2006) the \mathbf{H} matrix is assumed to be diagonal whereas the \mathbf{Q} matrix is non-diagonal. The assumption of a diagonal \mathbf{H} matrix, which implies mutually uncorrelated deviations of yields of various maturities from the yield curve, is quite common. It is also used for computational tractability. On the other hand, the assumption of an unrestricted \mathbf{Q} (non-diagonal) matrix allows the shocks of the three factors to be correlated. Diebold et al. (2006) extended the dynamic Nelson-Siegel (DNS) model by including observable macroeconomic variables (specifically, real activity, inflation, and the monetary policy instrument) to study the interaction between the macroeconomy and the yield curve. Therefore, the macroeconomic variables are added to the set of space variables, and Equation (5.6) is replaced with

$$\boldsymbol{\beta}_t = \boldsymbol{\mu} + \sum_{j=1}^p \boldsymbol{\Phi}_j \boldsymbol{\beta}_{t-j} + \mathbf{B} \mathbf{X}_t + \boldsymbol{\eta}_t, \quad (5.7)$$

where vector \mathbf{X}_t is a $r \times 1$ vector of exogenous macroeconomic variables observable at time t and \mathbf{B} is a $3 \times r$ matrix of regression coefficients with r representing the number of observable variables.

5.4.1 Estimation based on the Kalman filter

The dynamic Nelson-Siegel (DNS) model of Diebold et al. (2006) is a linear Gaussian state-space model. The vector of latent factors $\boldsymbol{\beta}_t$ is therefore optimally estimated using the Kalman filter given past and current observations up to time t , i.e. $\mathbf{Y}_t = \{\mathbf{y}_1, \dots, \mathbf{y}_t\}$. The initial state vector is assumed to be normally distributed with initial conditions $\boldsymbol{\beta}_0 \sim N(\boldsymbol{\alpha}_0, \boldsymbol{\Sigma}_0)$, where $\boldsymbol{\alpha}_0, \boldsymbol{\Sigma}_0$ are assumed to be known. Define $\mathbf{b}_{t|t-1}$ as the minimum mean square linear estimator of $\boldsymbol{\beta}_t$ given $\mathbf{Y}_{t-1} = \{\mathbf{y}_1, \dots, \mathbf{y}_{t-1}\}$ with mean square error matrix $\mathbf{P}_{t|t-1}$. For given values of $\mathbf{b}_{t|t-1}$ and $\mathbf{P}_{t|t-1}$, the Kalman filter computes $\mathbf{b}_{t|t}$ and $\mathbf{P}_{t|t}$, when observation \mathbf{y}_t is available, using the following filtering step

$$\mathbf{b}_{t|t} = \mathbf{b}_{t|t-1} + \mathbf{K}_t \boldsymbol{\varepsilon}_t,$$

$$\mathbf{P}_{t|t} = [\mathbf{I} - \mathbf{K}_t \boldsymbol{\Lambda}(\lambda)] \mathbf{P}_{t|t-1},$$

where $\boldsymbol{\varepsilon}_t = \mathbf{y}_t - E(\mathbf{y}_t | \mathbf{Y}_{t-1}) = \mathbf{y}_t - \boldsymbol{\Lambda}(\lambda) \mathbf{b}_{t|t-1}$ is the error prediction vector, $\mathbf{F}_t = \text{Var}(\boldsymbol{\varepsilon}_t) = \boldsymbol{\Lambda}(\lambda) \mathbf{P}_{t|t-1} \boldsymbol{\Lambda}(\lambda)' + \mathbf{H}$ is the prediction error covariance matrix and $\mathbf{K}_t = \mathbf{P}_{t|t-1} \boldsymbol{\Lambda}(\lambda)' \mathbf{F}_t^{-1}$ is called the *Kalman gain*. The minimum mean square linear estimator of the state vector for the next period $t+1$, given $\mathbf{Y}_t = \{\mathbf{y}_1, \dots, \mathbf{y}_t\}$,

can be obtained by the following prediction step

$$\begin{aligned}\mathbf{b}_{t+1|t} &= (\mathbf{I} - \Phi)\boldsymbol{\mu} + \Phi\mathbf{b}_{t|t} + \mathbf{B}\mathbf{X}_{t+1}, \\ \mathbf{P}_{t+1|t} &= \Phi\mathbf{P}_{t|t}\Phi' + \mathbf{Q},\end{aligned}$$

For a given time series, $\mathbf{y}_1, \dots, \mathbf{y}_T$, and initial values $\mathbf{b}_{1|0} = \boldsymbol{\alpha}_0$ and $\mathbf{P}_{1|0} = \boldsymbol{\Sigma}_0$, the parameters that specify the state-space model, $\boldsymbol{\theta} = \{\boldsymbol{\mu}, \Phi, \mathbf{A}, \Lambda(\lambda), \mathbf{Q}, \mathbf{H}\}$, can be estimated recursively for $t = 1, \dots, T$ via the Kalman filter by maximising the log-likelihood function constructed via the prediction error decomposition, and is given by

$$l(\boldsymbol{\theta}) = -\frac{NT}{2} \log 2\pi - \frac{1}{2} \sum_{t=1}^T \log |\mathbf{F}_t| - \frac{1}{2} \sum_{t=1}^T \boldsymbol{\varepsilon}_t' \mathbf{F}_t^{-1} \boldsymbol{\varepsilon}_t. \quad (5.8)$$

5.4.2 Handling missing data

In our sample there are missing observations related to maturities or time periods. An attractive feature of the state-space framework is its ability to treat time series that have been observed irregularly over time. Suppose, at a given time t , we observe some, but not all, values of observation vector $\mathbf{y}_t = [y_t(\tau_1), \dots, y_t(\tau_N)]'$. We define the partition of the $N \times 1$ observation vector $\mathbf{y}_t = [\mathbf{y}_t^{(1)'}; \mathbf{y}_t^{(2)'}]'$, where the first $N_t^{(1)} \times 1$ vector $\mathbf{y}_t^{(1)}$ is observed and the second $N_t^{(2)} \times 1$ vector $\mathbf{y}_t^{(2)}$ is unobserved, where $N_t^{(1)} + N_t^{(2)} = N$. The partitioned observation equation can be given as

$$\begin{pmatrix} \mathbf{y}_t^{(1)} \\ \mathbf{y}_t^{(2)} \end{pmatrix} = \begin{pmatrix} \boldsymbol{\Lambda}^{(1)}(\lambda) \\ \boldsymbol{\Lambda}^{(2)}(\lambda) \end{pmatrix} \boldsymbol{\beta}_t + \begin{pmatrix} \boldsymbol{\varepsilon}_t^{(1)} \\ \boldsymbol{\varepsilon}_t^{(2)} \end{pmatrix}, \quad (5.9)$$

where $\boldsymbol{\Lambda}^{(1)}(\lambda)$ and $\boldsymbol{\Lambda}^{(2)}(\lambda)$ are partitioned $N_t^{(1)} \times 3$ and $N_t^{(2)} \times 3$ factor loading matrices respectively, while $\boldsymbol{\varepsilon}_t^{(1)}$ and $\boldsymbol{\varepsilon}_t^{(2)}$ are partitioned $N_t^{(1)} \times 1$ and $N_t^{(2)} \times 1$ error vectors, respectively, with the measurement covariance matrix between the observed and unobserved parts being written as follows

$$\text{Cov} \begin{pmatrix} \boldsymbol{\varepsilon}_t^{(1)} \\ \boldsymbol{\varepsilon}_t^{(2)} \end{pmatrix} = \begin{pmatrix} H_t^{(1)} & H_t^{(12)} \\ H_t^{(21)} & H_t^{(2)} \end{pmatrix}.$$

Consequently, at the times of the missing observations, where $\mathbf{y}_t^{(2)}$ is not observed, Equation (5.4) is replaced by

$$\mathbf{y}_t^{(1)} = \boldsymbol{\Lambda}^{(1)}(\lambda)\boldsymbol{\beta}_t + \boldsymbol{\varepsilon}_t^{(1)}, \quad \boldsymbol{\varepsilon}_t^{(1)} \sim N(0, \mathbf{H}^{(1)}), \quad (5.10)$$

where now the observation equation is $N_t^{(1)}$ -dimensional at time t . The Kalman filter proceeds exactly as in the standard case, provided that \mathbf{y}_t , $\boldsymbol{\Lambda}(\lambda)$ and \mathbf{H} are replaced by $\mathbf{y}_t^{(1)}$, $\boldsymbol{\Lambda}^{(1)}(\lambda)$ and $\mathbf{H}_t^{(1)}$ respectively at relevant time points. It is clear that the dimensionality of the observation equation evolves over time, but this does not affect

the validity of the filtering recursion. Once the state-space model parameters are estimated, $\hat{\theta} = \{\hat{\mu}, \hat{\Phi}, \hat{A}, \Lambda(\hat{\lambda}), \hat{Q}, \hat{H}\}$, we can obtain the missing observations in the vector of missing data $\mathbf{y}_t^{(2)}$ at any point in time $t = 1, \dots, T$. In this respect, each element j in the vector of missing yields $\mathbf{y}_t^{(2)}$ can be optimally predicted as follows

$$\mathbf{y}_t^{(2,j)} = \Lambda^{(2,j)}(\hat{\lambda})\hat{\mathbf{b}}_{t|t} + k \sqrt{\left(\Lambda^{(2,j)}(\hat{\lambda}) \hat{\mathbf{P}}_{t|t} \Lambda^{(2,j)}(\hat{\lambda})'\right)}, \quad (5.11)$$

where $\Lambda^{(2,j)}(\hat{\lambda})$ is the j row of the factor loading coefficient matrix and k is a scale parameter, which is set to a pre-specified value, and controls the deviation of the missing observation from its expected value.

5.5 Estimation of marginal yield curves for each country

We want to relate the evolution of the European sovereign yield curves under study to movements in European measures of liquidity and credit quality, study the relationships between the latent factors and these measures, and analyse their implications for monetary policy and portfolio risk management. There have been several attempts in the literature to explore the linkages between various macroeconomic factors such as inflation, measures for real economic activity, monetary policy instruments etc. and the yield curve (see for example, [Ang and Piazzesi \(2003\)](#), [Piazzesi \(2005\)](#), [Diebold et al. \(2006\)](#), [Balfoussia and Wickens \(2007\)](#), [Rudebusch and Wu \(2008\)](#), [Wright \(2011\)](#), among others). Nevertheless, to the best of our knowledge, so far, there have not been many studies in the literature that directly incorporate observable liquidity and credit quality variables into the state-space specification of the dynamic Nelson-Siegel (DNS) model as regression covariates. Several studies have shown that yield spreads can be explained by differences in credit quality and liquidity (see for example, [Duffie et al. \(2003\)](#), [Longstaff et al. \(2005\)](#), [Ericsson and Renault \(2006\)](#), [Beber et al. \(2009\)](#), among others). Therefore, the inclusion of credit quality and liquidity measures into the yield curve modelling specification can provide useful insight into the evolution of the yield curve and yield term premia.

Within this framework, we fit for each country in our sample, the dynamic Nelson-Siegel (DNS) model, augmented with common and country-specific macroeconomic and financial variables. Specifically, we employ the following variables: inflation for each country (INF_t), a liquidity measure for the European bond markets (LIQ_t), a credit quality measure for the European bond markets (CR_t), and major exchange rates against the Euro such as the US Dollar/Euro exchange rate (USD_t), the British Pound/Euro exchange rate (GBP_t) and the Japanese Yen/Euro exchange rate (JPY_t). The inclusion of observable variables in the state vector specification, however, does not only enable the study of the interaction between the macroeconomy and the yield curve but also removes the effect of these variables from the

errors of the fitted models, which will be used in the second stage of our cross-country analysis. We model the dynamic movements of L_t , S_t , C_t employing four alternative autoregressive specifications: AR(1), AR(2), VAR(1) and VAR(2). The best fitting model for each country is selected on the basis of information criteria. We assume that the transition error covariance matrix \mathbf{Q} is a diagonal matrix, whereas the measurement error covariance matrix \mathbf{H} is a non-diagonal first-order autoregressive covariance structure with heterogenous variances.

Table 5.5.1 reports results from Akaike’s information criterion (AIC) (Akaike, 1974) and Schwarz’s Bayesian information criterion (BIC) (Schwarz, 1978). We note that, with the exception of Italy, both information criteria agree on the selection of the best fitting model for each country. For the sake of parsimony, we follow the BIC criterion in the selection process. Therefore, an autoregressive model of order one, AR(1), is selected for the majority of the countries in our sample (more specifically, Italy, France and the UK). On the other hand, a vector autoregressive model of order one, VAR(1), is selected for Germany and a vector autoregressive model of order two, VAR(2), for Spain.

Table 5.5.1: Information Criteria results

Country	AIC Criterion				BIC Criterion			
	AR(1)	AR(2)	VAR(1)	VAR(2)	AR(1)	AR(2)	VAR(1)	VAR(2)
IT	-32 191.81	-24 013.91	-32207.70	-23 268.28	-31972.40	-23 778.83	-31 956.95	-22 970.51
DE	-47 887.49	-47 314.10	-47978.91	-35 758.84	-47 668.08	-47 079.02	-47728.15	-35 461.07
ES	-31 567.73	-29 254.50	-30 296.98	-31966.09	-31 348.32	-29 019.42	-30 046.23	-31668.32
FR	-46823.89	-39 690.03	-39 950.16	-43 592.55	-46604.48	-39 454.95	-39 699.40	-43 294.78
UK	-37823.17	-34 484.70	-35 710.73	-27 263.17	-37603.76	-34 249.62	-35 459.98	-26 965.40

This table reports results from the Akaike Information Criterion (AIC) and the Bayesian Information Criterion (BIC) for each country in four different model specifications: AR(1), AR(2), VAR(1), VAR(2). Bold values indicate minimum AIC and BIC estimates for each country across alternative model specifications.

After selecting the best fitting model for each country, we use the Kalman smoother to obtain optimal extractions of the latent level, slope and curvature factors. Figure 5.5.1 plots the estimated factors for each country together for the purpose of a comparative analysis. As expected, the level factor for all countries is positive ranging between 2.06 and 7.64. Consistent with the cross-sectional average of the raw yields, the level factor estimates of the peripheral countries have the highest average values, followed by those of France, the UK and Germany. The Spanish level factor also appears to be the most volatile. In contrast, the slope and curvature estimates assume both positive and negative values. The standard deviations of the slope factors for Italy, Spain and Germany are roughly the same but larger than those for France and the UK, while the standard deviations of the curvature factors differ considerably in size. The UK curvature factor volatility is 3.36 and almost double

in size when compared with the French curvature factor, which is the second most volatile among the curvature factor estimates.

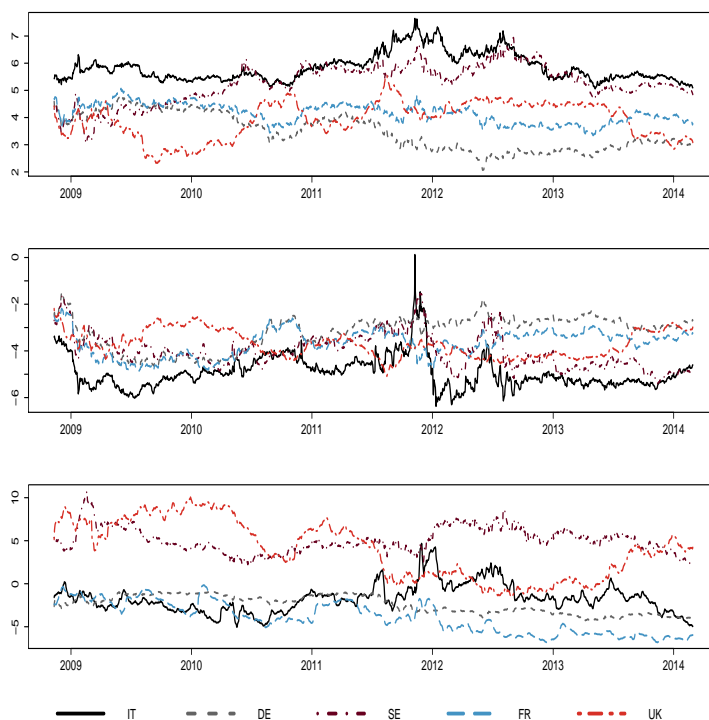


Figure 5.5.1: Estimates of the latent level (upper graph), slope (middle graph) and curvature (bottom graph) factors extracted using the Kalman smoother for Italy, Germany, Spain, France and the United Kingdom.

Figure 5.5.2 reports the cross-country correlation estimates for each factor. Interestingly, the correlation estimates of the level, slope and curvature for both the peripheral and the core Eurozone countries are large in size and positive. In contrast, the factor correlation estimates between any pair of a peripheral and a core Eurozone country are either positive and less pronounced or negative. The UK level factor is positively correlated with the Spanish and Italian level factors and negatively correlated with the German and French level factors. Additionally, the UK slope factor is negatively correlated with the slope factors of all of the Eurozone countries, while the curvature factor is negatively correlated with the curvature factors of the peripheral Eurozone countries and positively correlated with the curvature factors of the core Eurozone countries. As expected, the correlation estimates between the latent factors of the UK and those of the core Eurozone countries are much larger in size than the correlation estimates between the latent factors of the UK and those of the peripheral Eurozone countries possibly reflecting the common credit quality characteristics among these economies.

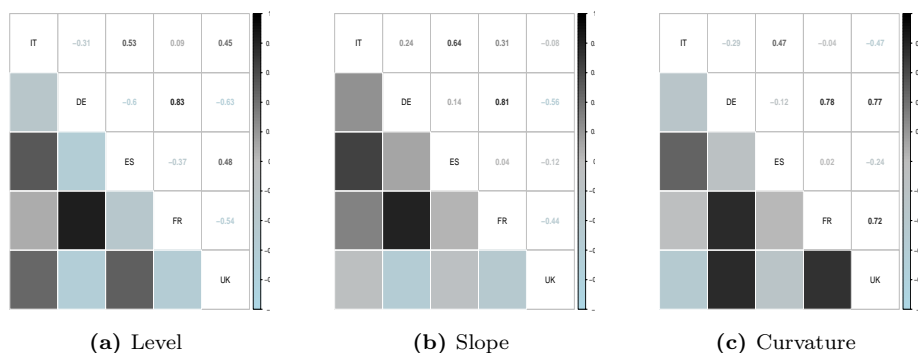


Figure 5.5.2: This figure presents cross-country correlation estimates for the latent level, slope and curvature factors extracted from the Kalman smoother.

To further investigate the linear dependence between the latent factor estimates of the countries under study, we perform a principal component analysis (PCA). Table 5.5.2 reports the principal component decomposition of the latent level, slope and curvature factor estimates. The proportion of the variation explained by the first principal component (PC1) for each of the latent factors is relatively small. Specifically, the first principal component (PC1) explains 58.50%, 48.36% and 54.18% of the variation of the level, slope and curvature factors, respectively. The total variation explained by the first two principal components (PC1 and PC2) is approximately 80% for each set of factors.

Table 5.5.2: Principal component analysis of the latent level, slope and curvature factors.

Panel A: Variation explained by each principal component (eigenvalues).

PCA	Level		Slope		Curvature	
	Variation explained (%)	Total variation explained (%)	Variation explained (%)	Total variation explained (%)	Variation explained (%)	Total variation explained (%)
PC1	58.50	58.50	48.36	48.36	54.18	54.18
PC2	24.38	82.88	29.09	77.45	27.84	82.02
PC3	10.05	92.93	13.26	90.71	10.61	92.63
PC4	5.58	98.51	6.29	97.00	4.31	96.94
PC5	1.49	100.00	3.00	100.00	3.06	100.00

Panel B: Country loadings (eigenvectors).

Country	Level		Slope		Curvature	
	PC1	PC2	PC1	PC2	PC1	PC2
IT	0.30	0.73	-0.36	0.59	-0.31	0.59
DE	-0.53	0.23	-0.56	-0.26	0.55	0.20
ES	0.45	0.29	-0.27	0.67	-0.20	0.67
FR	-0.44	0.58	-0.54	-0.25	0.49	0.40
UK	0.48	0.05	0.43	0.27	0.57	0.02

This table reports the principal component decomposition of the latent level, slope and curvature factor estimates. Panel A reports eigenvalues and the proportion of the total variation, expressed in percentages, in the latent factors explained by each principal component. Panel B reports the first and second eigenvectors or country loadings (denoted by PC1 and PC2) which correspond to the first and second eigenvalues, respectively.

The country loadings in the construction of the first and second principal components (the eigenvectors corresponding to the ranked eigenvalues), reported in Panel B of Table 5.5.2, are also of great interest because their corresponding signs and relative size can reveal important characteristics of the latent factor estimates and consequently of the yield curves of the countries in the sample. The loadings of PC1 for the level factors tend to be negatively signed for the core Eurozone countries and positively signed for the peripheral Eurozone countries and the UK, whereas those of PC2 are all positive. An increase in the PC1 of the level factors (keeping everything else constant) implies an increase in the level factors of the peripheral Eurozone countries and the UK and a decline in the level factors of the core Eurozone countries. This translates into a parallel upward shift in the yield curves of Italy, Spain and the UK and a parallel downward shift in the yield curves of Germany and France. In contrast, the loadings of PC1 for the slope factors are all negative, except for the UK, while the PC2 loadings show a sign pattern similar to that of the level PC1 loadings.

In addition, the PC1 loadings for the curvature factors appear positively signed for the core Eurozone countries and the UK and negatively signed for the peripheral Eurozone countries, whereas those of PC2 are all positive. We also note that Germany has the largest contribution to the construction of the first principal component (PC1) for the level and slope factors and the second largest contribution for the curvature factors as suggested by the respective loadings of -0.53, -0.56 and 0.55. This illustrates the country's leading role in explaining the variation of the latent level, slope and curvature factor estimates. The correlation analysis and the principal component analysis provide clear qualitative evidence that the sovereign yield curves of the peripheral and core Eurozone countries are negatively correlated, supporting the view that markets separate Eurozone members into two distinct groups of countries: the peripheral and the core Eurozone countries.¹³ The positive PC1 and PC2 country loadings for the UK also highlight the investors' tendency to differentiate between Eurozone and non-Eurozone countries.

5.5.1 Significance of coefficients

As explained, the dynamic interaction of the European sovereign yield curves with macroeconomic and financial variables, and in particular with liquidity and credit quality measures is one of the main concerns of this study. In this regard, significance testing and sensitivity analysis can provide useful insight into the response

¹³Saka et al. (2014), working with European sovereign credit default swap (CDS) data, also support the argument that investors separate Eurozone members into two distinct groups of countries (periphery versus core). They also argue that this discrimination was more intense before the implicit Outright Monetary Transactions (OMT) programme announcement on 26 July 2012.

of the yield curves to abrupt changes in the macroeconomic and financial environment. Table 5.5.3 reports the estimated coefficients and the corresponding p -values of macroeconomic and financial variables in the state specification of the dynamic Nelson-Siegel (DNS) model for each country.

Table 5.5.3: Estimates of macroeconomic and financial variables

Variables	Italy		Germany		Spain		France		United Kingdom	
	estimate	p -value	estimate	p -value						
Level : Inflation	0.0033	0.3884	0.1832	0.0000	-0.0018	0.4539	-0.0019	0.5586	0.0110	0.3115
Level : GBP	0.1409	0.1212	-1.4292	0.0007	0.0666	0.4633	0.1670	0.0098	-0.5275	0.1160
Level : JPY	0.0000	0.9674	0.0518	0.0000	-0.0004	0.2412	-0.0001	0.5935	-0.0028	0.0053
Level : USD	0.0078	0.8660	-2.3414	0.0000	0.0749	0.1441	-0.0464	0.1543	-0.4769	0.0031
Level : Liquidity	-0.0203	0.0637	0.3516	0.0000	-0.0280	0.0120	-0.0189	0.0205	0.0203	0.6223
Level : iTraxx	0.0003	0.0300	0.0045	0.0000	0.0004	0.0113	0.0001	0.3519	0.0007	0.1134
Slope : Inflation	-0.0020	0.7811	-0.0942	0.0000	0.0069	0.0608	0.0066	0.0721	-0.0177	0.1073
Slope : GBP	-0.1767	0.3033	0.6870	0.0049	-0.1879	0.1940	-0.1011	0.1749	-0.3627	0.2856
Slope : JPY	-0.0001	0.8257	-0.0285	0.0000	-0.0002	0.7088	-0.0001	0.6802	0.0010	0.3171
Slope : USD	0.1318	0.1306	1.2250	0.0000	0.1764	0.0300	0.0596	0.1128	0.1345	0.4070
Slope : Liquidity	-0.0398	0.0545	-0.1719	0.0000	-0.0054	0.7627	0.0143	0.1306	-0.0926	0.0264
Slope : iTraxx	0.0003	0.2726	-0.0028	0.0000	0.0003	0.1659	0.0000	0.8780	-0.0003	0.5022
Curvature : Inflation	0.0151	0.2889	-0.0280	0.0000	-0.0071	0.3083	-0.0197	0.0345	0.0340	0.1710
Curvature : GBP	0.6810	0.0444	-0.0560	0.5602	0.4766	0.0786	-0.1247	0.5104	1.4403	0.0652
Curvature : JPY	0.0007	0.5813	-0.0002	0.4450	-0.0014	0.1414	-0.0008	0.2827	0.0045	0.0486
Curvature : USD	0.1356	0.4271	-0.0293	0.5307	-0.1425	0.3483	0.1085	0.2480	0.1928	0.6039
Curvature : Liquidity	-0.0897	0.0291	-0.0323	0.0046	0.0181	0.5814	0.0492	0.0380	0.2674	0.0046
Curvature : iTraxx	0.0016	0.0008	0.0002	0.1084	0.0001	0.8249	-0.0002	0.4771	-0.0031	0.0024

This table reports the estimated coefficients of macroeconomic and financial variables and the corresponding p -values for each country in the sample.

At first glance we note that the macroeconomic and financial variables appear highly significant at 5% level for Germany, especially in the latent level and slope specification. In contrast, the significance of these variables for the peripheral Eurozone countries, France and the UK is less pronounced at the same confidence level. The liquidity and credit quality measures appear sporadically significant in the latent factor specification of these countries. In particular, the liquidity variable is negative and significant for the curvature factor, while the iTraxx index is positive and significant in both the level and the curvature factor for Italy. In this respect, an increase in the liquidity proxy (widening of the 3m Eurepo-Euribor spread) results in a decline in the curvature factor, which primarily affects the medium-term interest rates.

In contrast, an increase in the iTraxx index, which implies greater credit risk in the European bond markets, tilts the yield curve upward. In addition, the liquidity coefficient is negatively signed whereas the credit coefficient is positively signed and both are significant at 5% in the Spanish level factor specification. Therefore, a decline in liquidity in the European bond markets induces a parallel downward shift, while an increase of the iTraxx index tends to cause a parallel upward shift in

the Spanish yield curve. The liquidity and credit proxies are also significant at 5% in the specification of almost all latent factors for Germany. Moreover, the liquidity proxy appears significant for the French level and curvature factors as well as the UK slope and curvature factors, while the credit proxy is significant only for the UK curvature factor.

5.5.2 Sensitivity analysis

The impact of a change in the liquidity (3-month Euribor-Eurepo spread) and credit (iTraxx index) quality measures on the term structure of sovereign yields can be assessed through a sensitivity analysis. Table 5.5.4 reports the change, measured in basis points, in the term structure of average interest rates for each country in response to a two standard deviation increase in the average value of liquidity and credit measures, respectively. As shown in Table 5.5.4, a two standard deviation increase in the liquidity proxy reduces the yields across all maturities for Italy, Germany and Spain, while having a positive effect on the short-term and medium-term French yields and a negative effect on the long-term yields, thus reducing the slope of the French yield curve.

On the other hand, a liquidity shock has a negative effect on the short-term UK rates and a positive effect on the medium-term and long-term UK rates, thus increasing the slope of the yield curve. In addition, the German yield curve is the most sensitive to liquidity changes. On average, a two standard deviation liquidity shock reduces the German yields by 4.34 basis points, while the impact on Italian and Spanish yields is 3.58 and 1.92 basis points, respectively. It can also be seen that a liquidity shock affects more heavily the short-end part of the Italian and Spanish yield curves, whereas the German medium-term yields are more sensitive to a shock in liquidity than corresponding short-term and long-term yields. On the other hand, the French and UK yield curves seem to be less sensitive to liquidity shocks. On average, French and UK yields are expected to increase by 0.22 and 0.94 basis points, respectively.

In contrast, a two standard deviation shock in the credit quality measure is expected to have a positive impact on the average Spanish, Italian and French yields and a negative impact on the German and UK yields. Italian and Spanish short-term yields are more sensitive to credit measure shocks than longer-term yields. The French yields are less sensitive to a two standard deviation change in the average value of the credit quality measure. On the other hand, the German yields are expected to decline on average by 1.68 basis points. However, a credit shock tends to have a negative impact on the short and medium-term yields and a positive impact on the longer-term yields. The UK yields are also expected to decline on average by

1.1 basis points in response to a two standard deviation change in the credit quality measure.

The third column in Table 5.5.4 reports the changes in the term structure of average sovereign yields that are caused by a simultaneous two standard deviation increase in both liquidity and credit quality measures. It essentially combines the first two columns of Table 5.5.4. As expected, the German yields are the most sensitive to simultaneous changes in liquidity and credit quality measures, which yield an average decline of approximately 6 basis points in the term structure of interest rates. The medium-term German rates respond to these changes more than the short-term and long-term rates.

The Spanish and Italian yields are also sensitive to abrupt changes in liquidity and credit quality measures. However, a simultaneous two standard deviation increase in these measures raises the average yields by 2.76 and 1.68 basis points, respectively. In contrast, French and UK yields are less sensitive to these changes. French yields are expected to increase on average by 0.29 basis points whereas UK yields to decline by 0.17 basis points.

Table 5.5.4: Sensitivity analysis

Maturity	Liquidity shock					Credit shock					Combined shock				
	IT	DE	ES	FR	UK	IT	DE	ES	FR	UK	IT	DE	ES	FR	UK
12	-4.28	-0.20	-2.63	0.30	-4.52	5.04	-0.42	6.23	0.36	2.41	0.76	-0.62	3.60	0.65	-2.12
24	-4.62	-3.43	-2.42	0.84	-3.10	6.30	-2.73	5.86	-0.03	1.00	1.68	-6.16	3.44	0.81	-2.10
36	-4.63	-5.10	-2.24	0.99	-1.87	6.73	-3.70	5.54	-0.18	-0.13	2.10	-8.80	3.30	0.81	-2.00
48	-4.48	-5.85	-2.10	0.94	-0.82	6.73	-3.91	5.26	-0.22	-1.02	2.25	-9.76	3.16	0.72	-1.84
60	-4.25	-6.07	-1.98	0.79	0.08	6.50	-3.71	5.01	-0.19	-1.70	2.25	-9.78	3.03	0.60	-1.63
72	-4.00	-6.00	-1.88	0.61	0.84	6.17	-3.30	4.80	-0.14	-2.22	2.17	-9.30	2.91	0.48	-1.37
84	-3.76	-5.77	-1.81	0.43	1.50	5.82	-2.81	4.61	-0.07	-2.58	2.06	-8.58	2.81	0.36	-1.09
96	-3.53	-5.48	-1.74	0.26	2.05	5.47	-2.30	4.45	-0.01	-2.82	1.93	-7.77	2.70	0.25	-0.77
108	-3.33	-5.16	-1.69	0.10	2.52	5.15	-1.80	4.30	0.05	-2.96	1.81	-6.96	2.61	0.15	-0.44
120	-3.15	-4.84	-1.65	-0.04	2.91	4.85	-1.34	4.18	0.11	-3.00	1.70	-6.18	2.52	0.07	-0.09
180	-2.53	-3.59	-1.56	-0.52	4.06	3.81	0.38	3.74	0.30	-2.35	1.28	-3.20	2.18	-0.21	1.71
240	-2.19	-2.83	-1.57	-0.78	4.39	3.23	1.37	3.50	0.41	-0.97	1.05	-1.46	1.93	-0.37	3.42
360	-1.84	-2.06	-1.64	-1.04	4.17	2.64	2.39	3.27	0.52	1.99	0.80	0.34	1.63	-0.52	6.17
Mean	-3.58	-4.34	-1.92	0.22	0.94	5.26	-1.68	4.67	0.07	-1.10	1.68	-6.02	2.76	0.29	-0.17

This table reports the change, measured in basis points, in the term structure of average sovereign yields for each country in our sample that is caused by a positive shock (2 standard deviation increase) in the liquidity (Liquidity shock column) and credit quality measures (Credit shock column) as well as by a shock in both liquidity and credit quality measures simultaneously (Combined shock column).

It is also of great interest to investigate the impact of liquidity and credit quality shocks on the yield spreads of European sovereign bonds and their relative importance across the term structure. Within this framework, we can directly relate changes in the European liquidity and credit quality measures to changes in the

sovereign yield spreads and quantify their effects. Table 5.5.5 reports the changes in the spreads, at selected maturities, of the European sovereign yields that result from a two standard deviation increase in the liquidity and credit quality measures as well as from a shock in both measures simultaneously. A negative sign indicates a narrowing in the yield spread of the corresponding sovereign bonds, while a widening in the yield spread is accompanied by a positive sign.

Table 5.5.5: Cross-country sensitivity analysis

<i>Panel A: Liquidity shock</i>										
Maturity	IT-DE	IT-ES	IT-FR	IT-UK	DE-ES	DE-FR	DE-UK	ES-FR	ES-UK	FR-UK
12	-4.08	1.65	-4.57	0.25	-2.43	0.50	-4.32	-2.92	1.90	4.82
36	0.47	2.39	-5.62	-2.76	2.86	6.09	3.23	-3.23	-0.37	-2.86
60	1.82	2.27	-5.04	-4.32	4.09	6.86	6.15	-2.77	-2.06	-0.72
120	1.69	1.50	-3.11	-6.06	3.19	4.80	7.75	-1.61	-4.56	2.95
240	0.65	0.62	-1.41	-6.58	1.27	2.06	7.23	-0.79	-5.96	5.17
360	0.22	0.20	-0.80	-6.02	0.41	1.01	6.23	-0.60	-5.82	5.22

<i>Panel B: Credit shock</i>										
Maturity	IT-DE	IT-ES	IT-FR	IT-UK	DE-ES	DE-FR	DE-UK	ES-FR	ES-UK	FR-UK
12	5.46	1.19	4.68	2.63	6.65	0.77	2.82	5.87	3.82	1.29
36	10.43	-1.20	6.92	6.86	9.24	3.52	3.57	5.72	5.67	0.05
60	10.21	-1.48	6.69	8.20	8.72	3.52	2.01	5.20	6.72	-1.51
120	6.19	-0.67	4.74	7.86	5.52	1.45	-1.67	4.07	7.18	-3.11
240	1.86	0.27	2.82	4.21	2.13	-0.96	-2.35	3.09	4.47	-1.39
360	0.25	0.63	2.12	0.65	0.88	-1.87	-0.40	2.75	1.28	1.47

<i>Panel C: Combined shock</i>										
Maturity	IT-DE	IT-ES	IT-FR	IT-UK	DE-ES	DE-FR	DE-UK	ES-FR	ES-UK	FR-UK
12	1.38	2.84	0.11	2.88	4.22	1.27	-1.50	2.95	5.72	2.77
36	10.91	1.19	1.30	4.11	12.10	9.61	6.80	2.49	5.30	-2.81
60	12.03	0.78	1.65	3.88	12.82	10.38	8.16	2.43	4.66	-2.23
120	7.88	0.82	1.63	1.79	8.70	6.25	6.08	2.46	2.62	-0.16
240	2.51	0.89	1.41	-2.37	3.39	1.09	4.88	2.30	-1.48	3.78
360	0.46	0.83	1.32	-5.37	1.29	-0.86	5.83	2.15	-4.54	6.69

This table reports the change, measured in basis points, in the spreads of the European sovereign yields, at selected maturities, which results from a positive shock (2 standard deviation increase) in the liquidity (Panel A) and credit quality measures (Panel B) as well as from a shock in both measures simultaneously (Panel C).

We note that the yield spreads between the German bonds and the bonds of the peripheral countries rise in response to a two standard deviation increase in the liquidity or credit quality measures (with the exception of a liquidity shock in the 12-month spread). The 36-month and 60-month yield spreads are the most sensitive to these changes. A liquidity shock positively affects the German-French and German-UK spreads (with the exception of a liquidity shock in the 12-month German-UK spread), while a credit shock raises the spreads of the short-term and medium-term bonds and reduces the spreads of the long-term bonds. Moreover, the spread of the Italian-Spanish yields widens because Italian yields are more sensitive and

exhibit a greater decline in response to a two standard deviation increase in the liquidity measure than Spanish yields. The impact of a credit shock on the Italian-Spanish yield spreads varies across maturities. Short-term and long-term spreads are positively related to changes in the credit quality measure, whereas medium-term spreads are negatively related to it. Moreover, the spreads between the yields of the peripheral Eurozone countries and those of France and the UK are also negatively related to a liquidity shock and positively related to a credit shock, possibly reflecting the fact that the credit quality of the French and the UK economy is superior to that of the peripheral Eurozone countries. The behaviour of French-UK yield spreads is also mixed. Short-term and long-term spreads tend to rise, while medium-term spreads tend to decline in response to an increase in the liquidity or credit quality measures.

5.6 Covariance regression

In this Section, we employ the covariance regression model of [Hoff and Niu \(2012\)](#), which parametrises the covariance matrix of a multivariate response vector as a parsimonious quadratic function of explanatory variables, to model the cross-country covariance structure of sovereign yields, at selected maturities, using country-specific liquidity (bid-ask yield spreads) and credit quality (credit default swap (CDS) spreads) measures as explanatory variables in the regression structure. The proposed analysis provides a simple and flexible way of relating the heteroscedasticity of European sovereign yields, at certain maturities, to country-specific liquidity and credit quality measures and assessing their impact and relative importance in explaining the behaviour of the covariance structure over-time. It also provides a distinct way to quantify the effects of country-specific liquidity and credit shocks on the linear dependence between European sovereign yields and analyse their implications for policy and portfolio management.

5.6.1 Covariance regression model

The covariance regression model of [Hoff and Niu \(2012\)](#) proposes a parsimonious way to parametrise the covariance structure of a multivariate response vector as a function of explanatory variables. Let $\mathbf{y} \in \mathbb{R}^p$ be a random multivariate response vector and $\mathbf{x} \in \mathbb{R}^q$ be a vector of explanatory variables. [Hoff and Niu \(2012\)](#) propose a simple and flexible method for modelling and estimating the covariance matrix $\Sigma_x = \text{Cov}[\mathbf{y}|\mathbf{x}]$, the conditional covariance of \mathbf{y} given \mathbf{x} . In its simplest form, Σ_x can be expressed as

$$\Sigma_x = \Psi + \mathbf{B}\mathbf{x}\mathbf{x}^T\mathbf{B}^T, \quad (5.12)$$

where Ψ is a $p \times p$ positive-definite matrix and \mathbf{B} is a $p \times q$ matrix of coefficients. Therefore, the resulting covariance function is positive-definite for all values of \mathbf{x}

because the covariance is equal to a “baseline” covariance matrix Ψ plus a $p \times p$ positive-definite rank-1 matrix that depends on \mathbf{x} . Hoff and Niu (2012) also show that the covariance regression model has a random-effects model representation. The random-effects representation for a rank-1 covariance regression model, given observed data $\mathbf{y}_1, \dots, \mathbf{y}_t$, can be written as

$$\mathbf{y}_t = \boldsymbol{\mu}_{\mathbf{x}_t} + \gamma_t \times \mathbf{B}\mathbf{x}_t + \boldsymbol{\varepsilon}_t, \quad (5.13)$$

where $E[\boldsymbol{\varepsilon}_t] = \mathbf{0}$, $\text{Cov}[\boldsymbol{\varepsilon}_t] = \Psi$, $E[\gamma_t] = 0$, $\text{Var}[\gamma_t] = 1$ and $E[\gamma_t \times \boldsymbol{\varepsilon}_t] = \mathbf{0}$. The covariance matrix for \mathbf{y}_t given \mathbf{x}_t can then be derived as

$$\begin{aligned} E[(\mathbf{y}_t - \boldsymbol{\mu}_{\mathbf{x}_t})(\mathbf{y}_t - \boldsymbol{\mu}_{\mathbf{x}_t})^T] &= E[\gamma_t^2 \mathbf{B}\mathbf{x}_t\mathbf{x}_t^T\mathbf{B}^T + \gamma_t(\mathbf{B}\mathbf{x}_t\boldsymbol{\varepsilon}_t^T + \boldsymbol{\varepsilon}_t^T\mathbf{x}_t^T\mathbf{B}^T) + \boldsymbol{\varepsilon}_t\boldsymbol{\varepsilon}_t^T] \\ &= \mathbf{B}\mathbf{x}_t\mathbf{x}_t^T\mathbf{B}^T + \Psi \\ &= \Sigma_{\mathbf{x}_t}. \end{aligned} \quad (5.14)$$

The model in Equation (5.13) can also be represented as a factor analysis model and expressed as

$$\begin{pmatrix} y_{1,t} - \mu_{x_{1,t}} \\ \vdots \\ y_{p,t} - \mu_{x_{p,t}} \end{pmatrix} = \gamma_t \times \begin{pmatrix} \mathbf{b}_1^T \mathbf{x}_t \\ \vdots \\ \mathbf{b}_p^T \mathbf{x}_t \end{pmatrix} + \begin{pmatrix} \varepsilon_{1,t} \\ \vdots \\ \varepsilon_{p,t} \end{pmatrix}, \quad (5.15)$$

where $\{\mathbf{b}_1, \dots, \mathbf{b}_p\}$ denote the rows of \mathbf{B} . The latent factor γ_t essentially describes the additional unit-level variability beyond that represented by the error term $\boldsymbol{\varepsilon}_t$, while the vectors $\{\mathbf{b}_1, \dots, \mathbf{b}_p\}$ describe how this additional variability is shared across the p different response vectors. For example, large values of \mathbf{b}_j indicate large heteroscedasticity in y_j as a function of \mathbf{x} . Additionally, the direction of vectors \mathbf{b}_j and \mathbf{b}_k determines the direction of the linear dependence between y_j and y_k , i.e. whether y_j and y_k are positively or negatively correlated.

5.6.2 Parameter estimation via the EM-algorithm

Given the random-effects representation of the model, described in the previous Section, Hoff and Niu (2012) show that parameter estimation can be executed using maximum likelihood estimation via the EM-algorithm.¹⁴ The maximum likelihood estimation via the EM-algorithm relies on the conditional distribution of $\{\gamma_1, \dots, \gamma_T\}$

¹⁴Hoff and Niu (2012) also show that model parameters can be estimated using a Bayesian setting via the Gibbs sampler. In this study, we present only the maximum likelihood estimation procedure via the EM-algorithm, which is also employed to estimate model parameters in the empirical part of this study.

given $\{\mathbf{Y}, \mathbf{X}, \Psi, \mathbf{B}\}$. Consider response data $\mathbf{Y} = (\mathbf{y}_1^T, \dots, \mathbf{y}_T^T)$ observed under conditions $\mathbf{X} = (\mathbf{x}_1^T, \dots, \mathbf{x}_T^T)$. Under the assumption that all error terms are normally distributed, that is

$$\begin{aligned}\gamma_1, \dots, \gamma_T &\stackrel{\text{i.i.d.}}{\sim} \text{normal}(0, 1), \\ \varepsilon_1, \dots, \varepsilon_T &\stackrel{\text{i.i.d.}}{\sim} \text{multivariate normal}(\mathbf{0}, \Psi), \\ \mathbf{y}_t &= \boldsymbol{\mu}_{x_t} + \gamma_t \times \mathbf{B}\mathbf{x}_t + \varepsilon_t,\end{aligned}$$

the conditional distribution of $\{\gamma_t, \dots, \gamma_n\}$ given $\{\mathbf{Y}, \mathbf{X}, \Psi, \mathbf{B}\}$ can be derived as

$$\begin{aligned}\{\gamma_t | \mathbf{Y}, \mathbf{X}, \Psi, \mathbf{B}\} &\sim \text{normal}(m_t, v_t), \text{ where} \\ v_t &= (1 + \mathbf{x}_t^T \mathbf{B}^T \Psi^{-1} \mathbf{B}\mathbf{x}_t)^{-1}, \\ m_t &= v_t (\mathbf{y}_t - \boldsymbol{\mu}_{x_t})^T \Psi^{-1} \mathbf{B}\mathbf{x}_t.\end{aligned}$$

The EM-algorithm maximises the expected value of the complete data log-likelihood, $l(\mathbf{A}, \mathbf{B}, \Psi) = \log p(\mathbf{Y} | \mathbf{A}, \mathbf{B}, \Psi, \mathbf{X}, \mathbf{x})$, iteratively.¹⁵ The log-likelihood, derived from the multivariate normal density, is

$$l(\mathbf{A}, \mathbf{B}, \Psi) = -\frac{1}{2} \left[T p \log(2\pi) + T \log |\Psi| + \sum_{t=1}^T (\mathbf{y}_t - [\mathbf{A} + \gamma_t \mathbf{B}]\mathbf{x}_t)^T \Psi^{-1} (\mathbf{y}_t - [\mathbf{A} + \gamma_t \mathbf{B}]\mathbf{x}_t) \right]. \quad (5.16)$$

The EM-algorithm proceeds as follows. Given current estimates $(\hat{\mathbf{A}}, \hat{\mathbf{B}}, \hat{\Psi})$ of $(\mathbf{A}, \mathbf{B}, \Psi)$, the first step of the EM-algorithm computes, $m_t = E[\gamma_t | \hat{\mathbf{A}}, \hat{\mathbf{B}}, \hat{\Psi}, \mathbf{y}_t]$ and $v_t = \text{Var}[\gamma_t | \hat{\mathbf{A}}, \hat{\mathbf{B}}, \hat{\Psi}, \mathbf{y}_t]$, which are then plugged into the likelihood in Equation (5.16), yielding

$$\begin{aligned}E[l(\mathbf{A}, \mathbf{B}, \Psi) | \hat{\mathbf{A}}, \hat{\mathbf{B}}, \hat{\Psi}] \\ = -\frac{1}{2} \left[T p \log(2\pi) + T \log |\Psi| + \sum_{t=1}^T E[(\hat{\mathbf{e}}_t - \gamma_t \mathbf{B}\mathbf{x}_t)^T \mathbf{A}^{-1} (\hat{\mathbf{e}}_t - \gamma_t \mathbf{B}\mathbf{x}_t) | \hat{\mathbf{A}}, \hat{\mathbf{B}}, \hat{\Psi}] \right],\end{aligned} \quad (5.17)$$

¹⁵The matrix \mathbf{A} denotes the coefficient matrix of the mean function. Hoff and Niu (2012) assume that the mean function is linear, i.e. $\boldsymbol{\mu}_x = \mathbf{A}\mathbf{x}$, using the same regressors as in the covariance function. For ease of presentation, we follow the notation of Hoff and Niu (2012) in the rest of this Section. Note, that the heteroscedasticity in the response vector is modelled separately from the mean in the empirical part of this Section.

where $\hat{\mathbf{e}}_t = \mathbf{y}_t - \hat{\mathbf{A}}\mathbf{x}_t$ and

$$\begin{aligned} & \mathbb{E}[(\hat{\mathbf{e}}_t - \gamma_t \mathbf{B}\mathbf{x}_t)^T \Psi^{-1} (\hat{\mathbf{e}}_t - \gamma_t \mathbf{B}\mathbf{x}_t) | \hat{\mathbf{A}}, \hat{\mathbf{B}}, \hat{\Psi}] \\ &= (\hat{\mathbf{e}}_t - m_t \mathbf{B}\mathbf{x}_t)^T \Psi^{-1} (\hat{\mathbf{e}}_t - m_t \mathbf{B}\mathbf{x}_t) + v_t \mathbf{x}_t^T \mathbf{B}^T \Psi^{-1} \mathbf{B}\mathbf{x}_t \\ &= (\hat{\mathbf{e}}_t - m_t \mathbf{B}\mathbf{x}_t)^T \Psi^{-1} (\hat{\mathbf{e}}_t - m_t \mathbf{B}\mathbf{x}_t) + s_t \mathbf{x}_t^T \mathbf{B}^T \Psi^{-1} \mathbf{B}\mathbf{x}_t s_t, \end{aligned}$$

with $s_t = v_t^{1/2}$. The second step of the EM-algorithm is to maximise the expected log-likelihood. Following Hoff and Niu (2012), we construct the $2T \times 2q$ matrix $\tilde{\mathbf{X}}$ whose t -th row is $(\mathbf{x}_t^T, m_t \mathbf{x}_t^T)$ and whose $(T+t)$ -th row is $(\mathbf{0}_q^T, s_t \mathbf{x}_t^T)$ and the $2T \times p$ matrix $\tilde{\mathbf{Y}}$ given by $(\mathbf{Y}^T, \mathbf{0}_{T \times p}^T)^T$. In this respect, the expected value of the complete data log-likelihood can be re-written as

$$\mathbb{E}[l(\mathbf{A}, \mathbf{B}, \Psi) | \hat{\mathbf{A}}, \hat{\mathbf{B}}, \hat{\Psi}] = -\frac{1}{2} \left[Tp \log(2\pi) + T \log |\Psi| + \text{tr} \left([(\tilde{\mathbf{Y}} - \tilde{\mathbf{X}}\tilde{\mathbf{C}}^T) [(\tilde{\mathbf{Y}} - \tilde{\mathbf{X}}\tilde{\mathbf{C}}^T)^T \Psi^{-1}] \right) \right], \quad (5.18)$$

with $\mathbf{C} = (\mathbf{A}, \mathbf{B})$. The EM-algorithm obtains the new values $(\check{\mathbf{A}}, \check{\mathbf{B}}, \check{\Psi})$ by maximising the expected log-likelihood. Given the fact that the expected log-likelihood has the same form as the log-likelihood for normal multivariate regression, the new values $(\check{\mathbf{A}}, \check{\mathbf{B}}, \check{\Psi})$ are given by

$$\begin{aligned} (\check{\mathbf{A}}, \check{\mathbf{B}}) &= \check{\mathbf{C}} = \tilde{\mathbf{Y}}^T \tilde{\mathbf{X}} (\tilde{\mathbf{X}}^T \tilde{\mathbf{X}})^{-1}, \\ \check{\Psi} &= \frac{1}{T} (\tilde{\mathbf{Y}} - \tilde{\mathbf{X}}\check{\mathbf{C}}^T)^T (\tilde{\mathbf{Y}} - \tilde{\mathbf{X}}\check{\mathbf{C}}^T). \end{aligned}$$

The procedure is repeated until convergence.

5.7 Covariance regression results

We work with the one-step ahead prediction errors obtained by applying the Kalman Filter to the state-space model defined in Section 5.4.1. Specifically, for each country $j = \{\text{Italy (IT), Germany (DE), Spain (ES), France (FR), United Kingdom (UK)}\}$ in our sample, the one-step ahead prediction errors $\boldsymbol{\varepsilon}_{j,t}$ can be obtained as follows

$$\boldsymbol{\varepsilon}_{j,t} = \mathbf{y}_{j,t} - \mathbb{E}(\mathbf{y}_{j,t} | \mathbf{Y}_{j,t-1}) = \mathbf{y}_{j,t} - \mathbf{\Lambda}(\hat{\lambda}_j) \hat{\boldsymbol{\beta}}_{j,t|t-1}, \quad (5.19)$$

where $\mathbf{y}_{j,t}$ is the vector of the observed yields, $\mathbf{y}_{j,t} = [y_{j,t}(\tau_1), \dots, y_{j,t}(\tau_N)]'$, $\mathbf{\Lambda}(\hat{\lambda}_j)$ is the estimated factor loading coefficient matrix and $\hat{\boldsymbol{\beta}}_{j,t|t-1}$ is the predicted mean of latent vector $\boldsymbol{\beta}_t$ for country j .

As explained, the focus in the second part of the empirical analysis is on relating the heteroscedasticity of European sovereign yields to country-specific liquidity and

credit quality measures. We work with the errors obtained from the estimated dynamic Nelson-Siegel (DNS) model for each country, and not with the raw yields for two main reasons. Firstly, we want to remove the temporal dependence from the observed yields and, hence, remove the effects of autocorrelation from the covariance regression results. Secondly, we want to remove the effects of country-specific macroeconomic and financial variables, as well as of broader measures of liquidity and credit quality, from the covariance regression results. Thus, the first part of the empirical analysis can also be viewed as a filtering stage for the second part of the covariance regression analysis.

After obtaining the errors for each country j , we rearrange them by maturity. Therefore, the response vector \mathbf{y}_t in Equation (5.13) represents a 5×1 vector where each element is a prediction error for each country j , maturity τ_i and time period t , i.e., $\mathbf{y}_t = [y_{1,t}(\tau_i), \dots, y_{5,t}(\tau_i)]'$. On the other hand, the vector of explanatory variables \mathbf{x}_t is a 10×1 vector that includes liquidity measures (bid-ask spreads), $x_{j,t}^s(\tau_i)$, and credit quality measures (credit default swap (CDS) spreads), $x_{j,t}^c(\tau_i)$, for each country j , maturity τ_i and time period t , i.e. $\mathbf{x}_t = [x_{1,t}^s(\tau_i), \dots, x_{5,t}^s(\tau_i), x_{1,t}^c(\tau_i), \dots, x_{5,t}^c(\tau_i)]'$. In this respect, the matrix \mathbf{B} in Equation (5.13) is a 5×10 matrix that describes how additional variability is manifested across the 5 different response variables.

Figure 5.7.1 highlights the statistical significance results, at 5% level, of the estimated coefficients of matrix \mathbf{B} in the covariance regression model in Equation (5.12) at 24, 60, 120, 240 and 360-month maturities.¹⁶ The selection of these maturities enables the study of the interaction between country-specific liquidity and credit quality measures and the covariation in the sovereign yields across the entire maturity spectrum (specifically, at short-term, medium-term and long-term maturities). The white cells in Figure 5.7.1 indicate significance of the corresponding coefficients at 5% level, while the black cells indicate insignificance at the same confidence level. Each country pair, displayed in Figure 5.7.1, corresponds to 1 of the 15 unique elements of the 5×5 covariance matrix Σ_x . For example, the IT-DE pair denotes the covariance between Italy and Germany, whereas pairs of the same country index, such as IT-IT, denote the variance of this particular country - in this particular case, the variance of prediction errors for Italy at the selected maturity. In addition, the second country index indicates the origin of the liquidity and credit quality explanatory variables. For example, the IT-DE cell that corresponds to the country-specific

¹⁶Ideally, we would have preferred to also include covariance regression results corresponding to the 12-month maturity, which is the shortest maturity period in our dataset. However, as shown in Section 5.3, more than half of the 12-month Spanish bid-ask spreads are missing and thus interpolated spreads could have significantly affected the covariance regression results at this specific maturity. As a result, in order to avoid incorrect inference and to maintain data consistency, we decided not to report covariance results for the 12-month maturity data.

liquidity measures (bid-ask spreads) in Figure 5.7.1a, denotes the statistical significance of the German bid-ask spreads on the covariation between Italian and German prediction errors.

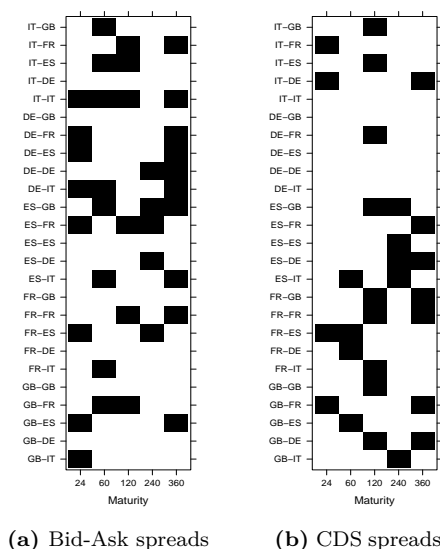


Figure 5.7.1: This figure demonstrates the significance of the estimated coefficients, at selected maturities, from the covariance regression model. White cells indicate significance at 5% level, while black cells indicate insignificance of the estimated coefficients at 5% level. Figure 5.7.1a presents the significance of country-specific liquidity measures (bid-ask spreads), whereas Figure 5.7.1b presents the significance of country-specific credit measures (credit default swap (CDS) spreads) in explaining the covariation for each individual pair. The first country of each pair represents the row, while the second country represents the column of matrix B in Equation (5.12). In addition, the second country indicates the origin of the country-specific explanatory variable in the covariance regression model.

At first glance, country-specific liquidity and credit quality measures appear highly significant in explaining the heteroscedasticity of the prediction errors across maturities. It seems that credit quality measures are slightly more significant than the corresponding liquidity measures. In total, the liquidity and credit quality coefficient estimates appear significant in the covariance regression specification 88 and 96 out of 125 times, respectively. The liquidity measures are slightly less significant at the 360-month maturity, whereas the credit quality measures are less significant at the 120-month maturity. Nevertheless, we cannot identify any distinct pattern between these measures across term structure maturities.

Furthermore, the German bid-ask spreads are significant in explaining the covariance for Italian-German, German-UK and French-German prediction errors, whereas the UK bid-ask spreads are significant in explaining the covariation for German-UK and French-UK prediction errors across all maturities. In general, the German bid-ask spreads tend to be the most significant liquidity measures followed by the UK bid-ask spreads. In contrast, the Italian and Spanish credit default swap (CDS) spreads

are the most significant country-specific credit variables. In particular, the Italian credit measures are important in explaining the covariation in the German-Italian errors, whereas the Spanish credit variables are significant in explaining the covariance of German-Spanish errors across term structure maturities.

Figure 5.7.2 plots the direction of the estimated coefficients in the covariance regression model. The white cells indicate negatively-signed coefficients, whereas the black cells indicate positively-signed coefficients. We note that the majority of the liquidity coefficients are negatively-signed, whereas the signs of the credit coefficients are almost equally split. Specifically, there are 75 coefficients corresponding to liquidity measures and 62 coefficients corresponding to credit measures that are negatively-signed (out of 125 in total for each set of variables) across all maturities, respectively. Nevertheless, the direction of the estimated coefficients cannot provide a clear view of the level and direction of the correlation as implied by the covariance regression model. To facilitate the analysis, we calculate time-series correlations for each country-pair across all maturities. Table 5.7.1 reports the time-series average correlation estimates.

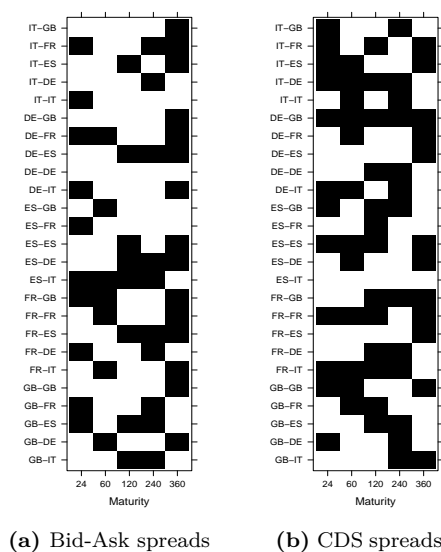


Figure 5.7.2: This figure demonstrates the direction of the estimated coefficients, at selected maturities, from the covariance regression model. The white cells indicate negatively-signed estimated coefficients, while the black cells indicate positively-signed estimated coefficients. Figure 5.7.2a presents the signs of the country-specific liquidity measures (bid-ask spreads) whereas Figure 5.7.2b presents the signs of the country-specific credit measures (credit default swap (CDS) spreads). The first country in each pair represents the row, while the second country represents the column of matrix B in Equation (5.12). In addition, the second country indicates the origin of the country-specific explanatory variable in the covariance regression model.

Table 5.7.1: Time-series average correlation estimates

Country	Maturity				
	24	60	120	240	360
IT-DE	-0.10	-0.17	0.39	0.75	0.25
IT-ES	0.35	0.46	0.64	0.28	0.63
DE-ES	-0.05	-0.16	0.07	0.01	-0.01
IT-FR	0.11	0.33	0.57	0.68	0.30
DE-FR	0.03	0.04	0.75	0.84	0.46
ES-FR	0.11	0.27	0.19	0.12	0.31
IT-UK	-0.01	-0.11	0.26	0.25	0.14
DE-UK	0.43	0.57	0.28	0.42	0.08
ES-UK	-0.16	-0.10	0.14	0.02	0.07
FR-UK	-0.39	-0.23	0.18	0.31	-0.01

This table reports the time-series average correlation estimates, at selected maturities, for each pair of countries as implied by the covariance regression model estimates.

We notice that the majority of time-series average correlation estimates are positive. The negative correlation estimates mainly correspond to 24 and 60-month maturities; however, these estimates turn positive for the majority of the pairs at 120, 240 and 360-month maturities. The correlation estimates between the peripheral Eurozone countries are all positive across the maturity spectrum. France is also positively correlated with the peripheral Eurozone countries and Germany across all maturities. In contrast, Germany is weakly correlated with Spain, while the German-Italian correlation is more pronounced across all maturities. In particular, the correlation between German and Italian prediction errors is negative at the 24 and 60-month maturities and positive at the 120, 240 and 360-month maturities, with the positive estimates being much more pronounced than the negative correlation estimates. The correlation estimates for the UK are mixed. The UK-German correlation is positive across all maturities reaching its highest level, 0.57, at 60-month maturity. On the other hand, the UK is negatively correlated with Italy, Spain and France at shorter maturities, i.e. at 24 and 60-month maturities, and positively correlated for longer maturities, i.e. at 120, 240 and 360-month maturities (with the exception of the UK-France correlation at 360-month maturity, which is negative and quite small).

To investigate the impact of country-specific liquidity and credit quality measures on the correlation structure of prediction errors, we re-estimate the covariance regression model in Equation (5.13) using either liquidity or credit quality measures as explanatory variables. Table 5.7.2 reports the time-series average correlation estimates at 24, 60, 120, 240 and 360-month maturities, respectively. The direction of the correlation coefficients implied by either liquidity or credit quality measures is almost identical across maturities. Similar to the regression results of the complete set in Table 5.7.1, the correlation estimates tend to be positively-signed across maturities for most of the country pairs under study. Moreover, the correlation estimates

in Table 5.7.2 do not differ significantly in magnitude indicating that country-specific liquidity and credit quality measures contribute to the covariation of the prediction errors to a similar extent.

Table 5.7.2: Time-series average correlation estimates

Country	Liquidity measures					Credit measures				
	24	60	120	240	360	24	60	120	240	360
IT-DE	-0.15	-0.16	0.44	0.80	0.22	-0.11	-0.13	0.44	0.71	0.25
IT-ES	0.36	0.50	0.68	0.25	0.61	0.37	0.41	0.63	0.26	0.61
DE-ES	-0.10	-0.18	0.16	0.01	-0.05	-0.05	-0.15	0.14	-0.02	-0.01
IT-FR	0.11	0.35	0.58	0.60	0.28	0.10	0.36	0.58	0.72	0.29
DE-FR	0.02	0.01	0.76	0.76	0.48	0.03	0.06	0.77	0.84	0.46
ES-FR	0.19	0.30	0.21	0.11	0.29	0.11	0.19	0.18	0.10	0.33
IT-UK	-0.03	-0.09	0.22	0.28	0.08	-0.01	-0.06	0.25	0.21	0.10
DE-UK	0.42	0.58	0.18	0.31	0.05	0.42	0.56	0.23	0.43	0.06
ES-UK	-0.31	-0.18	0.20	0.00	0.00	-0.14	-0.10	0.18	0.01	0.04
FR-UK	-0.50	-0.23	0.08	0.16	-0.04	-0.41	-0.20	0.18	0.31	-0.03

This table reports the time-series average correlation estimates, at selected maturities, for each pair of countries as implied by the covariance regression model estimates. The Liquidity measures column reports correlation estimates employing only country-specific liquidity measures (bid-ask spreads) as explanatory variables. The Credit measures column reports correlation estimates using only country-specific credit quality measures (cds spreads) as explanatory variables

Furthermore, the likelihood ratio test statistics and the corresponding p -values, reported in Table 5.7.3, clearly reject the restricted covariance regression models in favour of the unrestricted model where both country-specific credit quality and liquidity variables are employed in the covariance regression specification.

Table 5.7.3: Likelihood ratio test results

Maturity	Liquidity measures		Credit measures	
	LR-statistic	p -value	LR-statistic	p -value
24	1113.33	0.00	275.12	0.00
60	1307.23	0.00	657.37	0.00
120	1146.33	0.00	637.22	0.00
240	1190.20	0.00	905.90	0.00
360	456.90	0.00	292.02	0.00

This table reports likelihood ratio test results from the fit of alternative covariance regression models. The Liquidity measures column reports likelihood ratio statistics and the corresponding p -values from the fit of covariance regression models using country-specific liquidity measures as explanatory variables (restricted model) at 24, 60, 120, 240 and 360-month maturities. The Credit measures column reports likelihood ratio statistics and the corresponding p -values from the fit of covariance regression models using country-specific credit measures as explanatory variables (restricted model) at 24, 60, 120, 240 and 360-month maturities. The unrestricted covariance model uses both country-specific liquidity and credit quality measures as explanatory variables. All test statistics are Chi-square with 25 degrees of freedom.

5.7.1 Conditional covariance results: low and high-equity market volatility

So far the analysis has been concentrated on the unconditional behaviour of liquidity, credit quality and sovereign yields. In this Section, we attempt to understand how this relation is altered in the face of changes to the market environment. In particular, we analyse the behaviour of liquidity, credit quality and sovereign yields when equity markets are perceived to be volatile. The flight of capital out of equity markets and into fixed-income markets, especially during periods of elevated market volatility, is well-documented in the literature (see for example, [Connolly et al., 2005](#); [Underwood, 2009](#), among others). Following [Beber et al. \(2009\)](#), we use the VSTOXX index as a measure of perceived European equity market volatility. The VSTOXX index is constructed using implied option prices written on the Euro Stoxx 50 index and thus reflects market expectations of European equity market volatility. The VSTOXX index data are downloaded from Bloomberg. We proxy for equity market volatility by conditioning on periods where the VSTOXX index is above its time-series median.

Therefore, our conditional analysis entails estimating the covariance regression model in Equation (5.13) having conditioned the sample on periods of low-equity market volatility (calm period) and high-equity market volatility (stress period). Figure 5.7.1 plots the significance of country-specific liquidity and credit quality measures across both sub-periods. The credit default swap (CDS) variables appear slightly more significant than bid-ask spread variables in the calm period. In total, the credit quality measures appear significant at 5% level 79 out of 125 times, whereas the liquidity proxies are significant at 5% level 72 out of 125 times. The significance of explanatory variables in the covariance regression specification has altered in the crisis period. The significance of credit quality measures increased over this period. In particular, credit quality measures appear significant in explaining the covariation of the prediction errors 89 out of 125 times across maturities. In contrast, the significance of liquidity measures has lessened in the crisis period. In total, liquidity measures appear significant in the covariance regression model 65 out of 125 times across term structure maturities.

Moreover, the German bid-ask spreads are the most significant country-specific liquidity measures, whereas the Spanish credit default swap (CDS) spreads are the most significant country-specific credit quality measures in the calm period. In contrast, the Spanish bid-ask spreads and the UK credit default swap (CDS) data are the least significant liquidity and credit quality measures in this period, respectively. The Italian bid-ask spreads appear to be the most significant country-specific liquidity measures in the crisis period, while the French liquidity variables are the least

significant in the same period. Furthermore, the credit default swap (CDS) spreads of the peripheral Eurozone countries and Germany are the most significant country-specific credit proxies, while the French credit default swap (CDS) data are the least significant country-specific credit measures in the crisis period. In Figure 5.7.2, we also note that liquidity and credit quality measures tend to be more significant for the shorter-term yields than for the longer-term yields in the calm period. In contrast, the bid-ask spread variables are less significant for the shorter-term yields than for the longer-term yields in the crisis period, whereas the credit default swap (CDS) data appear less significant for the 360-month maturity and almost equally significant for the remaining maturities in the same period.

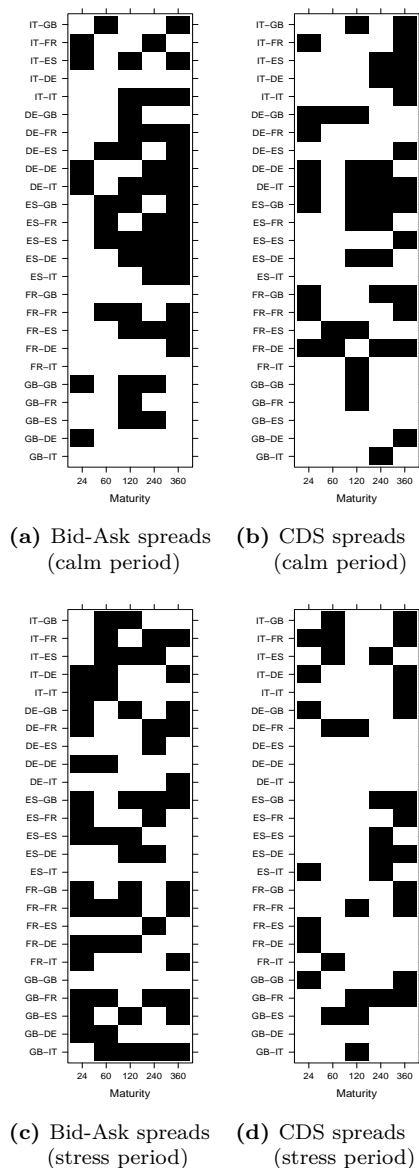


Figure 5.7.3: This figure demonstrates the significance of the estimated coefficients, at selected maturities, from the covariance regression model in calm and stress periods. White cells indicate significance at 5% level, while Black cells indicate insignificance of the estimated coefficient at 5% level. Figure 5.7.3a presents the significance of country-specific liquidity measures (bid-ask spreads), whereas Figure 5.7.3b presents the significance of country-specific credit measures (credit default swap (CDS) spreads) in explaining the covariation for each individual pair of countries in the calm period. Figure 5.7.3c presents the significance of country-specific liquidity measures (bid-ask spreads), whereas Figure 5.7.3d presents the significance of country-specific credit measures (credit default swap (CDS) spreads) in explaining the covariation for each individual pair of countries in the stress period. The first country of each pair represents the row, while the second country represents the column of matrix \mathbf{B} in Equation (5.12). In addition, the second country indicates the origin of the country-specific explanatory variable in the covariance regression model.

Table 5.7.4 reports the time-series average correlation estimates implied by the covariance regression model in both sub-periods. At first glance, we notice that the time-series average correlation estimates differ significantly in magnitude and direction for the majority of country pairs across both sub-periods. In particular, almost all correlation coefficients tend to be positively-signed and rather pronounced for the 120 and 240-month maturities in the low-equity volatility period. The largest positively-signed correlation coefficient in the calm period is 0.80 for the Italy-Spain and Italy-Germany country pairs at 120 and 240-month maturities, respectively. Most of the negatively-signed correlation estimates reported in the calm period correspond to the 24 and 60-month maturities with the France-UK pair at the 24-month maturity being the largest negative correlation coefficient. The correlation structure across maturities has altered in the high-equity volatility period. We notice that several of the correlation estimates have changed direction. In particular, 14 out of 50 correlation coefficients changed direction between the calm and the stress sub-period. Of these 14 correlation changes, 9 coefficients turned from positive to negative whereas 5 coefficients turned from negative to positive.

The 240-month maturity correlation coefficient for the Germany-France country pair, which is equal to 0.93, is the largest positively-signed correlation estimate in the stress period. In contrast, the correlation coefficient for the France-UK country pair is -0.25, which is the largest negatively-signed correlation estimate in the stress period. The correlation estimates for the peripheral Eurozone countries are positive across all maturities and sub-periods; however, the correlation estimates tend to be more pronounced in the calm period than in the stress period. The correlation between Germany and France is also positive and significant for most of the pairs analysed, especially for the medium and long-term maturities. The correlation between Germany and the peripheral Eurozone countries varies across maturities and sub-periods. Short-term correlations tend to be negative whereas medium and long-term correlations tend to be positive across both sub-periods. The majority of German-UK correlation coefficients tend to be positively signed and rather significant, while the correlations between the UK and the peripheral Eurozone countries as well as France vary across maturities and sub-periods.

Table 5.7.4: Time-series average correlation estimates

Country	Calm period					Stress period				
	24	60	120	240	360	24	60	120	240	360
IT-DE	0.00	-0.24	0.57	0.80	0.30	-0.16	-0.07	0.32	0.76	0.18
IT-ES	0.29	0.63	0.80	0.23	0.67	0.42	0.32	0.43	0.33	0.60
DE-ES	-0.15	-0.14	0.47	-0.03	-0.09	-0.02	-0.12	-0.16	0.02	0.00
IT-FR	-0.06	0.35	0.76	0.41	0.09	0.18	0.28	0.47	0.77	0.37
DE-FR	-0.20	0.02	0.73	0.50	0.28	0.18	0.06	0.75	0.93	0.53
ES-FR	0.10	0.43	0.53	0.10	0.14	0.17	0.06	-0.05	0.12	0.40
IT-UK	0.15	-0.27	0.35	0.43	0.25	-0.12	0.01	0.18	0.08	-0.03
DE-UK	0.45	0.62	0.48	0.60	0.25	0.42	0.49	-0.02	0.19	-0.11
ES-UK	-0.23	-0.26	0.29	0.06	0.08	-0.04	0.10	0.11	-0.01	0.03
FR-UK	-0.67	-0.22	0.40	0.21	-0.02	-0.24	-0.25	-0.01	0.24	-0.03

This table reports the time-series average correlation estimates, at selected maturities, for each pair of countries as implied by the covariance regression model estimates for calm and stress periods.

5.7.2 Covariance regression sensitivity analysis

The advantage of our modelling strategy is that we can quantify the effects on the sovereign yields from a shock in any of the country-specific liquidity and credit measures. In other words, we can assess the impact of country-specific liquidity and credit quality shocks not only on the yield curve of the country which experiences the shock but also on the yield curves of the remaining countries and, therefore, study the linkages between European sovereign yields and potential spillover effects. In this Section, we describe in detail the sensitivity analysis procedure, which is essentially based on the full state-space model representation. Denote the complete set of all country and maturity yields as \mathbf{Y}_t , where each element $y_{j,t}(\tau_i)$ represents a zero-coupon bond yield at maturity τ_i ($i = 1, \dots, N$) for country j ($j = 1, \dots, d$) at time t ($t = 1, \dots, T$):

$$\mathbf{Y}_t = \begin{pmatrix} y_{1,t}(\tau_1) & \dots & y_{d,t}(\tau_1) \\ \vdots & \vdots & \vdots \\ y_{1,t}(\tau_N) & \dots & y_{d,t}(\tau_N) \end{pmatrix}.$$

Denote by \mathbf{M}_t the set of the Nelson-Siegel term structure regression model of [Diebold et al. \(2008\)](#), where each element $f(\tau_i; \boldsymbol{\beta}_{j,t}, \boldsymbol{\theta}_j)$ is a 1×3 vector of the i -th row of the $\boldsymbol{\Lambda}(\lambda_j)$ $\boldsymbol{\beta}_{j,t}$ matrix, with $\boldsymbol{\beta}_{j,t}$ representing the vector of latent factors, $\boldsymbol{\Lambda}(\lambda_j)$ is the $N \times 3$ factor loadings matrix and $\boldsymbol{\theta}_j$ denotes the set of parameters for each country j . Also denote by $\boldsymbol{\Lambda}$ the set of all factor loading matrices $\boldsymbol{\Lambda}(\lambda_j)$. The resulting $N \times 3d$ \mathbf{M}_t and $\boldsymbol{\Lambda}$ matrices are given by:

$$\mathbf{M}_t = \begin{pmatrix} f(\tau_1; \boldsymbol{\beta}_{1,t}, \boldsymbol{\theta}_1) & \dots & f(\tau_1; \boldsymbol{\beta}_{d,t}, \boldsymbol{\theta}_d) \\ \vdots & \vdots & \vdots \\ f(\tau_N; \boldsymbol{\beta}_{1,t}, \boldsymbol{\theta}_1) & \dots & f(\tau_N; \boldsymbol{\beta}_{d,t}, \boldsymbol{\theta}_d) \end{pmatrix} \quad \text{and} \quad \boldsymbol{\Lambda} = \left(\boldsymbol{\Lambda}(\lambda_1), \dots, \boldsymbol{\Lambda}(\lambda_d) \right).$$

As explained in Section 5.4, the time-series dynamics of latent factors $\beta_{j,t} = [L_{j,t}, S_{j,t}, C_{j,t}]'$ for each country j are modelled as autoregressive processes augmented with observable variables. The total observation model with all countries and maturities can be written as follows

$$\begin{pmatrix} y_{1,t}(\tau_1) \\ \vdots \\ y_{1,t}(\tau_N) \\ \vdots \\ y_{d,t}(\tau_1) \\ \vdots \\ y_{d,t}(\tau_N) \end{pmatrix} = \begin{pmatrix} f(\tau_1; \beta_{1,t}, \theta_1) \\ \vdots \\ f(\tau_N; \beta_{1,t}, \theta_1) \\ \vdots \\ f(\tau_1; \beta_{d,t}, \theta_d) \\ \vdots \\ f(\tau_N; \beta_{d,t}, \theta_d) \end{pmatrix} + \begin{pmatrix} \varepsilon_{1,t}(\tau_1) \\ \vdots \\ \varepsilon_{1,t}(\tau_N) \\ \vdots \\ \varepsilon_{d,t}(\tau_1) \\ \vdots \\ \varepsilon_{d,t}(\tau_N) \end{pmatrix} + \begin{pmatrix} \zeta_{1,t}(\tau_1) \\ \vdots \\ \zeta_{1,t}(\tau_N) \\ \vdots \\ \zeta_{d,t}(\tau_1) \\ \vdots \\ \zeta_{d,t}(\tau_N) \end{pmatrix}, \quad (5.20)$$

where $\varepsilon_{j,t} = [\varepsilon_{j,t}(\tau_1), \dots, \varepsilon_{j,t}(\tau_N)]'$ and $\zeta_{i,t} = [\zeta_{i,t}(\tau_i), \dots, \zeta_{i,t}(\tau_i)]'$.

We assume that $\mathbb{E}[\varepsilon_{j,t} \varepsilon'_{l,t}] = 0 \forall j, l \text{ s.t. } j \neq l$, $\mathbb{E}[\zeta_{i,t} \zeta'_{l,t}] = 0 \forall i, l \text{ s.t. } i \neq l$ and $\mathbb{E}[\varepsilon_{j,t}(\tau_i) \zeta_{j,t}(\tau_i)] = 0 \forall j, i$. We also assume that

$$\begin{pmatrix} \varepsilon_{j,t}(\tau_1) \\ \vdots \\ \varepsilon_{j,t}(\tau_N) \end{pmatrix} \sim \mathbf{N}_N(\mathbf{0}, \mathbf{H}_j) \quad \text{and} \quad \begin{pmatrix} \zeta_{1,t}(\tau_i) \\ \vdots \\ \zeta_{d,t}(\tau_i) \end{pmatrix} \sim \mathbf{N}_d(\mathbf{0}, \Sigma_{i,t}),$$

where \mathbf{H}_j is the covariance matrix of the *transition errors* in the dynamic Nelson-Siegel model of Diebold et al. (2008), which is modelled as a non-diagonal first-order autoregressive covariance structure with heterogenous variances for each country j . In contrast, $\Sigma_{i,t}$ denotes the cross-country covariance structure of $\zeta_{i,t}$ errors at maturity τ_i . As shown above, $\Sigma_{i,t}$ is modelled as a parsimonious quadratic function of explanatory variables $\mathbf{x}_{i,t}$, that is

$$\Sigma_{i,t} = \Psi_i + \mathbf{B}_i \mathbf{x}_{i,t} \mathbf{x}_{i,t}^T \mathbf{B}_i^T.$$

Therefore, the distribution of $\varepsilon_{j,t}$ and $\zeta_{i,t}$ for all countries $j = 1, \dots, d$, maturities $\tau_i = \tau_1 \dots, \tau_N$, and time periods $t = 1, \dots, T$ can be written as

$$\begin{pmatrix} \varepsilon_{1,t}(\tau_1) \\ \vdots \\ \varepsilon_{1,t}(\tau_N) \\ \vdots \\ \varepsilon_{d,t}(\tau_1) \\ \vdots \\ \varepsilon_{d,t}(\tau_N) \end{pmatrix} \sim \mathbf{N}_{N \times d}(\mathbf{0}, \mathbf{H}_\varepsilon) \quad \text{and} \quad \begin{pmatrix} \zeta_{1,t}(\tau_1) \\ \vdots \\ \zeta_{d,t}(\tau_1) \\ \vdots \\ \zeta_{1,t}(\tau_N) \\ \vdots \\ \zeta_{d,t}(\tau_N) \end{pmatrix} \sim \mathbf{N}_{d \times N}(\mathbf{0}, \Sigma_{\zeta_t}),$$

where $\mathbf{H}_\varepsilon = \bigoplus_{j=1}^d \mathbf{H}_j$ and $\Sigma_{\zeta,t} = \bigoplus_{i=1}^N \Sigma_{i,t} = \bigoplus_{i=1}^N (\Psi_i + \mathbf{B}_i \mathbf{x}_{i,t} \mathbf{x}_{i,t}^T \mathbf{B}_i^T)$. To quantify the effects on the sovereign yields from a shock to any of the country-specific liquidity and credit quality measures in vector $\mathbf{x}_{i,t}$, we proceed as follows. Let $\tilde{\mathbf{y}}_t$ be the vector of observable sovereign yields sorted by country at each particular maturity τ_i at time t , that is

$$\tilde{\mathbf{y}}_t = \begin{pmatrix} y_{1,t}(\tau_1) \\ \vdots \\ y_{d,t}(\tau_1) \\ \vdots \\ y_{1,t}(\tau_N) \\ \vdots \\ y_{d,t}(\tau_N) \end{pmatrix} = \mathbf{R} \text{vec}(\mathbf{Y}_t) = \mathbf{R} \begin{pmatrix} y_{1,t}(\tau_1) \\ \vdots \\ y_{1,t}(\tau_N) \\ \vdots \\ y_{d,t}(\tau_1) \\ \vdots \\ y_{d,t}(\tau_N) \end{pmatrix}, \quad (5.21)$$

where \mathbf{R} is a permutation matrix that premultiplies and re-orders the vector of observed yields $\text{vec}(\mathbf{Y}_t)$ into the new $\tilde{\mathbf{y}}_t$ vector. We then proceed as follows:

Stage 1: Premultiply $\tilde{\mathbf{y}}_t$ by $\Sigma_{\zeta,t}^{-1/2}$ to obtain the new vector of transformed yields $\check{\mathbf{y}}_t$ in order to account for the cross-country dependence across the maturity spectrum:

$$\check{\mathbf{y}}_t = \Sigma_{\zeta,t}^{-1/2} \tilde{\mathbf{y}}_t = \Sigma_{\zeta,t}^{-1/2} \mathbf{R} \text{vec}(\mathbf{Y}_t).$$

Stage 2: Given the estimated parameters $\hat{\boldsymbol{\theta}}_1, \dots, \hat{\boldsymbol{\theta}}_d$, obtained from the Kalman-filter for each particular country j in Section 5.4, premultiply, using the permutation matrix \mathbf{R} , the matrix of factor loadings $\text{vec}(\boldsymbol{\Lambda})$ and the covariance matrix \mathbf{H}_ε by $\Sigma_{\zeta,t}^{-1/2}$ to obtain the corresponding transformed $\check{\boldsymbol{\Lambda}}_t$ and $\check{\mathbf{H}}_\varepsilon$, respectively:

$$\check{\boldsymbol{\Lambda}}_t = \Sigma_{\zeta,t}^{-1/2} \boldsymbol{\Lambda} = \Sigma_{\zeta,t}^{-1/2} \mathbf{R} \begin{pmatrix} \boldsymbol{\Lambda}(\hat{\lambda}_1) \\ \vdots \\ \boldsymbol{\Lambda}(\hat{\lambda}_d) \end{pmatrix} \quad \text{and} \quad \check{\mathbf{H}}_\varepsilon = \mathbf{R}^T \Sigma_{\zeta,t}^{-1/2} \mathbf{R} \mathbf{H}_\varepsilon \mathbf{R}^T (\Sigma_{\zeta,t}^{-1/2})^T \mathbf{R}.$$

Stage 3: Separate the transformed set of $\check{\mathbf{y}}_t$, $\check{\boldsymbol{\Lambda}}_t$ and $\check{\mathbf{H}}_\varepsilon$ into country specific components $\check{\mathbf{y}}_{j,t}$, $\check{\boldsymbol{\Lambda}}_t(\lambda_j)$ and $\check{\mathbf{H}}_j$ for each of the $j = 1, \dots, d$ countries:

$$\check{\mathbf{y}}_{j,t} = \begin{pmatrix} \check{y}_{j,t}(\tau_1) \\ \vdots \\ \check{y}_{j,t}(\tau_N) \end{pmatrix}, \quad \begin{pmatrix} \check{\boldsymbol{\Lambda}}_t(\lambda_1) \\ \vdots \\ \check{\boldsymbol{\Lambda}}_t(\lambda_d) \end{pmatrix} = \mathbf{R}^T \check{\boldsymbol{\Lambda}}_t \quad \text{and} \quad \check{\mathbf{H}}_\varepsilon = \begin{pmatrix} \check{\mathbf{H}}_1 & & \\ & \ddots & \\ & & \check{\mathbf{H}}_d \end{pmatrix},$$

where $\check{\mathbf{H}}_j$ is the subset of the $\check{\mathbf{H}}_\varepsilon$ matrix corresponding to country j .

Stage 4: Given the set of transformed $\check{\mathbf{y}}_{j,t}$, $\check{\mathbf{\Lambda}}_t(\lambda_j)$ and $\check{\mathbf{H}}_j$ we run, separately for each case, the Kalman-filter keeping all static parameters fixed to obtain the new set of latent factors $\check{\boldsymbol{\beta}}_{j,t} = [\check{L}_{j,t}, \check{S}_{j,t}, \check{C}_{j,t}]'$ for each country j .

State 5: Given the new set of latent factors $\check{\boldsymbol{\beta}}_{j,t} = [\check{L}_{j,t}, \check{S}_{j,t}, \check{C}_{j,t}]'$ and static parameter estimates $\hat{\boldsymbol{\theta}}_j$ we can obtain the predicted $\check{\mathbf{y}}_t$ yields for each country j as follows:

$$\mathbf{y}_{j,t}^* = \mathbb{E}(\check{\mathbf{y}}_{j,t} | \check{\mathbf{y}}_{j,t-1}) = \check{\mathbf{\Lambda}}(\lambda_j) \check{\boldsymbol{\beta}}_{j,t}.$$

State 6: After obtaining the predicted yields $\mathbf{y}_{j,t}^*$ for each country j we re-arrange them by maturity and pre-multiply by $\boldsymbol{\Sigma}_{\zeta,t}^{-1/2}$ to transform them to their initial scale:

$$\tilde{\mathbf{y}}_t^* = \begin{pmatrix} \tilde{y}_{1,t}^*(\tau_1) \\ \vdots \\ \tilde{y}_{d,t}^*(\tau_1) \\ \vdots \\ \tilde{y}_{1,t}^*(\tau_N) \\ \vdots \\ \tilde{y}_{d,t}^*(\tau_N) \end{pmatrix} = \boldsymbol{\Sigma}_{\zeta,t}^{1/2} \mathbf{R} \begin{pmatrix} y_{1,t}^*(\tau_1) \\ \vdots \\ y_{1,t}^*(\tau_N) \\ \vdots \\ y_{d,t}^*(\tau_1) \\ \vdots \\ y_{d,t}^*(\tau_N) \end{pmatrix} \quad (5.22)$$

Stage 7: To assess the impact of a shock in any of the \mathbf{x}_t variables we repeat the above procedure twice. Given the estimated parameters from the dynamic Nelson-Siegel and covariance regression models we follow the above procedure and obtain the set of predicted yields $\tilde{\mathbf{y}}_t^{*(1)}$. We then repeat the **Stage 1 - Stage 6** procedure allowing for a shock to any of the \mathbf{x}_t variables of our interest and obtain the new set of predicted yields $\tilde{\mathbf{y}}_t^{*(2)}$. The difference of the two sets of predicted yields, i.e. $\tilde{\mathbf{y}}_t^{*(2)} - \tilde{\mathbf{y}}_t^{*(1)}$, indicates the impact of a shock in the \mathbf{x}_t variables on the yield curves of the countries under study and consequently on their corresponding spreads.

5.7.3 Covariance regression sensitivity analysis results

Table 5.8.1 reports the time-series average change in the cross-country spreads, at selected maturities, after inducing a one standard deviation shock in the country-specific liquidity (Spreads columns) and credit quality variables (CDS columns), as well as a shock of the same magnitude in both variables simultaneously (Both columns). In addition, each panel in Table 5.8.1 reports the sensitivity analysis results from the shocks in liquidity and credit quality variables corresponding to each particular country. For example, the panel *Italian shock* reports the changes in all possible cross-country spreads after stress-testing the Italian liquidity and credit proxies at 24, 60, 120, 240 and 360-month maturities.

The sensitivity analysis results in Table 5.8.1 show that shocks to country-specific liquidity and credit variables have a significant impact on cross-country spreads. Nevertheless, the impact of these shocks differs across country-pairs and maturities. In general, it seems that credit shocks have, on average, a greater impact on cross-country spreads than liquidity shocks of the same magnitude. In addition, shocks to country-specific liquidity and credit quality variables appear to have a greater impact on 60, 120 and 240-month than on 24 and 360-month yields. The results are also in line with the time-series average correlation estimates reported in Table 5.7.1 indicating that the correlation estimates are much stronger for most of the country-pairs at these particular maturities. We also note that shocks in the country-specific liquidity and credit quality variables may have opposite effects on cross-country spreads. For example, the Italian-UK spread at 24-month maturity shrinks by approximately 12 basis points after a shock to the Italian bid-ask spreads. In contrast, a shock in the Italian CDS spreads suggests an increase of approximately 81.5 basis points in the Italian-UK spread indicating that investors react to country-specific liquidity and credit quality shocks in different ways.

As shown in the *Italian shock* panel of Table 5.8.1, the shocks in the Italian liquidity and credit quality variables have significant effects on cross-country spreads, which reach their maximum values at the 120-month maturity for most of the country-pairs. It can also be seen that the effects on the cross-country spreads differ across maturities. For example, a shock in the Italian CDS spreads suggests a reduction in the Italian-UK spread by approximately 28 basis points at the 120-month maturity, while the same shock suggests a widening of the Italian-UK spread by approximately 24 basis points at the 240-month maturity. The results confirm that investors' perceptions differ not only conditional on the shock type but also conditional on the investment horizon. The results also reveal significant spillover effects between European countries. For example, an Italian bid-ask shock at 120-month maturity widens the Spanish-French spread by approximately 27 basis points, while a shock of the same magnitude in the Italian CDS spreads suggests an increase of approximately 33 basis points in the Spanish-French spread.

The shocks to the Spanish liquidity and credit quality proxies have similar effects on the cross-country spreads. The greatest change in the cross-country spreads from a shock to the Spanish bid-ask spreads is an increase by approximately 77 basis points in the Italian-UK spread, while a shock in the Spanish CDS spreads has its greatest impact on the Spanish-UK spread, which increases by approximately 212 basis points at the 60-month maturity. The impact of the Spanish shocks is more pronounced in the 60, 120 and 240-month maturity cross-country spreads. We also note that Spanish shocks at 60-month maturity bring about a significant increase in the majority of cross-country spreads. On average, it seems that the shocks in the

Spanish liquidity and credit quality variables are the ones with the greatest impact on cross-country spreads, highlighting the strong dependence between the Spanish economy and the other European economies under study.

The shocks in the German and French variables also have a great impact on cross-country spreads. Nevertheless, their effects are, on average, less intense than those of the shocks corresponding to the peripheral Eurozone countries. It can be seen in Table 5.8.1 that shocks in the German CDS spreads have a positive impact on almost all cross-country spreads at 60, 120, 240 and 360-month maturities. On average, the impact of German credit shocks is more pronounced at the 60 and 120-month maturities, while the corresponding liquidity shocks appear more profound at 120 and 240-month maturities. On the other hand, the shocks in the French variables have a greater impact on cross-country spreads at 60 and 240-month maturities. In addition, the shocks in the UK liquidity and credit quality variables tend to have, on average, the least significant impact on cross-country spreads across term structure maturities. The greatest effect from a shock in the UK bid-ask spreads is a decline in the Spanish-UK spread by approximately 49 basis points at 360-month maturity, whereas the greatest impact from a shock in the UK CDS spreads is a fall by approximately 32 basis points in the French-UK spread at 60-month maturity.

In addition, Figures 5.8.1 and 5.8.2 visualise the time-series average change in the term structure of European sovereign yields after a shock in the country-specific liquidity and credit variables at 24, 60, 120 and 240-month maturities. We note that shocks in the short-term liquidity and credit quality variables, especially at 24-month maturity, are the most persistent ones across the maturity spectrum. It seems that the effects of the shocks in the short-term country-specific liquidity and credit quality variables are transmitted from the short-term yields to the medium-term and long-term maturity yields. For example, it can be seen in Figure 5.8.1a that a shock in the Spanish bid-ask spreads at 24-month maturity has a significant impact on up to at least 240-month maturity European sovereign yields. In contrast, the shocks in the medium-term and longer-term variables appear to affect the yields only at those maturities where the shock has taken place. It can be seen, for instance, that shocks at 120 and 240-month maturities bring about a significant shift in the yields at these particular tenors, whereas yields corresponding to different tenors remain relatively unaffected.

Tables 5.8.2 and 5.8.3 report sensitivity analysis results, with the sample having been conditioned on periods of low-equity market volatility (calm period) and high-equity market volatility (stress period), respectively. Similar to the unconditional sensitivity analysis results, shocks in country-specific variables appear to have a different impact on cross-country spreads across the term structure. The results correspond-

ing to the low-equity market volatility in Table 5.8.2 indicate that country-specific shocks in liquidity and credit quality variables have a greater impact on 60, 120 and 240-month maturities. In general, it is the shocks in the Spanish bid-ask spreads and credit quality variables that have, on average, the greatest impact on cross-country spreads over this period. In addition, shocks in the Italian, German and French liquidity and credit quality measures affect considerably the cross-country spreads, while shocks in the UK proxies seem to have, on average, the least significant impact on spreads in the low-equity market volatility period.

The behaviour of cross-country spread changes in the high-equity market volatility period is not remarkably different from the behaviour of the corresponding spread changes in the low-equity market volatility period for the majority of country pairs. As shown in Table 5.8.3, the impact of country-specific shocks on time-series average cross-country spread changes varies across maturities and shock types. Shocks tend to have a stronger impact on spreads at 60, 120 and 240-month tenors. In agreement with the unconditional and low-equity market volatility results, the Spanish shocks are the ones that have, on average, the greatest impact on cross-country spreads in the high-equity market volatility period. The Italian, German and French shocks also appear to have a great impact on cross-country spreads, while shocks in the UK liquidity and credit proxies tend to have the least significant impact on cross-country spread changes in the high-equity market volatility period. Furthermore, Figures 5.8.3 and 5.8.4 show the behaviour of the European sovereign yield changes over time after a shock in the liquidity and credit quality variables at 24, 60, 120 and 240-month maturities. The grey shaded areas correspond to the high-equity market volatility period. In general, we note that the changes in the yields due to shocks in country-specific liquidity and credit quality measures are more pronounced for all European sovereign yields in the high-equity market volatility period than in the low-equity market volatility period highlighting the dynamic interplay between equity and fixed income markets.

To sum up, the covariance regression results suggest that country-specific liquidity and credit quality measures are important in explaining the covariation of European sovereign yields unconditionally, as well as conditional on periods of low and high-equity market volatility. The explanatory power of credit quality measures appears to be slightly more significant than that of the corresponding liquidity measures in the low-equity market volatility period, whereas their explanatory power is relatively more profound over the high-equity market volatility period. The credit and liquidity measures of the peripheral European countries also appear rather significant over these sub-periods. The implied correlation estimates are, on average, more pronounced at the 120 and 240-month maturities, for most of the country-pairs under consideration. Nevertheless, the correlation estimates vary across tenors and

time periods.

The covariance regression sensitivity analysis results also reveal important linkages and spillover effects among European economies. The country-specific liquidity and credit quality shocks have a remarkable impact on European sovereign yields, while their effects vary significantly across maturities and time periods. Specifically, European sovereign yields tend to react more to shocks in country-specific measures at 60, 120 and 240-month maturities and over periods of heightened equity market volatility. Moreover, Spanish shocks entail, on average, the greatest changes in the cross-country spreads both unconditionally and conditionally on time. In addition, the European sovereign yield changes appear more pronounced in periods of high-equity market volatility, while the cross-country spread changes vary across both sub-periods.

5.8 Conclusions

We jointly model the dynamic evolution of Euro-area sovereign yield curves and their dependence structure using market-wide and country-specific measures of liquidity and credit quality. We investigate the significance of liquidity and credit concerns in explaining sovereign yield changes and sovereign yield heteroscedasticity unconditionally, as well as conditional on times of heightened equity market volatility, and we quantify the effects of market-wide and country-specific liquidity and credit shocks on sovereign yield curves and cross-country spreads.

Our main empirical findings are that both market-wide and country-specific liquidity and credit quality measures are significant in explaining the dynamic behaviour of sovereign yield curves and their dependence structure; however, their importance varies across countries with different credit qualities and investment horizons. The conditional covariance analysis results also suggest that country-specific credit quality measures are remarkably more significant in explaining the heteroscedasticity of sovereign yields than the corresponding liquidity measures in periods of high-equity market volatility, highlighting investors' heightened concerns regarding the credit quality of Euro-area economies during stress periods. The sensitivity analysis results also reveal significant spillover effects highlighting the strong dependence among Euro-area economies.

Table 5.8.1: Sensitivity analysis: Cross-country spreads

Countries	Maturity 24			Maturity 60			Maturity 120			Maturity 240			Maturity 360		
	Spreads	CDS	Both	Spreads	CDS	Both	Spreads	CDS	Both	Spreads	CDS	Both	Spreads	CDS	Both
<i>Italian shock</i>															
IT-DE	-1.28	-21.65	-20.06	-4.82	-3.75	-8.20	-23.28	17.60	-38.11	-21.72	45.66	16.84	1.22	4.76	5.51
IT-ES	-3.24	25.95	25.94	2.85	21.36	21.81	33.17	-22.84	-13.18	27.66	-5.31	2.67	0.84	2.26	3.22
IT-FR	3.75	-37.23	-29.50	1.89	-0.92	1.73	-6.00	55.85	-2.45	-45.82	80.96	1.17	0.35	-4.76	-3.08
IT-UK	-11.91	81.55	73.79	1.37	-15.29	-21.31	-51.03	-27.66	-38.78	-30.90	23.99	3.62	14.91	2.70	16.22
DE-ES	-4.51	4.30	5.89	-7.67	-25.11	-30.00	9.89	-5.24	-78.73	5.94	31.22	19.51	2.06	7.02	8.73
DE-FR	-5.03	15.58	9.45	-6.71	-2.83	-9.93	-17.28	-38.25	-35.66	-10.39	35.29	-15.67	0.87	9.53	8.60
DE-UK	-10.63	103.20	93.84	6.19	-11.54	-13.11	27.75	45.26	0.67	-9.18	-21.68	-13.22	-13.69	2.06	-10.71
ES-FR	0.52	-11.28	-3.56	-0.96	-22.28	-20.08	27.18	33.01	-43.06	-18.16	66.51	3.83	1.20	-2.50	0.14
ES-UK	-15.14	107.50	99.73	-1.48	-36.65	-43.12	-17.86	-50.50	-79.40	-3.24	9.55	6.29	15.76	4.96	19.44
FR-UK	-15.66	118.78	103.29	-0.52	-14.37	-23.04	14.76	53.24	6.06	14.92	35.50	2.45	14.56	7.47	19.30
<i>German shock</i>															
IT-DE	-1.71	-12.89	-15.28	-2.61	30.29	36.50	-3.19	31.45	27.25	-4.65	59.59	56.88	-0.30	7.12	6.28
IT-ES	-1.59	-3.57	-5.94	-0.94	6.40	5.22	-1.86	42.90	27.75	2.33	19.45	33.29	1.50	2.11	-0.57
IT-FR	-1.30	-9.61	-9.31	4.69	11.29	21.17	-15.73	51.05	26.70	29.23	3.24	22.18	1.17	-2.15	-3.03
IT-UK	-6.33	-3.90	-14.05	4.40	63.71	81.84	-22.23	12.51	-6.62	-16.09	8.99	-17.19	-44.40	22.51	-15.20
DE-ES	-3.31	-16.45	-21.22	-1.67	23.89	31.28	-5.04	74.35	55.00	-2.33	79.04	90.17	-3.12	9.22	5.71
DE-FR	-0.41	-3.28	-5.97	-7.30	19.00	15.33	12.55	-19.59	0.55	33.89	21.86	0.21	-1.47	9.27	9.31
DE-UK	-4.62	8.99	1.23	7.01	33.42	45.34	19.04	18.95	33.87	-11.43	-5.36	18.11	44.10	-15.40	21.48
ES-FR	-2.90	-13.18	-15.25	5.63	4.89	15.96	-17.59	93.95	54.45	31.56	22.69	55.47	-1.64	-0.05	-3.60
ES-UK	-7.93	-7.46	-19.99	5.34	57.31	76.62	-24.08	55.41	21.12	-13.76	28.44	16.10	-47.22	24.62	-15.77
FR-UK	-5.03	5.71	-4.74	-0.28	52.42	60.66	-6.49	8.27	3.05	23.85	5.75	17.90	13.11	24.67	-12.18
<i>Spanish shock</i>															
IT-DE	-3.29	-3.11	-13.69	26.20	85.35	156.55	53.21	-11.39	-1.82	50.12	-25.26	-17.37	0.34	0.72	0.10
IT-ES	-1.94	-11.69	-3.64	0.95	69.14	134.26	-1.74	6.49	29.84	2.78	19.72	27.13	0.62	2.35	4.34
IT-FR	-2.67	20.22	16.34	23.18	7.32	71.60	52.69	-32.61	24.24	31.54	-47.39	-44.62	3.27	3.49	5.39
IT-UK	-5.34	-23.17	-38.23	76.58	113.93	211.00	39.94	17.34	-12.36	36.50	-21.88	-22.39	-22.17	66.89	81.83
DE-ES	-5.23	-14.80	-33.73	25.26	183.18	319.50	51.47	-4.90	28.03	27.59	-5.55	9.76	0.96	3.07	4.44
DE-FR	-0.62	-23.33	-30.03	3.02	78.03	84.95	0.52	21.22	-26.06	-15.90	-12.36	-7.24	-2.94	-2.77	-5.29
DE-UK	-2.05	-20.06	-24.54	50.37	28.58	54.45	13.27	-28.73	10.54	-13.62	3.39	-5.02	22.51	8.16	23.71
ES-FR	-4.61	8.53	-3.70	22.24	105.15	234.55	50.95	-26.12	54.09	9.00	-27.67	-17.49	3.90	5.84	9.73
ES-UK	-7.28	-34.86	-58.27	75.63	211.76	373.95	38.20	23.83	17.49	13.97	-2.16	4.74	-21.55	69.24	86.17
FR-UK	-2.67	-43.39	-54.57	53.40	106.61	139.39	-12.75	49.95	6.33	4.96	25.51	22.23	-7.02	63.40	76.44
<i>French shock</i>															
IT-DE	2.70	6.37	11.42	-12.46	-26.56	25.10	-11.76	-11.25	-20.20	-47.46	-55.51	-107.79	0.15	-6.37	-4.81
IT-ES	-0.56	-0.78	-5.87	1.24	25.70	72.83	-0.68	14.73	13.71	5.34	32.53	27.10	0.31	2.58	3.23
IT-FR	2.27	-1.36	0.75	6.44	67.77	136.61	-3.63	9.52	6.21	-30.71	17.72	-15.84	0.66	3.85	4.45
IT-UK	6.76	3.60	19.21	-77.79	-96.41	-124.07	-0.58	-3.18	-1.33	-11.28	16.92	16.82	15.57	-15.78	7.65
DE-ES	2.14	5.60	5.55	-13.70	27.82	126.61	-12.45	3.48	-6.49	-42.11	-107.79	-96.09	0.46	-10.27	-9.36
DE-FR	0.43	7.74	10.68	-18.91	-33.05	-15.87	-8.13	-20.77	-26.41	16.75	73.23	91.95	-0.50	-10.21	-9.26
DE-UK	4.05	-2.78	7.79	-65.32	-63.59	15.73	-11.18	-8.06	-18.87	36.17	72.42	124.61	-15.41	9.41	-12.46
ES-FR	1.71	-2.14	-5.13	5.20	122.15	238.12	-4.32	24.25	19.92	-25.36	-34.56	-62.69	0.97	-0.05	-0.10
ES-UK	6.20	2.82	13.34	-79.03	-42.03	-22.56	-1.27	11.54	12.38	-5.94	-35.36	-30.03	15.88	-19.68	3.10
FR-UK	4.48	4.96	18.47	-84.23	-96.64	-0.14	3.05	-12.71	-7.54	19.42	-0.80	32.66	14.91	-12.84	3.20
<i>UK shock</i>															
IT-DE	-3.49	5.65	2.07	-2.87	-10.14	-15.08	1.06	10.82	13.58	-16.70	8.87	-7.77	-1.66	-1.89	-3.90
IT-ES	-2.35	5.55	0.52	2.25	-12.95	-12.56	-8.76	-0.01	-8.20	-5.02	3.46	0.03	1.53	-0.58	1.71
IT-FR	-1.26	12.10	8.18	0.18	3.59	0.27	-12.29	11.57	0.78	-15.36	8.31	-7.05	3.32	0.70	3.53
IT-UK	-11.13	1.80	-10.13	5.02	-28.23	-23.85	-10.69	-1.98	-12.64	-6.07	-2.58	-9.71	-46.15	-10.55	-55.77
DE-ES	-5.84	11.20	2.59	-5.12	5.59	-2.52	-7.71	10.81	5.38	-21.72	12.33	-7.74	-4.51	-2.63	-6.93
DE-FR	-2.23	-6.45	-6.11	-3.05	-13.73	-15.35	13.35	-0.75	12.80	1.35	-0.56	0.72	-4.98	-2.59	-7.44
DE-UK	-7.64	-3.85	-12.20	7.89	-18.09	-8.77	11.75	12.80	26.22	10.63	-11.45	-1.94	44.48	8.66	51.86
ES-FR	-3.61	17.65	8.70	-2.07	19.32	12.83	-21.05	11.56	-7.42	-20.37	11.77	-7.02	0.47	-0.04	0.51
ES-UK	-13.48	7.35	-9.61	2.77	-12.50	-11.29	-19.45	-1.99	-20.84	-11.09	0.88	-9.68	-48.99	-11.28	-58.79
FR-UK	-9.87	-10.30	-18.31	4.84	-31.82	-24.12	1.60	-13.54	-13.43	9.28	-10.58	-2.67	17.00	-11.24	26.84

The table reports the time-series average cross-country spread changes after a shock (1 standard deviation increase) in country-specific liquidity (Spreads columns) and credit quality variables (CDS columns) as well as a shock of the same magnitude to both country-specific liquidity and credit quality variables simultaneously (Both columns).

Table 5.8.2: Sensitivity analysis: Cross-country spreads (calm period)

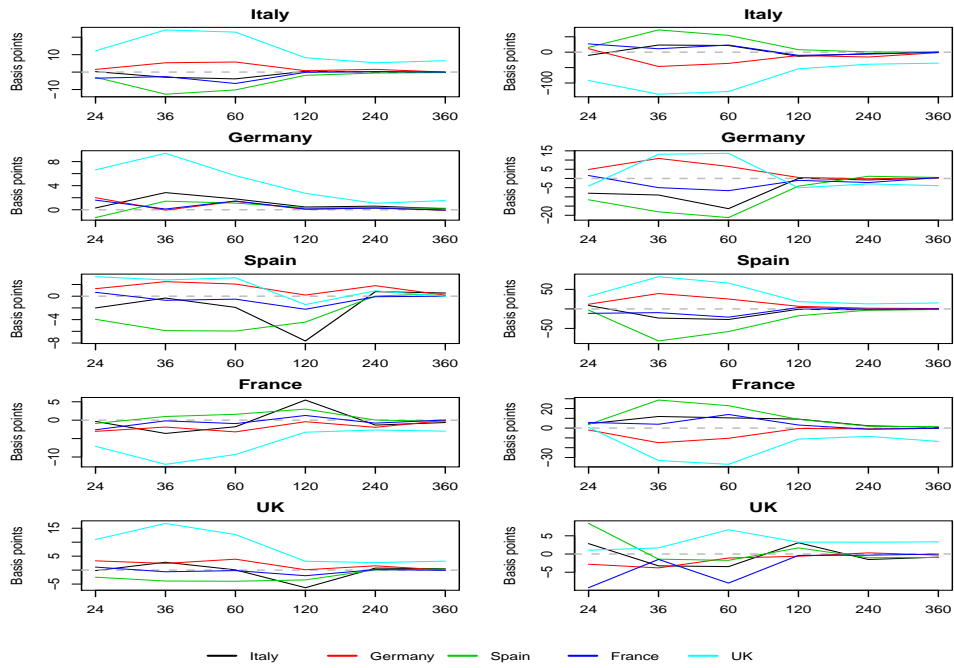
Countries	Maturity 24			Maturity 60			Maturity 120			Maturity 240			Maturity 360		
	Spreads	CDS	Both	Spreads	CDS	Both	Spreads	CDS	Both	Spreads	CDS	Both	Spreads	CDS	Both
<i>Italian shock</i>															
IT-DE	-3.11	-23.15	-22.03	-6.21	-6.31	-10.56	-26.72	27.00	-36.30	-16.10	49.54	19.58	1.12	6.78	7.02
IT-ES	-0.26	34.14	33.56	3.68	33.77	32.91	38.32	-26.65	-14.83	43.79	-9.11	22.41	1.25	3.88	4.58
IT-FR	1.24	-38.27	-30.62	2.24	0.79	3.85	-6.03	64.65	2.17	-62.80	81.29	-24.15	0.03	-5.43	-4.00
IT-UK	-14.60	84.07	76.85	4.30	-3.74	-6.66	-57.64	-19.09	-30.66	-44.61	13.76	-16.64	18.68	7.69	20.30
DE-ES	-7.67	10.99	11.53	-9.89	-40.07	-43.48	11.59	0.35	-78.92	27.69	40.43	41.99	2.37	10.67	11.60
DE-FR	-4.35	15.12	8.60	-8.45	-7.10	-14.41	-20.69	-37.65	-38.46	-29.04	31.75	-32.02	1.09	12.21	11.02
DE-UK	-11.49	107.23	98.88	10.51	2.57	3.90	30.91	46.09	-5.64	-28.51	-33.77	-33.34	-17.56	-0.91	-13.28
ES-FR	-3.32	-4.14	2.93	-1.44	-32.98	-29.07	32.29	38.00	-40.46	-19.02	72.18	-1.74	1.28	-1.55	0.58
ES-UK	-19.16	118.21	110.41	0.62	-37.51	-39.58	-19.32	-45.74	-73.28	-0.82	4.65	5.77	19.93	11.58	24.88
FR-UK	-15.84	122.35	107.47	2.06	-4.53	-10.51	-31.29	0.84	-32.82	12.00	67.53	1.32	18.65	13.12	24.30
<i>German shock</i>															
IT-DE	-1.79	-7.70	-10.13	1.64	42.26	52.69	-0.94	42.28	38.80	-5.21	71.71	72.65	0.05	7.01	8.77
IT-ES	0.01	2.46	0.86	1.24	2.11	5.38	-3.12	49.36	30.17	-3.92	24.18	34.97	-3.86	2.48	0.07
IT-FR	-1.28	8.26	9.54	9.02	23.57	37.21	-15.62	59.69	32.22	39.56	2.94	25.80	3.31	-3.99	-2.22
IT-UK	-4.01	-37.44	-47.53	6.05	62.05	81.60	-23.72	8.32	-13.14	-20.49	14.81	-2.44	-61.77	24.86	-19.03
DE-ES	-1.78	-14.99	-15.81	4.48	45.97	59.67	-4.06	91.64	68.97	-9.13	95.89	107.62	-3.81	9.49	8.85
DE-FR	-0.51	-15.96	-19.66	-7.38	18.69	15.48	14.69	-17.41	6.58	44.76	-6.97	-28.90	-3.26	11.00	11.00
DE-UK	-2.23	-29.73	-37.40	4.41	19.79	28.91	22.79	33.96	51.94	-15.29	-12.65	5.54	61.82	-17.85	27.80
ES-FR	-1.27	0.97	3.85	11.86	27.28	44.20	-18.75	109.05	62.39	35.63	27.12	60.77	-0.56	-1.51	-2.15
ES-UK	-4.00	-44.73	-53.22	8.90	65.76	88.58	-26.85	57.68	17.03	-24.42	38.99	32.53	-65.64	27.34	-18.96
FR-UK	-2.74	-45.70	-57.06	-2.97	38.48	44.39	-8.10	-31.53	-37.55	60.05	5.68	28.24	58.36	28.85	10.08
<i>Spanish shock</i>															
IT-DE	-0.61	-34.61	-44.60	42.00	124.82	224.58	61.26	-6.25	8.81	51.08	-17.17	-14.71	-1.08	-3.05	-4.98
IT-ES	0.39	17.33	34.68	12.35	154.80	242.50	10.58	13.87	38.31	-19.52	29.64	44.17	0.46	1.12	2.22
IT-FR	3.48	5.03	6.02	41.43	32.76	124.25	57.07	-31.04	23.01	31.36	-58.87	-61.84	3.02	1.74	3.72
IT-UK	-13.11	-65.68	-83.97	77.42	123.66	242.05	37.63	22.67	-16.87	34.12	-31.72	-38.37	-13.65	96.98	113.48
DE-ES	-5.83	-56.77	-84.11	55.96	281.22	468.69	71.84	7.62	47.12	31.56	12.47	29.46	-0.62	-1.93	-2.76
DE-FR	-4.09	-14.96	-3.96	0.58	92.06	100.33	4.19	24.79	-14.19	-19.72	-34.05	-28.62	-4.10	-4.80	-8.71
DE-UK	-12.50	-31.08	-35.90	35.42	-1.16	17.47	23.62	2.30	25.68	-16.96	-14.55	-23.66	12.58	17.70	36.14
ES-FR	-1.74	-17.13	-33.48	55.38	189.16	368.35	67.65	-17.18	61.31	11.84	-29.23	-17.66	3.48	2.86	5.94
ES-UK	-18.32	-87.84	-123.48	91.38	280.06	486.16	48.21	36.54	21.44	14.60	-2.08	5.80	-13.19	98.10	115.70
FR-UK	-16.59	-59.15	-39.87	36.00	90.90	117.80	-19.43	53.72	-39.88	-2.76	20.96	17.28	9.95	95.23	109.76
<i>French shock</i>															
IT-DE	4.91	11.62	18.99	-36.38	-40.75	-9.91	-12.76	-12.49	-21.76	-49.47	-67.71	-74.79	0.08	-7.33	-5.48
IT-ES	-0.87	14.31	6.11	17.60	7.57	51.62	-1.19	16.69	15.57	2.82	6.65	1.06	1.40	-3.67	-3.16
IT-FR	3.21	9.38	11.07	-4.01	32.19	100.28	-3.73	11.00	7.81	-33.54	24.92	-13.98	0.00	4.91	4.74
IT-UK	9.43	-7.47	12.44	-77.26	-102.64	-130.57	-0.07	-5.27	-1.62	-12.27	22.91	21.59	25.17	-9.25	23.17
DE-ES	4.04	25.94	25.10	-53.98	-31.58	43.32	-13.95	4.20	-6.19	-46.64	-126.64	-73.72	1.48	-11.00	-8.63
DE-FR	1.70	2.25	7.92	-32.37	-52.74	-15.50	-9.04	-23.49	-29.57	15.93	92.63	112.24	0.07	-12.25	-10.22
DE-UK	4.52	-19.10	-6.55	-40.88	-61.88	-40.91	-12.70	-7.22	-6.48	37.20	90.62	147.81	-25.09	1.92	-28.65
ES-FR	2.34	23.69	17.17	-21.61	41.37	153.50	-4.91	27.69	23.39	-30.71	-42.09	-75.41	1.41	1.25	1.58
ES-UK	8.56	6.84	18.55	-94.86	-93.46	-77.35	-1.25	11.42	13.96	-9.45	-44.10	-39.84	26.57	-12.92	20.01
FR-UK	6.21	-16.85	1.37	-73.25	-134.83	-56.41	3.66	-16.27	-9.43	15.08	2.01	29.38	25.16	7.45	18.43
<i>UK shock</i>															
IT-DE	-2.67	5.14	0.03	-0.56	-17.91	-20.96	3.53	11.77	17.76	-19.29	10.40	-8.76	-1.31	-2.07	-4.38
IT-ES	-1.17	6.81	-0.17	2.64	13.97	10.93	-10.73	0.61	-9.75	-7.89	4.29	-2.25	-3.26	-1.22	-3.42
IT-FR	1.87	8.06	3.76	-1.85	6.02	-1.94	-12.48	12.17	1.55	-14.88	8.49	-5.85	5.48	1.64	5.62
IT-UK	-13.68	3.39	-11.02	11.07	-28.57	-19.85	-8.77	-3.19	-10.93	-7.06	-1.65	-10.45	-53.11	-18.04	-67.63
DE-ES	-6.32	11.95	-0.14	-3.20	-2.34	-8.43	-7.20	12.39	8.01	-27.18	14.70	-11.01	-4.57	-3.29	-7.80
DE-FR	-4.54	-2.92	-3.73	1.29	-23.94	-19.02	16.01	-0.40	16.21	4.40	-1.92	2.90	-6.79	-3.71	-10.00
DE-UK	-11.01	-1.74	-11.05	11.63	-10.65	1.11	12.30	14.96	28.69	12.22	-12.05	-1.69	51.80	15.97	63.26
ES-FR	-1.78	14.87	3.58	-4.49	21.60	10.59	-23.21	12.79	-8.20	-22.78	12.78	-8.10	2.22	0.42	2.20
ES-UK	-17.33	10.21	-11.19	8.43	-12.99	-7.32	-19.50	-2.58	-20.69	-14.96	2.65	-12.70	-56.37	-19.26	-71.05
FR-UK	-15.55	-4.66	-14.78	12.92	-34.59	-17.91	3.71	-15.36	-12.49	1.63	10.13	4.59	51.87	12.96	66.53

The table reports the time-series average cross-country spread changes corresponding to the low-equity market volatility period (Calm period) after a shock (1 standard deviation increase) in country-specific liquidity (Spreads columns) and credit quality variables (CDS columns) as well as a shock of the same magnitude to both country-specific liquidity and credit quality variables simultaneously (Both columns).

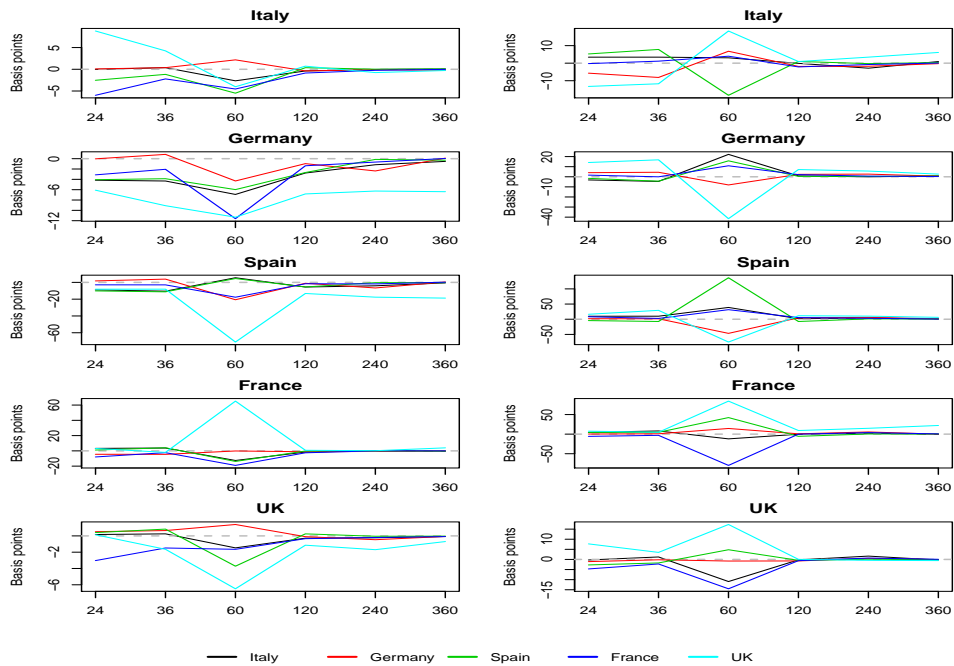
Table 5.8.3: Sensitivity analysis: Cross-country spreads (stress period)

Countries	Maturity 24			Maturity 60			Maturity 120			Maturity 240			Maturity 360		
	Spreads	CDS	Both	Spreads	CDS	Both	Spreads	CDS	Both	Spreads	CDS	Both	Spreads	CDS	Both
<i>Italian shock</i>															
IT-DE	0.56	-20.16	-18.08	-3.44	-1.19	-5.83	-19.83	8.20	-39.93	-27.34	41.79	14.10	1.32	2.75	4.01
IT-ES	-1.91	17.76	18.33	2.01	8.96	10.70	28.03	-19.03	-11.52	-9.34	19.77	17.07	-0.43	-0.63	-1.86
IT-FR	6.27	-36.19	-28.38	1.53	-2.62	-0.38	-5.96	47.05	-7.06	-28.84	80.62	26.48	0.68	-4.10	-2.16
IT-UK	-9.22	79.02	70.73	-1.56	-26.83	-35.96	-44.42	-36.23	-46.91	-17.19	34.21	23.87	11.15	-2.28	12.14
DE-ES	-1.35	-2.39	0.24	-5.45	-10.15	-16.53	8.19	-10.83	-78.54	-15.81	22.02	-2.97	1.75	3.38	5.87
DE-FR	-5.71	16.03	10.30	-4.97	1.43	-5.45	-13.87	-38.85	-32.87	1.50	32.06	5.61	0.64	6.84	6.17
DE-UK	-9.77	99.18	88.81	1.87	-25.64	-30.13	24.58	44.43	6.98	10.14	-7.58	9.77	-9.83	5.03	-8.13
ES-FR	4.35	-18.43	-10.06	-0.48	-11.58	-11.08	22.06	28.02	-45.67	-17.31	60.85	9.40	1.11	-3.46	-0.31
ES-UK	-11.13	96.78	89.06	-3.58	-35.79	-46.66	-16.39	-55.26	-85.52	-5.67	14.44	6.80	11.58	-1.65	14.00
FR-UK	-15.48	115.21	99.11	-3.10	-24.21	-35.58	38.45	83.28	39.85	11.64	-2.73	-2.61	10.47	1.81	14.31
<i>German shock</i>															
IT-DE	-1.64	-18.07	-20.43	-6.85	18.31	20.31	-5.44	20.63	15.70	-4.10	47.48	41.11	-0.66	7.22	3.79
IT-ES	-3.20	0.16	-6.19	0.97	16.50	17.42	-0.59	36.44	25.33	-8.58	-6.16	10.74	1.77	-1.73	1.21
IT-FR	-1.33	-27.48	-28.15	0.36	-0.99	5.13	-15.84	42.41	21.18	18.91	3.54	18.57	-0.96	-0.32	-3.83
IT-UK	-8.65	29.65	19.43	2.76	65.36	82.07	-20.73	16.70	-0.11	-11.69	3.18	-31.95	-27.03	20.17	-11.38
DE-ES	-4.84	-17.91	-26.63	-7.83	1.81	2.89	-6.03	57.07	41.03	4.48	62.18	72.72	-2.42	8.95	2.58
DE-FR	-0.31	9.40	7.72	-7.21	19.30	15.18	10.41	-21.78	-5.48	16.25	43.93	22.55	0.31	7.54	7.62
DE-UK	-7.01	47.72	39.87	9.61	47.05	61.76	15.29	3.93	15.81	-7.58	1.93	30.69	26.38	-12.94	15.17
ES-FR	-4.53	-27.32	-34.35	-0.61	-17.49	-12.28	-16.43	78.85	46.50	27.49	18.25	50.18	-2.73	1.41	-5.04
ES-UK	-11.85	29.80	13.24	1.79	48.86	64.65	-21.32	53.14	25.22	-3.11	17.88	-0.34	-28.80	21.90	-12.59
FR-UK	-7.32	57.12	47.58	2.40	66.35	76.94	4.89	25.71	21.29	-18.54	-0.37	1.38	-26.07	20.48	-7.55
<i>Spanish shock</i>															
IT-DE	-5.96	28.39	90.46	10.41	45.89	22.16	45.16	-16.53	-76.46	49.16	-33.35	-104.65	1.75	4.49	-150.08
IT-ES	1.33	-1.21	31.28	15.84	-16.51	92.39	-14.06	-0.89	85.39	25.55	-9.79	125.48	-0.78	-3.58	118.93
IT-FR	-8.82	35.41	99.90	4.93	-18.12	-47.40	48.32	-34.18	-38.53	31.71	-35.90	-90.52	3.53	5.24	-148.21
IT-UK	2.43	19.34	80.75	75.74	104.20	113.59	42.25	12.01	-71.86	38.88	-12.03	-142.67	-30.69	36.81	-105.10
DE-ES	-4.63	27.17	-132.92	-5.44	85.14	36.54	31.10	-17.42	-21.40	23.62	-23.56	131.72	2.53	8.07	72.14
DE-FR	2.86	-7.02	53.79	5.47	64.00	-64.21	-3.16	17.64	-21.68	17.45	2.55	149.02	-1.78	-0.74	58.62
DE-UK	8.39	-9.05	139.85	65.33	58.31	225.19	2.91	-28.54	-34.94	-10.28	21.32	85.66	32.43	-1.39	15.51
ES-FR	-7.49	34.19	34.03	-10.91	21.13	-43.04	34.26	-35.07	-108.49	6.17	-26.11	-48.27	4.31	8.81	-132.80
ES-UK	3.76	18.12	14.88	59.89	143.45	117.94	28.18	11.12	-141.82	13.34	-2.24	-118.39	-29.90	40.39	-128.99
FR-UK	11.25	-16.07	94.68	70.80	122.32	174.59	6.07	23.83	-11.18	7.17	23.87	56.08	-23.99	31.57	-22.31
<i>French shock</i>															
IT-DE	0.49	1.13	3.85	11.46	-12.36	60.11	-10.76	-10.00	-18.64	-45.44	-43.30	-89.36	0.23	-5.40	-4.14
IT-ES	-0.24	-15.87	-17.85	-15.12	43.82	94.04	-0.18	12.76	11.84	-7.87	37.55	32.27	0.78	4.13	5.94
IT-FR	1.33	-12.10	-9.57	16.90	103.35	172.94	-3.54	8.04	4.61	-27.88	10.53	-17.69	1.31	2.78	4.16
IT-UK	4.08	14.67	25.99	-78.31	-90.18	-117.56	-1.10	-1.10	-1.04	-10.30	10.93	12.06	5.97	-22.30	-7.86
DE-ES	0.24	-14.74	-14.00	26.57	87.22	209.91	-10.94	2.76	-6.80	-37.58	-80.85	-118.45	-0.55	-9.53	-10.08
DE-FR	-0.84	13.22	13.43	-5.44	-13.36	-16.25	-7.22	-18.05	-23.24	10.80	47.06	64.89	-1.08	-8.18	-8.31
DE-UK	3.59	13.54	22.13	-15.53	-27.48	72.37	-9.66	-8.91	-17.60	35.15	54.22	101.41	-5.74	16.90	3.72
ES-FR	1.09	-27.97	-27.42	32.02	202.93	322.74	-3.72	20.80	16.44	-20.01	-27.02	-49.97	0.53	-1.35	-1.78
ES-UK	3.84	-1.20	8.13	-63.19	9.41	32.24	-1.28	11.66	10.80	-2.43	-26.62	-20.22	5.19	-26.43	-13.81
FR-UK	2.75	26.77	35.56	-95.21	-40.85	56.12	-2.44	9.14	5.64	17.58	0.40	29.75	4.66	-25.08	-12.03
<i>UK shock</i>															
IT-DE	-4.32	6.17	4.11	-5.18	-2.38	-9.20	-1.42	9.87	9.40	-14.12	7.34	-6.78	-2.02	-1.72	-3.43
IT-ES	-1.05	4.28	1.21	1.85	-15.89	-12.58	-6.79	-0.64	-6.64	2.14	-2.63	-2.30	2.43	0.25	2.63
IT-FR	-4.39	16.14	12.60	2.21	1.15	2.48	-12.11	10.96	0.01	-15.83	8.13	-8.24	1.15	-0.25	1.44
IT-UK	-8.59	0.21	-9.24	-1.03	-27.90	-27.84	-12.61	-0.76	-14.36	-5.08	-3.52	-8.98	-39.18	-3.05	-43.90
DE-ES	-5.37	10.45	5.33	-7.03	13.52	3.38	-8.21	9.23	2.76	-16.26	9.97	-4.48	-4.45	-1.96	-6.06
DE-FR	0.07	-9.97	-8.49	-7.38	-3.52	-11.69	10.69	-1.09	9.39	1.71	-0.79	1.46	-3.16	-1.46	-4.87
DE-UK	-4.27	-5.96	-13.35	4.15	-25.53	-18.64	11.19	10.63	23.75	9.04	-10.86	-2.19	37.17	1.34	40.47
ES-FR	-5.44	20.42	13.82	0.35	17.04	15.07	-18.90	10.33	-6.63	-17.97	10.76	-5.93	-1.28	-0.50	-1.19
ES-UK	-9.64	4.49	-8.02	-2.89	-12.01	-15.26	-19.40	-1.40	-21.00	-7.22	-0.89	-6.67	-41.61	-3.30	-46.54
FR-UK	-4.20	-15.93	-21.84	-3.24	-29.05	-30.33	0.51	11.72	14.37	10.75	-11.65	-0.74	-17.88	-2.80	-12.86

The table reports the time-series average cross-country spread changes corresponding to the high-equity market volatility period (Stress period) after a shock (1 standard deviation increase) in country-specific liquidity (Spreads columns) and credit quality variables (CDS columns) as well as a shock of the same magnitude to both country-specific liquidity and credit quality variables simultaneously (Both columns).

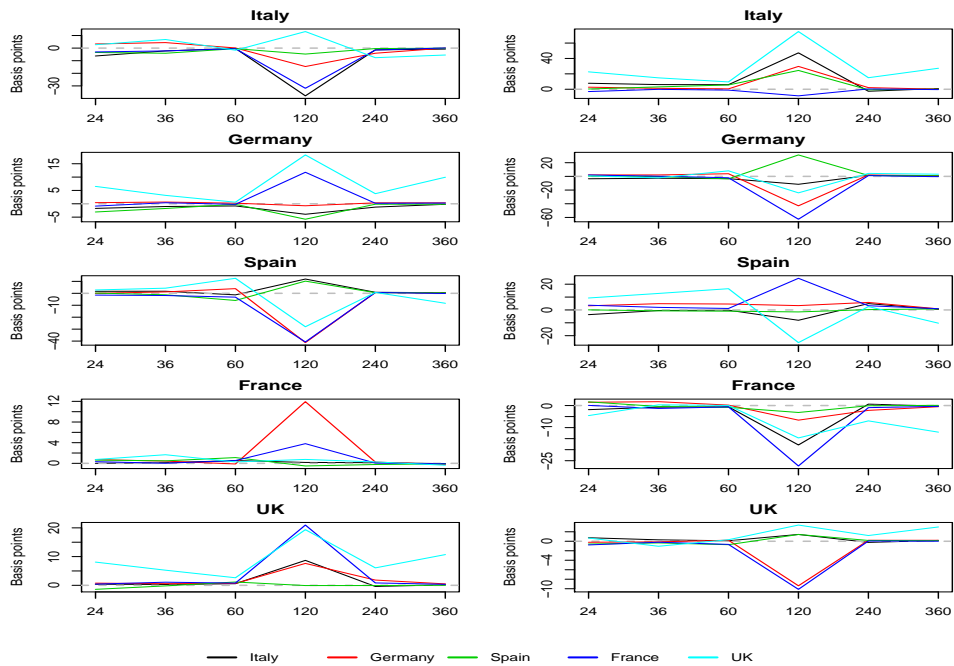


(a) Spread changes after liquidity and credit shocks at 24-month maturity

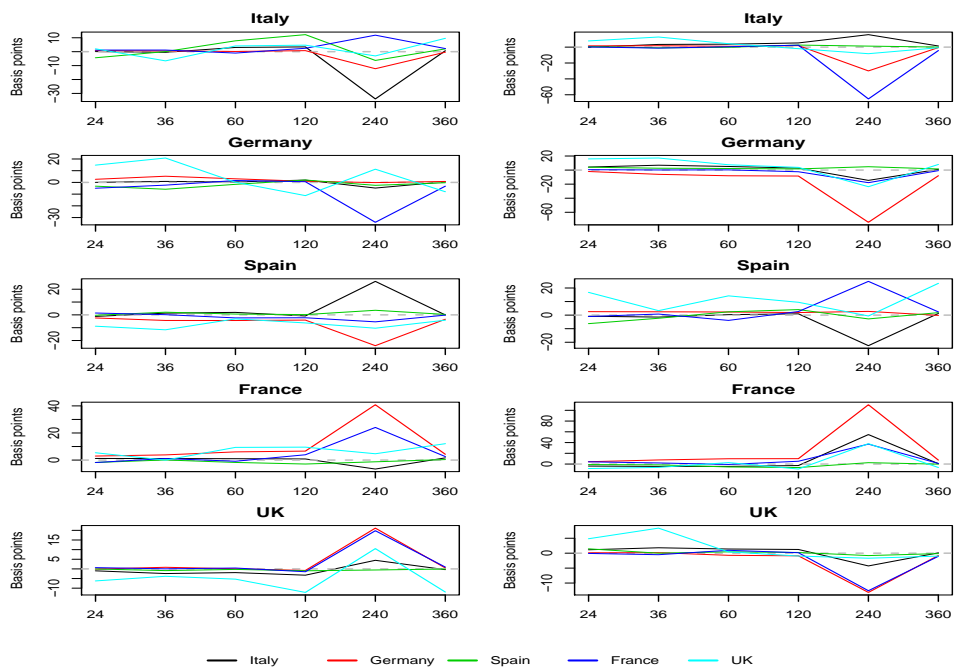


(b) Spread changes after liquidity and credit shocks at 60-month maturity

Figure 5.8.1: This figure shows the time-series average change in the European bond yields at 24, 36, 60, 120, 240 and 360-month maturities after a shock in the liquidity and credit quality variables at 24 and 60-month maturities. The left-sided graphs show the time-series average change in the European bond yields that results from a shock of one standard deviation in the bid-ask spreads (liquidity shock) for each particular country. The right-sided graphs show the time-series average change in the European bond yields that results from a shock of one standard deviation in the credit default swap (CDS) spreads (credit shock) for each particular country.

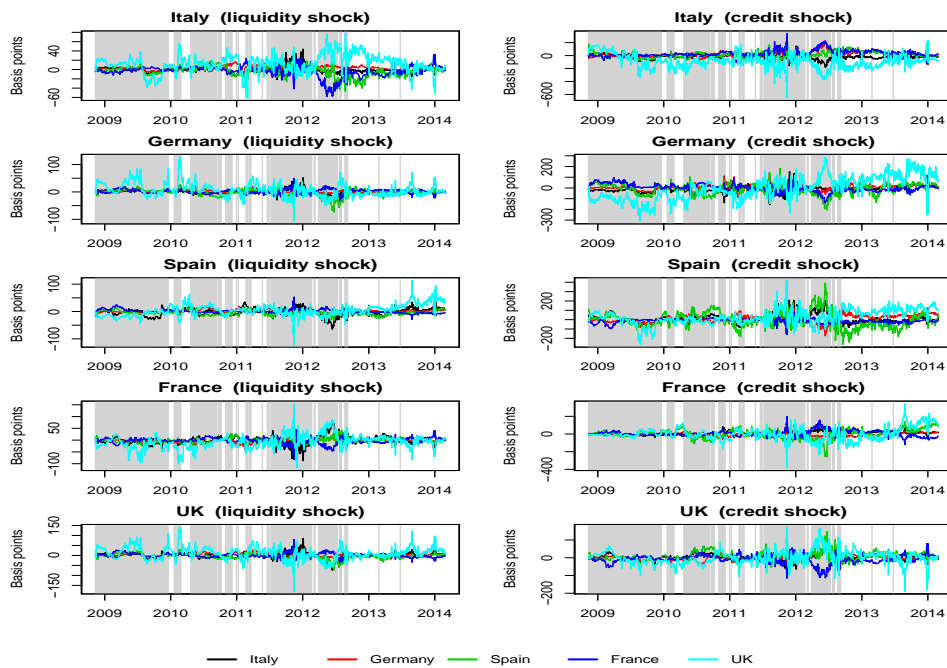


(a) Spread changes after liquidity and credit shocks at 120-month maturity

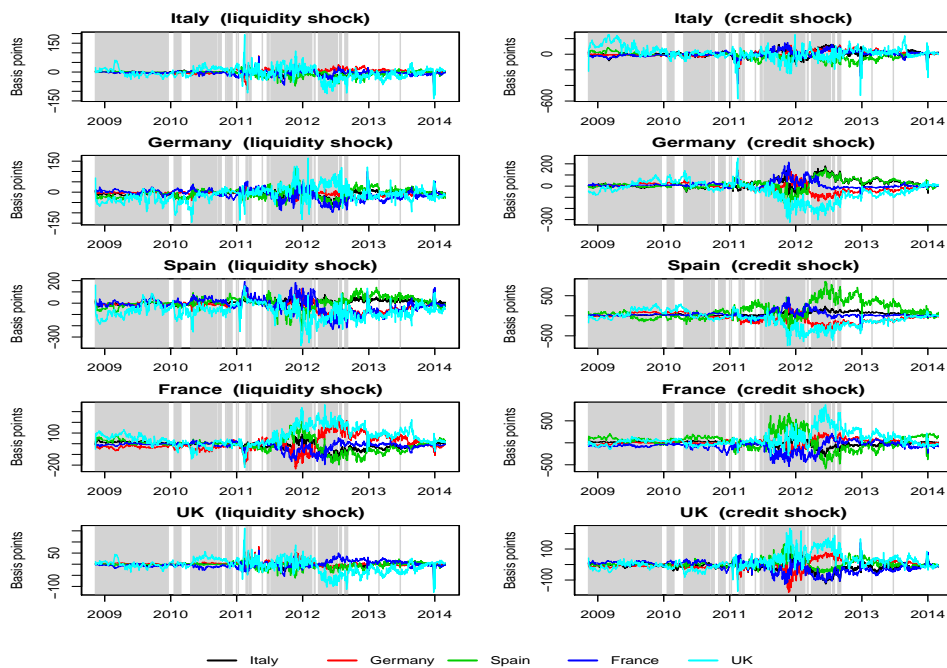


(b) Spread changes after liquidity and credit shocks at 240-month maturity

Figure 5.8.2: This figure shows the time-series change in the European bond yields at 24, 36, 60, 120, 240 and 360-month maturities after a shock in the liquidity and credit quality variables at 120 and 240-month maturities. The left-sided graphs show the time-series average change in the European bond yields that results from a shock of one standard deviation in the bid-ask spreads (liquidity shock) for each particular country. The right-sided graphs show the time-series average change in the European bond yields that results from a shock of one standard deviation in the credit default swap (CDS) spreads (credit shock) for each particular country.

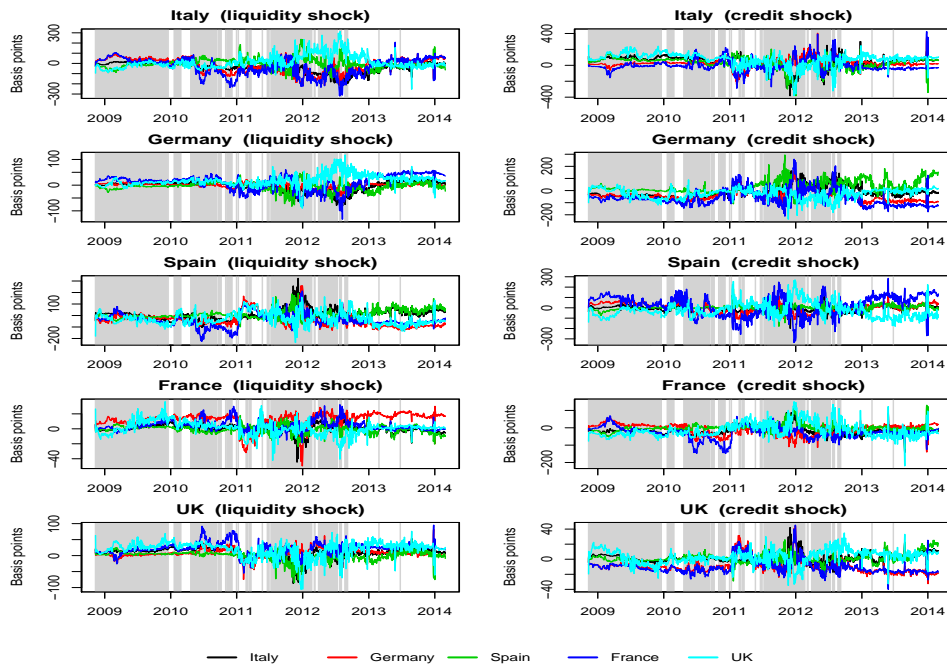


(a) Spread changes at 24-month maturity

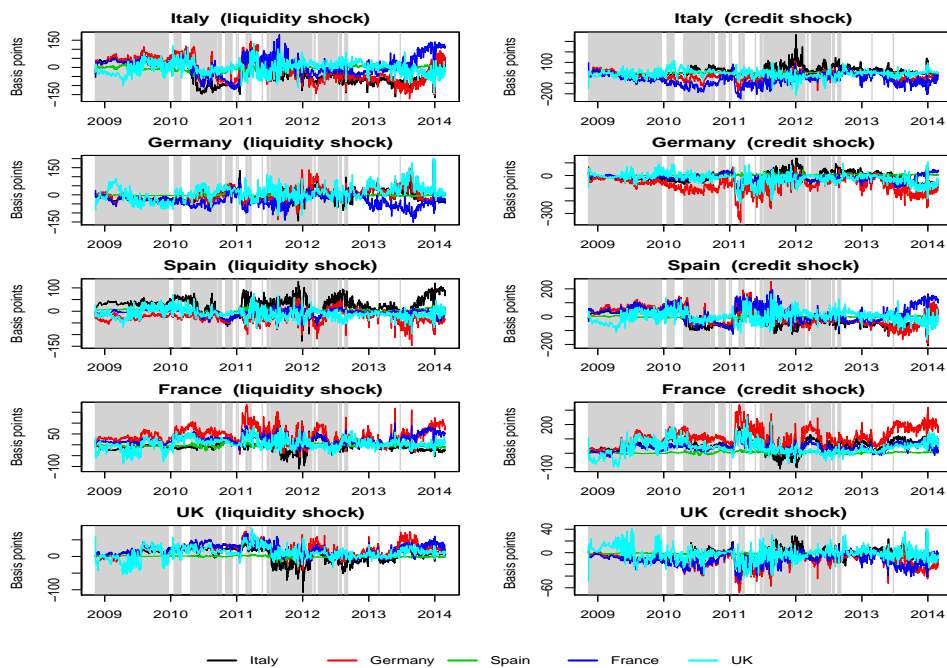


(b) Spread changes at 60-month maturity

Figure 5.8.3: This figure shows the time-series change in the European bond yields after a shock in the liquidity and credit quality variables at 24 and 60-month maturities. The left-sided graphs show the change in the European bond yields that results from a shock of one standard deviation in the bid-ask spreads (liquidity shock) for each particular country. The right-sided graphs show the change in the European bond yields that results from a shock of one standard deviation in the credit default swap (CDS) spreads (credit shock) for each particular country. The grey shaded area corresponds to the high-equity market volatility period.



(a) Spread changes at 120-month maturity



(b) Spread changes at 240-month maturity

Figure 5.8.4: This figure shows the time-series change in the European bond yields after a shock in the liquidity and credit quality variables at 120 and 240-month maturities. The left-sided graphs show the change in the European bond yields that results from a shock of one standard deviation in the bid-ask spreads (liquidity shock) for each particular country. The right-sided graphs show the change in the European bond yields that results from a shock of one standard deviation in the credit default swap (CDS) spreads (credit shock) for each particular country. The grey shaded area corresponds to the high-equity market volatility period.

Chapter 6

Conclusions and further research

6.1 Conclusions

This PhD thesis deals primarily with the modelling of multivariate distributions of financial data and introduces distinct methodologies to address significant financial modelling challenges in the risk and interest rate modelling literature. In this respect, each Chapter of the current PhD thesis explores alternative research questions, concentrates on multiple segments of the financial markets and employs different modelling techniques that take into account the stylised features and complex dependence dynamics of financial data. In particular, Chapter 3 relates to the risk modelling of energy portfolios and employs a semi-parametric approach to model the marginal series and a pair-copula construction principle (PCC) to model the dependence structure of portfolios' constituents, while Chapter 4 focuses on systemic risk measurement in the European banking sector introducing a new approach for calculating systemic risk, which uses copula distribution functions. Finally, Chapter 5 centers on the joint modelling of European sovereign yield curves and associates their dynamic interaction with market-wide and country-specific measures of liquidity and credit quality.

More specifically, Chapter 3 introduces a combination of extreme value theory (EVT) methods and the pair-copula construction principle (PCC) to model the joint distribution of energy portfolios and forecast portfolios' risk exposures. Within this framework, a two-step estimation procedure is followed, where standard univariate time series models are fitted in the series in the first stage and the resulting standardised residuals are used in the second stage for modelling the dependence structure. In contrast to the traditional parametric modelling approaches, our approach combines pseudo maximum likelihood fitting of time series models and extreme value theory to model the tails of the resulting innovations distribution. The dependence structure of the portfolio is modelled using a canonical vine copula modelling approach. The vine factorisation is specified according to the empirical rule of [Czado et al. \(2012\)](#) and the copula family selection is based on Akaike's information criterion (AIC). An alternative asymmetric vine specification, based on the theoretical and empirical results of [Joe et al. \(2010\)](#) and [Nikoloulopoulos et al. \(2012\)](#), is also proposed. In particular, the selected Student- t copula families in level 1 of the vine are replaced by copula families that imply asymmetric tail dependence, whereas the

Independence copula is employed for those pairs that cannot reject the assumption of independence. We show how the proposed modelling approach can be used for forecasting portfolios' *Value-at-Risk* (*VaR*) and *Conditional-Value-at-Risk* (*CVaR*). In this context, portfolio *VaR* and *CVaR* forecasts are computed by five alternative modelling specifications, while the evaluation of their forecasting performance is performed using standard statistical and loss function techniques. In general, the statistical tests for all models show good unconditional and conditional coverage. Nevertheless, the asymmetric vine model shows superior performance according to its *VaR* and *CVaR* results over alternative model specifications at extreme quantiles.

The empirical results provide new insight into the study of multivariate extremes and also support the findings of [Joe et al. \(2010\)](#) and [Nikoloulopoulos et al. \(2012\)](#). It seems that the asymmetric vine model combined with semi-parametric marginals provides a better fit in the tails of the joint distribution and hence better risk estimates when compared to the entirely AIC selected vine model and alternative competitive risk models. Although the data sample does not show significant evidence of tail asymmetries, it seems that the use of asymmetric copulas instead of the likelihood-selected Student-*t* copulas in level 1 of the vine structure, as well as the employment of Independence copulas for those pairs that do not reject the assumption of independence, may improve the fit in the tails of the joint density and as a consequence the accuracy of risk estimates. It is believed that the employment of asymmetric vine models in portfolios that exhibit more pronounced asymmetric tail dependences can further highlight the superior performance of the model at extreme quantiles.

In addition, Chapter 4 introduces a new methodology to estimate the systemic risk in the European banking sector building upon the *Conditional Value-at-Risk* (*CoVaR*) methodology, which was originally proposed by [Adrian and Brunnermeier \(2011\)](#) and subsequently modified by [Girardi and Ergün \(2013\)](#) to address the inefficiencies in dependence modelling arising from the original *CoVaR* definition. In this Chapter, we show that *CoVaR* can be estimated using analytical expressions for a broad range of copula families for both alternative definitions. The new Copula *CoVaR* methodology is also extended to a dynamic framework. In this context, systemic risk estimates derived from this approach reflect the time-varying dependence of the financial series involved in the estimation procedure. Furthermore, we extend the Copula *CoVaR* methodology to alternative “co-risk” measures such as the *Conditional Expected Shortfall* (*CoES*) and also show how the new framework can facilitate the implementation of stress-testing exercises, which are useful for analysing the impact of extreme market conditions on systemic risk.

The Copula *CoVaR* methodology is subsequently applied to measure the contribution of a large set of European financial institutions to systemic risk. In the empirical analysis, the assessment of systemically important financial institutions is performed following the *CoVaR* definition of Girardi and Ergün (2013) due to the favourable dependence modelling properties of this definition and the fact that systemic risk estimates generated from this framework can be statistically evaluated for unconditional and conditional coverage. The empirical analysis is also performed using alternative distribution assumptions in the marginal series and the dependence structure, as well as alternative risk metrics such as *CoVaR* and *CoES*. The empirical analysis also includes a number of panel regressions to assess the impact of several macroeconomic and financial variables as well as of institution-specific variables on systemic risk contribution.

The main empirical results highlight the importance of taking into account the asymmetries in the marginal series and the dependence structure. The selection of inappropriate marginals may cause significant bias in the selection of dependence models and provide erroneous results. In addition, the statistical backtesting results favour the employment of Skewed-*t* over Gaussian marginals for systemic risk modelling. The average systemic risk estimates deviate significantly across alternative marginal specifications but are robust across different risk metrics within the same marginal specifications. Several large European institutions such as BBVA, UBS, Deutsche Bank, Credit Suisse and BNP Paribas appear to be among the most systemic European financial institutions. In addition, the Spanish and French banks appear to be the most systemic banking sectors in Europe according to their average contribution to systemic risk. Finally, the effects of the implied market volatility, of funding liquidity and of the change in the credit spread and the short-term interest rates are significant in explaining systemic risk estimates and show an asymmetric response between the pre-crisis and crisis periods. This behaviour is partly attributed to the coordinated intervention of central banks in response to the financial crisis. With respect to bank-specific characteristics, the size and leverage variables appear to be the most robust determinants of systemic risk, implying that bigger and highly leveraged financial institutions may contribute more to systemic risk.

Finally, Chapter 5 introduces an approach for modelling jointly the dynamic dependence between several European sovereign yield curves and relating it to broader European and country-specific measures of liquidity and credit quality both unconditionally and conditional on periods of heightened uncertainty in equity markets. To model the multiple forms of dependence found in the European sovereign yield curves, we follow a two-step procedure that entails modelling the yield curve dynamics for each individual country using the macro-finance Nelson-Siegel model of Diebold et al. (2006) and modelling the heteroskedasticity of the prediction errors

obtained from the fit of the yield curve models employing the covariance regression model of Hoff and Niu (2012). In this regard, the latent factor dynamics in the macro-finance Nelson-Siegel model of Diebold et al. (2006) are modelled as autoregressive processes augmented with observable macroeconomic and financial variables. In addition, market-wide liquidity and credit quality measures are included in the latent factor specification to assess the interaction between the European liquidity and credit measures and the sovereign yield curves. Subsequently, the covariance matrix of the European sovereign yield prediction errors is modelled as a function of country-specific liquidity and credit quality measures to assess the impact of idiosyncratic country risks on the yield curves and cross-country European spreads.

In the empirical analysis, we model the yield curve dynamics for Germany, France, Spain, Italy and the United Kingdom and relate them to market-wide and country-specific liquidity and credit measures. The main empirical results suggest that investors separate European countries into distinct groups, based on their overall credit quality, as well as on whether they are Eurozone members or not. The statistical analysis results also highlight the importance of market-wide liquidity and credit quality measures in explaining the dynamics of sovereign yield curves. Moreover, the sensitivity analysis results highlight a unique negative relationship between the German yields and shocks to European liquidity and credit quality measures supporting the view that investors in the fixed income markets regard the German bonds as a safe haven in periods of increased illiquidity and credit uncertainty. In addition, the results highlight the importance of country-specific liquidity and credit quality measures in explaining the covariation of sovereign yields both unconditionally and conditional on periods of increased volatility in equity markets. It is shown that investors are more concerned with the credit quality than the liquidity of sovereign debt instruments and that European sovereign yields are more sensitive to shocks in liquidity and credit quality variables in times when equity markets are perceived as more volatile. Finally, it is shown that shocks to Spanish liquidity and credit quality measures have the greatest impact on the cross-country spreads indicating investors' increased concerns over the country's financial stability and suggesting significant spillover effects among European economies.

6.2 Further research

Undoubtedly, the research ideas and methodologies presented in each Chapter of this PhD thesis can be further improved and extended in multiple directions. Possible improvements may include exploration of alternative parametric distribution assumptions for marginal and dependence modelling, consideration of different estimation techniques that exhibit alternative optimality properties, exploration of non-standard model selection procedures, consideration of alternative dynamics in

the specification of dependence parameters, employment of additional observed factors that affect the dependence of the financial variables analysed and exploration of alternative data sets that correspond to diverse market conditions and reflect alternative distribution characteristics. In addition, the proposed research ideas and methodologies are non-exclusive and non-limited to the applications presented in this PhD thesis but can be easily extended to alternative financial applications such as portfolio selection, portfolio hedging or asset pricing and shed light on additional research questions that have not been addressed in the present PhD thesis.

In particular, in Chapter 3, the selection of asymmetric copula families in level 1 of the vine need not be entirely based on empirical and theoretical scatter and function plots comparisons but can also be based, as proposed by [Nikoloulopoulos et al. \(2012\)](#), on the comparison between the empirical tail dependence of the data being modelled and the theoretical tail dependence of the corresponding asymmetric copula families. Moreover, the fit of the semi-parametric marginals and the canonical vine copula model can be improved by re-estimating the models at fixed periods of time, i.e., every month, when considering forecasting applications. All risk measure forecasts presented in this study are obtained using a static multivariate model. The marginals and the vine model are estimated using a fixed estimation sample and portfolio *VaR* and *CVaR* forecasts are obtained conditional on the estimated model parameters. This approach is clearly faster, especially when considering large-scale portfolio forecasting evaluations, and it also eliminates the possibility of over-fitting the data. However, the portfolio dependence structure may not be constant over time but rather time-varying and hence a static model may be insufficient to describe it and lead to incorrect inference.

A potentially interesting and, at the same time, challenging topic for further research is to develop multivariate models in the context of pair-copula construction (PCC) that will allow time-varying dependence, while being computationally tractable for large dimensional problems. In general, various time-varying copula models have been proposed in the literature where the copula functional form is fixed and its parameter is allowed to vary over time as a function of lagged information (see for example, [Patton 2004, 2006](#); [Jondeau and Rockinger 2006](#); [Christoffersen et al. 2012](#), among others) or where the functional form of the copula varies over time (see for example, [Rodriguez 2007](#); [Chollete et al. 2009](#); [Garcia and Tsafack 2011](#); [Markwat et al. 2012](#), among others). Nevertheless, the majority of these models are limited to relatively small dimensions and cannot comfortably accommodate larger-scale dependence modelling problems.

In addition, the modelling approach presented in Chapter 3 can be employed not only for passive but also for active portfolio risk management. There is abundant room for further research on the use of vine copulas for conditional asset allocation. In principle, the aim of conditional asset allocation is to find the optimal portfolio allocation for the next time period. In general, the optimal asset allocation follows the mean-variance approach of [Markowitz \(1952\)](#). It is clear that the next period's returns and covariance matrix are not known *ex-ante* but can be estimated using the forecasted returns derived from the vine model. The conditional asset allocation can also be extended beyond the standard mean-variance approach - to alternative approaches where the optimal portfolio is obtained after incorporating the downside risk into the asset allocation model. For example, an alternative approach could be to construct portfolios by maximising expected returns subject to a *VaR* or *CVaR* constraint. It is therefore possible to obtain optimal portfolio weights and thus re-balance portfolios according to the selected risk measure and the resulting weights. Furthermore, this approach could also be employed to build a trading strategy that fits the risk profile of an investor.

A natural extension of the *Copula CoVaR* methodology presented in Chapter 4 would be to increase the number of conditioning events and consider the scenario where more than one institution is in distress. Currently, the general *CoVaR* representation depends on the conditional distribution of returns representing the entire financial system given that a single institution is in financial distress. Several studies in the finance literature, however, find that there is more extremal dependence in periods of heightened market uncertainty (see for example, [Longin and Solnik 2001](#); [Ang and Chen 2002](#); [Jondeau and Rockinger 2006](#); [Chollete et al. 2009](#), among others). It is possible therefore that more than one financial institution may find itself in distress at the same time. This scenario is not unrealistic given the extensive business ties between financial institutions, many of which have emerged in the last decade. In this regard, further research should be undertaken to investigate the impact of several financial institutions being in distress simultaneously on the stability of the financial system and the economy as a whole. The pair-copula construction methodology can be directly associated with this study and provide further flexibility to the modelling of the dependence structure between the returns of the financial system and those of financial institutions.

In future investigations, it might be possible to study the spillover effects of systemic risk on individual financial institutions. As described in Chapter 4, the *CoVaR* measures an institution's contribution to systemic risk. Nevertheless, the adverse effects of systemic risk on the financial stability of an individual institution can also be measured by reversing the conditioning event in the original *CoVaR* definition. Another area for future research would be to explore whether systemic risk can be

successfully forecasted. Unquestionably, this is a significant area for further investigation, with important practical implications for the regulatory community and the financial system. So far, most studies have focused on developing alternative quantitative systemic risk models. To the best of our knowledge, the number of studies that focus on systemic risk forecasting is rather limited. In this regard, we believe that our methodology can contribute to this segment of the literature and provide further insight into systemic risk forecasting.

Certainly, the proposed *Copula CoVaR* framework can be further improved in many ways. A great challenge would be to provide analytical expressions for both *CoVaR* definitions beyond the class of Archimedean copulas.¹ Furthermore, alternative marginals and time-varying specifications can also be used to assess the model's performance under different assumptions in the marginal series and the dependence structure. The methodology can also be extended to take into account changing market conditions by assuming a varying copula functional form or introducing multiple regimes through time. Moreover, there is a large number of observable macroeconomic and financial variables that can be directly incorporated in the marginal series and copula dependence dynamics and assess their effects on the conditional dependence between the returns of the financial system and those of financial institutions. Finally, more efficient methods can be employed to estimate the models (e.g. full maximum likelihood methods) and to reduce misspecification in the marginal series (e.g. semi-parametric methods).

A great challenge with reference to Chapter 5 would be to extend the model of Hoff and Niu (2012) to elliptical copula families that allow for asymmetric dependence in the tails. This is an important issue for further research since the multivariate Gaussian distribution implied in the model of Hoff and Niu (2012) does not allow for tail dependence. However, it is possible that the yield prediction errors may exhibit strong dependence among extreme values and therefore the assumption of normality might be inappropriate for capturing the distribution characteristics of the data being modelled. Further work is also required in the estimation procedure of the proposed methodology. The current estimation approach is characterised by two main steps; in the first step, the yield curve for each individual country is estimated separately and the covariance of the prediction errors obtained from this process is modelled as a function of country-specific liquidity and credit quality measures in the second step. In this respect, it may be possible to build a procedure that performs the estimation of the entire model in one step and thus improve the model's relative efficiency.

¹General solutions have also been proposed for elliptical copula families, i.e., Gaussian and Student-*t* copulas for the *CoVaR* definition in Girardi and Ergün (2013).

There are also multiple ways to improve the present study and apply this framework to alternative financial applications. For example, the three-factor macro-finance Nelson-Siegel model of [Diebold et al. \(2006\)](#), employed to model the yield curve dynamics for each individual country, can be easily extended to incorporate more factors in the spirit of the [Svensson \(1994\)](#) model. In addition, the macro-finance Nelson-Siegel model of [Diebold et al. \(2006\)](#) can be extended by treating the loading parameter λ as a stochastically time-varying latent factor and by introducing time-varying volatility into the variance specification of the disturbances as shown in [Koopman et al. \(2010\)](#). Furthermore, the dynamics of the latent factors as well as the transition error covariance matrices can be modelled assuming more complex specifications. It is also important to note that additional observable macroeconomic and financial variables can be used in the latent factor specification, which may act as additional control variables, and alternative proxies for market-wide liquidity and credit measures. Additionally, the quality of country-specific liquidity and credit measures is very important in the covariance regression models and thus alternative proxies, especially for country-specific liquidity measures, should be considered.

Finally, the proposed methodology can find useful applications in various areas of financial modelling. For example, the stress testing procedure described in Chapter 5 may be used as a risk management tool for portfolio managers and investors in the fixed-income markets to assess the impact of particular shocks in the liquidity and credit quality measures on relevant debt instruments and to relate them directly to the corresponding yield spreads and fixed-income portfolios analysed. The methodology may also be useful for the study of the sources of risk premia and cross-market dynamics, which may have important implications for monetary policy and financial stability. It can also have significant practical implications for the pricing of underlying instruments and the hedging strategy of relevant contracts.

Bibliography

- Aas, Kjersti, and Daniel Berg, 2009, Models for construction of multivariate dependence - a comparison study, *The European Journal of Finance* 15, 639–659.
- Aas, Kjersti, Claudia Czado, Arnoldo Frigessi, and Henrik Bakken, 2009, Pair-copula constructions of multiple dependence, *Insurance: Mathematics and Economics* 44, 182–198.
- Abberger, Klaus, 2005, A simple graphical method to explore tail-dependence in stock-return pairs, *Applied Financial Economics* 15, 43–51.
- Acharya, Viral V., and Lasse Heje Pedersen, 2005, Asset pricing with liquidity risk, *Journal of Financial Economics* 77, 375–410.
- Acharya, Viral V., Lasse Heje Pedersen, Thomas Philippon, and Matthew P. Richardson, 2012, Measuring systemic risk, SSRN Scholarly Paper ID 2013815, Social Science Research Network, Rochester, NY.
- Adrian, Tobias, and Markus K. Brunnermeier, 2011, CoVaR, Staff Reports 348, Federal Reserve Bank of New York.
- Adrian, Tobias, and Hyun Song Shin, 2010, Liquidity and leverage, *Journal of Financial Intermediation* 19, 418–437.
- Akaike, Hirotugu, 1974, A new look at the statistical model identification, *IEEE Transactions on Automatic Control* 19, 716–723.
- Alter, Adrian, and Andreas Beyer, 2014, The dynamics of spillover effects during the European sovereign debt turmoil, *Journal of Banking & Finance* 42, 134–153.
- Amihud, Yakov, Haim Mendelson, and Lasse Heje Pedersen, 2005, *Liquidity and Asset Prices* (Now Publishers Inc).
- Ané, Thierry, and Cécile Kharoubi, 2003, Dependence Structure and Risk Measure, *The Journal of Business* 76, 411–438.
- Ang, Andrew, and Geert Bekaert, 2002a, International Asset Allocation With Regime Shifts, *Review of Financial Studies* 15, 1137–1187.
- Ang, Andrew, and Geert Bekaert, 2002b, Regime Switches in Interest Rates, *Journal of Business & Economic Statistics* 20, 163–182.
- Ang, Andrew, and Joseph Chen, 2002, Asymmetric correlations of equity portfolios, *Journal of Financial Economics* 63, 443–494.

- Ang, Andrew, and Monika Piazzesi, 2003, A no-arbitrage vector autoregression of term structure dynamics with macroeconomic and latent variables, *Journal of Monetary Economics* 50, 745–787.
- Ang, Andrew, Monika Piazzesi, and Min Wei, 2006, What does the yield curve tell us about GDP growth?, *Journal of Econometrics* 131, 359–403.
- Angelidis, Timotheos, and Stavros Antonios Degiannakis, 2007, Backtesting VaR Models: An Expected Shortfall Approach, Working paper, University of Crete, Department of Economics.
- Balduzzi, Pierluigi, Edwin J. Elton, and Clifton T. Green, 2001, Economic News and Bond Prices: Evidence from the U.S. Treasury Market, *The Journal of Financial and Quantitative Analysis* 36, 523–543.
- Balfoussia, Hiona, and Mike Wickens, 2007, Macroeconomic Sources of Risk in the Term Structure, *Journal of Money, Credit and Banking* 39, 205–236.
- Balkema, August A., and Laurens De Haan, 1974, Residual Life Time at Great Age, *The Annals of Probability* 2, 792–804.
- Bandein-Roche, Karen J., and Kung-Yee Liang, 1996, Modelling failure-time associations in data with multiple levels of clustering, *Biometrika* 83, 29–39.
- Bao, Jack, Jun Pan, and Jiang Wang, 2011, The Illiquidity of Corporate Bonds, *The Journal of Finance* 66, 911–946.
- Beber, Alessandro, Michael W. Brandt, and Kenneth A. Kavajecz, 2009, Flight-to-Quality or Flight-to-Liquidity? Evidence from the Euro-Area Bond Market, *Review of Financial Studies* 22, 925–957.
- Bedford, Tim, and Roger M. Cooke, 2001, Probability Density Decomposition for Conditionally Dependent Random Variables Modeled by Vines, *Annals of Mathematics and Artificial Intelligence* 32, 245–268.
- Bedford, Tim, and Roger M. Cooke, 2002, Vines: A New Graphical Model for Dependent Random Variables, *The Annals of Statistics* 30, 1031–1068.
- Belgorodski, Natalia, 2010, Selecting pair-copula families for regular vines with application to the multivariate analysis of European stock market indices, Diploma thesis, Technische Universität München, Germany, <http://mediatum.ub.tum.de/doc/1079284/1079284.pdf>.
- Berkowitz, Jeremy, Peter Christoffersen, and Denis Pelletier, 2009, Evaluating Value-at-Risk Models with Desk-Level Data, *Management Science* 57, 2213–2227.

- Bianchi, Francesco, Haroon Mumtaz, and Paolo Surico, 2009, The great moderation of the term structure of UK interest rates, *Journal of Monetary Economics* 56, 856–871.
- Billio, Monica, Mila Getmansky, Andrew W. Lo, and Lorian Pelizzon, 2012, Econometric measures of connectedness and systemic risk in the finance and insurance sectors, *Journal of Financial Economics* 104, 535–559.
- Bisias, Dimitrios, Mark Flood, Andrew W. Lo, and Stavros Valavanis, 2012, A Survey of Systemic Risk Analytics, *Annual Review of Financial Economics* 4, 255–296.
- Börger, Reik H, Álvaro Cartea, Ruediger Kiesel, and Gero Schindlmayr, 2007, A Multivariate Commodity Analysis and Applications to Risk Management, Birkbeck working papers in economics and finance, Birkbeck, Department of Economics, Mathematics & Statistics.
- Bouyè, Eric, and Mark Salmon, 2009, Dynamic copula quantile regressions and tail area dynamic dependence in forex markets, *The European Journal of Finance* 15, 721–750.
- Brechmann, Eike Christain, and Claudia Czado, 2013, Risk management with high-dimensional vine copulas: An analysis of the Euro Stoxx 50, *Statistics & Risk Modeling* 30, 307–342.
- Brechmann, Eike Christain, Claudia Czado, and Kjersti Aas, 2012, Truncated regular vines in high dimensions with application to financial data, *Canadian Journal of Statistics* 40, 68–85.
- Brechmann, Eike Christian, 2010, Truncated and simplified regular vines and their applications, Diploma thesis, Faculty of Mathematics, Technische Universität München, Germany, <http://mediatum.ub.tum.de/doc/1079285/1079285.pdf>.
- Brechmann, Eike Christian, and Ulf Schepsmeier, 2013, Modeling dependence with C-and D-vine copulas: The R-package CDVine, *Journal of Statistical Software* 52, 1–27.
- Brownlees, Christian T., and Robert F. Engle, 2012, Volatility, Correlation and Tails for Systemic Risk Measurement, SSRN Scholarly Paper ID 1611229, Social Science Research Network, Rochester, NY.
- Brunnermeier, Markus K., 2009, Deciphering the liquidity and credit crunch 2007–2008, *Journal of Economic Perspectives* 23, 77–100.
- Brunnermeier, Markus K., Andrew Crockett, Charles A.E. Goodhart, Avinash Persaud, and Hyun Song Shin, 2009, *The fundamental principles of financial regulation* (Centre for Economic Policy Research, London).

- Brunnermeier, Markus K., and Lasse Heje Pedersen, 2009, Market Liquidity and Funding Liquidity, *Review of Financial Studies* 22, 2201–2238.
- Byström, Hans N. E., 2005, Extreme value theory and extremely large electricity price changes, *International Review of Economics & Finance* 14, 41–55.
- Chen, Long, David A. Lesmond, and Jason Wei, 2007, Corporate Yield Spreads and Bond Liquidity, *The Journal of Finance* 62, 119–149.
- Cherubini, Umberto, and Elisa Luciano, 2001, Value-at-risk Trade-off and Capital Allocation with Copulas, *Economic Notes* 30, 235–256.
- Cherubini, Umberto, Elisa Luciano, and Walter Vecchiato, 2004, *Copula Methods in Finance* (John Wiley & Sons).
- Chollete, Lorán, Andréas Heinen, and Alfonso Valdesogo, 2009, Modeling International Financial Returns with a Multivariate Regime-switching Copula, *Journal of Financial Econometrics* 7, 437–480.
- Chordia, Tarun, Asani Sarkar, and Avanidhar Subrahmanyam, 2001, Common determinants of bond and stock market liquidity: the impact of financial crises, monetary policy, and mutual fund flows, Staff Reports 141, Federal Reserve Bank of New York.
- Chordia, Tarun, Asani Sarkar, and Avanidhar Subrahmanyam, 2005, An Empirical Analysis of Stock and Bond Market Liquidity, *Review of Financial Studies* 18, 85–129.
- Christensen, Jens H.E., Francis X. Diebold, and Glenn D. Rudebusch, 2011, The affine arbitrage-free class of Nelson-Siegel term structure models, *Journal of Econometrics* 164, 4–20.
- Christoffersen, Peter, 1998, Evaluating Interval Forecasts, *International Economic Review* 39, 841–862.
- Christoffersen, Peter, Vihang Errunza, Kris Jacobs, and Hugues Langlois, 2012, Is the Potential for International Diversification Disappearing? A Dynamic Copula Approach, *Review of Financial Studies* 25, 3711–3751.
- Christoffersen, Peter, and Denis Pelletier, 2004, Backtesting Value-at-Risk: A Duration-Based Approach, *Journal of Financial Econometrics* 2, 84–108.
- Clarke, Kevin A., 2007, A Simple Distribution-Free Test for Nonnested Model Selection, *Political Analysis* 15, 347–363.
- Connolly, Robert, Chris Stivers, and Licheng Sun, 2005, Stock Market Uncertainty and the Stock-Bond Return Relation, *Journal of Financial and Quantitative Analysis* 40, 161–194.

- Covitz, Dan, and Chris Downing, 2007, Liquidity or Credit Risk? The Determinants of Very Short-Term Corporate Yield Spreads, *The Journal of Finance* 62, 2303–2328.
- Cox, John C., Jonathan E. Ingersoll, Jr., and Stephen A. Ross, 1985, A Theory of the Term Structure of Interest Rates, *Econometrica* 53, 385–407.
- Czado, Claudia, 2010, Pair-Copula Constructions of Multivariate Copulas, in Piotr Jaworski, Fabrizio Durante, Wolfgang Karl Härdle, and Tomasz Rychlik, eds., *Copula Theory and Its Applications*, number 198 in Lecture Notes in Statistics, 93–109 (Springer).
- Czado, Claudia, Ulf Schepsmeier, and Aleksey Min, 2012, Maximum likelihood estimation of mixed C-vines with application to exchange rates, *Statistical Modelling* 12, 229–255.
- Dai, Qiang, and Kenneth J. Singleton, 2000, Specification Analysis of Affine Term Structure Models, *The Journal of Finance* 55, 1943–1978.
- Danielsson, Jon, and Casper G. de Vries, 1997, Tail index and quantile estimation with very high frequency data, *Journal of Empirical Finance* 4, 241–257.
- Das, Sanjiv Ranjan, and Raman Uppal, 2004, Systemic Risk and International Portfolio Choice, *The Journal of Finance* 59, 2809–2834.
- de Jong, Frank, and Joost Driessen, 2012, Liquidity Risk Premia in Corporate Bond Markets, *Quarterly Journal of Finance* 02, 1250006.
- Dewachter, Hans, and Marco Lyrio, 2006, Macro Factors and the Term Structure of Interest Rates, *Journal of Money, Credit, and Banking* 38, 119–140.
- Dick-Nielsen, Jens, Peter Feldhütter, and David Lando, 2012, Corporate bond liquidity before and after the onset of the subprime crisis, *Journal of Financial Economics* 103, 471–492.
- Diebold, Francis X., and Canlin Li, 2006, Forecasting the term structure of government bond yields, *Journal of Econometrics* 130, 337–364.
- Diebold, Francis X., Canlin Li, and Vivian Z. Yue, 2008, Global yield curve dynamics and interactions: A dynamic Nelson-Siegel approach, *Journal of Econometrics* 146, 351–363.
- Diebold, Francis X., Glenn D. Rudebusch, and S. Borağan Aruoba, 2006, The macroeconomy and the yield curve: a dynamic latent factor approach, *Journal of Econometrics* 131, 309–338.
- Dobrić, Jadran, and Friedrich Schmid, 2005, Nonparametric estimation of the lower tail dependence λ_L in bivariate copulas, *Journal of Applied Statistics* 32, 387–407.

- Duffee, Gregory R., 2002, Term Premia and Interest Rate Forecasts in Affine Models, *The Journal of Finance* 57, 405–443.
- Duffie, Darrell, and Rui Kan, 1996, A Yield-Factor Model of Interest Rates, *Mathematical Finance* 6, 379–406.
- Duffie, Darrell, and Jun Pan, 1997, An overview of value at risk, *The Journal of Derivatives* 4, 7–49.
- Duffie, Darrell, Lasse Heje Pedersen, and Kenneth J. Singleton, 2003, Modeling Sovereign Yield Spreads: A Case Study of Russian Debt, *The Journal of Finance* 58, 119–159.
- Embrechts, Paul, Andrea Höing, and Alessandro Juri, 2003a, Using copulae to bound the Value-at-Risk for functions of dependent risks, *Finance and Stochastics* 7, 145–167.
- Embrechts, Paul, Claudia Kluppelberg, and Thomas Mikosch, 1999a, *Modelling Extremal Events*, second edition (Springer).
- Embrechts, Paul, Filip Lindskog, and Alexander McNeil, 2003b, Modelling Dependence with Copulas and Applications to Risk Management, in S. T. Rachev, ed., *Handbook of Heavy Tailed Distributions in Finance* (Elsevier).
- Embrechts, Paul, Alexander McNeil, and Daniel Straumann, 1999b, Correlation: pitfalls and alternatives, *Risk* 12, 69–71.
- Embrechts, Paul, Alexander McNeil, and Daniel Straumann, 2002, Correlation and dependence in risk management: properties and pitfalls, in *Risk Management: Value at Risk and Beyond*, 176–223 (Cambridge University Press).
- Embrechts, Paul, Alexander McNeil, and Daniel Straumann, 2003c, Modelling dependence with copulas and applications to risk management, in S. T. Rachev, ed., *Handbook of Heavy Tailed Distributions in Finance: Handbooks in Finance* (Elsevier).
- Embrechts, Paul, Sidney I. Resnick, and Gennady Samorodnitsky, 1999c, Extreme value theory as a risk management tool, *North American Actuarial Journal* 30–41.
- Engle, Robert, 2002, Dynamic conditional correlation, *Journal of Business & Economic Statistics* 20, 339–350.
- Engle, Robert, Eric Jondeau, and Michael Rockinger, 2014, Systemic Risk in Europe, *Review of Finance* rfu012.
- Ericsson, Jan, and Olivier Renault, 2006, Liquidity and Credit Risk, *The Journal of Finance* 61, 2219–2250.

- Fantazzini, Dean, 2009, The effects of misspecified marginals and copulas on computing the value at risk: A Monte Carlo study, *Computational Statistics & Data Analysis* 53, 2168–2188.
- Fernández, Carmen, and Mark F. J. Steel, 1998, On Bayesian Modeling of Fat Tails and Skewness, *Journal of the American Statistical Association* 93, 359–371.
- Fischer, Matthias, Christian Köck, Stephan Schlüter, and Florian Weigert, 2009, An empirical analysis of multivariate copula models, *Quantitative Finance* 9, 839–854.
- Fisher, Nicholas I., and Paul Switzer, 1985, Chi-plots for assessing dependence, *Biometrika* 72, 253–265.
- Fisher, Nicholas I., and Paul Switzer, 2001, Graphical assessment of dependence: Is a picture worth 100 tests?, *The American Statistician* 55, 233–239.
- Fong Chan, Kam, and Philip Gray, 2006, Using extreme value theory to measure value-at-risk for daily electricity spot prices, *International Journal of Forecasting* 22, 283–300.
- Garcia, René, and Georges Tsafack, 2011, Dependence structure and extreme co-movements in international equity and bond markets, *Journal of Banking & Finance* 35, 1954–1970.
- Gauthier, Céline, Alfred Lehar, and Moez Souissi, 2012, Macroprudential capital requirements and systemic risk, *Journal of Financial Intermediation* 21, 594–618.
- Gençay, Ramazan, and Faruk Selçuk, 2004, Extreme value theory and Value-at-Risk: Relative performance in emerging markets, *International Journal of Forecasting* 20, 287–303.
- Genest, Christian, 2007, Everything You Always Wanted to Know about Copula Modeling but Were Afraid to Ask, *Journal of Hydrologic Engineering* 12, 347–368.
- Genest, Christian, and Jean-Claude Boies, 2003, Detecting Dependence With Kendall Plots, *The American Statistician* 57, 275–284.
- Genest, Christian, Kilani Ghoudi, and Louis-Paul Rivest, 1995, A semiparametric estimation procedure of dependence parameters in multivariate families of distributions, *Biometrika* 82, 543–552.
- Genest, Christian, and Louis-Paul Rivest, 1993, Statistical inference procedures for bivariate Archimedean copulas, *Journal of the American Statistical Association* 88, 1034–1043.
- Giannone, Domenico, Michele Lenza, Huw Pill, and Lucrezia Reichlin, 2012, The ECB and the interbank market, *The Economic Journal* 122, 467–486.

- Girardi, Giulio, and A. Tolga Ergün, 2013, Systemic risk measurement: Multivariate GARCH estimation of CoVaR, *Journal of Banking & Finance* 37, 3169–3180.
- Glosten, Lawrence R., Ravi Jagannathan, and David E. Runkle, 1993, On the Relation between the Expected Value and the Volatility of the Nominal Excess Return on Stocks, *The Journal of Finance* 48, 1779–1801.
- Goldreich, David, Bernd Hanke, and Purnendu Nath, 2005, The Price of Future Liquidity: Time-Varying Liquidity in the U.S. Treasury Market, *Review of Finance* 9, 1–32.
- González-Hermosillo, Brenda, and Christian A. Johnson, 2014, Transmission of Financial Stress in Europe: The Pivotal Role of Italy and Spain, But Not Greece, SSRN Scholarly Paper ID 2445460, Social Science Research Network, Rochester, NY.
- Goyenko, Ruslan, Avanidhar Subrahmanyam, and Andrey Ukhov, 2011, The Term Structure of Bond Market Liquidity and Its Implications for Expected Bond Returns, *Journal of Financial and Quantitative Analysis* 46, 111–139.
- Haff, Ingrid Hobæk, 2013, Parameter estimation for pair-copula constructions, *Bernoulli* 19, 462–491.
- Hameed, Allaudeen, Wenjin Kang, and S. Viswanathan, 2010, Stock Market Declines and Liquidity, *The Journal of Finance* 65, 257–293.
- Heath, David, Robert Jarrow, and Andrew Morton, 1992, Bond Pricing and the Term Structure of Interest Rates: A New Methodology for Contingent Claims Valuation, *Econometrica* 60, 77–105.
- Heinen, Andréas, and Alfonso Valdesogo, 2008, Asymmetric CAPM Dependence for Large Dimensions: The Canonical Vine Autoregressive Copula Model, SSRN Scholarly Paper ID 1297506, Social Science Research Network, Rochester, NY.
- Ho, Thomas S. Y., and Sang-Bin Lee, 1986, Term Structure Movements and Pricing Interest Rate Contingent Claims, *The Journal of Finance* 41, 1011–1029.
- Hoff, Petter D., and Xiaoyue Niu, 2012, A Covariance Regression Model, *Statistica Sinica* 22, 729–753.
- Hong, Yongmiao, Jun Tu, and Guofu Zhou, 2007, Asymmetries in Stock Returns: Statistical Tests and Economic Evaluation, *Review of Financial Studies* 20, 1547–1581.
- Hördahl, Peter, Oreste Tristani, and David Vestin, 2006, A joint econometric model of macroeconomic and term-structure dynamics, *Journal of Econometrics* 131, 405–444.

- Hosking, Jonathan R.M., and James R. Wallis, 1987, Parameter and quantile estimation for the generalized Pareto distribution, *Technometrics* 29, 339–349.
- Huang, Xin, Hao Zhou, and Haibin Zhu, 2009, A framework for assessing the systemic risk of major financial institutions, *Journal of Banking & Finance* 33, 2036–2049.
- Hull, John C., 1990, Pricing interest-rate-derivative securities, *Review of Financial Studies* 3, 573–592.
- Hull, John C., and Alan D. White, 1998, Value at Risk When Daily Changes in Market Variables are not Normally Distributed, *The Journal of Derivatives* 5, 9–19.
- Hurlin, Christophe, and Christophe Pérignon, 2011, Margin Backtesting, SSRN Scholarly Paper ID 2001988, Social Science Research Network, Rochester, NY.
- Joe, Harry, 1996, Families of m -variate distributions with given margins and $m(m - 1)/2$ bivariate dependence parameters, in Ludger Rüschendorf, Berthold Schweizer, and Michael Dee Taylor, eds., *Distributions with fixed marginals and related topics*, 120–141 (Hayward: Institute of Mathematical Statistics).
- Joe, Harry, 1997, *Multivariate Models and Multivariate Dependence Concepts* (CRC Press).
- Joe, Harry, and Taizhong Hu, 1996, Multivariate Distributions from Mixtures of Max-Infinitely Divisible Distributions, *Journal of Multivariate Analysis* 57, 240–265.
- Joe, Harry, Haijun Li, and Aristidis K. Nikoloulopoulos, 2010, Tail dependence functions and vine copulas, *Journal of Multivariate Analysis* 101, 252–270.
- Jondeau, Eric, and Michael Rockinger, 2006, The Copula-GARCH model of conditional dependencies: An international stock market application, *Journal of International Money and Finance* 25, 827–853.
- Jorion, Philippe, 2001, *Value at Risk: The New Benchmark for Managing Financial Risk* (McGraw-Hill).
- Kempf, Alexander, Olaf Korn, and Marliese Uhrig-Homburg, 2012, The term structure of illiquidity premia, *Journal of Banking & Finance* 36, 1381–1391.
- Kim, Gunky, Mervyn J. Silvapulle, and Paramsothy Silvapulle, 2007, Comparison of semiparametric and parametric methods for estimating copulas, *Computational Statistics & Data Analysis* 51, 2836–2850.
- Koenker, Roger, and Gilbert Bassett, 1978, Regression quantiles, *Econometrica* 46, 33–50.

- Kole, Erik, Kees Koedijk, and Marno Verbeek, 2007, Selecting copulas for risk management, *Journal of Banking & Finance* 31, 2405–2423.
- Koopman, Siem Jan, Max I. P. Mallee, and Michel Van der Wel, 2010, Analyzing the Term Structure of Interest Rates Using the Dynamic Nelson-Siegel Model With Time-Varying Parameters, *Journal of Business & Economic Statistics* 28, 329–343.
- Kozicki, Sharon, and P. A. Tinsley, 2001, Shifting endpoints in the term structure of interest rates, *Journal of Monetary Economics* 47, 613–652.
- Krishnamurthy, Arvind, 2002, The bond/old-bond spread, *Journal of Financial Economics* 66, 463–506.
- Kupiec, Paul H, 1995, Techniques for verifying the accuracy of risk measurement models, *The Journal of Derivatives* 3, 73–84.
- Kurowicka, Dorota, and Roger M. Cooke, 2006, *Uncertainty Analysis with High Dimensional Dependence Modelling* (John Wiley & Sons).
- Liu, Jun, Francis A. Longstaff, and Ravit E. Mandell, 2006, The Market Price of Risk in Interest Rate Swaps: The Roles of Default and Liquidity Risks, *The Journal of Business* 79, 2337–2359.
- Longin, François, and Bruno Solnik, 1995, Is the correlation in international equity returns constant: 1960-1990?, *Journal of International Money and Finance* 14, 3–26.
- Longin, François, and Bruno Solnik, 2001, Extreme Correlation of International Equity Markets, *The Journal of Finance* 56, 649–676.
- Longstaff, Francis A., 2004, The Flight-to-Liquidity Premium in U.S. Treasury Bond Prices, *The Journal of Business* 77, 511–526.
- Longstaff, Francis A., Sanjay Mithal, and Eric Neis, 2005, Corporate Yield Spreads: Default Risk or Liquidity? New Evidence from the Credit Default Swap Market, *The Journal of Finance* 60, 2213–2253.
- Lopez, Jose A., 1998, Regulatory evaluation of value-at-risk models, Technical report, Federal Reserve Bank of New York.
- Lopez, Jose A., 1999, Methods for evaluating value-at-risk estimates, Technical report, Federal Reserve Bank of San Francisco.
- Lòpez-Espinosa, Germàn, Antonio Moreno, Antonio Rubia, and Laura Valderrama, 2012, Short-term wholesale funding and systemic risk: A global CoVaR approach, *Journal of Banking & Finance* 36, 3150–3162.

- López-Espinosa, Germàn, Antonio Rubia, Laura Valderrama, and Miguel Antòn, 2013, Good for one, bad for all: Determinants of individual versus systemic risk, *Journal of Financial Stability* 9, 287–299.
- Mainik, Georg, and Eric Schaanning, 2014, On dependence consistency of CoVaR and some other systemic risk measures, *Statistics & Risk Modeling*, 31, 49–77.
- Markowitz, Harry, 1952, Portfolio Selection, *The Journal of Finance* 7, 77–91.
- Markwat, Thijs D., Erik Kole, Van Dijk, and Dick J. C., 2012, Time Variation in Asset Return Dependence: Strength or Structure?, SSRN Scholarly Paper ID 1460648, Social Science Research Network, Rochester, NY.
- McNeil, Alexander J., 2008, Sampling nested Archimedean copulas, *Journal of Statistical Computation and Simulation* 78, 567–581.
- McNeil, Alexander J., and Rüdiger Frey, 2000, Estimation of tail-related risk measures for heteroscedastic financial time series: an extreme value approach, *Journal of Empirical Finance* 7, 271–300.
- Mendes, Beatriz Vaz de Melo, Mariângela Mendes Semeraro, and Ricardo P. Câmara Leal, 2010, Pair-copulas modeling in finance, *Financial Markets and Portfolio Management* 24, 193–213.
- Mills, Frederick C., 1927, The behavior of prices, *NBER* .
- Min, Aleksey, and Claudia Czado, 2010, Bayesian Inference for Multivariate Copulas Using Pair-Copula Constructions, *Journal of Financial Econometrics* 8, 511–546.
- Monfort, Alain, and Jean-Paul Renne, 2014, Decomposing Euro-Area Sovereign Spreads: Credit and Liquidity Risks, *Review of Finance* 18, 2103–2151.
- Nelsen, Roger B., 2007, *An Introduction to Copulas*, Second edition (Springer).
- Nelson, Charles R., and Andrew F. Siegel, 1987, Parsimonious Modeling of Yield Curves, *The Journal of Business* 60, 473–489.
- Nicolò, Gianni De, and Marcella Lucchetta, 2011, Systemic Risks and the Macroeconomy, Working Paper 16998, National Bureau of Economic Research.
- Nikoloulopoulos, Aristidis K., Harry Joe, and Haijun Li, 2012, Vine copulas with asymmetric tail dependence and applications to financial return data, *Computational Statistics & Data Analysis* 56, 3659–3673.
- Patton, Andrew J., 2004, On the Out-of-Sample Importance of Skewness and Asymmetric Dependence for Asset Allocation, *Journal of Financial Econometrics* 2, 130–168.

- Patton, Andrew J., 2006, Modelling asymmetric exchange rate dependence, *International Economic Review* 47, 527–556.
- Piazzesi, Monika, 2005, Bond Yields and the Federal Reserve, *Journal of Political Economy* 113, 311–344.
- Pickands, James, 1975, Statistical inference using extreme order statistics, *The Annals of Statistics* 3, 119–131.
- Poon, Ser-Huang, Michael Rockinger, and Jonathan Tawn, 2004, Extreme Value Dependence in Financial Markets: Diagnostics, Models, and Financial Implications, *Review of Financial Studies* 17, 581–610.
- Rachev, S. T., 2003, *Handbook of Heavy Tailed Distributions in Finance: Handbooks in Finance* (Elsevier).
- Reiss, Rolf-Dieter, and Michael Thomas, 1997, *Statistical Analysis of Extreme Values with Applications to Insurance, Finance, Hydrology and Other Fields* (Birkhäuser Verlag).
- Rodriguez, Juan Carlos, 2007, Measuring financial contagion: A Copula approach, *Journal of Empirical Finance* 14, 401–423.
- Rudebusch, Glenn D., and Tao Wu, 2008, A Macro-Finance Model of the Term Structure, Monetary Policy and the Economy, *The Economic Journal* 118, 906–926.
- Saka, Orkun, Ana-Maria Fuertes, and Elena Kalotychou, 2014, ECB Policy and Eurozone Fragility: Was De Grauwe Right?, SSRN Scholarly Paper ID 2459882, Social Science Research Network, Rochester, NY.
- Sarma, Mandira, Susan Thomas, and Ajay Shah, 2003, Selection of Value-at-Risk models, *Journal of Forecasting* 22, 337–358.
- Savu, Cornelia, and Mark Tiede, 2009, Hierarchies of Archimedean copulas, *Quantitative Finance* 10, 295–304.
- Schepsmeier, Ulf, 2010, Maximum likelihood estimation of C-vine pair-copula constructions based on bivariate copulas from different families, Diploma thesis, Technische Universität München, Germany, <http://mediatum.ub.tum.de/doc/1079296/1079296.pdf>.
- Schestag, Raphael, Philipp Schuster, and Marliese Uhrig-Homburg, 2013, Measuring Liquidity in Bond Markets, SSRN Scholarly Paper ID 2328370, Social Science Research Network, Rochester, NY.
- Schwarz, Gideon E., 1978, Estimating the dimension of a model, *The Annals of Statistics* 6, 461–464.

- Segoviano, Miguel A., and Charles Goodhart, 2009, Banking stability measures, Financial markets group, London School of Economics and Political Science.
- Shambaugh, Jay C., 2012, The Euro's Three Crises, *Brookings Papers on Economic Activity* .
- Sklar, Abe, 1959, Fonctions de répartition à n dimensions et leurs marges, *Publications del'Institut de Statistique de L'Université de Paris*, 8, 229–231.
- Svensson, Lars E. O., 1994, Estimating and Interpreting Forward Interest Rates: Sweden 1992 - 1994, Working Paper 4871, National Bureau of Economic Research.
- Thompson, Samuel B., 2011, Simple formulas for standard errors that cluster by both firm and time, *Journal of Financial Economics* 99, 1–10.
- Underwood, Shane, 2009, The cross-market information content of stock and bond order flow, *Journal of Financial Markets* 12, 268–289.
- Vasicek, Oldrich, 1977, An equilibrium characterization of the term structure, *Journal of Financial Economics* 5, 177–188.
- Vayanos, Dimitri, 2004, Flight to Quality, Flight to Liquidity, and the Pricing of Risk, Working Paper 10327, National Bureau of Economic Research.
- Vuong, Quang H., 1989, Likelihood Ratio Tests for Model Selection and Non-Nested Hypotheses, *Econometrica* 57, 307–333.
- Weiß, Gregor, and Marcus Scheffer, 2012, Smooth Nonparametric Bernstein Vine Copulas, Paper 1210.2043, arXiv.org.
- Weiß, Gregor N. F., and Marcus Scheffer, 2015, Mixture pair-copula-constructions, *Journal of Banking & Finance* 54, 175–191.
- Whelan, Niall, 2004, Sampling from Archimedean copulas, *Quantitative Finance* 4, 339–352.
- Wong, Alfred Y-T., and Tom Pak Wing Fong, 2011, Analysing interconnectivity among economies, *Emerging Markets Review* 12, 432–442.
- Wright, Jonathan H., 2011, Term Premia and Inflation Uncertainty: Empirical Evidence from an International Panel Dataset, *The American Economic Review* 101, 1514–1534.
- Yu, Wei-Choun, and Donald M. Salyards, 2009, Parsimonious modeling and forecasting of corporate yield curve, *Journal of Forecasting* 28, 73–88.
- Yu, Wei-Choun, and Eric Zivot, 2011, Forecasting the term structures of Treasury and corporate yields using dynamic Nelson-Siegel models, *International Journal of Forecasting* 27, 579–591.

Zhou, Chen, 2010, Are banks too big to fail? Measuring systemic importance of financial institutions, *International Journal of Central Banking* 6, 205–250.